

Chemical Modification of Alginates in Organic Media

Siddhesh Nitin Pawar

Dissertation submitted to the faculty of the Virginia Polytechnic Institute and State University in
partial fulfillment of the requirements for the degree of

**Doctor of Philosophy
In
Macromolecular Science and Engineering**

Kevin J. Edgar, Committee Chair
S. Richard Turner
Judy S. Riffle
Charles E. Frazier
Maren Roman

April 30, 2013
Blacksburg, VA

Keywords: Alginate, derivatization, regioselective, acetate, modification, DS, gelling, microbeads, esters, drug delivery, naringenin, solubility, enhancement

Copyright 2013, Siddhesh N. Pawar

Chemical Modification of Alginates in Organic Media

Siddhesh Nitin Pawar

Abstract

Alginates are (1→4) linked linear copolysaccharides composed of β -D-mannuronic acid (M) and its C-5 epimer, α -L-guluronic acid (G). Several strategies to synthesize organically modified alginate derivatives have been reported, but almost all chemistries are performed in either aqueous or aqueous-organic media. The ability to react alginates homogeneously in organic solvents would open up access to a wide range of new chemistries and derivatives. However, past attempts have been restricted by the absence of methods for alginate dissolution in organic media. We therefore report a strategy to solubilize tetrabutylammonium (TBA) salts of alginic acid in polar aprotic solvents containing tetrabutylammonium fluoride (TBAF).

Acylation of TBA-alginate was performed in DMSO/TBAF to get products with DS_{acetyl} up to ≈ 1.0 . We further report that by using appropriate solvent conditions, placement of acyl groups can be controlled to achieve either random or M-selective substitution. Alginate acetates synthesized in an M-selective fashion were used to study the ability of these derivatives to form Ca-crosslinked hydrogels. Detailed structure-property analyses were performed to identify acetylation reaction conditions and product properties that may be ideal for hydrogel formation. Furthermore, alginate esters were synthesized via modification of carboxylate groups on the backbone. These derivatives dissolved in polar aprotic solvents without the need to add TBAF. A proof of concept study showed their utility in the solubility enhancement of the poorly water soluble flavonoid naringenin.

Acknowledgements

First and foremost, I would like to thank my graduate advisor, Prof. Kevin J. Edgar, whose expertise, support and guidance enabled me to bring our research goals to fruition. His research and managements styles have truly brought out the best in me, and have influenced me deeply through my graduate career. His penchant for hard work, high thinking, kindheartedness and generosity are life's lessons, for which I will forever be grateful.

I wish to express deep gratitude towards my graduate committee members, Prof. Riffle, Prof. Turner, Prof. Frazier and Prof. Roman. Their guidance and suggestions have proven most valuable through my research. More importantly, I wish to thank them for being remarkable educators in this noble profession; you will be a constant source of inspiration to me in my life.

I would like to acknowledge our collaborators from Norway, Prof. Gudmund Skjåk-Bræk and Dr. Anne Tøndervik for sending us generous quantities of specialized alginates which are not commercially available. I would also like to thank our collaborator Prof. Emmanuel Opara from Wake Forest Institute of Regenerative Medicine (WFIRM) for all our joint efforts in successfully forming Ca-crosslinked alginate acetates. I wish to thank FMC Biopolymer for providing us with food grade alginates for our studies. I thank Dr. Hugo Azurmendi for assistance with NMR, Ms. Suzanne Barnes for performing and analyzing aqueous SEC data, and Mr. Joshua Moore for his assistance in the laboratory. I wish to give a big thanks to all my past and present colleagues in the cellulose research group – Junia Pereira, Haoyu Liu, Joyann Marks, Xueyan Zheng, Ruoran Zhang, Xiangtao Meng, Thomas Simerly, Dr. Daiqiang Xu, Dr. Carter Fox, Dr. Bin Li and Dr. Nilanjana Kar.

I would like to extend my deep gratitude towards organizations that funded this work – the Sustainable Engineered Materials Institute (SEMI) at Virginia Tech and USDA (Grant No. 2011-67009-20090). A special thanks to the Institute for Critical Technology and Applied Science (ICTAS) for providing top-class research facilities, and Macromolecules and Interfaces Institute (MII) for academic support.

Last but not the least, this accomplishment is dedicated to the people in my life who matter most and have inspired me to become who I am. I thank my parents for the blood, sweat and tears they have spent in successfully raising me. I thank my grandparents, sister, uncles, aunts and their families for their unending love. I wish to thank Ms. Sneha Kelkar for being a solid support through this journey. Last but not least, I would like to thank Prof. Thomas W. Smith, my Master's thesis advisor for being an inspiring mentor throughout my graduate school career.

Table of Contents

Abstract.....	iii
Acknowledgements.....	iii
List of Figures	viii
List of Schemes.....	xiv
List of Tables	xvi
Chapter 1: Dissertation Overview.....	1
Chapter 2: Literature Review on the Derivatization of Alginates.....	3
2.1 Abstract.....	3
2.2 Introduction.....	4
2.3 Description of alginates	5
2.3.1 Biosynthesis	5
2.3.2 Manufacture	6
2.3.3 Structure determination.....	8
2.3.4 Physical properties	10
2.3.5 Chemical properties	13
2.4 Alginate modification	16
2.4.1 Acetylation of alginates	17
2.4.2 Phosphorylation of alginates.....	29
2.4.3 Sulfation of alginates	31
2.4.4 Hydrophobic modification	35
2.4.5 Attachment of cell signaling molecules.....	45
2.4.6 Covalent crosslinking of alginates	54
2.4.7 Graft copolymerization of alginates.....	64
2.5 Conclusions.....	71
2.6 References.....	73
2.7 Copyright Authorization	83
Chapter 3: Organic Dissolution of Alginates and Epimer-selective Acetylation Thereof.....	84
3.1 Abstract.....	84
3.2 Introduction.....	84

3.3 Experimental.....	87
3.3.1 Materials and methods	87
3.3.2 Synthesis of TBA-alginate.....	91
3.3.3 Homogeneous synthesis of alginate acetate in DMSO/TBAF using acetic anhydride	91
3.3.4 Heterogeneous synthesis of alginate acetate in DMSO	92
3.3.5 Homogeneous synthesis of alginate acetate in DMSO/TBAF using acetyl chloride.....	93
3.3.6 Homogeneous synthesis of alginate propionate in DMSO/TBAF using propionic anhydride ..	94
3.3.7 Synthesis of anhydrous DMSO/TBAF solvent system.....	95
3.4 Results and discussion	96
3.5 Conclusions.....	111
3.6 Supporting information	112
3.7 References.....	118
3.8 Copyright Authorization	122
Chapter 4: Ca ⁺² -Induced Gelation of Alginate Acetates for Tailored Hydrogels	123
4.1 Abstract.....	123
4.2 Introduction.....	124
4.3 Experimental	127
4.3.1 Materials	127
4.3.2 Synthesis of TBA-alginate.....	128
4.3.3 Synthesis of alginate acetate	129
4.3.4 Synthesis of Ca-alginate beads	130
4.3.5 DS _{NMR} measurement	130
4.3.6 DS _{Titration} measurement	131
4.3.7 FTIR measurement.....	132
4.3.8 SEC analysis	133
4.3.9 Viscosity measurement	133
4.3.10 Imaging of Microbeads	134
4.3.11 Mechanical Strength Testing of Microbeads	134
4.3.12 Statistical evaluation of data	135
4.4 Results and Discussion	135
4.5 Conclusions.....	153
4.6 Supporting information.....	156

4.7 References.....	174
Chapter 5: Synthesis of Alginate Esters via Carboxyl Group Modification.....	179
5.1 Abstract.....	179
5.2 Introduction.....	180
5.3 Experimental.....	184
5.3.1 Materials	184
5.3.2 Synthesis of TBA-alginate.....	185
5.3.3 Synthesis of benzyl alginate.....	186
5.3.4 Synthesis of methyl alginate	187
5.3.5 Synthesis of ethyl alginate	188
5.3.6 Synthesis of butyl alginate	188
5.3.7 Saponification of esters.....	189
5.3.8 NMR Analysis	189
5.3.9 FTIR measurement.....	191
5.3.10 Elemental analysis.....	191
5.3.11 DS measurement by titration.....	191
5.3.12 Synthesis of solid dispersions	192
5.3.13 Alginate ester solubility in water	192
5.3.14 Nar calibration curves	193
5.3.15 Measurement of % drug loading.....	193
5.3.16 Nar release studies	193
5.4 Results and Discussion	194
5.5 Conclusion	209
5.6 Supporting information.....	211
5.7 References.....	228
Chapter 6: Summary and Future Work.....	231
6.1 References.....	237

List of Figures

Figure 2.1: Bacterial alginate biosynthesis pathway ⁹	6
Figure 2.2: Schematic showing alginate extraction procedure from algae	8
Figure 2.3: Representative alginate structure: (a) chain conformation and (b) block distribution	9
Figure 2.4: Anomeric region in the ¹ H-NMR spectra of alginates containing varying M contents. Peak assignments as described by Grasdalen, H. ²⁷	10
Figure 2.5: Possible junction points in alginates. (a) GG/GG junctions, (b) MG/MG junctions, and (c) GG/MG junctions. ³⁰	12
Figure 2.6: Important parameters governing alginate derivatization	17
Figure 2.7: Viscosity of alginate acetate plotted against corresponding DS value (represented as ‘degree of acetylation’) ⁴⁶	19
Figure 2.8: Dependence of the modulus of rigidity (G) on DS (represented as "D.a.") in acetylated Ca-alginate gels ⁵³	24
Figure 2.9: Partial dissolution of TBA-alginate in DMSO (left) and complete dissolution in DMSO/TBAF (right) at a TBAF concentration of 1.1% (w/v). Alginate concentration in both vials was 15 mg/mL ²⁸	26
Figure 2.10: Shift in the SEC chromatograms to longer elution times for alginate acetates shown in Table 2.4, recorded over increasing reaction time ²⁸	29
Figure 2.11: (a) Viscosity vs. concentration (C) plot for PGA (empty squares) and PGA-C12 (half-filled squares) at a shear rate of 0.06 (1/s) and (b) Viscosity vs. NaCl concentration (Cs) plot for PGA (empty squares) and PGA-C12 (half-filled squares) at a fixed polymer concentration of 1.2 g/dL and shear rate of 0.06 (1/s) ⁶⁸	39
Figure 2.12: (a) Alg-C ₁₂ adsorption at the air water interface and (b) Alg-C ₁₂ +DTAB adsorption at the air water interface ⁷³	41

Figure 2.13: Schematic illustration of the encapsulation of the hydrophobic moieties on Alg-CONH-C ₈ by the β -CD truncated cone ⁷⁶	45
Figure 2.14: Schematic describing the synthesis of Amylose-g-Alg ¹³²	68
Figure 2.15: Schematic showing the temperature dependent behavior in PNIPAAm-g-Alg hydrogels ¹³³ ..	69
Figure 2.16: Schematic showing the effect of pH and ionic strength on PDMAEMA-g-OAlg hydrogels ¹³⁴	71
Figure 3.1: Partial dissolution of alginate M063 in DMSO (left) and complete dissolution in DMSO/TBAF (right) at a TBAF concentration of 1.1% (w/v). Alginate concentration in both vials was 15 mg/mL.....	99
Figure 3.2: ¹ H-NMR spectrum of alginate acetate synthesized from alginate M063	101
Figure 3.3: FTIR spectrum of alginate acetate synthesized from alginate M063	101
Figure 3.4: ¹ H-NMR spectrum of alginate acetate synthesized from alginate M100. Peak A represents H-3 from M residues monoacetylated at position 3. Peak B represents H-3 from M residues diacetylated at positions 2 and 3. Peaks A and B assigned according to previously published literature ⁴⁹	105
Figure 3.5: ¹ H-NMR spectra of homogeneously acetylated alginates from Table 3.3. Peak A represents H-3 from M residues monoacetylated at position 3. Peak B represents H-3 from M residues diacetylated at positions 2 and 3. Peaks A and B assigned according to previously published literature ⁴⁹	106
Figure 3.6: ¹ H-NMR spectra of heterogeneously acetylated alginates from Table 3.3. Peak A represents H-3 from M residues monoacetylated at position 3. Peak B represents H-3 from M residues diacetylated at positions 2 and 3. Peak C represents H-1 from unreacted GGG, MGG and GGM triad sequences. Peak D represents H-5 from unreacted GGG triad sequences. Peaks A, B, C and D were assigned according to previously published literature ⁴⁹⁻⁵⁰	108
Figure 3.7: Right-shift in the SEC chromatograms obtained using light scattering for the alginate acetates shown in Table 3.4, recorded over increasing reaction time.....	111
Figure 3.8: ¹ H-NMR of M063 TBA-alginate.....	112

Figure 3.9: FTIR of M063 TBA-alginate.....	113
Figure 3.10: ¹ H-NMR for product 2 shown in Table 3.4	113
Figure 3.11: FTIR for product 2 shown in Table 3.4	114
Figure 3.12: ¹ H-NMR for product 7 shown in Table 3.2	114
Figure 3.13: FTIR for product 7 shown in Table 3.2	115
Figure 3.14: ¹ H-NMR for product 8 shown in Table 3.2	115
Figure 3.15: FTIR for product 8 shown in Table 3.2	116
Figure 3.16: (a) ¹ H-NMR spectra and (b) DLS intensity plots for TBA-alginate partially dissolved in DMSO and completely dissolved in DMSO/TBAF. ¹ H-NMR spectra show integration of the DMSO-d ₆ solvent peak at 2.5 ppm against the polymer backbone region between 3.3-5.0 ppm.	117
Figure 4.1: ¹ H-NMR spectrum of alginate acetate A.P10.Ac20 from Table 4.2. HDO peak suppression used during acquisition	139
Figure 4.2: FTIR spectrum of alginate acetate A.P10.Ac20 from Table 4.2	140
Figure 4.3: ¹ H-NMR spectrum of alginate acetate A.P10.Ac20 from Table 4.2. HDO peak suppression carried out post acquisition using NMR processing software.....	141
Figure 4.4: Potentiometric titration [pH] plot for alginate acetate A.P10.Ac20 from Table 4.2	142
Figure 4.5: Potentiometric titration derivative [d(pH)] plot for alginate acetate A.P10.Ac20 from Table 4.2	143
Figure 4.6: SEC chromatograms of alginate acetates in Series I, II and III from Table 4.2	145
Figure 4.7: Microscopic images of capsules formed using alginate acetates from Table 4.2.....	147
Figure 4.8: Viscosity vs. shear rate plots for alginate acetates from Table 4.2 at various concentrations, measured at room temperature	150
Figure 4.9: SEC chromatograms of alginate acetates in Series IV from Table 4.2	151
Figure 4.10: (A) Osmotic and (B) mechanical stress effects, measured as % of broken microbeads. For osmotic stress test: 1.5% LVM vs. 5% A-Na, p < 0.001; 1.5% LVM vs. 5% A.P10.Ac2, no significant	

difference; 5% A-Na vs. 5% A.P10.Ac2, $p < 0.001$. For mechanical stress test: 1.5% LVM vs. 5% A-Na, no significant difference; 5% A-Na vs. 5% A.P10.Ac2, $p < 0.05$; 1.5% LVM vs. 5% A.P10.Ac2, $p < 0.05$.

.....	153
Figure 4.11: ^1H -NMR of TBA-alginate ‘A’	156
Figure 4.12: FTIR of TBA-alginate ‘A’	157
Figure 4.13: ^1H -NMR spectrum of alginate acetate A.P2.Ac20 from Table 4.2. HDO peak suppression pulse applied during acquisition	159
Figure 4.14: FTIR spectrum of alginate acetate A.P2.Ac20 from Table 4.2	160
Figure 4.15: ^1H -NMR spectrum of alginate acetate A.P2.Ac20 from Table 4.2. HDO peak suppression pulse applied during acquisition	161
Figure 4.16: FTIR spectrum of alginate acetate A.P2.Ac20 from Table 4.2	162
Figure 4.17: ^1H -NMR spectrum of alginate acetate A.P10.Ac2 from Table 4.2. HDO peak suppression pulse applied during acquisition	163
Figure 4.18: FTIR spectrum of alginate acetate A.P10.Ac2 from Table 4.2	164
Figure 4. 19: ^1H -NMR spectrum of alginate acetate A.P10.Ac5 from Table 4.2. HDO peak suppression pulse applied during acquisition	165
Figure 4.20: FTIR spectrum of alginate acetate A.P10.Ac5 from Table 4.2	166
Figure 4.21: ^1H -NMR spectrum of alginate acetate A.P10.Ac10 from Table 4.2. HDO peak suppression pulse applied during acquisition	167
Figure 4.22: FTIR spectrum of alginate acetate A.P10.Ac10 from Table 4.2	168
Figure 4.23: ^1H -NMR spectrum of alginate acetate B.P10.Ac10 from Table 4.2. HDO peak suppression pulse applied during acquisition	169
Figure 4.24: FTIR spectrum of alginate acetate B.P10.Ac10 from Table 4.2	170
Figure 4.25: ^1H -NMR spectrum of alginate acetate C.P10.Ac10 from Table 4.2. HDO peak suppression pulse applied during acquisition	171

Figure 4.26: FTIR spectrum of alginate acetate C.P10.Ac10 from Table 4.2	172
Figure 4.27: ^1H -NMR spectrum of alginate acetate D.P10.Ac10 from Table 4.2. HDO peak suppression pulse applied during acquisition	173
Figure 4.28: FTIR spectrum of alginate acetate D.P10.Ac10 from Table 4.2	174
Figure 5.1: ^1H and ^{13}C -NMR spectra of benzyl alginate with $\text{DS}_{\text{benzyl}} = 1.0$	197
Figure 5.2: FTIR spectrum of benzyl alginate with $\text{DS}_{\text{benzyl}} = 1.0$	198
Figure 5.3: ^1H -NMR spectra of benzyl alginate pre (top) and post hydrolysis (bottom)	200
Figure 5.4: Potentiometric titration [left] and d(pH) [right] plots for benzyl alginate	201
Figure 5.5: Stacked ^1H -NMR spectra of butyl alginates of varying M contents.....	202
Figure 5.6: Stacked ^{13}C -NMR spectra of butyl alginates of varying M contents	203
Figure 5.7: Nar release profiles studied at pH 1.2 (top) and pH 6.8 (bottom)	207
Figure 5.8: ^1H -NMR of TBA-alginate	212
Figure 5.9: FTIR of TBA-alginate	212
Figure 5.10: ^1H -NMR spectrum of benzyl alginate with DS 0.44 synthesized using BzBr	213
Figure 5.11: DQF-COSY spectrum of benzyl alginate M000	213
Figure 5.12: HMQC spectrum of benzyl alginate M000	214
Figure 5.13: DQF-COSY spectrum of benzyl alginate M060	215
Figure 5.14: HMQC spectrum of benzyl alginate M060	216
Figure 5.15: DQF-COSY spectrum of benzyl alginate M063	217
Figure 5.16: HMBC spectrum of benzyl alginate M063.....	218
Figure 5.17: DQF-COSY spectrum of benzyl alginate M100	219
Figure 5.18: HMQC spectrum of benzyl alginate M100	220
Figure 5.19: ^1H and ^{13}C -NMR of methyl alginate	221
Figure 5.20: FTIR of methyl alginate	222

Figure 5.21: ^1H and ^{13}C -NMR of ethyl alginate.....	223
Figure 5.22: FTIR of ethyl alginate	224
Figure 5.23: ^1H and ^{13}C -NMR of butyl alginate	225
Figure 5.24: FTIR of butyl alginate	226
Figure 5.25: ^1H -NMR of partially esterified alginates acquired in D_2O	227
Figure 5.26: Nar calibration curves obtained in pH 1.2 (left) and pH 6.8 (right) buffer	227
Figure 6.1: Proposed routes to synthesis of alginate acetoacetates.....	235
Figure 6.2: ^1H -NMR of alginate acetoacetate	236

List of Schemes

Scheme 2.1: Acid-catalyzed hydrolytic degradation of alginates	14
Scheme 2.2: Alkaline degradation of alginates by β -elimination	15
Scheme 2.3: Acetylation of alginate using pyridine/acetic anhydride. For acetylation in gel form, $M = Ca^{+2}$ and $M = Na^{+}$. ⁵² For homogeneous acetylation in DMSO/TBAF, $M = TBA^{+}$ and $M'' = -H$ or Na^{+} . ²⁸	22
Scheme 2.4: Phosphorylation of alginate ⁵⁶	30
Scheme 2.5: (a) Alginate sulfation using chlorosulfonic acid and (b) quaternization of alginate sulfate using 2,3-epoxypropyl trimethylammonium chloride.....	32
Scheme 2.6: Sulfation of alginates using DCC-sulfuric acid route ⁶⁰	33
Scheme 2.7: Sulfation of alginates using sodium bisulfite-sodium nitrite reagents ⁶¹	35
Scheme 2.8: Synthesis of BzIO-TEG-NH-Alg by periodate oxidation of sodium alginate followed by reductive amination using BzIO-TEG-NH ₂	36
Scheme 2.9: Synthesis of alginate amides by reaction of propylene glycol esters of alginate with dodecylamine	38
Scheme 2.10: Reaction scheme for the synthesis of Alg-C ₁₂	40
Scheme 2.11: Reaction scheme for the synthesis of Alg-CONH-C ₈	43
Scheme 2.12: Mechanism of carbodiimide mediated coupling of carboxylic acids to amines.....	44
Scheme 2.13: Reaction scheme for the synthesis of galactose substituted alginate	47
Scheme 2.14: Reaction scheme for the synthesis of galactosylated alginate (GA) using lactobionic lactone	52
Scheme 2.15: Reaction scheme for the synthesis of GRGDY containing alginates	53
Scheme 2.16: Mechanism for alginate crosslinking using epichlorohydrin	55

Scheme 2.17: (a) mechanism of acid catalyzed acetalization of vicinal hydroxyl groups, (b) reaction scheme for covalent crosslinking of Na-alginate using glutaraldehyde.....	57
Scheme 2.18: (a) mechanism for the synthesis of alginate amide derivative using CMPI activating agent, and (b) alginate crosslinking reaction using bifunctional amine reagent.....	61
Scheme 2.19: Sodium alginate crosslinking using adipic dihydrazide via reaction with PAG	63
Scheme 2.20: Synthesis of PDMAEMA-g-OAlg	70
Scheme 3.1: Acetylation of TBA-alginate.....	100
Scheme 5.1: General reaction scheme for esterification of alginates using alkyl halides	196
Scheme 5.2: Postulated side reaction of DMSO with benzyl bromide leading to the formation of benzyldimethyloxosulfonium salts of alginate	199
Scheme 6.1: Suggested route for acylation of benzyl alginate and subsequent hydrogenation to remove benzyl groups	233

List of Tables

Table 2.1: Solubility of alginates in various solvents at a concentration of 15 mg/mL.....	11
Table 2.2: Relative acetyl substitution ratios on M and G residues for alginates ⁵²	23
Table 2.3: Homogeneous and heterogeneous acetylation of alginates and the corresponding DS values..	27
Table 2.4: Molecular weight degradation of TBA-alginate during acetylation	28
Table 2.5: Substitution selectivity for alginates at various DS values, measured using ¹ H-NMR spectroscopy ⁸⁰	48
Table 2.6: Monomer and dyad compositions of galactosylated polymannuronan derivatives after epimerization ⁸²	50
Table 3.1: Solubility of alginates in various solvents at a concentration of 15 mg/mL.....	96
Table 3.2: Acylation of alginates and the corresponding DS values	103
Table 3.3: Homogeneous and heterogeneous acetylation of alginates and the corresponding DS values	104
Table 3.4: Molecular weight degradation of TBA-alginate during acetylation	110
Table 3.5: Experimental and theoretically calculated % elemental compositions of alginate acetates shown in Table 3.4	116
Table 4.1: Molecular weights, PDI, DP _n and M/G compositions of alginates A-D used in the study	136
Table 4.2: Molar ratios used for acetylation, DS values as measured by titration, and aqueous SEC results for corresponding products	137
Table 4.3: Viscosities of alginate acetates from Table 4.2 at various concentrations.....	149
Table 4.4: Osmotic and mechanical stress effects, measured as % of broken microbeads.....	153
Table 4.5: Elemental compositions and percent salt contents of TBA-alginates A-D.....	158
Table 4.6: Percent TBA contents of alginate acetates, corresponding average repeat unit molar masses and DS values, as measured by ¹ H-NMR and titration.....	158
Table 5.1: Comparison of DS _{benzyl} values measured using ¹ H NMR and titration	201

Table 5.2: Alginate esters, their DS values and corresponding solubility properties	204
Table 5.3: SD compositions, along with theoretical and actual drug loading.....	206
Table 5.4: Maximum percent Nar released and solubility enhancement factors for the SDs studied.....	209
Table 5.5: ^1H and ^{13}C -NMR peak shifts in butyl alginates	220

Chapter 1: Dissertation Overview

Alginate is an important commercial polysaccharide that is widely used in the food, textile and paper industries, and is having a growing impact in the biomedical applications area. The biosynthetic pathways used by nature to make alginates afford tremendous variability in their size, structure and function. Furthermore, identification of the genes involved in biosynthesis and isolation of various enzymes has enabled in vitro control over these parameters. However, the idea of being able to dissolve alginates in organic media to perform modifications has not been explored to its full potential. We believe that alginate derivatization in organic media, if made possible, could be coupled with the biochemical advancements to open up new and high impact areas of applications. The primary goal of this dissertation is therefore to study the organic dissolution of alginates followed by their derivatization in the solvents to make novel functional biomacromolecules.

A brief overview of this dissertation can be expressed as follows. In Chapter 2, a detailed literature review of alginate derivatization will be presented. In Chapter 3, we will examine results from basic dissolution studies, which prove that the tetrabutylammonium (TBA) salts of alginate can be made soluble in two component polar aprotic solvent systems such as DMSO/TBAF. Based on these studies, we will then describe methods to acetylate alginates in both random and M-selective fashions by –OH group modification. This will be followed by Chapter 4, wherein we will show that Ca-crosslinking of M-selective alginate acetates is possible to prepare tailored hydrogel beads. The effect of acetylation reaction conditions on the degree of substitution (DS) and molecular weight (MW) will be discussed, and conditions that are most suitable to form stable crosslinked beads will be identified. In Chapter 5, we will describe

methods to synthesize alginate esters via -COOH group modification. Using $\text{S}_{\text{N}}2$ substitution reactions in the presence of alkyl halides, alginate derivatives that are capable of dissolution in single component polar aprotic solvents can be prepared. The use of these derivatives in enhancing aqueous solubility of poorly soluble flavonoids, such as naringenin will be reported. Finally, in Chapter 6, we will provide closing arguments with a summary and future work discussion.

Chapter 2: Literature Review on the Derivatization of Alginates

(Used with permission of Elsevier: *Pawar S.N., Edgar K.J. Biomaterials 2012; 33(11), 3279-3305*)

2.1 Abstract

Alginates have become an extremely important family of polysaccharides because of their utility in preparing hydrogels at mild pH and temperature conditions, suitable for the encapsulation of sensitive biomolecules like proteins and nucleic acids, and even for living cells such as islets of Langerhans. In addition, the complex monosaccharide sequences of alginates, and our growing ability to create controlled sequences by the action of isolated epimerases upon the alginate precursor poly(mannuronic acid), create remarkable opportunities for understanding the relationship of properties to sequence in natural alginates (control of monosaccharide sequence being perhaps the greatest synthetic challenge in polysaccharide chemistry). There is however a trend in recent years to create “value-added” alginates, by performing derivatization reactions on the polysaccharide backbone. For example, chemical derivatization may enable alginates to achieve enhanced hydroxyapatite (HAP) nucleation and growth, heparin-like anticoagulation properties, improved cell-surface interactions, degradability, or tuning of the hydrophobic-hydrophilic balance for optimum drug release. The creation of synthetic derivatives therefore has the potential to empower the next generation of applications for alginates. Herein we review progress towards controlled synthesis of alginate derivatives, and the properties and applications of these derivatives.

2.2 Introduction

Alginates are unbranched polysaccharides consisting of 1→4 linked β -D-mannuronic acid (M) and its C-5 epimer α -L-guluronic acid (G). The natural copolymer is an important component of algae such as kelp, and is also an exopolysaccharide of bacteria including *Pseudomonas aeruginosa*. It is comprised of sequences of M (M-blocks) and G (G-blocks) residues interspersed with MG sequences (MG-blocks). While it is possible to obtain alginates from both algal and bacterial sources, commercially available alginates currently come only from algae. The copolymer composition, sequence and molecular weights vary with the source and species that produce the copolymer. Due to the abundance of algae in water bodies, there is a large amount of alginate material present in nature. Industrial alginate production is approximately 30,000 metric tons annually, and is estimated to comprise less than 10% of the bio-synthesized alginate material.¹ Therefore there is significant additional potential to design sustainable biomaterials based on alginates. The combination of chemical and biochemical techniques provide considerable potential for creating modified alginic acid derivatives with control over monosaccharide sequence and nature, location and quantity of substituents. This in turn enables the tailoring of alginate derivative properties such as solubility, hydrophobicity, affinity for specific proteins, and many others. Such modifications are complicated by key alginic acid properties including solubility, pH sensitivity, and complexity (which can make both synthetic control and analysis difficult). Both the promise and the difficulty of alginate modification have attracted much effort towards controlled derivatization.

The significance of alginates as natural polysaccharides in biomedicine can hardly be overstated. Alginates are currently used as wound dressing materials for the treatment of acute or chronic wounds.² They also play a crucial part in the progression of cystic fibrosis, wherein

bacterial biofilms formed from alginate gels are secreted by *Pseudomonas aeruginosa*.³ More importantly, use of alginate crosslinking to make hydrogels for cell encapsulation has proved to be most advantageous for biomedical applications.⁴⁻⁶ Worthy of mention is the role played by alginates gels in encapsulating islets of Langerhans for diabetes treatment.⁷ Chemical modification of alginates is used as a tool to attain one of two ends – (A) enhance existing properties (example: improvement of ionic gel strength by additional covalent crosslinking, increase hydrophobicity of the backbone, improve biodegradation, or achieve greater HAP nucleation and growth), or (B) introduce completely new properties otherwise not existing in unmodified alginates (example: afford anticoagulant properties, provide chemical/biochemical anchors to interact with cell surfaces or bestow temperature dependent characteristics such as lower critical solution temperature). In short, alginate derivatization is the most convenient way to achieve both inherent property enhancement and new property introduction. We herein review the chemical routes to such modifications, and the resulting properties achieved.

2.3 Description of alginates

2.3.1 Biosynthesis

Recent progress in biosynthesis of bacterial alginates has been reviewed in several excellent articles.⁸⁻¹¹ Alginate biosynthesis (**Figure 2.1**) involves the oxidation of a carbon source to acetyl-CoA, which enters the TCA cycle to be converted to fructose-6-phosphate *via* gluconeogenesis. Fructose-6-phosphate then undergoes a series of biosynthetic transformations to be eventually converted to GDP-mannuronic acid, which acts as a precursor to alginate synthesis. In general, the biosynthetic operation can be broken down into four stages: (1) GDP-mannuronic acid precursor synthesis; (2) cytoplasmic membrane transfer and polymerization to

polymannuronic acid; (3) periplasmic transfer and modification; and (4) export through the outer membrane. Post-polymerization modification of alginates occurs at stage (3), where polymannuronic acid is acetylated at the O-2 and/or O-3 positions by several transacetylases.¹²⁻¹⁴. Epimerization is then performed by a family of epimerase enzymes to convert some non-acetylated M residues to G residues.¹⁴⁻¹⁷. Finally, alginate is released from the cell through transmembrane porins.

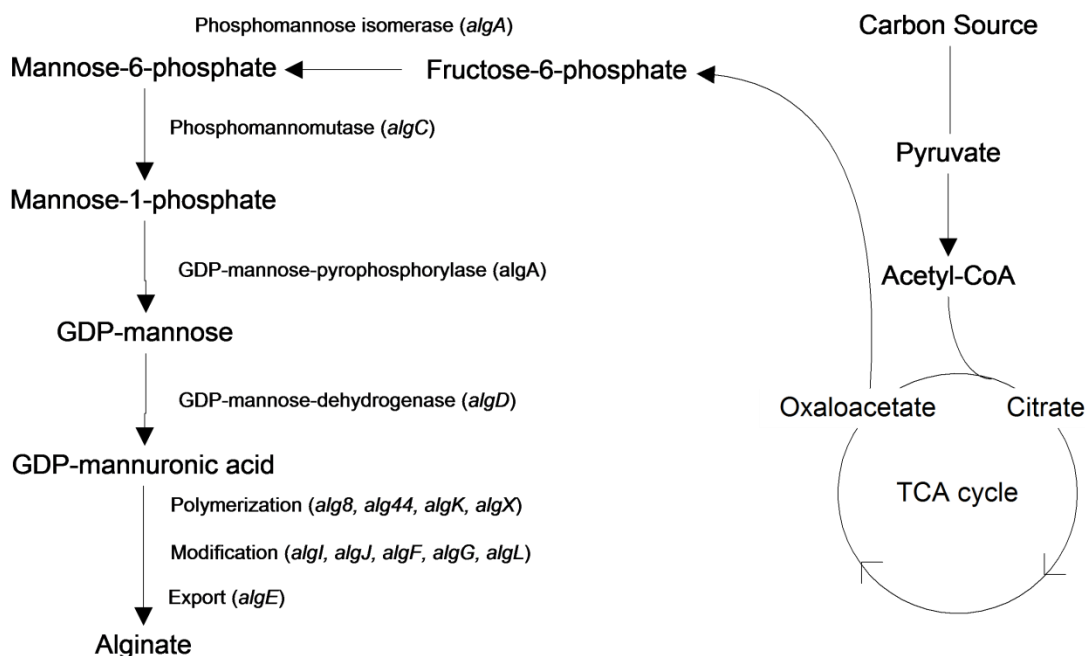


Figure 2.1: Bacterial alginate biosynthesis pathway⁹

2.3.2 Manufacture

Current commercial production of alginates is based entirely on algal sources, with upto 30,000 metric tons produced annually. Alginates occur in brown algae in the intracellular matrix as gels containing sodium, calcium, magnesium, strontium and barium ions, such that the counterion composition is determined by the ion-exchange equilibrium with sea water. A

schematic of the alginate extraction procedure is represented in **Figure 2.2**. The first step in the extraction process is removal of the counterions by proton exchange using 0.1-0.2 M mineral acid. In the second step, insoluble alginic acid is solubilized by neutralization with alkali such as sodium carbonate or sodium hydroxide to form sodium alginate. Rigorous separation processes such as sifting, flotation, centrifugation and filtration follow in order to remove particulate matter. Sodium alginate is then precipitated directly by alcohol, calcium chloride or a mineral acid. The product is dried and milled. Alginates obtained using the described procedure contains several mitogens (agents that induce cell mitosis) and cytotoxic impurities making them unsuitable for biomedical applications. Ultrapure, amitogenic and biocompatible alginates which are suitable for biomedical purposes have therefore been prepared using more rigorous extraction processes. Free flow electrophoresis was applied as one technique to remove mitogenic impurities from commercial alginates.¹⁸ This method was however not suitable for large scale processing because it was time consuming and required expensive electrophoresis equipment. A chemical extraction method was therefore described using Ba-alginate gels.¹⁹ Ba⁺² ions show higher affinity towards alginates compared to Ca⁺² ions. Ba-alginate gels are therefore stable in acidic and neutral pH environments, but disintegrate under alkaline pH conditions. Mitogenic contaminants were first eluted from Ba-alginate beads by treatment with various solutions followed by ethanol extraction, after which the pure alginate beads were dissolved in alkaline solutions. Finally the solution was dialyzed, Ba⁺² exchanged for Na⁺ ions and pure, biocompatible alginate precipitated from ethanol.

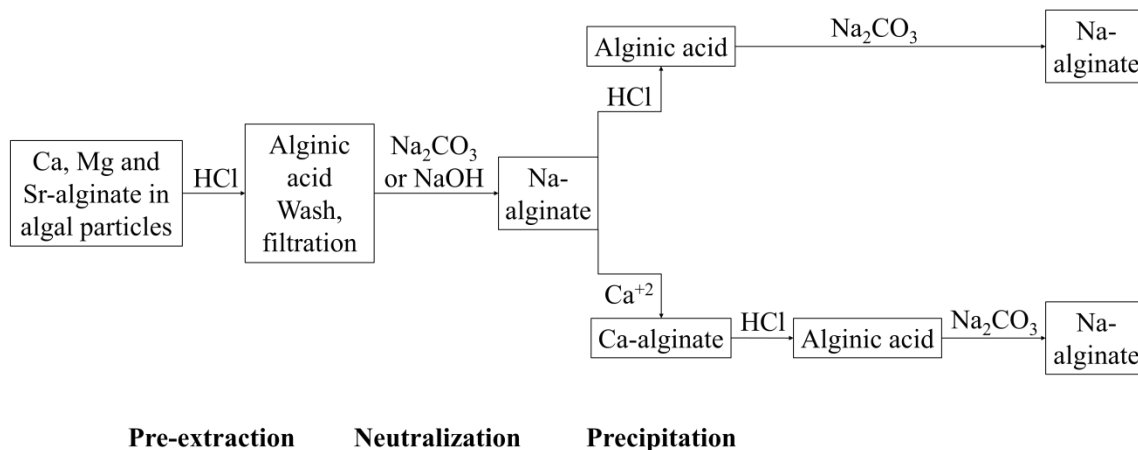


Figure 2.2: Schematic showing alginate extraction procedure from algae

2.3.3 Structure determination

The first report on the chemical structure of alginates appeared as early as 1966. Larsen et al. described in detail the partial hydrolysis of alginates followed by fractionation to obtain alginates containing different copolymer compositions.²⁰ Fractionation yielded a soluble (hydrolysable) fraction and an insoluble (resistant) fraction. The resistant fractions consisted of molecules which had either mainly M rich or mainly G rich residues, while the hydrolysable fractions consisted of a high proportion of alternating MG residues. A structure was therefore proposed which consisted of M-blocks, G-blocks, and hydrolysable MG alternating blocks. A representative structure of the alginate backbone is shown in **Figure 2.3** where (a) shows the chain conformation and (b) shows the typical block distribution. Larsen et al. later employed free boundary electrophoresis to examine the hydrolysis products isolated by fractionation.²¹ The results confirmed the presence of M-blocks, G-blocks and alternating MG blocks. Computer driven mathematical models were also used in understanding the alginate microstructure.²²⁻²⁴ The

clearest understanding of alginate backbone structure was however achieved only using ^1H and ^{13}C -NMR spectroscopy.

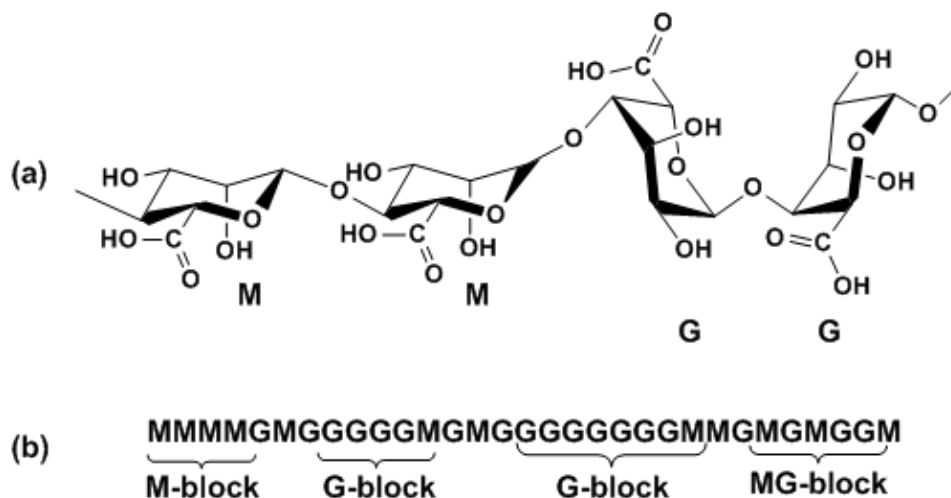


Figure 2.3: Representative alginate structure: (a) chain conformation and (b) block distribution

Penman et al. described a method for the determination of M/G ratio in alginates using peak ratios obtained from the ^1H -NMR spectrum.²⁵ Grasdalen et al. later showed that ^1H -NMR can also yield fractions of the four dyads MM, MG, GM and GG.²⁶ **Figure 2.4** shows the anomeric region in the ^1H -NMR spectra of alginates with varying M contents. The monomer and dyad fractions were obtained using the following equations, where I_A , I_B and I_C are the intensities of the three peaks labeled A, B and C respectively.

$$F_G = \frac{I_A}{I_B + I_C} \quad F_{GG} = \frac{I_C}{I_B + I_C} \quad F_{GG} + F_{GM} = F_G \quad F_{MM} + F_{MG} = F_{MG}$$

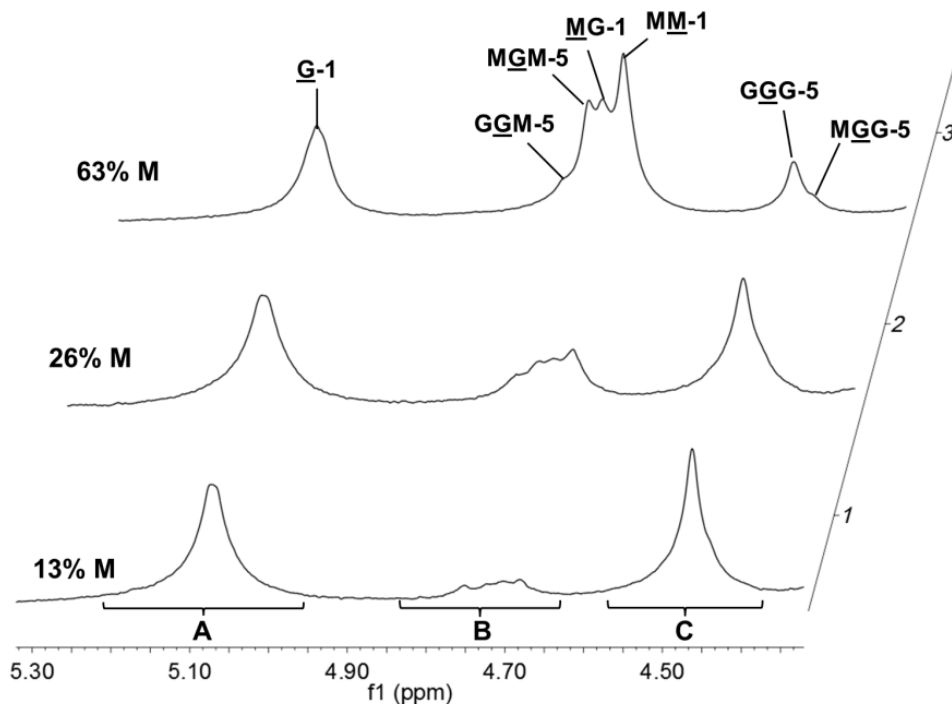


Figure 2.4: Anomeric region in the ^1H -NMR spectra of alginates containing varying M contents. Peak assignments as described by Grasdalen, H.²⁷

2.3.4 Physical properties

2.3.4.1 Solubility

The solubility of alginates in water is governed by four parameters – a) pH of the solvent, b) ionic strength of the medium, c) presence of gelling ions in the solvent, and d) molecular weight. To make alginates soluble it is essential that the pH be above a certain critical value and the carboxylic acid groups be deprotonated. Changing the ionic strength of the medium affects solution properties such as polymer conformation, chain extension, viscosity and therefore solubility. Alginates gel in the presence of divalent cations such as Ca^{+2} , Sr^{+2} and Ba^{+2} . It is therefore necessary to have an aqueous solvent free of crosslinking ions to enable dissolution. The solubility of alginates in organic media requires formation of a tetrabutylammonium (TBA)

salt. We recently reported the complete dissolution of TBA-alginate in polar aprotic solvents containing tetrabutylammonium fluoride (TBAF).²⁸ The solubility of alginates depends strongly on the state of the backbone carboxylic acid groups. Alginic acid with its carboxylic acid groups in their protonated form was not fully soluble in any solvent system examined, including water. Na-alginate dissolved in water, but was not entirely soluble in any organic medium examined. TBA-alginate was completely soluble in water, ethylene glycol and polar aprotic solvents containing TBAF, but did not dissolve in any other solvent systems under consideration. **Table 2.1** shows the results of a detailed solubility study.²⁸

Table 2.1: Solubility of alginates in various solvents at a concentration of 15 mg/mL

	H ₂ O	EG	DMAc	DMF	DMSO	DMAc/ LiCl	DMF/ TBAF	DMSO/ TBAF	DMAc/ TBAF	DMI/ TBAF
Alginic acid	-	-	-	-	-	-	-	-	-	-
Na-alginate	+	-	-	-	-	-	-	-	-	-
TBA-alginate	+	+	-	-	-	-	+	+	+	+

(+) complete solubility and (-) partial or no solubility; EG = ethylene glycol

2.3.4.2 Ionic crosslinking

Alginate chelates with divalent cations to form hydrogels. Gel formation is driven by the interactions between G-blocks which associate to form tightly held junctions in the presence of divalent cations.²⁹ In addition to G-blocks, MG-blocks also participate, forming weak junctions.³⁰ Thus, *alginates with high G contents yield stronger gels*. The affinity of alginates towards divalent ions decreases in the following order: Pb > Cu > Cd > Ba > Sr > Ca > Co, Ni, Zn > Mn.³¹ Ca²⁺, however, is the most commonly used cation to induce alginate gel formation. A

pictorial representation of the three junction types possible in Ca-alginate gels is shown in **Figure 2.5**.

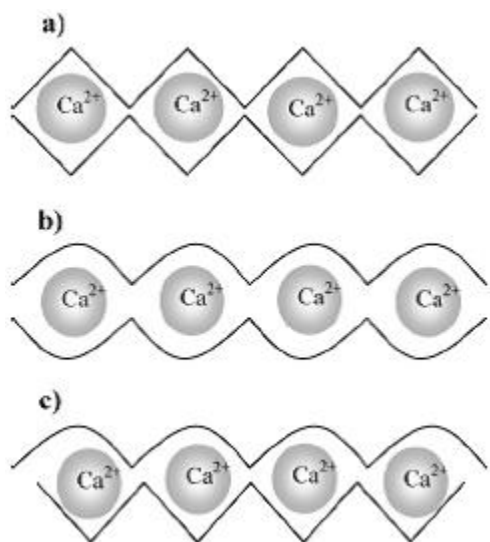


Figure 2.5: Possible junction points in alginates. (a) GG/GG junctions, (b) MG/MG junctions, and (c) GG/MG junctions.³⁰

Calcium crosslinking of alginates can be performed by two methods. The first is a “diffusion” method, wherein crosslinking ions diffuse into the alginate solution from an outside reservoir. The second is the “internal setting” method, where the ion source is located within the alginate solution and a controlled trigger (typically pH or solubility of the ion source) sets off the release of crosslinking ions into solution. The diffusion method yields gels having a Ca^{+2} ion concentration gradient across the thickness, while internal setting gives gels with uniform ion concentrations throughout.³² Diffusion set gels are typically made by dropping a Na-alginate solution into a CaCl_2 bath. Internal set gels typically use insoluble calcium salts such as CaCO_3 as a calcium source. A change in the pH caused by a slowly hydrolyzing lactone such as D-glucono- δ -lactone (GDL) triggers the release of Ca^{+2} ions internally and leads to gel formation.

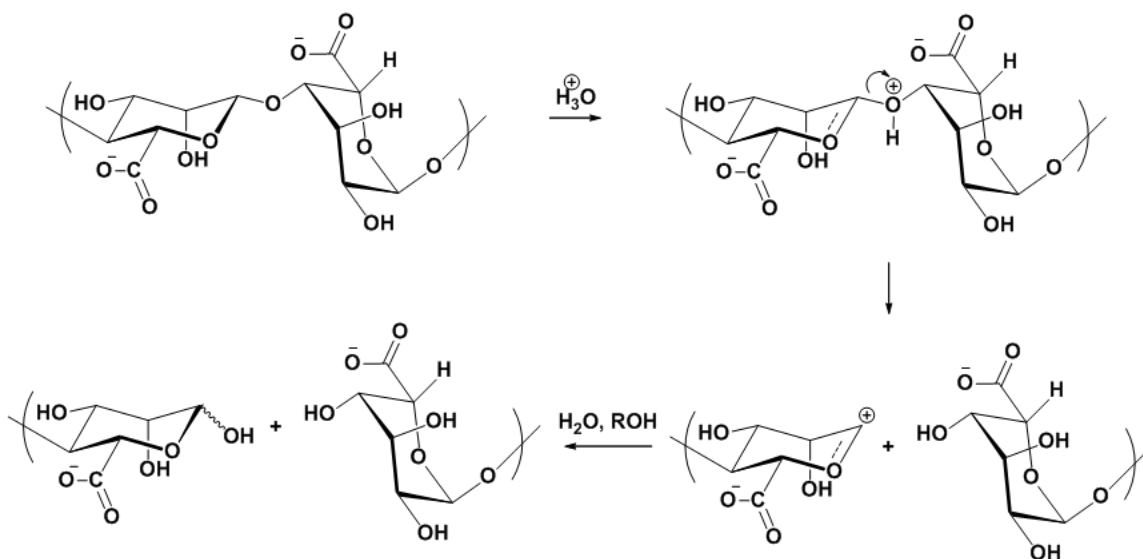
The encapsulation of cells within alginate gels is a preferred technique for immunoprotection and has been reviewed in several publications.⁴⁻⁶

2.3.4.3 Alginic acid gels

When the pH of alginate solutions is lowered below the pK_a of the uronic acids in a highly controlled fashion, acid gels are formed. Such gels are stabilized by an intermolecular hydrogen bonding network. Two methods are generally used to make acid gels.³³ In the first method, a slowly hydrolyzing lactone such as GDL is added to a solution of Na-alginate. In the second method, pre-formed Ca-alginate gels are converted to acid gels by proton exchange.

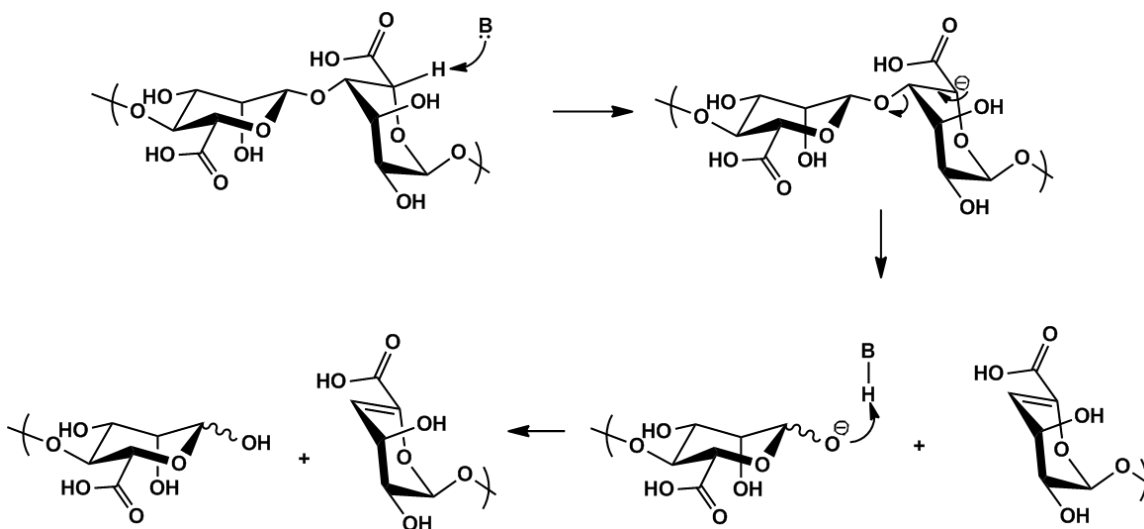
2.3.5 Chemical properties

Polysaccharides undergo hydrolytic cleavage under acidic conditions. The mechanism of acid hydrolysis of the glycosidic bond has been described by Timell.³⁴ It involves three steps: (1) protonation of the glycosidic oxygen to give the conjugate acid; (2) heterolysis of the conjugate acid forming a non-reducing end group and a carbonium-oxonium ion; and (3) rapid addition of water to the carbonium-oxonium ion, forming a reducing end group. The acid hydrolysis mechanism for alginates is illustrated in **Scheme 2.1**. Sodium alginate in the form of dry powder can be stored without degradation in a cool, dry place and away from sunlight for several months. The shelf life can be extended to several years by storing it in the freezer. Alginic acid degrades more rapidly than the sodium salt form. The reason for this enhanced degradation rate is thought to be intramolecular catalysis by the C-5 carboxyl groups.³⁵



Scheme 2.1: Acid-catalyzed hydrolytic degradation of alginates

The enzymatic degradation of alginates by lyase occurs by a β -elimination mechanism resulting in unsaturated compounds (**Scheme 2.2**).³⁶⁻³⁷ A similar degradation route is followed when they are subjected to strongly alkaline environments. The rate of degradation increases rapidly above pH 10.0 and below pH 5.0. Above a pH of 10.0, the degradation arises mostly from the β -elimination mechanism, while below 5.0 the degradation is mostly due to acid catalyzed hydrolysis.³⁸ The mechanism of β -elimination involves abstraction of the proton at C-5 position, which is enhanced by the electron-withdrawing effect of the carbonyl group at C-6 position. When the C-6 carboxyl group is ionized, the electron-withdrawing effect is moderated and abstraction of the C-5 proton is not as facile as when the carboxyl group is protonated.³⁹ However, the rate of abstraction is still sufficiently high to cause relatively rapid degradation at high pH.



Scheme 2.2: Alkaline degradation of alginates by β -elimination

Alginates are susceptible to chain degradation not only in the presence of acids or bases, but also at neutral pH values in the presence of reducing compounds. Alginates derived from brown algae contain varying amounts of phenolic compounds, depending on the algal species.⁴⁰ The rate of degradation in species containing a higher quantity of phenolics was shown to be much greater.⁴¹ A number of reducing compounds such as hydroquinone, sodium sulfite, sodium hydrogen sulfide, cysteine, ascorbic acid, hydrazine sulfate and leuco-methylene blue also caused degradation in alginates. The mechanism of degradation involves the formation of a peroxide leading to free radical creation, which eventually causes breakdown of the alginate chain.⁴² In addition, sterilization techniques such as heat treatment, autoclaving, ethylene oxide treatment and γ -irradiation cause alginate degradation.⁴³ In short, degradation is an important concern when subjecting alginates to various modification reactions. ***The chemistry and reaction conditions employed must therefore be chosen carefully*** so that rapid molecular weight loss does not occur during the synthesis of alginate derivatives.

2.4 Alginate modification

The derivatization and design strategies for alginates depend on three important parameters: solubility, reactivity and characterization (**Figure 2.6**). (A) **Solubility**: alginates may be dissolved in aqueous, organic or mixed aqueous-organic media for derivatization. The choice of solvent system can dictate the type of reagents that may be used for modification. In addition, the degree of alginate solubility in the solvent system can impact derivative substitution pattern. (B) **Reactivity**: alginates can be modified at the two secondary –OH positions (C-2 and C-3) or the one –COOH (C-6) position. The difference in reactivity between the two functional group types can be easily used to selectively modify either one of the two types. Selective modification of either the C-2 or C-3 hydroxyl group is challenging due to their minor reactivity differences. In addition, the reaction may be controlled in terms of selective modification of M or G residues. This may be achieved by taking advantage of the selective chelation of G-residues in Ca-alginate gels, or by using the partial solubility properties of alginates in certain solvent systems. More importantly, the reactivity of alginates towards acids, bases and reducing agents cannot be overlooked when performing derivatization reactions. Competitive degradation reactions can cause rapid molecular weight loss in short time periods. (C) **Characterization**: in order to understand the substitution patterns obtained for the alginate derivatives, it is often essential to have multiple alginate samples with a range of M/G ratios. In addition, derivatization of alginates enriched in M, G or MG blocks may be required to achieve a detailed understanding of the substitution patterns. A lack of commercial availability of alginates with controlled sequences may impede complete structural characterization of the derivatives. Due to the complex nature of the alginate copolysaccharide backbone, use of advanced analytical techniques is often necessary.

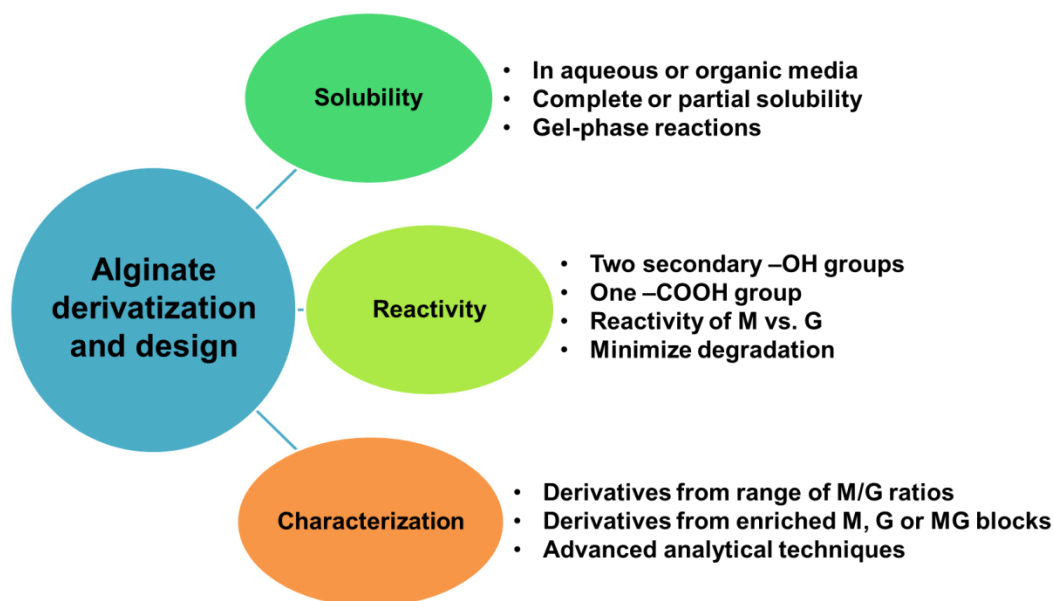


Figure 2.6: Important parameters governing alginate derivatization

In view of the aspects of alginate derivatization just described, we herein review the progress made in modification of these useful polysaccharides. We highlight important chemistries that have been reported in the literature to date, and discuss the properties attained and applications envisioned for the synthesized derivatives. Our goal is to present a clear and complete picture of the available methods for alginate modification, enabling the creation of successful strategies for synthesis of target alginate derivatives, and pointing out the areas where synthetic advances are still needed, through a solid understanding of the chemistry of this important polysaccharide.

2.4.1 Acetylation of alginates

Alginates as biosynthesized by bacteria are partially acetylated.¹²⁻¹⁴ The acetylation patterns govern both biosynthesis (by preventing epimerization of acetylated monosaccharides)

and biological functions of bacterial alginates. In vitro acetylation of alginates is therefore valuable to the understanding of structure-property relationships of bacterial alginates. The earliest known report addressing the chemical modification of alginates was published by Chamberlain et al., wherein acetylation of the hydroxyl groups of alginic acid was described.⁴⁴ The hydroxyl groups present in alginic acid yarn could not be reacted with acetic anhydride in the dry state due to strong H-bonding. However when swollen with water, the hydroxyl groups were available for reaction. Following the swelling process, solvent exchange was performed to replace water with glacial acetic acid. The alginic acid yarn swollen with glacial acetic acid was subjected to a mixture consisting of benzene, acetic anhydride and sulfuric acid catalyst. The yarn acetylated in this manner yielded alginic acid with 97.3% di-acetate, as determined from the total acetyl content. However, severe degradation was reported to occur during the reaction.

Wassermann reported the acetylation of alginic acid using ketene, a gaseous reagent.⁴⁴⁻⁴⁵ The reactive small molecule ketene was used as an acetylating agent, probably in order to avoid the alginate degradation caused by exposure to acetic acid or anhydride, and catalysts such as pyridine or strong acids. Acetylation was performed by swelling alginic acid fully in acetone, and then reacting with ketene at room temperature to form alginic acid acetate. The product was insoluble in water as well as in common organic solvents. Alginic acid acetate was converted to its Na- or Ca-salt forms by treatment with sodium or calcium hydroxide solutions respectively. Alternatively, Na- or Ca-alginate was directly reacted with ketene to form Na- or Ca-alginate acetates. Approximately one acetyl group was introduced per monosaccharide unit of the alginate chain, as determined by a titration method. Degradation during acetylation was assessed using viscosity measurements. While Na-alginate acetate and alginic acid acetate showed lower viscosities due to more rapid molecular weight loss, Ca-alginate acetate did not degrade to a very

large extent. Regioselectivity of the reaction and composition of the products were not reported, most likely due to the limited analytical methods available at that time.

Schweiger reported the synthesis of both partially and fully acetylated alginic acid derivatives using an acid catalyzed esterification technique.⁴⁶⁻⁴⁷ The reaction was performed by suspending alginic acid in a mixture of acetic acid and acetic anhydride containing perchloric acid. Products with DS values up to 1.85 were achieved at moderate temperatures without significant degradation. While $DS > 1.85$ was possible using higher temperatures, these conditions also led to significant molecular weight loss. Corroborating the phenomenon reported by Chamberlain et al.⁴⁴, the presence of water was essential to the availability of hydroxyl groups for acetylation. Strong H-bonds present in the dehydrated state prevented the hydroxyl groups from reacting. The viscosities of alginate acetates plotted against their corresponding DS values are shown in **Figure 2.7**.

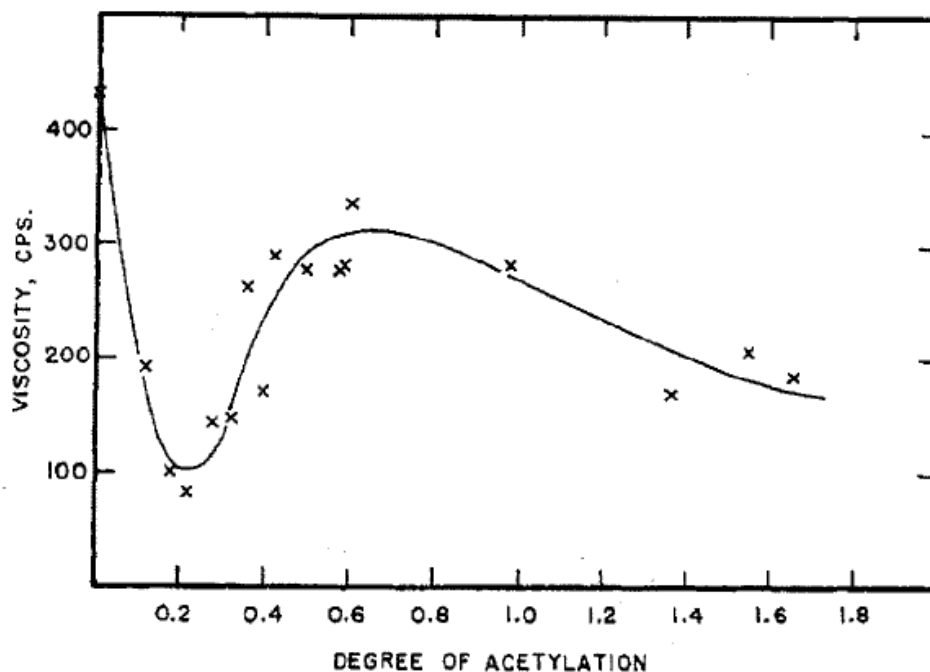


Figure 2.7: Viscosity of alginate acetate plotted against corresponding DS value (represented as ‘degree of acetylation’)⁴⁶

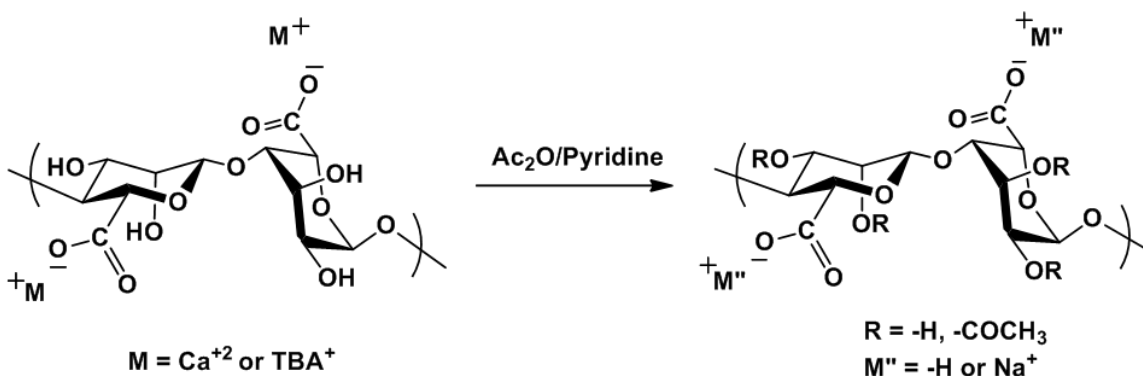
A hypothesis was presented based on the assumption that an increase in the solution viscosity is caused by the presence of free, unsubstituted and non-hydrogen bonded hydroxyl groups owing to their ability to associate with water molecules. A decrease in the solution viscosity on the other hand results from either (a) acid hydrolysis or (b) substitution of the free hydroxyls with acetyl groups. The initial decrease in viscosity up to DS ~ 0.2 is evident in **Figure 9**, and was attributed to a combined effect of (a) and (b). However, as the reaction progressed, H-bonding between the vicinal hydroxyl groups was overcome and an alginate monoacetate product was formed. An increase in the total number of free hydroxyl groups occurred as a result of more vicinal H-bonds being cleaved, resulting in a spike in the solution viscosity. A viscosity maximum was reached at DS ~ 0.7 . Beyond this maximum, the monoacetate sugars were acetylated further to form diacetates. This led to a reduction in the number of free hydroxyls and a corresponding decrease in viscosity. The presence of vicinal H-bonds was therefore thought to be an important factor causing alginate hydroxyl groups to have low reactivity. However, the hydroxyl group reactivity in monoacetylated alginate products was higher compared to unreacted alginates. This phenomenon was substantiated by kinetic data which indicated to a rapid increase in the reaction rate at DS values between 0.7-1.5. The increase in the reaction rate was associated with increasing availability of non H-bonded hydroxyl groups for acetyl substitution.

The partially and fully acetylated alginates were used as tools to enhance understanding of the chelate structure formed in ionically crosslinked alginate gels.⁴⁷ The addition of divalent ions to a solution of alginate diacetate (DS = 2.0) did not lead to gel formation. Furthermore, alginates with DS = 1.4 which contained monoacetylated and diacetylated, but no non-acetylated

saccharide residues resisted gel formation. This suggested that the presence of non-acetylated saccharide units was a must for chelate formation. It also indicated that the presence of hydroxyl groups was essential for ionic crosslinking, and that carboxylate anions were only partially responsible for gelation. Therefore, based on the data acquired a chelate structure was proposed wherein a single Ca^{+2} ion co-ordinated with two carboxylate groups and two vicinal hydroxyl groups belonging to the same sugar to form a gel. This proposed chelate structure was further supported by the fact that the tendency towards gelation was shown to be greater for alginates containing a higher fraction of unreacted uronic acid sugar residues.

While the early efforts to acetylate alginate were successful, they were limited in terms of structural characterization of the synthesized derivatives. These investigators were hampered by a lack of detailed knowledge about the composition and sequence of the alginate backbone, which was not achieved until a series of fundamental papers published in the 1960s-1980s illuminated the alginate copolysaccharide structure.^{20-23, 25, 27, 48-51} Early studies were also restricted by the absence of advanced techniques for structural analysis. DS values in alginate acetates were determined predominantly in these early papers using deacylation and titration methods to measure the acetyl content. Insight about the acetyl substitution variation between M and G monosaccharide residues, and the regioselectivity between the two secondary OH-groups on each, was possible only later through powerful characterization techniques such as NMR spectroscopy. Modern researchers are also advantaged by the availability of alginates with different M/G contents and sequences, by isolation from various organisms and by enzymatic preparation in vitro. Alginate variants having different block structures and sequences were not available until the biochemistry of alginates was better understood.⁸⁻¹¹

Acetylation of alginates coupled with a detailed analysis of the acetyl substitution pattern along the backbone was first reported by Skjåk-Bræk et al.⁵² The reaction was carried out by preparing Ca-alginate gel beads in aqueous media, then replacing water with pyridine via solvent exchange. The beads were then suspended in a mixture of pyridine-acetic anhydride at 38 °C to perform the acetylation reaction. **Scheme 2.3** shows the reaction scheme. Acetylated Ca-alginate beads were washed thoroughly with water, Ca^{+2} ions removed and exchanged with Na^{+} ions, and the final product dialyzed and freeze dried. Alternatively, acetylation was also performed using alginic acid. In all cases, the presence of water was essential for reaction to occur and the DS was found to depend on the amount of water present. The DS value reached maximum at a water content of ~20%. The reaction rate was fast for the first 40 min of reaction time, and then dropped off over the next 20 hours.



Scheme 2.3: Acetylation of alginate using pyridine/acetic anhydride. For acetylation in gel form, $\text{M} = \text{Ca}^{+2}$ and $\text{M} = \text{Na}^{+}$.⁵² For homogeneous acetylation in DMSO/TBAF, $\text{M} = \text{TBA}^{+}$ and $\text{M}'' = -\text{H} \text{ or } \text{Na}^{+}$.²⁸

The alginate acetate derivatives so prepared were characterized using ^1H -NMR spectroscopy. The anomeric and high field resonances overlapped, making accurate peak assignments difficult. The splitting patterns resulting from the O-acetyl peaks around ~2.0-2.2 were therefore used for substituent analysis. In order to make accurate peak assignments

possible, it was essential to have alginates enriched in certain block sequences and acetylate them to identify the peaks arising from their respective structures. By comparing the ^1H -NMR spectra of acetylated alginates enriched in G-blocks and M-blocks, the resonances at 2.04-2.06 ppm were assigned to the acetyl groups from monoacetylated G-residues. Using the relative changes in the peak intensities observed at varying DS values, signals arising from monoacetylated G-residues were identified and distinguished from diacetylated G-residues. ^1H -NMR spectra of acetates synthesized from alginates containing varying MG block sequences were compared, and the peaks arising from acetylated G-residues adjacent to G residues were distinguished from acetylated G-residues adjacent to M residues.

The relative acetyl substitution ratios for M and G residues were calculated and the results are summarized in **Table 2.2**. Alginate obtained from *L. hyperborea* with $F_G = 0.68$ was acetylated to two different DS values. At both DS values, the substitution favored M residues over G. In addition, when two alginates obtained from *L. hyperborea* and *A. nodosum* with varying F_G values were acetylated to the same DS values, substitution occurred preferentially on M residues. Therefore, selective acetylation of M-residues was possible through the reaction of Ca-alginate beads with pyridine and acetic anhydride.

Table 2.2: Relative acetyl substitution ratios on M and G residues for alginates⁵²

Alginate Source	F_G	DS	Acetylation (%)	
			M	G
<i>L. hyperborea</i>	0.68	0.1	>90	<10
<i>L. hyperborea</i>	0.68	0.40	80	20
<i>A. nodosum</i>	0.40	0.40	63	36

Skjåk-Bræk et al. also reported the effects of acetylation upon alginate properties.⁵³ Molecular weight measurements showed no significant degradation taking place during gel acetylation. The addition of acetyl groups to the backbone caused noticeable chain extension at

0.1M ionic strength. Even a small proportion of acetyl groups on the backbone played an important role in defining the polymer conformation. When Ca-alginate gels were formed, acetylation was found to severely diminish the ability of Ca^{+2} ions to induce conformational ordering. Consequently, lower strength gels resulted from acetylated alginates. On drying and re-swelling the Ca-alginate beads, the degree of swelling increased 500-fold from DS 0 to DS 0.65. This was a result of enhancement in the positive osmotic pressure resulting from a higher number of dissociating counterions per polymer chain, due to impairment of co-operative binding by the added acetyl groups. A plot of the moduli (G) of gels made from acetylated alginates vs. DS is shown in **Figure 2.8**. Even at low DS values where M residues were acetylated selectively, a large drop in modulus was recorded. Thus, to form Ca^{+2} junctions, it was important that both G- as well as M-residues remained unsubstituted.

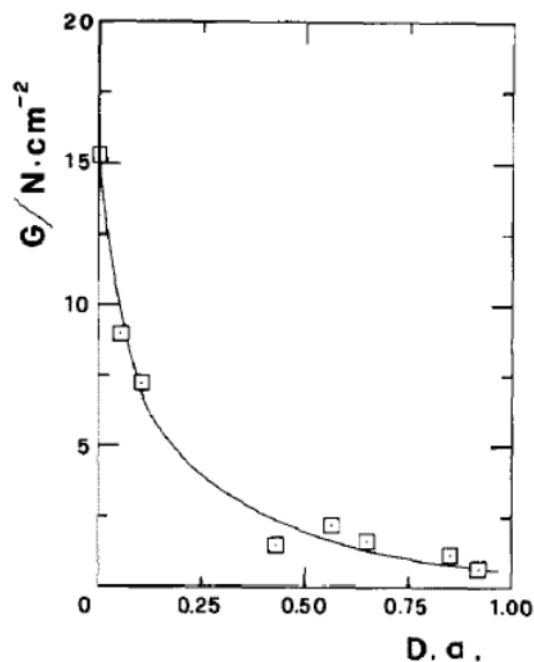


Figure 2.8: Dependence of the modulus of rigidity (G) on DS (represented as "D.a.") in acetylated Ca-alginate gels⁵³

We recently reported a strategy for acetylation of alginates by homogeneous dissolution of TBA-alginate in two-component organic solvent systems.²⁸ TBA-alginate dissolved completely in DMSO solutions containing TBAF. In the absence of TBAF, a heterogeneous mixture was formed with partial dissolution of TBA-alginate, as confirmed by ¹H-NMR and dynamic light scattering (DLS). **Figure 2.9** shows an image of the two mixtures. In addition to DMSO, dipolar aprotic solvents such as DMF, DMAc and DMI fully dissolved TBA-alginate in the presence of TBAF. Partial acetylation of alginates was achieved in all solvent systems using pyridine/acetic anhydride reagent under homogeneous conditions with DS ranging between 0.74-0.85. A maximum DS of ~1.0 was however achieved for acetylation under anhydrous conditions wherein TBAF was synthesized *in situ*⁵⁴, or by adding a second portion of acetic anhydride to the reaction mixture. The DS value for alginate acetates could not be increased significantly beyond ~1.0 under any attempted conditions. A potential explanation for this limited DS was based on monosaccharide ring electronic effects. The uronate ring in unreacted TBA-alginate contained one electron-withdrawing substituent at the C-5 position. During acetylation, the monoacetate product was formed first by reaction at one of the two hydroxyl groups. The monoacetylated uronate ring now had two electron-withdrawing substituents; the first was the C-5 carboxylate and the second was the acetyl substituent. It is likely that with two electron-withdrawing substituents present, the reactivity of the second hydroxyl group was significantly reduced. The DS value may therefore be limited to ~1.0 when pyridine/anhydride is used as the acylating reagent system.

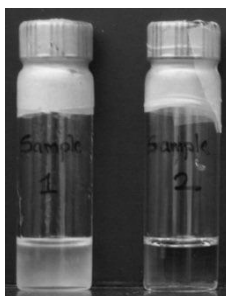


Figure 2.9: Partial dissolution of TBA-alginate in DMSO (left) and complete dissolution in DMSO/TBAF (right) at a TBAF concentration of 1.1% (w/v). Alginate concentration in both vials was 15 mg/mL²⁸

An alternate theory was based on the stereochemistry of the monosaccharide residues. In M residues, the 2-OH group is axial and can interact with the C-4 proton through 1,3-diaxial interactions, thus favoring substitution at the 3-OH position. In G residues the 3-OH group is axial and therefore interacts with the C-5 proton through 1,3-diaxial interactions. Substitution of the 2-OH position was hence favored on G units. Thus, in each monosaccharide, stereochemistry favored reaction of one out of the two hydroxyl groups, limiting the DS to ~ 1.0 . While these possible causes for an upper DS limit were postulated, they were not corroborated experimentally. In addition to acetates, propionylation of alginates was also reported using propionic anhydride and pyridine to obtain a product with DS = 0.31.

To better understand the selectivity of alginate acetylation, the reaction was performed using alginates containing varying M/G ratios. Under homogeneous reaction conditions, the DS values obtained were nearly identical (~ 0.8) across the entire range of alginate M/G ratios. This proved that the reaction was not selective for M vs. G, and that both M and G residues could be acetylated. ¹H-NMR peak assignments showed that both 2- and 3-OH positions on M residues could be acetylated under homogeneous conditions. Regioselectivity between the 2-OH and 3-

OH positions on G residues was however difficult to determine with certainty due to severe overlap of signals in the ^1H -NMR spectrum.

Acetylation of TBA alginates performed in DMSO without added TBAF, that is, under partly heterogeneous conditions, afforded more variable DS values compared to homogeneous acetylation. The products of heterogeneous reactions yielded DS values that varied with the M/G ratios of the starting polymers. The ^1H -NMR spectra of heterogeneously acetylated alginates showed a predominance of two peaks at shifts of 5.08 and 4.47 ppm respectively. This predominance was not observed in the case of homogeneous reaction products. Previous assignments for alginates have shown that the peak at ~5.08 ppm arises from the H-1 signal of G residues in GGG, MGG and GGM triads. The peak centered at ~4.47 ppm on the other hand arises from the H-5 signal of G-residues in GGG triads.²⁷ Thus, the predominance of the two peaks in heterogeneously acetylated alginates suggested that GGG triad sequences remained relatively unreacted. G-blocks were therefore preserved, resulting in selective acetylation of M residues. **Table 2.3** shows the DS values obtained for alginates with various M contents, under both homogeneous as well as heterogeneous conditions.

Table 2.3: Homogeneous and heterogeneous acetylation of alginates and the corresponding DS values

Alginate	DS_{Homogeneous}	DS_{Heterogeneous}
100% M	0.80	0.91
63% M	0.80	0.48
29% M	0.78	0.63
13% M	0.78	0.54
0% M	0.82	0.72

DS values measured using ^1H -NMR. All reactions employed TBA alginate at 100 mg/mL DMSO using alginate monosaccharide unit:pyridine:acetic anhydride molar ratio of 1:17:15; homogeneous reactions also employed 100 mg TBAF/mL DMSO.

The difference in DS values and distribution observed between homogeneous and heterogeneous reaction products was likely related to the partial solubility of TBA-alginate in DMSO. A possible explanation may be that the M-blocks have a higher affinity for DMSO, thus facilitating the selective acetylation of M residues. A contrasting picture was seen for homogeneous reactions in DMSO/TBAF, where all polymer chains were fully solubilized. Thus, there was equal accessibility to G-blocks, M-blocks and MG-blocks, which resulted in a statistical distribution of acetyl groups.

Table 2.4: Molecular weight degradation of TBA-alginate during acetylation

Reaction time	DS	M _n (kDa)	M _w (kDa)	PDI	DP
0 min	0	56.37	98.18	1.74	144
15 min	0.65	20.36	48.88	2.40	66
30 min	0.75	13.23	33.32	2.52	43
1 h	0.51	8.13	19.61	2.41	28
2 h	0.90	2.78	10.91	3.93	9

DS values measured using ¹H-NMR. All reactions were performed in 1% (w/v) DMSO/TBAF using M063 sample at 40 °C for 2 hours. Ac₂O was used as the acyl reagent with an Alg:Pyr:Acyl ratio of 1:17:15

As previously described in this review, alginates degrade via β -elimination at higher pH values.³⁸⁻³⁹ Pyridine is a mild base which nonetheless can degrade alginates. Furthermore, fluoride from TBAF is also known to be a strong base⁵⁵. Molecular weight measurements were therefore performed on alginate acetates that were reacted for different time periods, and compared to unreacted TBA-alginate. **Table 2.4** shows the obtained results, which clearly point to significant chain degradation. The starting DP (0 min) of 144 is reduced to 66 within the first 15 minutes of reaction. DP continues to decrease throughout the two hours of reaction time. **Figure 2.10** shows shifts in the SEC chromatograms to longer elution times for alginate acetate

as degradation proceeds. Thus in order to preserve the alginate molecular weight, it was desirable to minimize reaction times and temperatures.

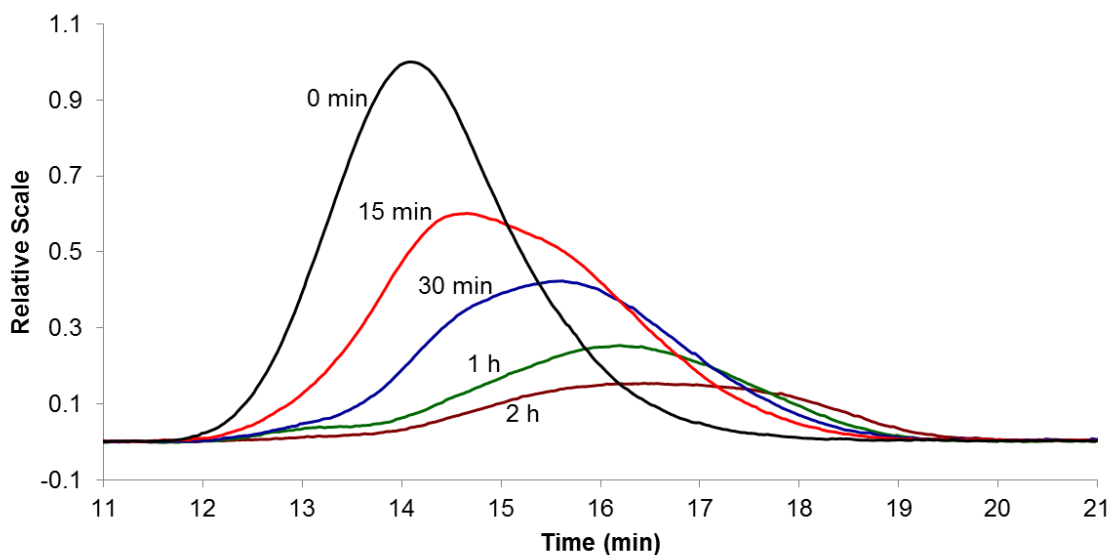
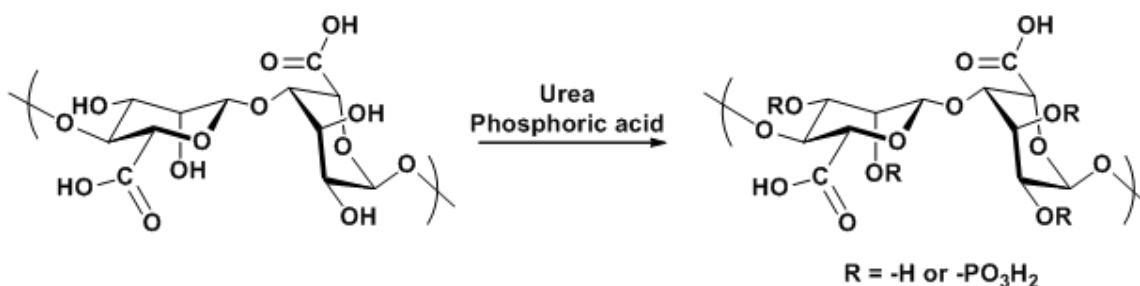


Figure 2.10: Shift in the SEC chromatograms to longer elution times for alginate acetates shown in Table 2.4, recorded over increasing reaction time²⁸

2.4.2 Phosphorylation of alginates

The synthesis of phosphorylated alginate derivatives was recently described to evaluate their ability to induce hydroxyapatite (HAP) nucleation and growth.⁵⁶ **Scheme 2.4** shows the reaction scheme. Phosphorylation was performed using urea/phosphoric acid reagent by creating a suspension of alginate in DMF. A maximum DS of 0.26 was achieved using an alginate:H₃PO₄:urea mole ratio of 1:20:70; the heterogeneous nature of the reaction apparently limited the maximum DS attainable. Phosphoric acid as a strong acid is likely to cause alginate molecular weight degradation. Accordingly, a 2-4 fold reduction in the value of M_w was reported for phosphorylated alginates compared to unreacted alginates.



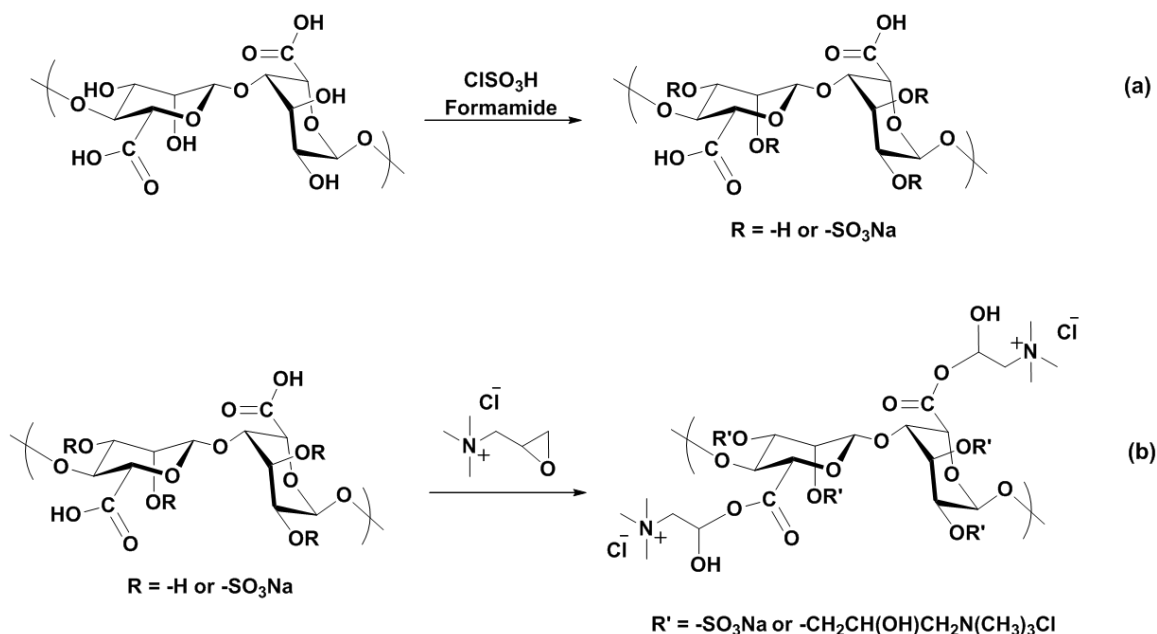
Scheme 2.4: Phosphorylation of alginate⁵⁶

The regioselectivity of phosphorylation with respect to four possible substitution sites (2-OH and 3-OH positions of each residue, G and M) was studied using NMR spectroscopy. A combination of NMR techniques including one-dimensional ^1H and ^{31}P , ^1H - ^1H COSY, ^1H - ^{31}P HMBC, ^1H - ^{31}P HMQC-TOCSY and ^1H - ^{13}C HSQC was used to carry out detailed peak assignments. The analysis pointed towards phosphate substitution on M residues such that a higher degree of phosphorylation occurred on the 3-OH group compared to the 2-OH group. This regioselectivity was a result of the higher reactivity of the equatorial 3-OH. The equatorial sites were more accessible compared to axial during phosphorylation. NMR spectroscopy also showed evidence for substitution occurring on G residues. However, the regioselectivity between 3-OH and 2-OH groups for G residues could not be cleanly measured because the correlations observed for G residues in a ^1H , ^{31}P -HMQC-TOCSY experiment were much weaker compared to those for M residues. Interestingly, these phosphorylated alginates were found to be incapable of forming Ca-crosslinked ionic gels. The reduction of molecular weight during reaction in addition to conformational changes resulting from phosphorylation were cited as causes for the inability of these alginate derivatives to form gels. However, Ca-crosslinked gels could be formed by blending unreacted alginate with phosphorylated alginate. Such gels formed using alginate blends showed higher resistance to calcium extraction compared to gels formed using only

unreacted alginates. The authors pointed out that the phosphate groups were likely to have participated in the chelation process, thus making the gels more stable.

2.4.3 Sulfation of alginates

Sulfation of polysaccharides, both enzymatically in nature as well as by chemical methods is known to provide blood-compatibility and anticoagulant activity.⁵⁷ Heparin is the most widely used naturally sulfated polysaccharide because of its ability to prevent blood from clotting.⁵⁸ It is therefore of interest to see whether alginate sulfates would possess similar anticoagulation properties. Yumin et al. first reported the sulfation of sodium alginate using chlorosulfonic acid in formamide.⁵⁹ The reaction scheme is depicted in **Scheme 2.5(a)**. Sulfates with DS up to 1.41 were obtained, and the values were measured using the %C to %S ratio from elemental analysis. The anticoagulant activity of alginate sulfates was measured using activated partial thrombosis time (APTT), thrombin time (TT) and prothrombin time (PT). Using APTT, anticoagulant activity of alginate sulfate was found to be comparable to heparin. But using PT, the activity was very low. Since APTT is based on an intrinsic coagulation pathway and PT is based on an external coagulation pathway, alginate sulfates were shown to have a greater influence on the intrinsic coagulation pathway.

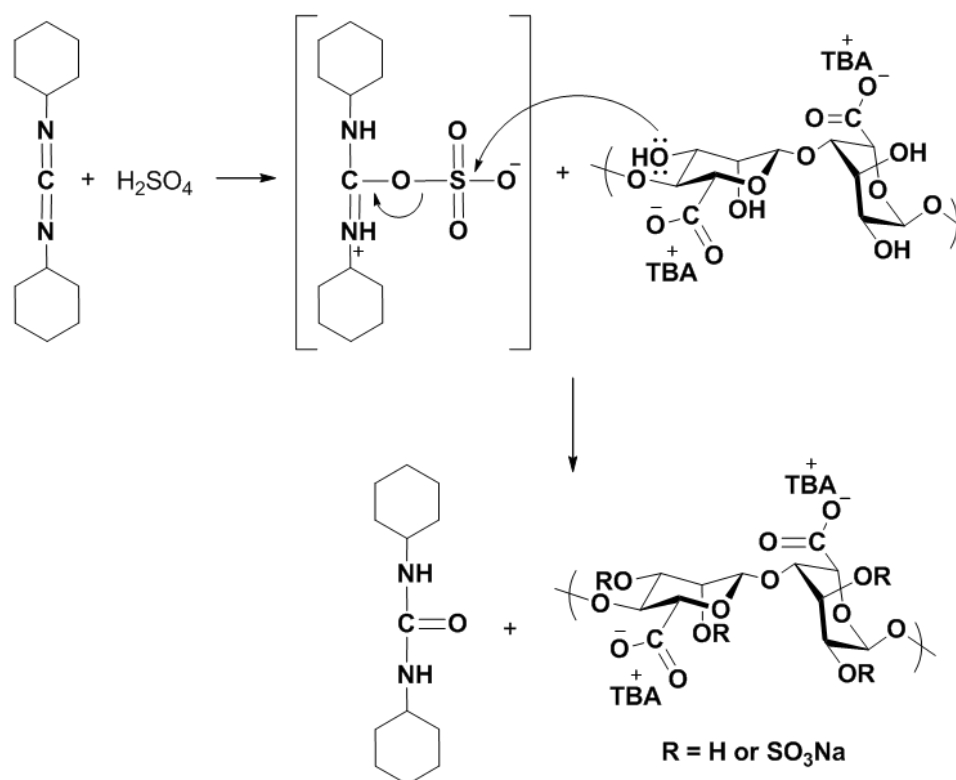


Scheme 2.5: (a) Alginate sulfation using chlorosulfonic acid and (b) quaternization of alginate sulfate using 2,3-epoxypropyl trimethylammonium chloride

While sulfation is beneficial in many cases, oversulfation is undesirable since it can cause side effects. Therefore to decrease the anticoagulant activity, alginate sulfates were reacted with 2,3-epoxypropyl trimethylammonium chloride to attach pendent quaternary amine groups (**Scheme 2.5(b)**). The number of quaternary ammonium groups attached was controlled by the moles of the epoxy reagent added. Both unsulfated hydroxyl and carboxylate groups added to the epoxy compound to append the quaternary ammonium salts. While the sulfation step required use of chlorosulfonic acid, most likely causing molecular weight loss, the epoxide condensation did not cause degradation. The anticoagulant activities of alginate sulfates were greatly reduced by attachment of the quaternary amines. Furthermore, the reduction of activity was proportional to the number of quaternary ammonium groups attached.

Cohen et al. reported the synthesis of alginate sulfates using carbodiimide coupling chemistry.⁶⁰ The hydroxyl groups were sulfated using a DCC-sulfuric acid reagent system such

that the carboxylate groups remained unreacted. The reaction mechanism (**Scheme 2.6**) is marked by the formation of a DCC- H_2SO_4 adduct which reacts with the hydroxyl nucleophile. The products were characterized using ^{13}C -NMR, and the spectra revealed that the C-1 and C-6 peak shifts did not change upon sulfation. The C-2 and C-3 peaks however shifted downfield, thus proving that the sulfate groups were added to either one or both hydroxyl positions. The use of a strong acid reagent caused substantial molecular weight loss. The average molecular weight decreased from 100 to 10 kDa during reaction, but was not affected by the M/G ratio.

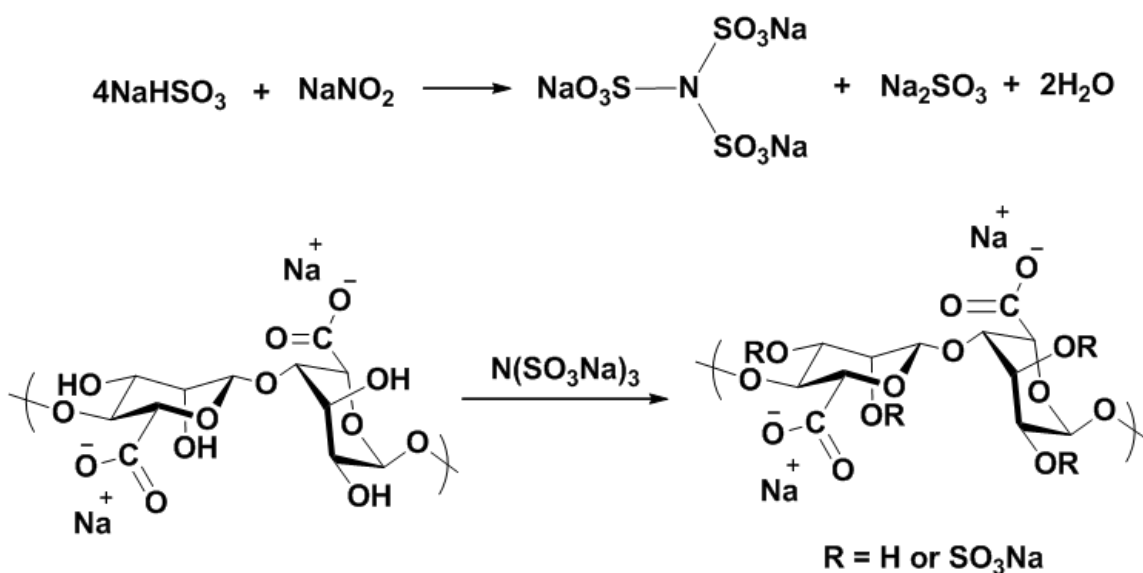


Scheme 2.6: Sulfation of alginates using DCC-sulfuric acid route⁶⁰

The binding of alginate sulfates to both heparin-binding and non-binding proteins was compared to unmodified alginates. While the sulfates bound strongly to heparin-binding proteins, unmodified alginates did not bind. Furthermore, both sulfates and unmodified alginates showed no affinity for heparin non-binding proteins. In nature, specific binding of growth factors

to heparin and heparan sulfate protects them from denaturation and proteolytic degradation. The ability of alginate sulfates to provide protection to growth factors and sustain their release was therefore studied. Ca-alginate microspheres were formed by blending alginate sulfates with unreacted alginates. A much more sustained release of bFGF growth factor was achieved from alginate/alginate sulfate microspheres compared to that from pure alginate microspheres. The sustained in vivo release of bFGF afforded enhanced angiogenic activity compared to non-specifically bound alginate.

Fan et al. reported the sulfation of alginates by an uncommon reagent prepared using sodium bisulfite and sodium nitrite in an aqueous solvent.⁶¹ Traditional sulfation reagents such as sulfuric acid, chlorosulfonic acid, sulfuryl chloride, sulfur trioxide and sulfamic acid cause hydrolytic degradation of alginates. The new synthetic route was therefore used to overcome this limitation of traditional reagents. The reaction was performed in water, wherein the sulfation reagent was first adjusted to the desired pH followed by addition of sodium alginates (**Scheme 2.7**). DS values for the derivatives were measured using barium sulfate nephelometry. An optimum DS value of 1.87 was achieved at pH 9.0, 40 °C and 2:1 mole ratio of reagent:uronic acid residue. Anticoagulant activities for the sulfated alginate derivatives were measured and the DS, molecular weight and concentration were found to be influential factors.



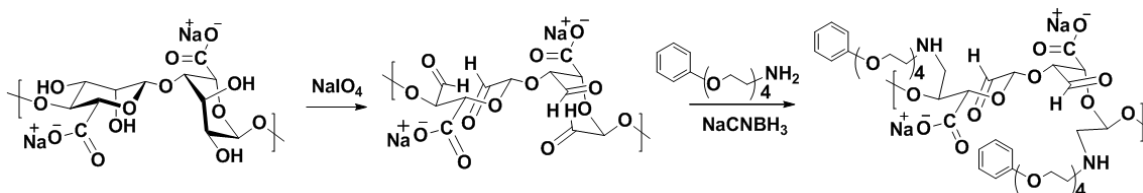
Scheme 2.7: Sulfation of alginates using sodium bisulfite-sodium nitrite reagents⁶¹

While the sulfation chemistries described thus far yield alginate sulfates, control over the placement of sulfate groups along the alginate backbone has not yet been achieved. It is known that most biological functions in sulfated polysaccharides are related to their sulfation pattern and sequence.⁶²⁻⁶³ Therefore, advances in controlled placement of sulfate groups along the alginate backbone may eventually translate into greater understanding and perhaps control of structure-property relationships in alginate sulfates.

2.4.4 Hydrophobic modification

Alginates are hydrophilic polysaccharides. In addition to hydrophilicity resulting from the two hydroxyl groups, the carboxylate ion enhances water solubility at pH 5 and above. The motivation for hydrophobic modification of alginates is therefore to transform the polysaccharide from its predominantly hydrophilic nature to a molecule with amphiphilic or hydrophobic characteristics. The most straightforward way to achieve this transformation is by covalent

attachment of hydrophobic moieties such as long alkyl chains or aromatic groups to the polymer backbone. Hubert et al. attempted the hydrophobic modification of sodium alginate by covalent attachment of short polyether chains to the alginate backbone.⁶⁴ Sodium alginate was first activated using sodium metaperiodate, which oxidized the two secondary hydroxyl groups to aldehyde groups. The aldehydes were then reacted with α -amino, ω -benzyloxy tetraoxyethylene ($\text{C}_6\text{H}_5(\text{OCH}_2\text{CH}_2)_4\text{NH}_2$, abbreviated as BzlO-TEG-NH₂) by reductive amination to yield a tetraoxyethylene functionalized amine derivative of alginate (BzlO-TEG-NH-Alg; **Scheme 2.8**). Through oxidization, alginate hydroxyl groups having low reactivity were converted to aldehydes having significantly higher reactivity. The carboxylate groups were preserved in the process, thus retaining the ability of the modified alginate to form ionic gels.



Scheme 2.8: Synthesis of BzlO-TEG-NH-Alg by periodate oxidation of sodium alginate followed by reductive amination using BzlO-TEG-NH₂

The amount of periodate reagent used for the reaction was calculated to be sufficient to oxidize 20% of the available uronate residues. A significant reduction in the viscosity was recorded on completion of this step due to molecular weight degradation and extension of chain conformation by ring opening. Breakdown of the alginate molecular weight in solutions containing periodate, as previously mentioned, depends on the sequence and distribution of M and G residues.⁶⁵ Alginates containing longer MG block sequences were found to degrade more rapidly than alginates containing shorter MG blocks. Partial oxidation of alginates may be

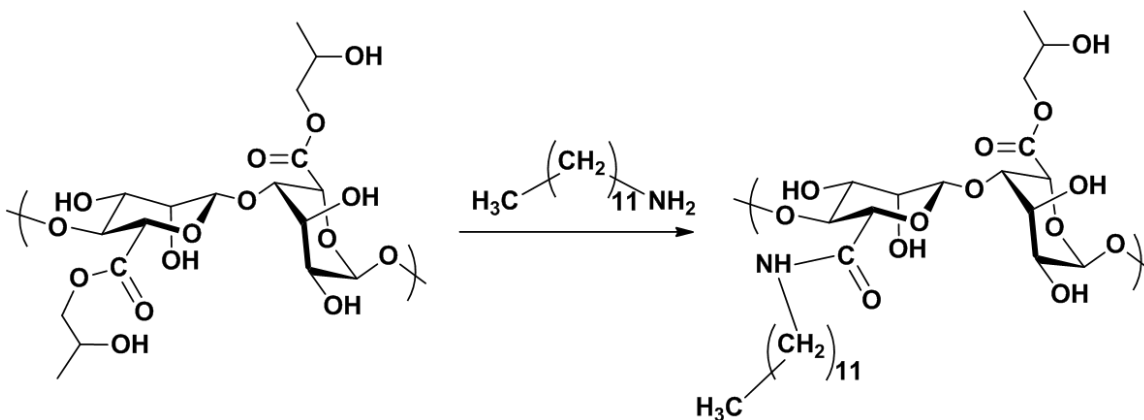
advantageous for biomedical applications because they degrade in aqueous media, while unmodified alginates do not.⁶⁶

The oxidized alginate derivative was reductively aminated with excess BzlO-TEG-NH₂ and sodium cyanoborohydride (NaCNBH₃) in phosphate buffer (pH 7). Due to the difficult removal of residual BzlO-TEG-NH₂, BzlO-TEG-NH-Alg was converted to its Ca-gel form and washed with ethanol. After the removal of residual BzlO-TEG-NH₂, the product was transformed back to its Na-salt form and characterized using ¹H and ¹³C-NMR. The DS value was however quantified using ¹³C-NMR, since the ¹H-NMR spectrum showed complex overlap occurring in both anomeric and high field regions. Based on the integration ratios of the benzyl aromatic carbons and the carboxylic carbon, the DS was calculated to be 0.12.

As the charged (anionic) alginate backbone is decorated with hydrophobic entities, two competing forces emerge - (a) repulsive interactions resulting from the charged carboxylate groups promote chain extension, and (b) attractive interactions resulting from the hydrophobic groups promote chain collapse. The result of these forces is the formation of high molecular weight aggregates in solution when (b) dominates (a). For BzlO-TEG-NH-Alg the electrostatic repulsive forces offset the hydrophobic attractive forces, preventing the formation of high molecular weight aggregates. This was contrary to the observation found in similar dextran derivatives (BzlO-TEG-NH-Dex), where high molecular weight aggregates were freely formed.⁶⁷ Dextran is an uncharged polysaccharide, and the absence of repulsive electrostatic forces in BzlO-TEG-NH-Dex caused hydrophobic interactions to dominate.

In addition to intramolecular effects, interactions in hydrophobically modified alginates are also present at the intermolecular level. Hubert et al. later presented evidence for this through the synthesis of C₁₂-linked alginate amide derivatives.⁶⁸ Propylene glycol esters of alginate

(PGA) with ~ 30% carboxylic acid groups esterified ($DS_{PG} \sim 0.3$) were substrates for nucleophilic displacement by dodecylamine (**Scheme 2.9**) to form the corresponding amides (PGA-C₁₂) with a $DS_{Amide} \sim 0.09$ (calculated based on nitrogen content analysis). The reaction was performed in the heterogeneous state by making a suspension of PGA in DMF.



Scheme 2.9: Synthesis of alginate amides by reaction of propylene glycol esters of alginate with dodecylamine

The change in viscosity of PGA solutions after C₁₂ modification was studied. **Figure 2.11(a)** shows the viscosity vs. concentration plots for both PGA and PGA-C₁₂. A large increase in PGA-C₁₂ viscosity with concentration was observed compared to that in PGA. This increase in PGA-C₁₂ viscosity was attributed to a combined effect of chain entanglements and intermolecular interactions between the hydrophobic dodecyl chains. Interactions at an intermolecular level lead to the formation of physically crosslinked domains. This effect was similar to that observed in hydrophobically modified hydroxyethyl cellulose (HMHEC) derivatives, wherein hydrophobically driven association between individual molecules leads to the formation of a three-dimensional network.⁶⁹ The viscosity increase in unmodified PGA resulted only from chain entanglements. The absence of intermolecular interactions and physically crosslinked domains prevented a large viscosity spike. The presence of intermolecular

hydrophobic interactions in PGA-C₁₂ was further confirmed when the ionic strength of the medium was varied. An increase in the salt concentration had an effect of screening the electrostatic repulsive forces leading to a more compact coil and higher viscosity. For PGA-C₁₂, in addition to the screening effect there was an enhancement of hydrophobic interactions with increase in ionic strength. The increase in viscosity with salt concentration was therefore found to be significantly higher for PGA-C₁₂ compared to PGA. **Figure 2.11(b)** shows the plot for viscosity vs. NaCl concentration for both PGA and PGA-C₁₂. An increase in the hydrophobicity of the environment was further created by increasing the PGA-C₁₂ concentration. A similar concentration dependent increase in hydrophobicity did not occur with PGA.

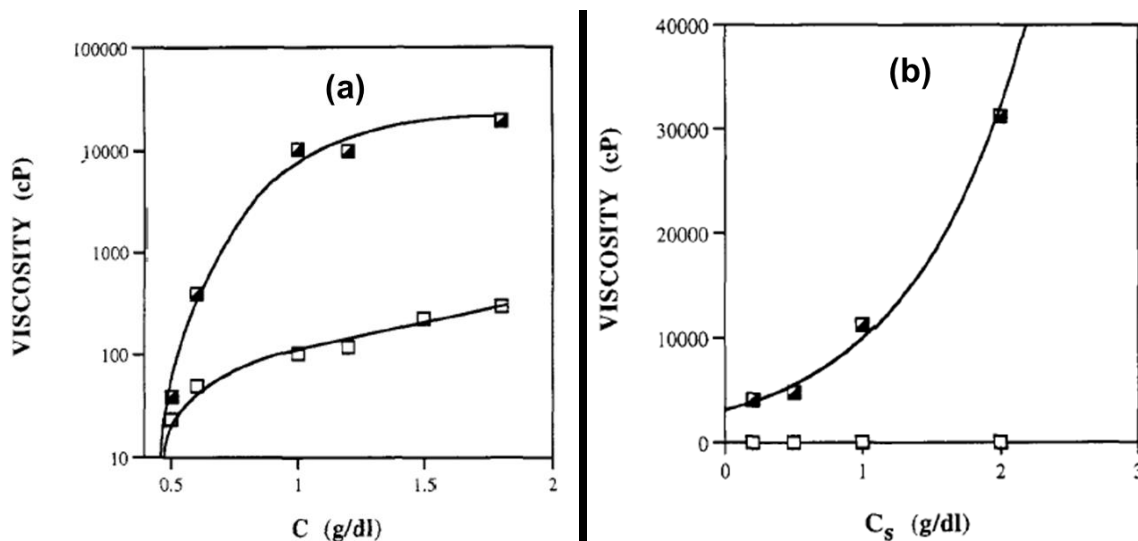
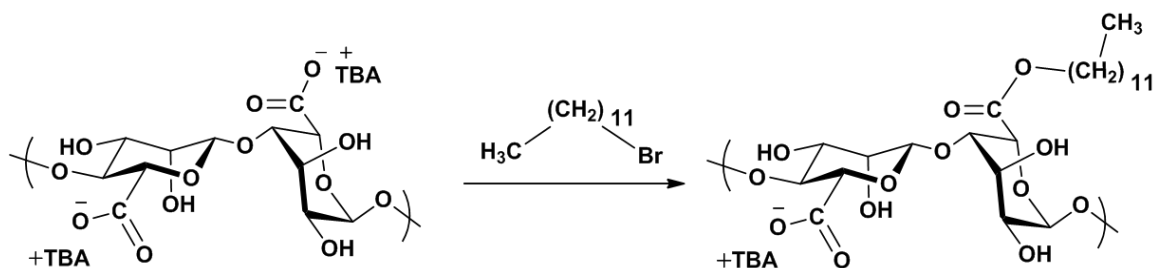


Figure 2.11: (a) Viscosity vs. concentration (C) plot for PGA (empty squares) and PGA-C₁₂ (half-filled squares) at a shear rate of 0.06 (1/s) and (b) Viscosity vs. NaCl concentration (C_s) plot for PGA (empty squares) and PGA-C₁₂ (half-filled squares) at a fixed polymer concentration of 1.2 g/dL and shear rate of 0.06 (1/s)⁶⁸

The synthesis of alginate amide derivatives with varying length hydrocarbon chains - PGA-C₈, PGA-C₁₄ and PGA-C₁₂ has been described.⁷⁰⁻⁷¹ Clear evidence for the increase in hydrophobic character of the polymer solution for long alkyl chain lengths was observed. The

rheological properties of PGA, PGA-C₁₂ and PGA-C₁₄ derivatives were studied in the semi-dilute aqueous regime, and a marked change was observed for the hydrophobically modified derivatives when compared to parent PGA.⁷² The intermolecular hydrophobic interactions between long alkyl chains were disrupted reversibly under high shear.

Hubert et al. also reported the synthesis of hydrophobically modified alginate derivatives starting from Na-alginate.⁷³ Dodecyl chains were covalently linked to the carboxylate groups on the backbone. TBA-alginate was first synthesized by converting Na-alginate to alginic acid and subsequent neutralization with TBA hydroxide. TBA-alginate was reported to be soluble in DMSO, but experiments in our laboratory have shown that TBA-alginate synthesized using a similar procedure was only partially soluble in DMSO.²⁸ The reaction was carried out using dodecyl bromide reagent via nucleophilic displacement (**Scheme 2.10**). The product (Alg-C₁₂) was purified by dialysis and subsequently freeze dried, with hydrophobe DS 0.12 as determined by gas chromatography after alkaline hydrolysis of the sample.



Scheme 2.10: Reaction scheme for the synthesis of Alg-C₁₂

The surface tension isotherms for Alg-C₁₂ and unreacted Na-alginate were compared by measuring the change in surface tension (σ) with concentration. The σ value for Na-alginate was surprisingly unchanged after C₁₂ modification. It was proposed that collapsed micellar structures formed due to intramolecular hydrophobic interactions. The dodecyl chains were buried inside

the micelles, protecting them from exposure to the adsorption interface. In addition, the charged alginate backbone made it incapable of folding at short distances and restricted orientation of the hydrophobic chains at the surface. **Figure 2.12(a)** shows a schematic of the adsorption of Alg- C_{12} at the air water interface in the presence of a high concentration of covalently attached long alkyl chains.

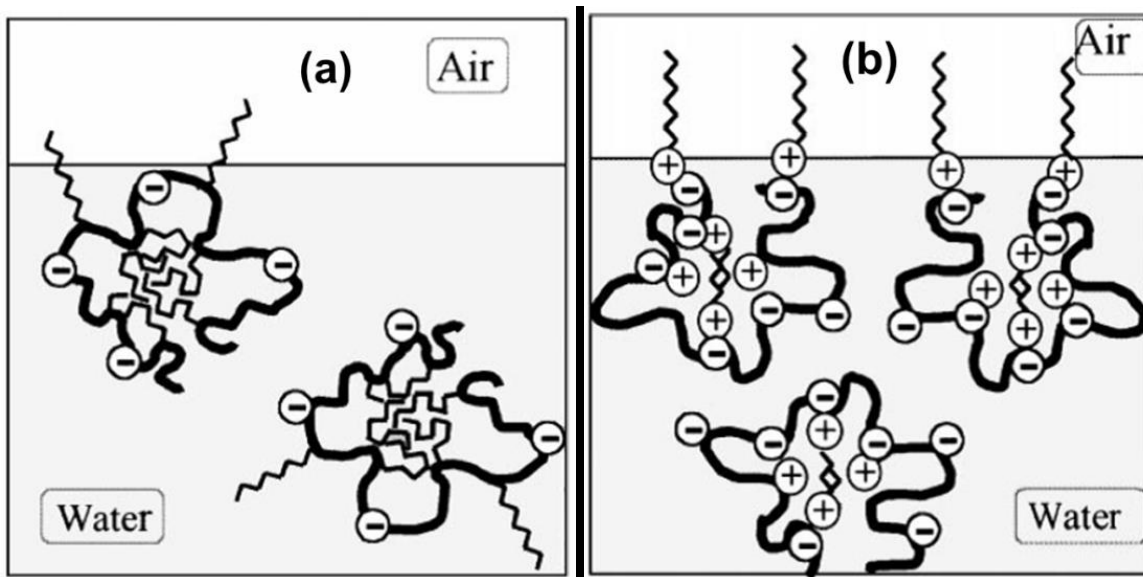


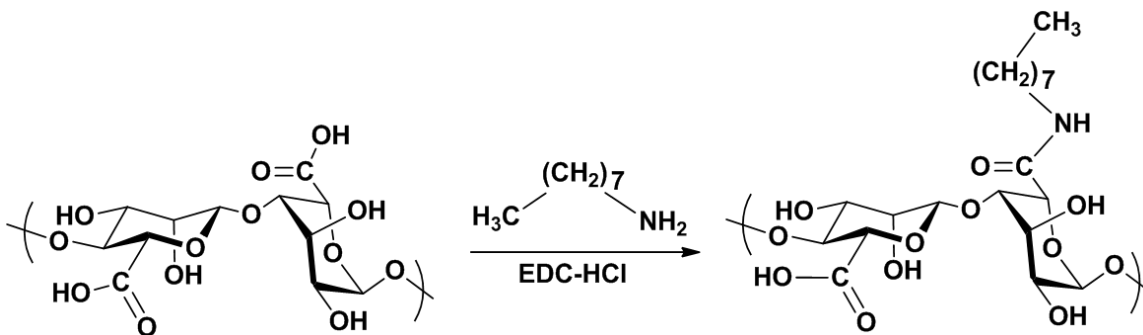
Figure 2.12: (a) Alg- C_{12} adsorption at the air water interface and (b) Alg- C_{12} +DTAB adsorption at the air water interface⁷³

While Alg- C_{12} did not show markedly enhanced adsorption activity, the addition of a cationic surfactant, dodecyltrimethylammonium bromide (DTAB) with Na-alginate showed a remarkable improvement in the surface adsorption. The surfactant possesses a C_{12} hydrophobic tail and a cationic head group which interacted ionically with the negative charges on the alginate backbone. Therefore, while the hydrophobic C_{12} chain was covalently linked in Alg- C_{12} , the C_{12} chain was bonded ionically to the alginate backbone in a mixture of Na-Alg + DTAB. At identical C_{12} molar concentrations, the ionically linked Na-Alg + DTAB showed almost a thousand-fold higher surface adsorption activity compared to the covalently linked Alg- C_{12} . In

other words, the electrostatically linked C₁₂ alkyl chains in Alg+DTAB were more densely aligned at the air-water interface than the covalently attached C₁₂ chains in Alg-C₁₂. **Figure 2.12(b)** shows a schematic of Alg +DTAB adsorption at the air-water interface. The labile nature of electrostatically attached C₁₂ alkyl chains allowed a free re-organization at the interface, while such re-organization was not possible when the chains were covalently linked to the alginate backbone. Dellacherie et al. later reported the physico-chemical properties of hydrophobically modified alginates in aqueous solution.⁷⁴ Fluorescence spectroscopy studies were performed which showed an increase in the hydrophobic character with increasing alkyl chain lengths.

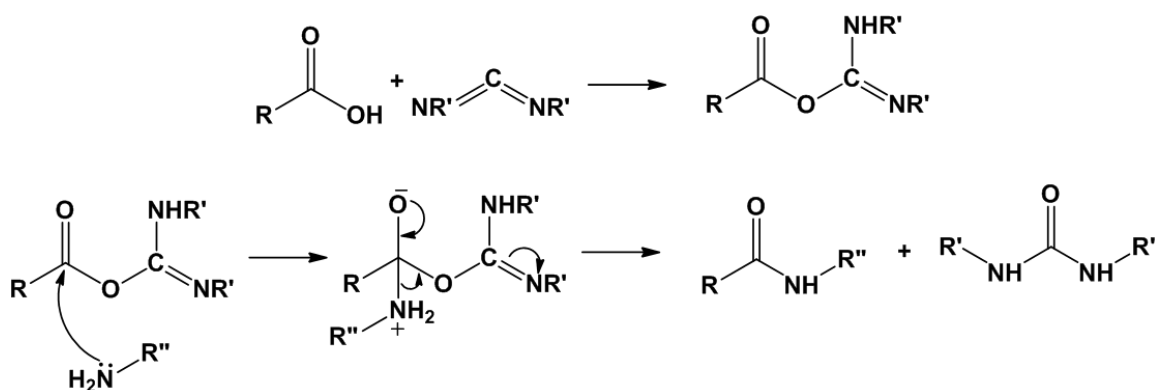
Production of microspheres based on hydrophobically modified alginates by a dispersion gelation method was reported by Leonard et al.⁷⁵ Gelation was induced in an aqueous solution of Alg-C₁₂ by the addition of NaCl. A dispersive shear stress was first applied to overcome the initially high solution viscosity of Alg-C₁₂. The solution was then dispersed in aq. NaCl to afford gel microparticles. Microparticle size was controlled by varying the applied shear stress. While the particles were stable in aqueous solutions for several days, they aggregated upon centrifugation. A small amount of CaCl₂ was therefore used during particle formation to strengthen the physical network by ion crosslinking. Increasing the polymer concentration in the starting mixture caused a slight increase in the particle size. Furthermore, at high DS values, small particle sizes could be achieved at low salt concentrations; while at low DS values, high salt concentrations were necessary to achieve the same size. Bovine serum albumin (BSA) was encapsulated within the Alg-C₁₂ gel microspheres. In water, the protein was released from unmodified alginate within a few hours, but BSA encapsulated in Alg-C₁₂ microspheres was not released for up to 5 days. In citrate solutions, no release of BSA encapsulated in Alg-C₁₂ microspheres was observed, whereas BSA encapsulated in unmodified alginate gel was released

instantaneously by dissolution of Ca-alginate beads. Sodium citrate is a Ca^{+2} chelating agent, and likely caused a rapid Na^{+} - Ca^{+2} exchange causing the beads to dissolve. The authors further cited that no BSA release occurred from Alg- C_{12} microspheres into the surrounding aqueous environment due to the stability of hydrophobic junctions within the gels.



Scheme 2.11: Reaction scheme for the synthesis of Alg-CONH-C₈

Nyström et al. reported the synthesis of hydrophobically modified alginate (Alg-CONH-C₈) by coupling n-octylamine to the backbone carboxylic acid groups using 1-ethyl-3-(3-dimethylaminopropyl)carbodiimide hydrochloride (EDC-HCl) ⁷⁶ (**Scheme 2.11**). A DS value up to 0.30 was measured using ¹H-NMR, using the ratio of methyl (from the C₈ chain) to anomeric protons, and was confirmed by elemental analysis. The effect of the M/G ratio and the sequence of the two monosaccharides on substitution pattern were however not reported. The mechanism of carbodiimide mediated coupling of carboxylic acids to amines is depicted in **Scheme 2.12**.



Scheme 2.12: Mechanism of carbodiimide mediated coupling of carboxylic acids to amines

The hydrophobic interactions occurring in Alg-CONH-C₈ were reversible in the presence of β -cyclodextrin (β -CD). β -CD was shown to have a noticeable effect on the Alg-CONH-C₈ chain length. Small-Angle Neutron Scattering (SANS) was used to calculate two physical parameters – persistence length (L) and correlation length (ξ). Persistence length is a measure of the stiffness of long polymer chains, whereas correlation length defines the average spatial extent of polymer concentration fluctuations resulting from thermal changes. When β -CD was added to a solution of Alg-CONH-C₈, the value of L increased while that of ξ decreased. The truncated cone structures in β -CD encapsulated the hydrophobic C₈ chains on Alg-CONH-C₈ causing a decrease in hydrophobic interactions. This in turn led to an increase in the net repulsive electrostatic forces, resulting in local stretching of polymer chains and higher L values. The decrease in ξ was a result of re-organization of the network, whereby the hydrophobic interactions fell apart to yield a homogeneous system devoid of junction points. **Figure 2.13** shows a schematic illustrating the encapsulation of hydrophobic C₈ moieties on Alg-CONH-C₈ by the β -CD truncated cone.

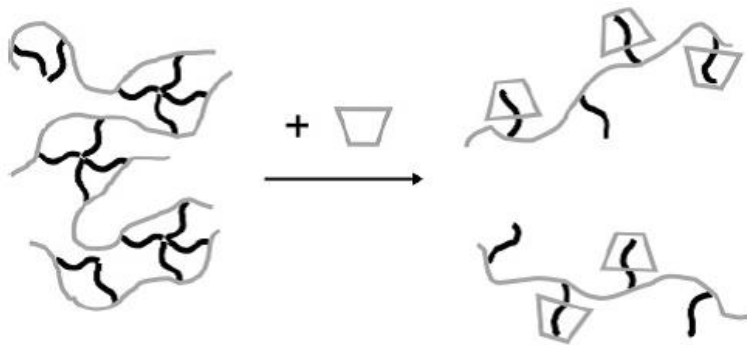


Figure 2.13: Schematic illustration of the encapsulation of the hydrophobic moieties on Alg-CONH-C₈ by the β -CD truncated cone⁷⁶

Nyström et al. later reported complex formation between Alg-CONH-C₈ and hydroxypropyl- β -CD (HP- β -CD) or polymerized β -CD (poly- β -CD).⁷⁷ On addition of HP- β -CD to a solution of Alg-CONH-C₈, a reduction in viscosity was observed. This viscosity reduction was an effect of encapsulation of the hydrophobic moieties by the HP- β -CD truncated cone, thus deactivating the hydrophobic interactions. Addition of poly- β -CD to a solution of Alg-CONH-C₈ showed more complex behavior, where the solution viscosities depended on the both poly- β -CD and Alg-CONH-C₈ concentrations.

2.4.5 Attachment of cell signaling molecules

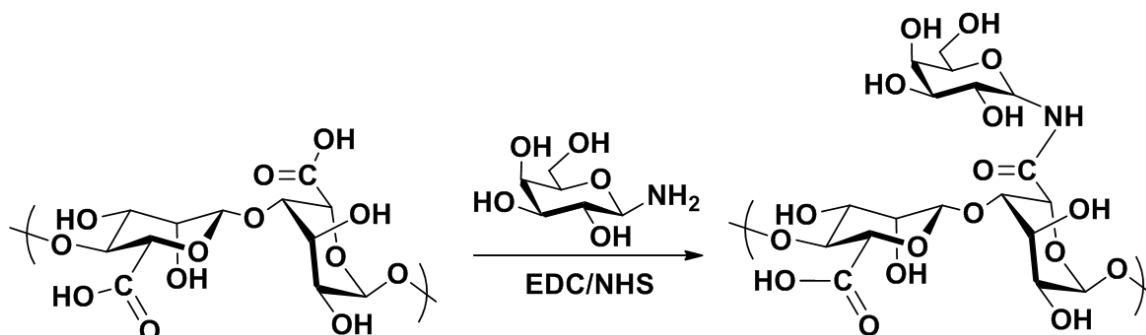
Alginates are important biomaterials in the area of bioengineering.⁷⁸ A critical requirement of such biomaterials is their ability to provide an environment that is both physically and chemically favorable to the presence of biological species such as living cells. In order to enhance the chemical interactions of alginate matrices with cells, they are functionalized with cell-specific ligands or extracellular signaling molecules. In addition to enhancement of the cellular interactions, functionalization may also play a role in controlling the growth,

differentiation and behavior of cells in culture. Alginates as biomaterials offer several advantages including hydrophilicity, biocompatibility and non-immunogenicity.⁷⁹ The ability of alginates to form gels capable of encapsulating cells, drugs and other biological entities is another important advantage for biological applications. However, a possible drawback is that cells do not adhere to alginates naturally. For that reason Mooney et al. have recently described alginates as “blank slates”.⁶ Chemical functionalization with cell signaling moieties is therefore crucial in order to overcome the low affinity of alginates to cell surfaces.

Skjåk-Bræk et al. reported the covalent attachment of galactose moieties to the alginate backbone for enhancement of hepatocyte cell recognition.⁸⁰ Hepatocytes perform a variety of metabolic functions in the normal liver. However, outside the liver they lose their function and are viable for only short time periods. The presence of an anchor material that provides mechanical support and immunoprotection to the cells prevents such loss of functionality and cell death. Alginates with their unique gel forming ability are considered very good matrix materials, providing a suitable environment for sustaining hepatocytes outside the organism. The surface of hepatocyte cell membranes possesses an asialoglycoprotein receptor (ASGPR), which binds and internalizes glycoproteins with terminal β -galactosyl residues. Galactose modified alginates capable of ionic gelation were therefore synthesized to be used as biomaterials for improved encapsulation and adhesion of hepatocytes.

The synthesis was performed by reaction of the alginate carboxylic acid groups with 1-amino-1-deoxy- β -D-galactose (Gal-1-NH₂) using aqueous carbodiimide chemistry (**Scheme 2.13**). An EDC/N-hydroxysulfosuccinimide (NHS) coupling reagent was used. The EDC/NHS coupling mechanism is similar to that depicted in **Scheme 2.12**, except the O-acylated urea

derivative formed in the first step is stabilized by conversion into an amine reactive sulfo-NHS ester, thus increasing the efficiency of EDC mediated coupling.



Scheme 2.13: Reaction scheme for the synthesis of galactose substituted alginate

The maximum achievable DS (measured by $^1\text{H-NMR}$) was 0.36 using 1.5 equivalents of Gal-1- NH_2 per monosaccharide unit at pH 4.5. $^1\text{H-NMR}$ spectroscopy was also used to identify the positions at which galactose substitution occurred on the alginate backbone. For accurate assignments of the new peaks that appeared in the anomeric region after derivatization, it was essential to obtain $^1\text{H-NMR}$ spectra of polymannuronate, G-enriched alginate and polyalternating MG, and their corresponding galactose substituted derivatives. Three new signals appeared in the anomeric region upon galactosylamine modification; signal (A) was assigned to the H-1 proton of galactosylamine linked to G-residues, signal (B) was assigned to the H-1 proton of a galactosylamine substituents linked to M residues neighboring G residues, and signal (C) resulted from a non-anomeric proton which experienced a peculiar environment like that of galactose moieties linked to diaxial GG dyads. The areas of these peaks corresponded to the fraction of galactosylamine linked to G-residues (A), the fraction of galactosylamine linked to M residues in alternating sequences (B), and the amount of galactosylamine residues linked to G residues neighboring G residues (C). The difference between peaks A and C was then used to calculate the fraction of substitution on G residues in alternating sequences. The fraction of

substituted M residues neighboring M residues could not be calculated due to overlapping signals in the 4.60-4.80 ppm region.

The difficult nature of the analytical problem at hand is clearly evident through this example.⁸⁰ The alginate derivatives studied in this case were modified only at the carboxylic acid position on the backbone. Increasing complexity arises in the NMR spectra when substitution occurs on the two hydroxyl groups in addition to the carboxyl group. For the galactosylamine substituted alginates, the positional selectivity present at various DS values is shown in **Table 2.5**. Based on the data, it was concluded that at low DS values, the reaction was more selective to G residues; as higher DS values were attained; M residues participated in the reaction. In addition, G residues neighboring M residues were more reactive than G residues neighboring G residues.

Table 2.5: Substitution selectivity for alginates at various DS values, measured using 1H-NMR spectroscopy⁸⁰

DS	Total Substitution on G (%)	Total Substitution on M (%)	Substitution on G adjacent to M (%)	Substitution on G adjacent to G (%)	Substitution on M adjacent to G (%)	Substitution on M adjacent to M (%)
0.07	7	-	7	-	-	-
0.19	19	-	7.2	11.8	-	-
0.36	29	7	7.3	21.7	7	-

The ability of galactose substituted alginate derivatives to form gel beads was studied. Substitution of galactose sugar residues on the alginate backbone caused a reduction in the number of available carboxylic acid groups, and impacted the bead size. Having galactose side chains caused conformational disordering within gels, whereby the junctions formed were held less tightly compared to unmodified alginates. A result of this effect was that larger bead volumes were achieved due to a net gain in hydration. Galactose moieties also interfered with the

polymer chain packing process during gel formation. When the gel beads were dried and rehydrated, the kinetics and thermodynamics of swelling were affected. Larger volume increases during rehydration resulted at high DS values. An increase in the DS was also found to decrease the affinity of alginates towards Ca^{+2} ions. Cytotoxicity studies were performed which showed that all of these Gal-substituted alginate derivatives were non-toxic.

The conformational effects resulting from the introduction of galactose moieties on the alginate backbone were studied using intrinsic viscosity, radius of gyration and chiro-optical property measurements.⁸¹ Galactose substitution on the alginate backbone led to a complex conformational change in solution. The presence of a fairly large moiety such as galactose in close proximity to the alginate backbone altered the conformational space available to the backbone. Additionally, when G residues in alternating sequences were substituted, the chain adopted a less extended conformation compared to the substitution of G residues in homopolymeric sequences. A decrease in the hydrodynamic radius was therefore observed at low DS values, when G residues neighboring M residues were substituted. As the DS value increased, G residues neighboring other G residues were substituted, and an increase in the hydrodynamic properties occurred.

Although galactose moieties were covalently attached to the alginate backbone, substitution on both M and G units was disadvantageous due to the loss of mechanical properties for the alginate gels. Skjåk-Bræk et al. therefore reported a method combining a chemical and enzymatic approach to achieve selective substitution on M residues.⁸² Since G units were not galactosylated, the mechanical properties of the ionotropic gels formed were not altered. A reaction scheme similar to that shown in **Scheme 2.13** was used wherein polymannuronan (with no G residues) was galactosylated first. Galactosylated polymannuronan was then subjected to

two different epimerase enzyme catalyzed reactions in a sequential fashion - AlgE4 and AlgE6. The function of the AlgE4 enzyme was to introduce long alternating MG sequences, while the function of AlgE6 was to introduce G-block sequences within the galactosylated polymannuronan backbone. Both enzymes catalyzed the epimerization of only those M residues that were not previously galactosylated. Therefore, all G residues introduced by epimerization were unsubstituted, and thus available for gel formation.

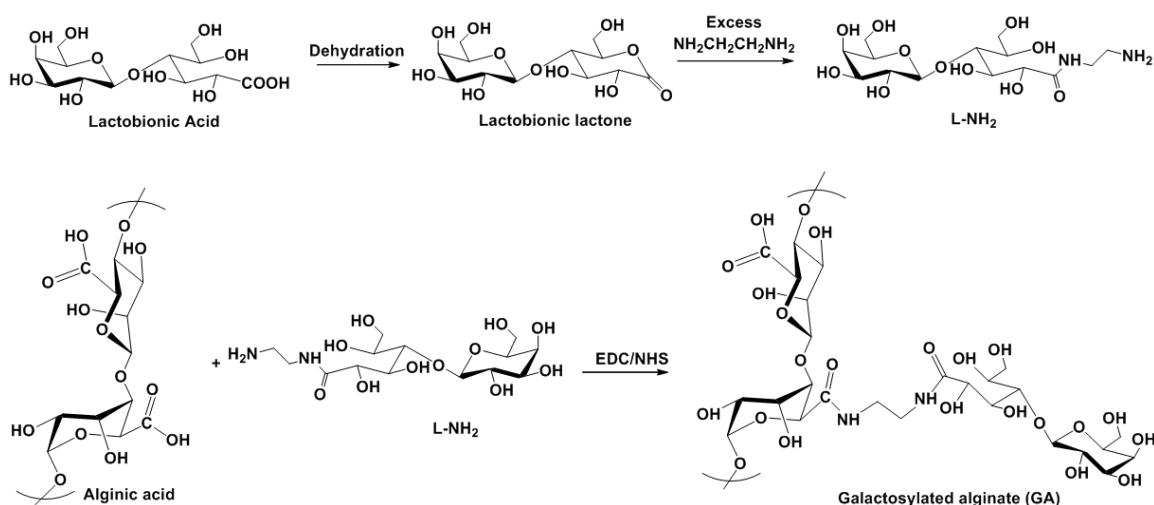
¹H-NMR spectroscopy was used to analyze the substitution patterns on the alginate backbone and to calculate the DS. Galactosylation of polymannuronan yielded a product with DS of 0.12. On introducing alternating MG sequences, a new signal at ~5.07 ppm appeared from the anomeric protons of the newly introduced G units. Relative peak area calculations for this peak showed that the F_G value was 0.33. While M residues neighboring unsubstituted M residues were epimerized to G residues, those neighboring galactosylated M residues did not epimerize. Enzyme activities were determined for both epimerization reactions using ratios of the experimentally achieved F_G , and theoretically calculated maximum achievable F_G values. Enzyme activity for the first step (AlgE4) was 86%, but dropped to 21% for the second epimerization (AlgE6) step. The monomer and dyad fractions calculated for all three derivatives are shown in **Table 2.6**.

Table 2.6: Monomer and dyad compositions of galactosylated polymannuronan derivatives after epimerization⁸²

Alginate	F_G	F_M	F_{GG}	$F_{GM/MG}$	F_{MM}
Galactosylated polymannuronan (MGal)	0	1	0	0	1
AlgE4 Treated MGal (MGalE4)	0.33	0.67	0	0.33	0.34
AlgE6 Treated MGalE4 (MGalE4E6)	0.45	0.55	0.16	0.29	0.26

To better understand the effect of the presence of galactose moieties on the epimerization reaction, galactosylated polymannuronan with a spacer group present between the galactose unit and mannuronan residue was synthesized. Carboxylic acid groups of mannuronic acid were coupled to *p*-aminophenyl- β -D-galactopyranoside (pNH₂Ph β Gal) using EDC/NHS coupling. The rigid spacer group did not significantly alter the epimerization of unmodified M residues. In addition, the amide bond was intact after exposure to both enzymes AlgE4 and AlgE6. Gel studies were performed with the galactosylated alginates. When the only source of G residues was from MG alternating sequences, the gels formed were based on the formation of interchain junctions. However, when the source of G residues was both MG alternating sequences and G-block sequences, “egg-box” (**Figure 2.5(A)**) structures were formed. The introduction of galactose units selectively on M residues caused faster gelling and higher gel strength compared to when galactose units were attached to both G and M residues. For gels that contained galactose units only on M residues, the alginate chains associated laterally with each other. This was contrary to gels made from alginates bearing galactosyl groups on both M and G residues, where the bulky galactose units on G residues sterically hinder lateral association among chains. Selective galactosylation of M residues also provided gels that were more stable to saline solutions, critical to in vivo performance.

Akaike et al. reported a strategy to galactosylate alginate using lactobionic lactone and ethylenediamine⁸³ (**Scheme 2.14**). Lactobionic acid was dehydrated to give lactobionic lactone in the first step. Then the lactone was reacted with excess ethylenediamine to form the monoamine terminated lactobionic lactone (L-NH₂). The free primary amine groups of L-NH₂ were then coupled with the carboxylic acid groups on the alginate backbone mediated by EDC/NHS. This afforded galactosylated alginates (GA) with DS 0.26 (elemental analysis).

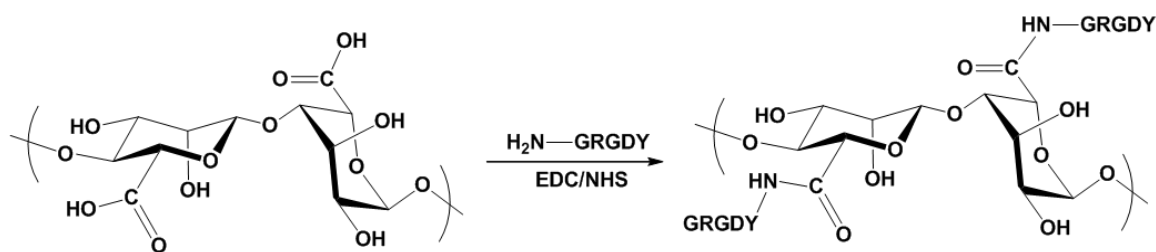


Scheme 2.14: Reaction scheme for the synthesis of galactosylated alginate (GA) using lactobionic lactone

The attachment of hepatocytes on to a GA coated polystyrene (PS) dish was studied. Hepatocyte attachment to GA was 55%, compared to 3% for PS coated with unmodified alginate. This clearly demonstrated that enhancement in hepatocyte attachment was caused by the linking of galactose residues to alginate. Furthermore, the number of hepatocytes attached was greater when the density of galactose residues on the GA coated surface was higher. Specific interaction of hepatocyte surfaces with galactose moieties was verified by poly-N-*p*-vinylbenzyl-D-lactoneamide (PVLA) competitive binding assay. The hepatocyte cells were encapsulated within calcium crosslinked GA gels. In order to maintain cell stability and liver-specific functions, the formation of three-dimensional hepatocyte spheroids within the anchoring matrix is essential. For calcium alginate gels formed using GA, more than 80% of the cells were found to aggregate forming uniformly distributed multicellular spheroids. In addition, aggregation increased as epidermal growth factor (EGF) and insulin were added. For calcium alginate gels formed using unmodified alginates, the hepatocyte cells did not aggregate. Hepatocytes are anchorage sensitive cells, which means that their functions in vitro and in vivo are regulated by

cell anchorage and cell aggregation.⁸⁴ GA thus enhanced liver related functions in encapsulated hepatocyte cells. Gels made from GA also showed higher cell viability compared to unmodified alginates.

Mooney et al. reported the linking of GRGDY cell adhesion peptide to alginates for enhancement of their interactions with mouse skeletal myoblasts.⁸⁵ Amine functional peptides were attached to the alginate carboxylic acid groups using EDC/NHS coupling (**Scheme 2.15**). The interaction of C2C12 mouse skeletal myoblasts with GRGDY containing alginates was studied. Myoblast cells seeded on to GRGDY-coupled alginate hydrogels attached and spread on the surface, while no attachment was observed on unmodified alginate control surfaces. The observed myoblast adhesion was a result of specific interactions with the GRGDY peptide sequences. Even though significant cell spreading occurred, the number of cells did not increase within the first 24 hours of seeding. At day 3, the number of cells increased slightly and reached an upper limit. Thereafter the number of cells decreased. This decrease was a result of the fusion of myoblasts into multinucleated microfibrils, an important step in the pathway to skeletal muscle differentiation.



Scheme 2.15: Reaction scheme for the synthesis of GRGDY containing alginates

Mooney et al. also reported the effect of variation of GRGDY ligand density and alginate M/G ratio on proliferation and differentiation of C2C12 skeletal myoblast cells.⁸⁶ With an increase in the alginate G-content, cell proliferation increased significantly. In addition, alginates

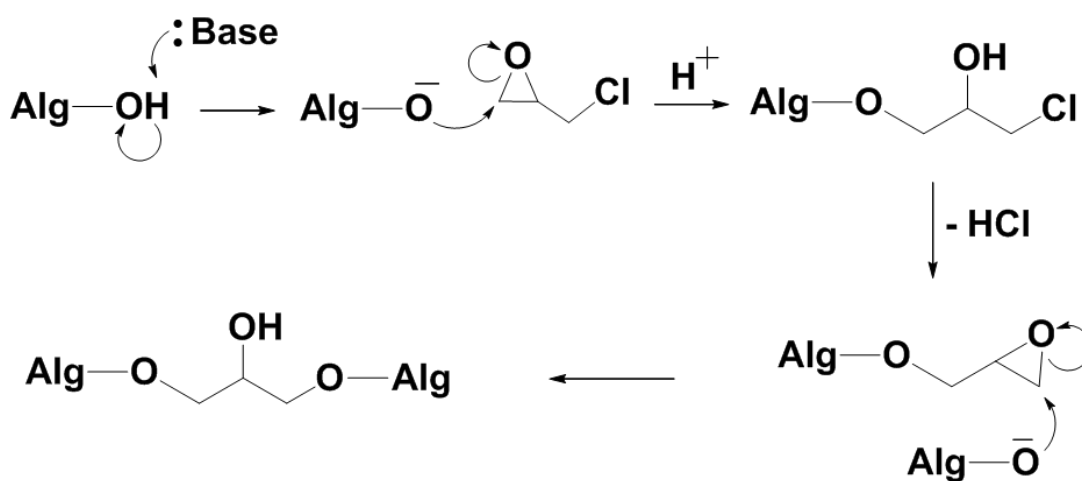
with high G-contents promoted extensive fusion of the myoblasts causing a corresponding increase in the levels of muscle creatine kinase (MCK) activity over time. Cell proliferation and differentiation was also dependent on the ligand density present on the alginate backbone. As the ligand density increased, the proliferation and spreading of myoblast cells improved and an increase in the cell count was recorded.

2.4.6 Covalent crosslinking of alginates

Ionic crosslinking of alginates in the presence of divalent cations is well known.⁸⁷ Such physical gels are used in a variety of areas including textile printing, paper coating, wound dressing, food additives and biotechnology.⁸⁸⁻⁸⁹ While the ionic gels are of great interest, covalent crosslinking of alginates yields matrices with improved mechanical properties. Ionic alginate gels are known to have limited stability in vivo. In physiological media, ion exchange with monovalent ions causes destabilization and rupture of the gel.⁹⁰ Chemical crosslinking is an attractive strategy for overcoming this drawback by creating more stable and robust networks. The methods used for covalent crosslinking of alginates and their applications are therefore reviewed.

Cascone et al. reported chemical crosslinking of alginates to make beads for affinity and ion exchange chromatography.⁹¹ In an ion exchange material, availability of the carboxylic acid groups on the alginate backbone is necessary. The carboxylic acid groups in Ca-alginate gels participate in ion crosslinking and are thus not available for ion exchange. Covalent crosslinking by reaction of the alginate hydroxyl groups for network formation is therefore essential for this application. This was achieved by reacting Ca-alginate beads with epichlorohydrin in the presence of aqueous NaOH. Calcium was later removed by multiple

treatments with sodium citrate solutions. Covalent polysaccharide network formation using epichlorohydrin is well known, and has been reported for starch and cellulose.⁹²⁻⁹⁴ The proposed mechanism for alginate crosslinking using epichlorohydrin is shown in **Scheme 2.16**. The crosslinked alginate beads were stable between a pH range of 1-13 and from 0-100 °C. They were also stable in high ionic strength media and polar solvents. In addition, large improvements in mechanical and chemical resistance properties were observed for covalently crosslinked alginates compared to Ca-alginate gels.



Scheme 2.16: Mechanism for alginate crosslinking using epichlorohydrin

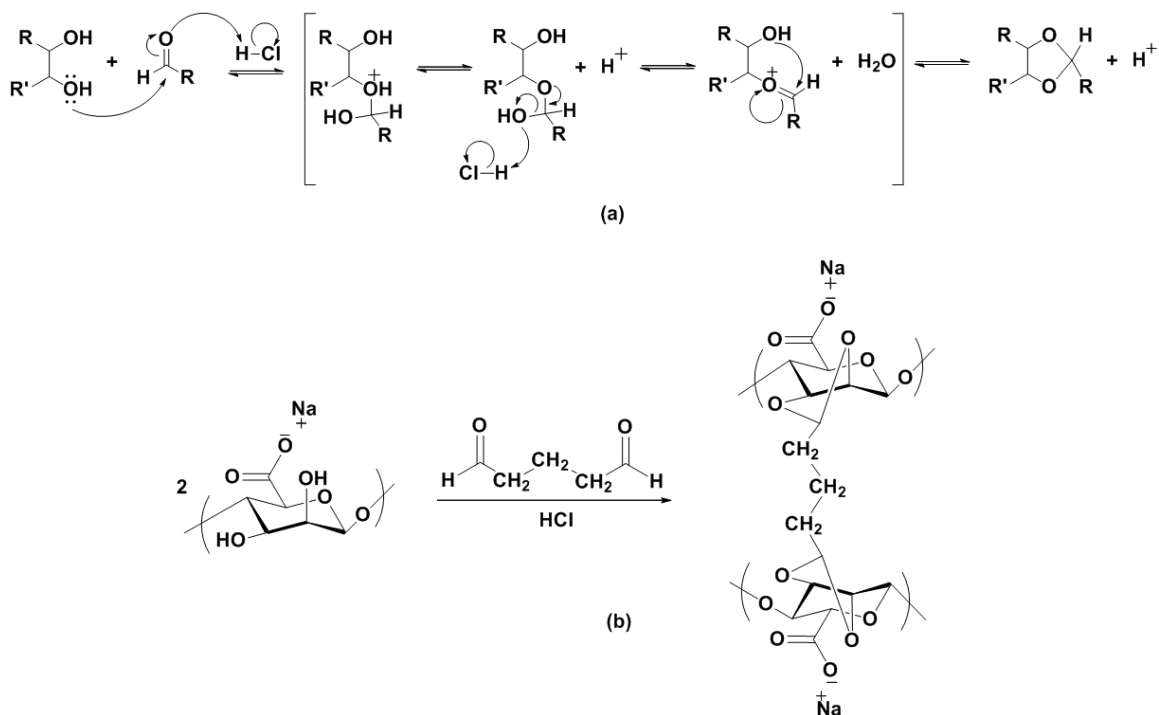
Skjåk-Bræk et al. reported base catalyzed covalent crosslinking of alginates with epichlorohydrin to form superswelling materials.⁹⁵ Ca-alginate beads were first prepared in water and the solvent was exchanged with 96% ethanol. The crosslinking reaction was performed by suspending the Ca-alginate beads in ethanol containing epichlorohydrin and NaOH. The synthesized beads were able to swell up to 100 times their dry volume without mass loss. Volume increase during re-swelling of dried beads was unaffected by the presence of non-ionic solutes such as glucose and glycerol. Ionic solutes such as NaCl and Na-galacturonate slightly

reduced the extent of volume increase. However, the reduction in degree of swelling due to the presence of ionic solutes was significantly lower in magnitude compared to synthetic superswelling materials like crosslinked polyacrylic acid.

Skjåk-Bræk et al. also studied the swelling behavior of covalently crosslinked alginate beads in the presence of monovalent and divalent cations.⁹⁶ On swelling the beads in water, ion concentration in the interior of the bead was high compared to the exterior. When the beads were swelled with monovalent salt solutions, the difference in ion concentration between the exterior and interior was lower, and caused a marked decrease in bead volume with increasing salt concentrations. Swelling with salt solutions of divalent (crosslinking) ions like Ca^{+2} , Sr^{+2} and Ba^{+2} showed hysteresis in the swelling curves - a feature displayed due to cation binding in alginate gels. This proved that alginates retain their ion-binding properties in the covalently linked state. By introducing divalent cations, physical crosslink sites were introduced in addition to the existing covalent linking sites, making stronger gels. Furthermore, the bead volume decreased as the pH of the swelling solution was reduced. Protonation of the alginate carboxylate groups at lower pH values reduced the difference between interior and exterior ion concentrations. This led to gel shrinkage. The change in gel volume as a function of ethanol addition showed that above a certain ethanol concentration, the gel transformed from a “dissolved” voluminous state to a “solid” compact state. A large volume decrease at high ethanol concentrations occurred due to precipitation-like behavior.

Yeom et al. reported the use of covalently crosslinked sodium alginate membranes for pervaporation separation.⁹⁷ Alginates are considered to be good membrane materials for dehydration of ethanol-water mixtures due to their ability to incorporate water into the hydrophilic membrane structure.⁹⁸ However, excess hydrophilicity may be disadvantageous as it

can cause low selectivity and poor membrane stability. Thus, chemical modification via covalent crosslinking was performed for membrane property enhancement. The *cis*-oriented vicinal hydroxyl groups at the C-2 and C-3 positions can react with glutaraldehyde to form acetal-linked alginate networks. **Scheme 2.17a** shows the mechanism for acid catalyzed acetal formation, while **Scheme 2.17b** shows the reaction scheme for glutaraldehyde crosslinking of alginates. Na-alginate films were first cast from aqueous solutions. The films were dried and reacted in an acetone solution containing glutaraldehyde and HCl. Crosslinking density in alginate films was controlled using the concentration of glutaraldehyde present in the reactive solution. Swelling measurements for the crosslinked films as well as Na-alginate films were performed in solutions containing varying ethanol:water ratios. The liquid volume fractions in Na-alginate films were higher compared to crosslinked films. In addition, crosslinked alginate films contained a higher fraction of ethanol compared to Na-alginate after absorption.



Scheme 2.17: (a) mechanism of acid catalyzed acetalization of vicinal hydroxyl groups, (b) reaction scheme for covalent crosslinking of Na-alginate using glutaraldehyde

Several reports on glutaraldehyde crosslinking of alginates for pervaporation separation have been described, wherein inorganic compounds such as zeolite, silicotungstic acid, aluminum-containing mesoporous silica and molecular sieves have been incorporated into the crosslinked network.⁹⁹⁻¹⁰³ Ko et al. demonstrated the use of glutaraldehyde crosslinked alginates to form superabsorbent fibers for use in disposable diapers and sanitary napkins.¹⁰⁴ Alginates crosslinked with divalent cations such as Ca^{+2} have low absorbency due to tightly packed junction points. Chemical crosslinking using glutaraldehyde enables high absorbency because linkers of adjustable lengths can be used to create crosslink junctions allowing more liquid to be absorbed. Saline absorption showed that an increase in the glutaraldehyde concentration caused a decrease in saline absorbency. Saline absorbency values were also dependent on the number of ionic groups present on the alginate. Deprotonation of the alginate acid groups increased saline absorbency by creation of a more hydrophilic environment. An important factor for application as superabsorbent materials is the extraction of uncrosslinked or partially crosslinked alginate chains into solution causing mass loss and reduction in absorbency. Reduced mass loss in synthetic urine solutions was reported compared to saline. Synthetic urine contains Ca^{+2} ions which result in the formation of ionic crosslinks in alginates. Ionic crosslinking in addition to the already existing covalent crosslinking helps in preventing the loss of alginate chains into solution.

Jegal et al. described the use of glutaraldehyde crosslinked Na-alginate membranes to separate the optical isomers of water-soluble α -amino acids (for example, mixtures of D-tryptophan and L-tryptophan).¹⁰⁵ Two important characteristics are required to create a membrane material for effective isomer separation – hydrophilicity and the presence of a large number of chiral centers. Alginates satisfy both requirements and are therefore suitable for

isomer separation. The degrees of alginate crosslinking and swelling govern the separation efficiency. Swelling increases the intermolecular distances of the molecules and makes larger chiral spaces. Such large chiral spaces are unsuitable as they allow the isomers to pass through without interaction with the chiral environment, resulting in low separation efficiency.

Riyajan et al. reported the use of a glutaraldehyde crosslinked alginate gel used for the encapsulation and controlled release of neem Azadirachtin-A (Aza-A).¹⁰⁶ Aza-A, an insecticidal tetranortriterpenoid, is highly unstable and degrades or isomerizes when exposed to light. One way to protect Aza-A from degradation is through microencapsulation within crosslinked alginate. The Aza-A entrapment efficiency was found to be a function of crosslinking time, wherein the efficiency decreased with increasing time. Beads crosslinked for shorter times swelled faster compared to the longer crosslinking times. The higher degree of crosslinking achieved by longer reaction times resulted in better control over the release properties of Aza-A. Entrapped Aza-A was released completely within 5, 10 and 25 hours in the case of beads crosslinked for 10, 20 and 30 min respectively. Controlled release from covalently crosslinked alginate matrices has been reported for other active molecules such neem seed oil (NSO).

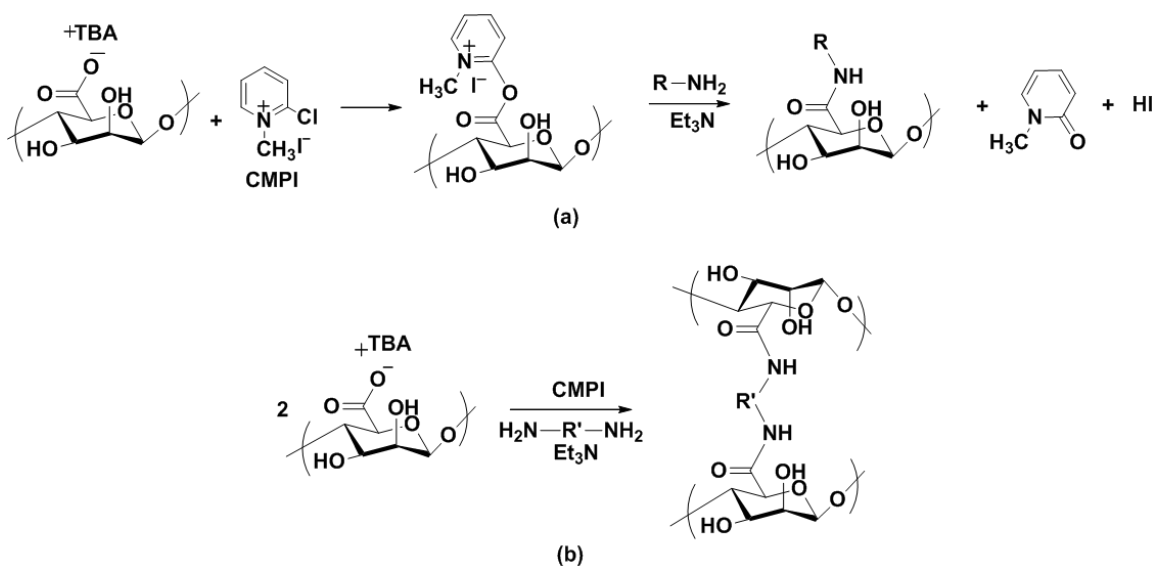
Neufeld et al. studied the reaction kinetics of alginate crosslinking by glutaraldehyde using equilibrium swelling measurements.¹⁰⁸ An equilibrium swelling model was used to calculate median pore sizes for the gels. The reaction rate was zero-order with respect to the alginate concentration, and independent of the alginate M/G composition and sequences. Thus, both M and G were equally reactive towards glutaraldehyde. However, the reaction rate increased with an increase in the alginate molecular weight. Higher molecular weights caused lower mobility of chains, thus improving the probability of collision with glutaraldehyde. Reaction rate was second-order with respect to glutaraldehyde concentration and first-order with

respect to the acid catalyst concentration. Lower temperatures slowed the rate of network formation due to the high activation energy associated with acid catalyzed acetalization reactions.

Neufeld et al. later reported the synthesis of thermodynamically controlled alginate network gels having pH-responsive properties.¹⁰⁹ Thermodynamic gels were synthesized by allowing the crosslinking reaction to reach equilibrium. The reaction rate was zero-order with respect to the initial alginate concentration, but the critical gel time decreased at higher alginate concentrations. Higher alginate fraction in mixtures led to a corresponding increase in the hydroxyl group concentration. This improved the probability of collision with the crosslinking reagent to form the gel. The reaction kinetics were also affected by the addition of a cosolvent to the aqueous media. Up to 10-20% water-miscible organic solvents were added as cosolvents without precipitation. Dipolar aprotic cosolvents such as acetone, dioxane and DMSO increase the rate of acetalization compared to pure water. The rate increase was an effect of the differential solubility of glutaraldehyde between external solvent and the solvent present in the interior of gel beads. Dipolar protic cosolvents such as 1-propanol, ethanol and methanol decreased the rate of acetalization compared to pure water. Alcohol groups from the cosolvent reacted with glutaraldehyde, resulting in a competitive side reaction and causing a decrease in crosslinking reaction rate. The pH-responsive properties of the crosslinked alginate gels were studied by subjecting them to stepwise pH-stimuli, and measuring the corresponding dynamic swelling response. At pH = 7.8, the carboxylic acid groups were deprotonated leading to increased hydrophilicity and electrostatic repulsion. This caused expansion of the network into a swollen state. At pH = 1.2 the carboxylic acid groups were protonated leading to charge

neutralization and limited solubility. This caused a rapid chain rearrangement and gel contraction by the expulsion of water from the network.

Barbucci et al. reported covalent crosslinking of alginate by amide bond formation.¹¹⁰ Covalently crosslinked hydrogels thus formed were used for the treatment of traumatic disorders of the intervertebral disc (IVD). An important component of IVD is nucleus pulposus (NP), a type II collagen matrix consisting of chondrocyte cells along with proteoglycans such as versican and hyaluronan. The typically encountered hyal-based hydrogels have a disadvantage due to rapid enzymatic degradation. Therefore, alginate hydrogel materials were examined as potential materials for NP replacement. Na-alginate was first converted to TBA-alginate and then dissolved in DMF for reaction. 2-Chloro-N-methyl pyridinium iodide (CMPI) was used to activate the carboxyl groups. A reactive diamine was then used along with triethylamine catalyst to yield crosslinked alginates. **Scheme 2.18** shows the reaction mechanism for synthesis of the alginate amide derivative using CMPI as an activating agent, and **(b)** shows the crosslinking reaction using a diamine.

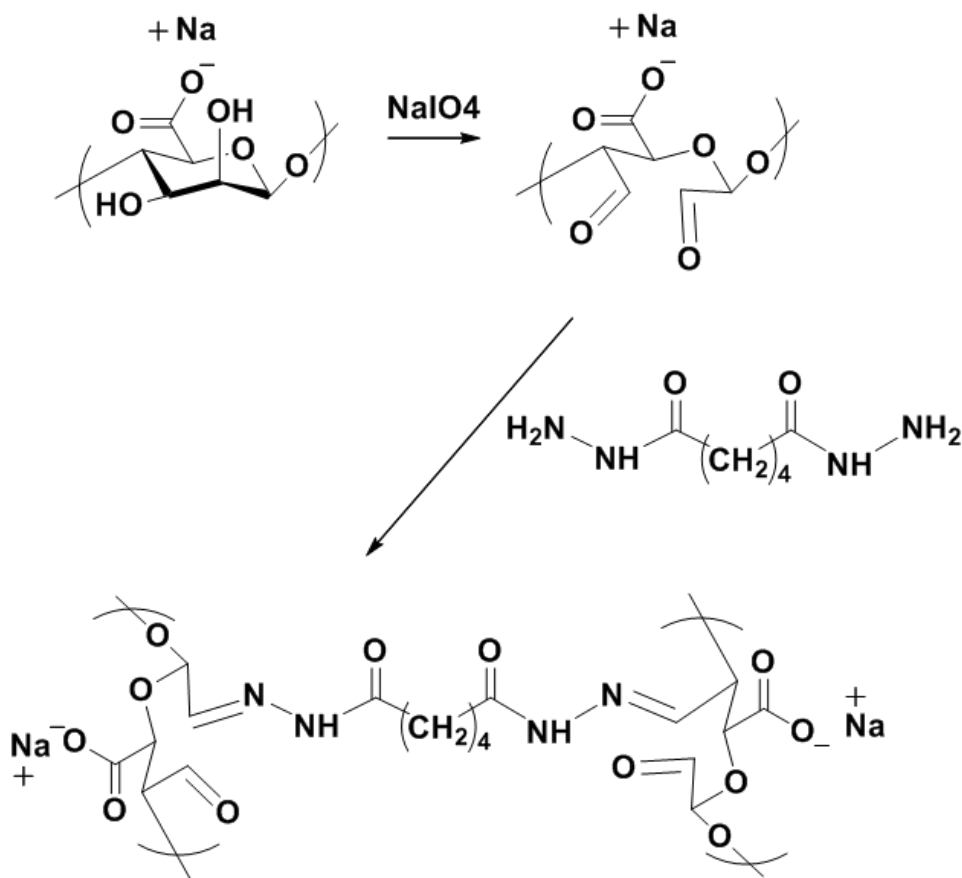


Scheme 2.18: (a) mechanism for the synthesis of alginate amide derivative using CMPI activating agent, and (b) alginate crosslinking reaction using bifunctional amine reagent

DS values were controlled using the CMPI stoichiometry. Water uptake and hydration kinetics revealed that the alginate hydrogel swelled up to 250%, while NP swelled up to 200%. Rheology studies showed a reversible sol-gel transition at a stress of 1270 Pa. This made the gels suitable for injection applications. Additionally, the modulus values for crosslinked alginate hydrogels were very close to those found in NP. Chondrocyte cells proliferated and maintained their ability to produce type II collagen within the alginate hydrogel matrix.

Johnson et al. reported the synthesis of crosslinked alginate hydrogels using water soluble carbodiimide chemistry.¹¹¹ Carboxylic acid groups on the alginate backbone reacted with hydroxyl groups to form a covalently crosslinked matrix. Na-alginate membranes were first cast from aqueous solutions, dried and then swollen in ethanol-water mixtures containing carbodiimide coupling reagent. An optimum water:ethanol ratio was essential for the reaction. At very low ethanol concentrations, sodium alginate membranes dissolved in the solvent mixture. At very low water concentrations, the carbodiimide coupling reagent was insoluble. The pH of crosslinking medium had a significant effect on final membrane swelling properties. At low pH values the carboxylic acid groups were protonated. Since the carbodiimide mediated coupling mechanism involves a protonated carboxylic acid, the crosslinking reaction was most efficient at low pH values. The degree of crosslinking increased with the carbodiimide concentration of the mixture and reached a stable value above 60 mM. The heats of fusion (ΔH_m) and melting points (T_m) of membranes crosslinked at various carbodiimide concentrations were measured. The ΔH_m values for crosslinked membranes were considerably larger than those of non-crosslinked membranes. Thus, crosslinking increased the crystalline character of the membranes.

Mooney et al. reported the synthesis of covalently crosslinked alginates by partial oxidation of the vicinal hydroxyl groups at the C-2 and C-3 positions.¹¹² Low molecular weight poly(guluronate) segments were partially oxidized using sodium periodate to form poly(aldehyde guluronate) [PAG], which was subsequently crosslinked using adipic dihydrazide (**Scheme 2.19**). The acyl hydrazone bonds linking the alginate chains were cleaved hydrolytically under aqueous conditions, making the gel degradable.



Scheme 2.19: Sodium alginate crosslinking using adipic dihydrazide via reaction with PAG

The degree of oxidation of alginate was controlled by varying the molar ratio of sodium periodate to uronate monosaccharides. With increasing dihydrazide concentration, a higher number of crosslinks were formed. However, the crosslinks involved both intermolecular and

intramolecular junctions. At an adipic dihydrazide concentration of 150 mM, an optimum number of intermolecular crosslink junctions was formed which maximized modulus value. The pH of the crosslinking mixture had a significant effect on the mechanical properties of the final gels. Crosslinking at pH 4.5 yielded gels with higher compressive moduli compared to pH 7.4. This was a result of optimal hydrazide reactivity towards aldehydes at low pH values. Compressive modulus values of the final gels were also controlled using the degree of oxidation of PAG, where an increased number of aldehyde groups on the PAG backbone yielded gels with higher modulus values.

2.4.7 Graft copolymerization of alginates

Graft copolymerization is a powerful method for modification of the physical and chemical properties of alginates. Grafting synthetic polymer chains to the alginate backbone can introduce hydrophobicity and steric bulkiness, which help protect the polysaccharide backbone from rapid dissolution and erosion. This in turn translates into a sustained release of active molecules from alginate matrices. Trivedi et al. reported the ceric ammonium nitrate (CAN)-induced grafting of poly(acrylonitrile) (PAN), poly(methyl acrylate) (PMA) or poly(methyl methacrylate) (PMMA) onto alginates.¹¹³ Homopolymer by-products were separated from the grafted alginates by solvent extraction. A comparison of the three different acrylate monomers showed that the grafting efficiency was highest for AN followed by MA followed by MMA. The homopolymer fractions formed showed a reverse trend where MMA polymerized to a greater extent compared to MA and AN. Similarly, Trivedi et al. reported alginate grafting using Fenton's reagent, another redox initiator system for grafting synthetic polymers onto alginates.¹¹⁴⁻¹¹⁵ An argument was presented wherein proton abstraction on the alginate backbone

was reported to have occurred by cleavage of the Alg-O-H bond to form Alg-O• radical. It may however be equally or more likely for proton abstraction to occur by cleavage of the ring C-H bonds giving rise to carbon centered radicals. It should be noted that for alginates as with other polysaccharides, grafting using a free radical initiator like CAN or Fenton's reagent is rather unselective, since all C-H bonds of the monosaccharides are labile due to the attached oxygen functionality. Therefore it can be expected that graft initiation points will occur at all monosaccharide carbons.

Singh et al. described the grafting of polyacrylamide (PAAm) onto alginates using a ceric-induced system.¹¹⁶⁻¹¹⁷ The advantage of using acrylamide (AAm) compared to AN, MA or MMA for radical grafting using CAN was that the homopolymer PAAm did not form in the mixture. In the case of AAm, radical formation takes place only on the alginate backbone leading exclusively to grafted products. PAAm grafted alginate (PAAm-g-Alg) was evaluated for its use as a commercial flocculant. The flocculation efficiency of the PAAm-g-Alg was studied for suspensions of kaolin, iron ore and coal fines, and its performance was found to be marginally better than that of commercial flocculants. Alginates containing longer PAAm grafts performed better than short grafts. Hydrolysis of the amide groups of PAAm-g-Alg was described through aqueous KOH treatment.¹¹⁸ When in contact with KOH under certain controlled conditions, the amide groups of PAAm-g-Alg can hydrolyze without causing alginate degradation. Hydrolyzed PAAm-g-Alg possessed enhanced flocculation and thickening characteristics vs. commercial flocculants.

Sa et al. reported the preparation of alginate based sustained release interpenetrating network (IPN) tablets.¹¹⁹ IPNs are formed when one polymer is crosslinked in the presence of another one. Such networks impart additional rigidity to simple crosslinked polymer matrices.

Alginate based IPNs were formed by mixing together Na-alginate with PAAm-g-Alg followed by Ca-crosslinking. The release of Diltiazem-HCl (DTZ) (a model water soluble drug) from the IPNs was studied. DTZ is a calcium channel blocker that is widely used for the treatment of angina pectoris, arrhythmia and hypertension. The DTZ release rate decreased as the ratio of PAAm-g-Alg:Na-alginate increased. Reduced swelling of the matrix and increased gel viscosity caused slow drug diffusion and hence sustained release.

Aminabhavi et al. described the glutaraldehyde crosslinking of PAAm-g-Alg to form membranes for pervaporation separation of water-isopropanol mixtures as well as water-tetrahydrofuran mixtures.¹²⁰⁻¹²¹ Li et al. reported the use of PMMA-g-Alg in forming composites with hydroxyapatite for the study of properties of the interface between the organic polymer and the inorganic material.¹²² Mollah et al. described an approach where 3-(trimethoxysilyl)propyl methacrylate was grafted onto Na-alginate to form films through casting. The films were soaked in a silane monomer mixture and were subsequently photocrosslinked to study the physico-mechanical properties of the networks formed.¹²³ Sa et al. described the synthesis of electrically responsive alginate based hydrogels by grafting PAAm to the backbone and subsequently hydrolyzing the amide.¹²⁴ Similar electro-responsive hydrogels were also described by Yang et al. by grafting poly(acrylic acid) (PAA) onto the alginate backbone.¹²⁵ The derivatives were used as transdermal drug delivery systems for ketoprofen, a model non-steroidal anti-inflammatory drug. On applying an electrical stimulus across the hydrogel, the positive counterion moved towards the negative electrode, but the negative carboxylate groups remained immobile. Consequently, an increased osmotic pressure near the positive electrode led to deswelling of the hydrogel, causing release of ketoprofen from the matrix. Kulkarni et al. also reported the use of hydrolyzed PAAm-g-Alg in forming IPNs with carboxymethyl cellulose (CMC) for the pH

dependent release of ketoprofen.¹²⁶ Pal et al. reported the use of microwave assisted synthesis for preparing PAAm-g-Alg polymers.¹²⁷ Liu et al. described the synthesis of PMMA-g-Alg using potassium ditelluratoargenate (III) as initiator.¹²⁸ Işıklan et al. reported the grafting of itaconic acid onto alginates using CAN as well as benzoyl peroxide initiators.¹²⁹⁻¹³⁰ Xiao et al. described the synthesis of polyvinyl alcohol grafted alginates (PVOH-g-Alg) to prepare ferromagnetic particles.¹³¹ Vinyl acetate (VAc) was first grafted to create PVAc-g-Alg which was subsequently hydrolyzed to yield PVOH-g-Alg. The resulting graft copolymer was physically crosslinked using Fe (II) ions. Fe (II) was subsequently oxidized to Fe (III), creating ferromagnetic microparticles containing entrapped Fe₃O₄.

Kadokawa et al. described a chemoenzymatic route to prepare amylose-grafted-alginates, and disintegrable beads thereof.¹³² Amylose can be prepared by a phosphorylase-catalyzed enzymatic polymerization initiated from a maltooligosaccharide primer. Thus, an amine functional maltooligosaccharide primer was first synthesized and attached to the alginate backbone via aqueous EDC/NHS coupling. Phosphorylase-catalyzed polymerization was then performed to propagate amylose chains from the alginate backbone (**Figure 2.14**). Amylose-g-Alg thus synthesized was used to form Ca-crosslinked gel beads containing entrapped fluorescein (a model dye). Release of the dye from the beads was studied as they were exposed to β -amylase, an enzyme that catalyzes amylose hydrolysis. Attachment of amylose chains impacted Ca-gel formation and for very long amylose chain lengths, gel formation did not occur. On β -amylase treatment, the gel beads disintegrated causing dye release.

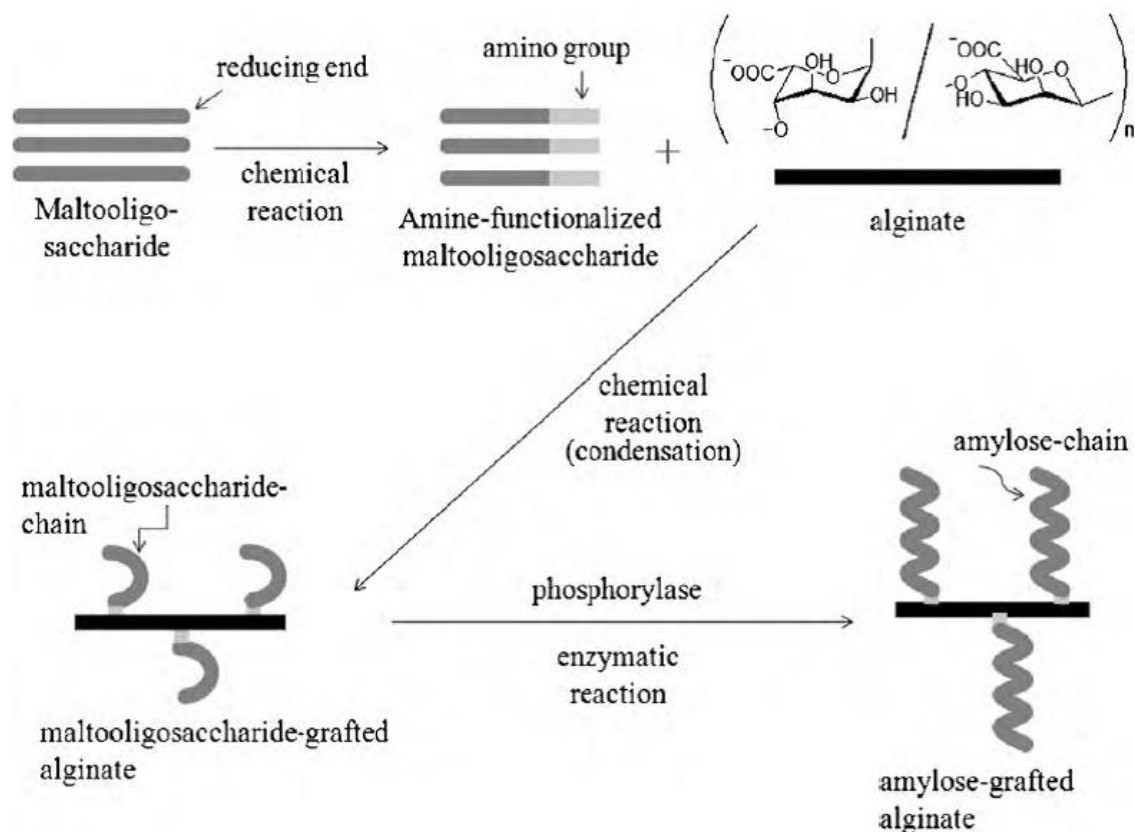


Figure 2.14: Schematic describing the synthesis of Amylose-g-Alg¹³²

Lee et al. described the grafting of poly(N-isopropylacrylamide) (PNIPAAm) to the alginate backbone to make temperature/pH responsive hydrogels.¹³³ PNIPAAm hydrogels are well known for their ability to show lower critical solution temperature (LCST) behavior in aqueous solutions at 32 °C. Alginates on the other hand show pH responsive behavior due to the presence of carboxylic acid groups on the backbone. The temperature and pH responsive properties of PNIPAAm and alginates were combined by a grafting technique. Amine terminal PNIPAAm (PNIPAAm-NH₂) was first synthesized and reacted with the carboxyl groups on the alginate backbone using EDC/NHS coupling. Hydrogel properties of bulk grafted PNIPAAm-g-Alg were compared to surface grafting of PNIPAAm onto Ca-hydrogel surfaces. Temperature dependent behavior of PNIPAAm-g-Alg hydrogels was evident through a noticeable decrease in

the swelling ratio above 30-35 °C. Such behavior was not observed in the case of non-grafted alginate gels. **Figure 2.15** shows a schematic representing the temperature dependent behavior of PNIPAAm-g-Alg hydrogels. The pH responsive behavior was evident through higher swelling ratios at increasing pH values due to chain expansion from the presence of ionic carboxylate groups on the backbone.

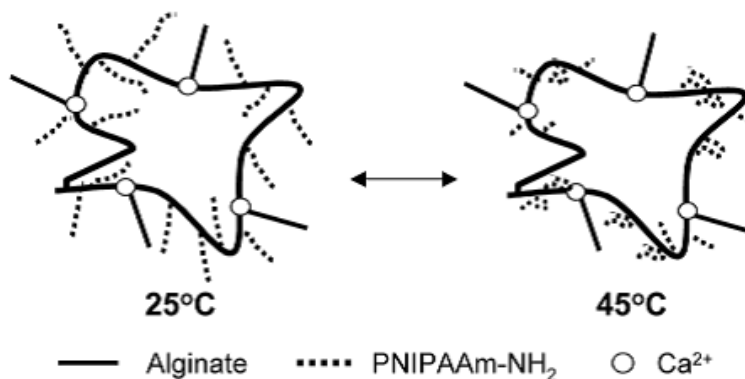
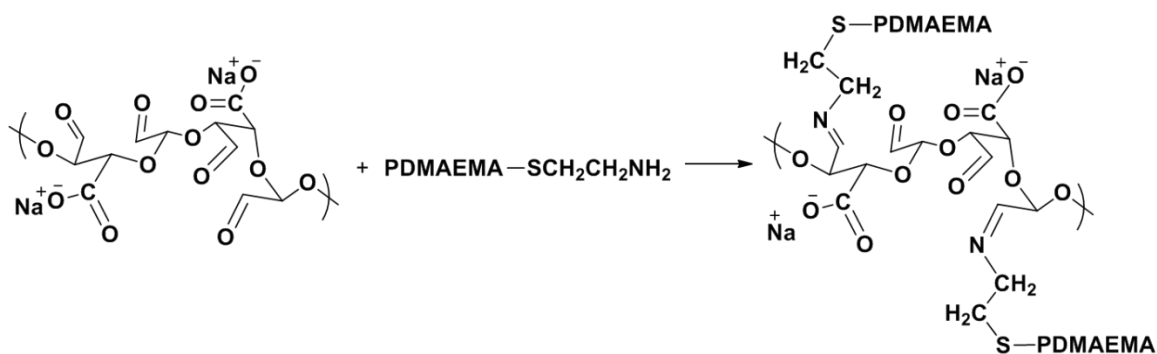


Figure 2.15: Schematic showing the temperature dependent behavior in PNIPAAm-g-Alg hydrogels¹³³

Liu et al. reported the grafting of poly((2-dimethylamino)ethyl methacrylate) (PDMAEMA) onto oxidized Na-alginate (OAlg) to study the in vitro controlled release behavior of BSA protein from the hydrogels.¹³⁴ PDMAEMA is a water soluble polymer with tertiary amine groups containing side chains, and exhibits LCST behavior. To use PDMAEMA for biomedical applications, the synthesis of PDMAEMA-g-OAlg hydrogel beads was described. As mentioned previously in this paper, Na-alginates do not degrade in aqueous media, but partially oxidized alginates do.⁶⁶ OAlg was therefore first synthesized from Na-alginate by periodate oxidation, wherein the vicinal 2-OH and 3-OH groups on the backbone were converted to aldehydes. The aldehyde groups were then reacted with amine terminal PDMAEMA to form a stable Schiff's base in the form of an imine (**Scheme 2.20**). Grafting of PDMAEMA chains to

the alginate chain allowed control over the equilibrium swelling ratio of hydrogels employing pH and ionic strength of the media. **Figure 2.16** shows an illustration of the swelling behavior. As the pH of the medium is increased above 3.0, ionization of the carboxylic acid groups takes place leading to the formation of polyelectrolyte complexes with the PDMAEMA cations. This causes a decrease in the equilibrium swelling ratio. Increasing the ionic strength (NaCl concentration) initially causes an increase in the swelling ratio due to disruption of the polyelectrolyte complexes, and later decreases the swelling ratio as the gel network is destroyed by Na-Ca ion exchange.



Scheme 2.20: Synthesis of PDMAEMA-g-OAlg

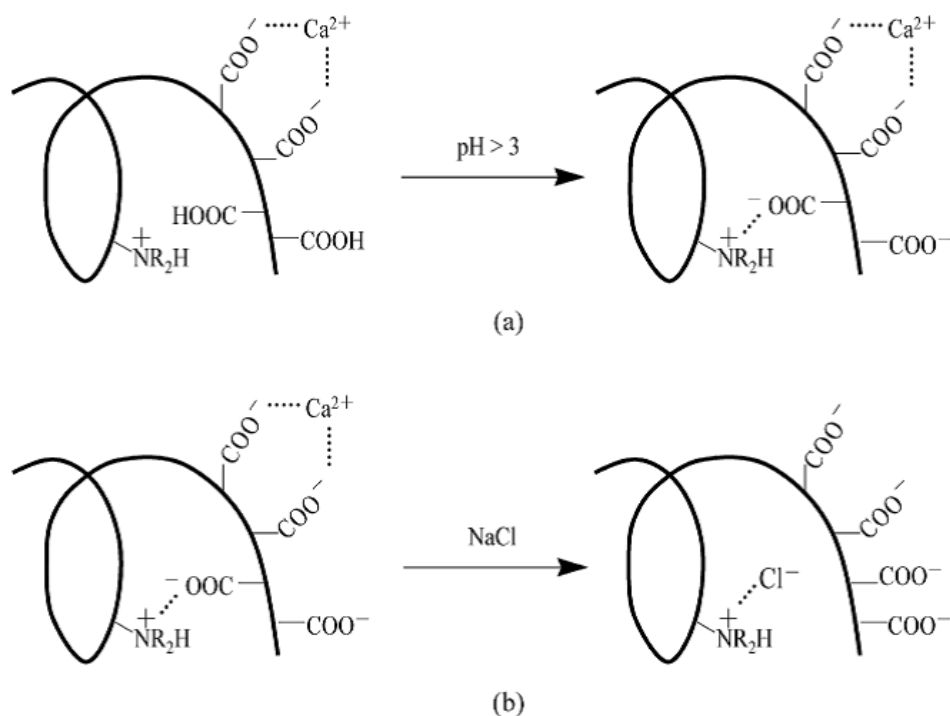


Figure 2.16: Schematic showing the effect of pH and ionic strength on PDMAEMA-g-OAlg hydrogels¹³⁴

2.5 Conclusions

Advances in the biochemistry of the complex alginate polysaccharides have provided opportunities to control monosaccharide *sequence* that are unique in polysaccharide chemistry¹³⁵. This provides insight into the structure-property relationships of alginates that can illuminate its important natural functions, for example in structural gels in kelp and in protective bacterial films made by *Pseudomonas aeruginosa* (which play a critical part in the progression of cystic fibrosis³). The developing ability to chemically modify alginate creates significant potential for tailoring alginate materials for particular applications. The ability of alginates to form hydrogels under mild pH and temperature conditions, along with the inherent biocompatibility of most alginates, makes these materials particularly attractive for biomedical

applications including drug delivery, tissue engineering, and implantation of protected living cells. More importantly, chemical derivatization is the most preferred method to create next generation alginate biomaterials having enhanced or altogether new properties. A thorough understanding of the chemistry of alginates is vital to this goal. Preparation of such tailored derivatives however has been limited by two main factors; the complete lack of organic solubility of alginic acid, and the proclivity for alginic acid to decompose under acidic, alkaline, and reductive conditions. Even so, the advent of carbonyl activating reagents that work in water, for example DCC and sulfonated N-hydroxysuccinimide, has permitted selective modification of the carboxyl groups of alginic acid. This permits not only modification of bulk properties like solubility, but also attachment of functional substituents like targeting ligands and fluorophores. Modification of the hydroxyl groups in aqueous media is more challenging, but has been accomplished under heterogeneous conditions, for example by gel acylation, and using techniques that can work in water, for example by acetal formation. The discovery of organic solvents for the tetrabutylammonium salts of alginic acid (TBAF in polar aprotic solvents) greatly expands the potential for alginate modification, encompassing a much wider variety of reagents. By analogy with cellulose¹³⁶, these new solvent systems should also enable enhanced exploration of chemoselectivity (e.g., OH vs. COOH reaction) and regioselectivity (M vs. G, 2-OH vs. 3-OH within each monosaccharide), because of the more selective reagents and milder conditions that are now possible. Such regio- and chemoselectivity should enable combined biochemical and chemical routes to alginate derivatives with exquisite control over both monosaccharide sequence and substitution position, to a degree unmatched in polysaccharide chemistry to date (the only comparable examples involve de novo synthesis of polysaccharides by laborious, standard carbohydrate chemistry involving multiple protection, deprotection and

glycosylation steps⁶²). In addition to the anticipation of progress against the important challenges of overcoming regiocontrol and chemoselectivity issues in alginate derivative synthesis, we can anticipate that researchers in the near future will be addressing analytical issues. The ability to use techniques like multidimensional NMR experiments, partial and full polysaccharide hydrolysis, combined LC/MS and GC/MS, and other spectroscopic and chromatographic techniques to give a more complete picture of substitution position and sequence will be essential accompaniment to the anticipated synthetic advances. In this way the great promise of alginates as biomaterials for biomedical and other applications can be fully realized.

2.6 References

1. Draget, K. I., Alginates. In *Handbook of Hydrocolloids*, Phillips, G. O., Williams, P.A., Ed. 2009; pp 379-395.
2. Boateng, J. S.; Matthews, K. H.; Stevens, H. N. E.; Eccleston, G. M., *J Pharm Sci-US* **2008**, 97 (8), 2892-2923.
3. Ramsey, D. M.; Wozniak, D. J., *Molecular Microbiology* **2005**, 56 (2), 309-22.
4. Zimmermann, H.; Shirley, S.; Zimmermann, U., *Current Diabetes Reports* **2007**, 7 (4), 314-320.
5. Ghidoni, I.; Chlapanidas, T.; Bucco, M.; Crovato, F.; Marazzi, M.; Vigo, D.; Torre, M.; Faustini, M., *Cytotechnology* **2008**, 58 (1), 49-56.
6. Lee, K. Y.; Mooney, D. J., *Prog. Polym. Sci.* **2012**, 37 (1), 106-126.

7. Soonshiong, P.; Feldman, E.; Nelson, R.; Heintz, R.; Yao, Q.; Yao, Z. W.; Zheng, T. L.; Merideth, N.; Skjåk-Bræk, G.; Espevik, T.; Smidsrød, O.; Sandford, P., *P Natl Acad Sci USA* **1993**, *90* (12), 5843-5847.
8. Hay, I. D.; Ur Rehman, Z.; Ghafoor, A.; Rehm, B. H. A., *J Chem Tech Biotech* **2010**, *85* (6), 752-759.
9. Remminghorst, U.; Rehm, B. H., *Biotechnol Lett* **2006**, *28* (21), 1701-12.
10. Gacesa, P., *Microbiology* **1998**, *144* (Pt 5), 1133-43.
11. Rehm, B. H. A.; Valla, S., *Appl Microbiol Biotechnol* **1997**, *48* (3), 281-288.
12. Franklin, M. J.; Ohman, D. E., *J Bacteriol* **2002**, *184* (11), 3000-7.
13. Franklin, M. J.; Douthit, S. A.; McClure, M. A., *J Bacteriol* **2004**, *186* (14), 4759-73.
14. Franklin, M. J.; Ohman, D. E., *J Bacteriol* **1993**, *175* (16), 5057-65.
15. Gimmetstad, M.; Sletta, H.; Ertesvag, H.; Bakkevig, K.; Jain, S.; Suh, S. J.; Skjåk-Bræk, G.; Ellingsen, T. E.; Ohman, D. E.; Valla, S., *J Bacteriol* **2003**, *185* (12), 3515-23.
16. Chitnis, C. E.; Ohman, D. E., *J Bacteriol* **1990**, *172* (6), 2894-900.
17. Franklin, M. J.; Chitnis, C. E.; Gacesa, P.; Sonesson, A.; White, D. C.; Ohman, D. E., *J Bacteriol* **1994**, *176* (7), 1821-30.
18. Zimmermann, U.; Klöck, G.; Federlin, K.; Hannig, K.; Kowalski, M.; Bretzel, R. G.; Horcher, A.; Entenmann, H.; Sieber, U.; Zekorn, T., *ELECTROPHORESIS* **1992**, *13* (1), 269-274.
19. Klöck, G.; Frank, H.; Houben, R.; Zekorn, T.; Horcher, A.; Siebers, U.; Wöhrle, M.; Federlin, K.; Zimmermann, U., *Applied Microbiology and Biotechnology* **1994**, *40* (5), 638-643.
20. Haug, A.; Larsen, B.; Smidsrød, O., *Acta Chem Scand* **1966**, *20*, 183-90.
21. Haug, A.; Larsen, B.; Smidsrød, O., *Acta Chem Scand* **1967**, *21*, 691-704.

22. Painter, T. J.; Smidsrød, O.; Haug, A., *Acta Chem Scand* **1968**, 22, 1637-48.
23. Larsen, B.; Smidsrød, O.; Painter, T. J.; Haug, A., *Acta Chem Scand* **1970**, 24, 726-8.
24. Smidsrod, O.; Whittington, S. G., *Macromolecules* **1969**, 2 (1), 42-44.
25. Penman, A.; Sanderson, G. R., *Carbohyd Res* **1972**, 25 (2), 273-282.
26. Grasdalen, H.; Larsen, B.; Smidsrød, O., *Carbohydr Res* **1979**, 68 (1), 23-31.
27. Grasdalen, H., *Carbohydr. Res.* **1983**, 118 (Jul), 255-260.
28. Pawar, S. N.; Edgar, K. J., *Biomacromolecules* **2011**, 12 (11), 4095-4103.
29. Sikorski, P.; Mo, F.; Skjåk-Bræk, G.; Stokke, B. r. T., *Biomacromolecules* **2007**, 8 (7), 2098-2103.
30. Donati, I.; Holtan, S.; Mørch, Y. A.; Borgogna, M.; Dentini, M.; Skjåk-Bræk, G., *Biomacromolecules* **2005**, 6 (2), 1031-40.
31. Morch, Y. A.; Donati, I.; Strand, B. L.; Skjak-Braek, G., *Biomacromolecules* **2006**, 7 (5), 1471-80.
32. Skjåk-Bræk, G.; Grasdalen, H.; Smidsrød, O., *Carbohydrate Polymers* **1989**, 10 (1), 31-54.
33. Draget, K. I.; Skjåk-Bræk, G.; Smidsrød, O., *Carbohydrate Polymers* **1994**, 25 (1), 31-38.
34. Timell, T. E., *Can. J. Chem.* **1964**, 42, 1456.
35. Smidsrød, O. H., A.; Larsen, B., *Acta Chem Scand* **1966**, 20, 1026-34.
36. Tsujino, I.; Saito, T., *Nature* **1961**, 192, 970-1.
37. Preiss, J.; Ashwell, G., *J Biol Chem* **1962**, 237 (2), 309-316.
38. Haug, A. L., B.; Smidsrød, O., *Acta Chem. Scand.* **1963**, 17, 1466-1468.
39. Haug, A. L., B.; Smidsrød, O., *Acta Chem. Scand.* **1967**, 21, 2859-2870.

40. Haug, A. L., B., *Acta Chem Scand* **1958**, 12, 650.
41. Smidsrød, O. H., A.; Larsen, B., *Acta Chem Scand* **1963**, 17, 1473.
42. Smidsrød, O. H., A.; Larsen, B., *Acta Chem Scand* **1963**, 17, 2628-2637.
43. Leo, W. J.; Mcloughlin, A. J.; Malone, D. M., *Biotechnol Progr* **1990**, 6 (1), 51-53.
44. Chamberlain, N. H., Cunningham, G.E., Speakman, J.B., *Nature* **1946**, 158, 553.
45. Wassermann, A., *J. Chem. Soc.* **1948**, 197.
46. Schweiger, R. G., *J. Org. Chem.* **1962**, 27 (5), 1786-1789.
47. Schweiger, R. G., *J. Org. Chem.* **1962**, 27 (5), 1789-1791.
48. Smidsrød, O.; Whittington, S. G., *Macromolecules* **1969**, 2 (1), 42-44.
49. Grasdalen, H.; Larsen, B.; Smidsrod, O., *Carbohydrate Research* **1979**, 68 (1), 23-31.
50. Grasdalen, H.; Larsen, B.; Smidsrød, O., *Carbohydr Res* **1977**, 56 (2), C11-C15.
51. Grasdalen, H.; Larsen, B.; Smidsrød, O., *Carbohydr Res* **1981**, 89 (2), 179-191.
52. Skjåk-Bræk, G.; Paoletti, S.; Gianferrara, T., *Carbohydr. Res.* **1989**, 185 (1), 119-129.
53. Skjåk-Bræk, G.; Zanetti, F.; Paoletti, S., *Carbohydrate Research* **1989**, 185 (1), 131-138.
54. Köhler, S.; Heinze, T., *Macromol. Biosci.* **2007**, 7 (3), 307-314.
55. Sun, H.; DiMagno, S. G., *J. Am. Chem. Soc.* **2005**, 127 (7), 2050-1.
56. Coleman, R. J.; Lawrie, G.; Lambert, L. K.; Whittaker, M.; Jack, K. S.; Grøndahl, L., *Biomacromolecules* **2011**, 12 (4), 889-897.
57. Alban, S.; Schauerte, A.; Franz, G., *Carbohydrate Polymers* **2002**, 47 (3), 267-276.
58. Linhardt, R. J., *J Med Chem* **2003**, 46 (13), 2551-2564.
59. Ronghua, H.; Yumin, D.; Jianhong, Y., *Carbohydrate Polymers* **2003**, 52 (1), 19-24.
60. Freeman, I.; Kedem, A.; Cohen, S., *Biomaterials* **2008**, 29 (22), 3260-3268.

61. Fan, L.; Jiang, L.; Xu, Y.; Zhou, Y.; Shen, Y.; Xie, W.; Long, Z.; Zhou, J., *Carbohydrate Polymers* **2011**, 83 (4), 1797-1803.
62. Gama, C. I.; Tully, S. E.; Sotogaku, N.; Clark, P. M.; Rawat, M.; Vaidehi, N.; Goddard, W. A.; Nishi, A.; Hsieh-Wilson, L. C., *Nat Chem Biol* **2006**, 2 (9), 467-473.
63. Rogers, C. J.; Clark, P. M.; Tully, S. E.; Abrol, R.; Garcia, K. C.; Goddard, W. A.; Hsieh-Wilson, L. C., *P Natl Acad Sci USA* **2011**, 108 (24), 9747-9752.
64. Carré, M.-C.; Delestre, C.; Hubert, P.; Dellacherie, E., *Carbohydr. Polym.* **1991**, 16 (4), 367-379.
65. Scott, J. E.; Tigwell, M. J.; Phelps, C. F.; Nieduszynski, I. A., *Carbohydrate Research* **1976**, 47 (1), 105-117.
66. Bouhadir, K. H.; Lee, K. Y.; Alsberg, E.; Damm, K. L.; Anderson, K. W.; Mooney, D. J., *Biotechnol Progr* **2001**, 17 (5), 945-950.
67. Marc Duval, J.; Delestre, C.; Carré, M.-C.; Hubert, P.; Dellacherie, E., *Carbohydrate Polymers* **1991**, 15 (3), 233-242.
68. Siquin, A.; Hubert, P.; Dellacherie, E., *Langmuir* **1993**, 9 (12), 3334-3337.
69. Maestro, A.; Gonzalez, C.; Gutierrez, J. M., *Journal of Rheology* **2002**, 46 (1), 127-143.
70. Siquin, A.; Hubert, P.; Dellacherie, E., *Polymer* **1994**, 35 (16), 3557-3560.
71. Siquin, A.; Houzelle, M. C.; Hubert, P.; Choplin, L.; Viriot, M. L.; Dellacherie, E., *Langmuir* **1996**, 12 (16), 3779-3782.
72. Siquin, A.; Hubert, P.; Marchal, P.; Choplin, L.; Dellacherie, E., *Colloids and Surfaces A: Physicochemical and Engineering Aspects* **1996**, 112 (2-3), 193-200.
73. Babak, V. G.; Skotnikova, E. A.; Lukina, I. G.; Pelletier, S.; Hubert, P.; Dellacherie, E., *J. Colloid Interface Sci.* **2000**, 225 (2), 505-510.

74. Pelletier, S.; Hubert, P.; Lapique, F.; Payan, E.; Dellacherie, E., *Carbohydr. Polym.* **2000**, *43* (4), 343-349.
75. Leonard, M.; Rastello de Boisseson, M.; Hubert, P.; Dellacherie, E., *Journal of Biomedical Materials Research Part A* **2004**, *68A* (2), 335-342.
76. Galant, C.; Kjoniksen, A. L.; Nguyen, G. T. M.; Knudsen, K. D.; Nystrom, B., *J. Phys. Chem. B* **2006**, *110* (1), 190-195.
77. Burckbuchler, V.; Kjoniksen, A. L.; Galant, C.; Lund, R.; Amiel, C.; Knudsen, K. D.; Nystrom, B., *Biomacromolecules* **2006**, *7* (6), 1871-1878.
78. Augst, A. D.; Kong, H. J.; Mooney, D. J., *Macromol Biosci* **2006**, *6* (8), 623-633.
79. Shapiro, L.; Cohen, S., *Biomaterials* **1997**, *18* (8), 583-590.
80. Donati, I.; Vetere, A.; Gamini, A.; Coslovi, A.; Campa, C.; Paoletti, S., *Biomacromolecules* **2003**, *4* (3), 624-631.
81. Donati, I.; Coslovi, A.; Gamini, A.; Vetere, A.; Campa, C.; Paoletti, S., *Biomacromolecules* **2004**, *5* (1), 186-196.
82. Donati, I.; Draget, K. I.; Borgogna, M.; Paoletti, S.; Skjåk-Bræk, G., *Biomacromolecules* **2005**, *6* (1), 88-98.
83. Yang, J.; Goto, M.; Ise, H.; Cho, C.-S.; Akaike, T., *Biomaterials* **2002**, *23* (2), 471-479.
84. Irwin, M. A., M.D., *The Liver: Biology and Pathobiology*. Fifth Edition ed.; 2009.
85. Rowley, J. A.; Madlambayan, G.; Mooney, D. J., *Biomaterials* **1999**, *20* (1), 45-53.
86. Rowley, J. A.; Mooney, D. J., *J. Biomed. Mater. Res.* **2002**, *60* (2), 217-223.
87. Mørch, Y. A.; Donati, I.; Strand, B. L.; Skjåk-Bræk, G., *Biomacromolecules* **2006**, *7* (5), 1471-80.

88. Draget, K. I. S., O.; Skjåk-Bræk, G., Alginates from Algae. In *Polysaccharides and Polyamides in the Food Industry: Properties, Production, and Patents*, Steinbüchel A.; Rhee, S. K., Ed. 2005; Vol. 1, pp 1-30.
89. Lee, K. Y.; Mooney, D. J., *Progress in Polymer Science* (0).
90. Thu, B.; Bruheim, P.; Espevik, T.; Smidsrød, O.; SoonShiong, P.; SkjakBraek, G., *Biomaterials* **1996**, 17 (11), 1069-1079.
91. Grasselli, M.; Diaz, L. E.; Cascone, O., *Biotechnol. Tech.* **1993**, 7 (10), 707-712.
92. Chang, C.; Zhang, L.; Zhou, J.; Zhang, L.; Kennedy, J. F., *Carbohydrate Polymers* **2010**, 82 (1), 122-127.
93. Zhou, J.; Chang, C.; Zhang, R.; Zhang, L., *Macromol Biosci* **2007**, 7 (6), 804-809.
94. Kartha, K. P. R.; Srivastava, H., *Starch/Stärke* **1985**, 37, 297-306.
95. Moe, S. T.; Skjåk-Bræk, G.; Smidsrød, O., *Food Hydrocolloids* **1991**, 5 (1-2), 119-123.
96. Moe, S. T.; Skjåk-Bræk, G.; Elgsaeter, A.; Smidsroed, O., *Macromolecules* **1993**, 26 (14), 3589-3597.
97. Yeom, C. K.; Lee, K.-H., *J. Appl. Polym. Sci.* **1998**, 67, 209-219.
98. Yeom, C. K.; Jegal, J. G.; Lee, K. H., *J Appl Polym Sci* **1996**, 62 (10), 1561-1576.
99. Patil, M. B.; Veerapur, R. S.; Bhat, S. D.; Madhusoodana, C. D.; Aminabhavi, T. M., *Desalination and Water Treatment* **2009**, 3 (1-3), 11-20.
100. Adoor, S. G.; Manjeshwar, L. S.; Bhat, S. D.; Aminabhavi, T. M., *Journal of Membrane Science* **2008**, 318 (1-2), 233-246.
101. Teli, S. B.; Gokavi, G. S.; Sairam, M.; Aminabhavi, T. M., *Separation and Purification Technology* **2007**, 54 (2), 178-186.

102. Patil, M. B.; Veerapur, R. S.; Patil, S. A.; Madhusoodana, C. D.; Aminabhavi, T. M., *Separation and Purification Technology* **2007**, 54 (1), 34-43.
103. Bhat, S. D.; Mallikarjuna, N. N.; Aminabhavi, T. M., *Journal of Membrane Science* **2006**, 282 (1-2), 473-483.
104. Kim, Y.-J.; Yoon, K.-J.; Ko, S.-W., *J. Appl. Polym. Sci.* **2000**, 78 (10), 1797-1804.
105. Kim, J. H.; Jegal, J.; Kim, J. H.; Lee, K. H.; Lee, Y., *J. Appl. Polym. Sci.* **2003**, 89 (11), 3046-3051.
106. Riyajan, S.-A.; Sakdapipanich, J., *Polym. Bull.* **2009**, 63 (4), 609-622.
107. Kulkarni, A. R.; Soppimath, K. S.; Aminabhavi, T. M.; Dave, A. M.; Mehta, M. H., *Journal of Controlled Release* **2000**, 63 (1-2), 97-105.
108. Chan, A. W.; Whitney, R. A.; Neufeld, R. J., *Biomacromolecules* **2008**, 9 (9), 2536-45.
109. Chan, A. W.; Whitney, R. A.; Neufeld, R. J., *Biomacromolecules* **2009**.
110. Leone, G.; Torricelli, P.; Chiumiento, A.; Facchini, A.; Barbucci, R., *J. Biomed. Mater. Res.-A* **2008**, 84A (2), 391-401.
111. Xu, J. B.; Bartley, J. P.; Johnson, R. A., *J. Appl. Polym. Sci.* **2003**, 90 (3), 747-753.
112. Bouhadir, K. H.; Hausman, D. S.; Mooney, D. J., *Polymer* **1999**, 40 (12), 3575-3584.
113. Shah, S. B.; Patel, C. P.; Trivedi, H. C., *Carbohydrate Polymers* **1995**, 26 (1), 61-67.
114. Shah, S. B.; Patel, C. P.; Trivedi, H. C., *Journal of Applied Polymer Science* **1994**, 51 (8), 1421-1426.
115. Shah, S. B.; Patel, C. P.; Trivedi, H. C., *Journal of Applied Polymer Science* **1994**, 52 (7), 857-860.
116. Tripathy, T.; Pandey, S. R.; Karmakar, N. C.; Bhagat, R. P.; Singh, R. P., *Eur Polym J* **1999**, 35 (11), 2057-2072.

117. Tripathy, T.; Singh, R. P., *Journal of Applied Polymer Science* **2001**, *81* (13), 3296-3308.
118. Biswal, D. R.; Singh, R. P., *Journal of Applied Polymer Science* **2004**, *94* (4), 1480-1488.
119. Mandal, S.; Basu, S. K.; Sa, B., *Carbohydrate Polymers* **2010**, *82* (3), 867-873.
120. Toti, U. S.; Aminabhavi, T. M., *Journal of Applied Polymer Science* **2004**, *92* (3), 2030-2037.
121. Kurkuri, M. D.; Kumbar, S. G.; Aminabhavi, T. M., *Journal of Applied Polymer Science* **2002**, *86* (2), 272-281.
122. Yang, W.; Zhang, L.; Wu, L.; Li, J.; Wang, J.; Jiang, H.; Li, Y., *Carbohydrate Polymers* **2009**, *77* (2), 331-337.
123. Mollah, M. Z. I.; Khan, M. A.; Hoque, M. A.; Aziz, A., *Carbohydrate Polymers* **2008**, *72* (2), 349-355.
124. Kulkarni, R. V.; Setty, C. M.; Sa, B., *Journal of Applied Polymer Science* **2010**, *115* (2), 1180-1188.
125. Yang, S.; Liu, G.; Cheng, Y.; Zheng, Y., *Journal of Macromolecular Science, Part A* **2009**, *46* (11), 1078-1082.
126. Kulkarni, R. V. S., B., *Current Drug Delivery* **2008**, *5*, 256-264.
127. Sen, G.; Singh, R. P.; Pal, S., *Journal of Applied Polymer Science* **2010**, *115* (1), 63-71.
128. Liu, Y.; Yang, L.; Li, J.; Shi, Z., *Journal of Applied Polymer Science* **2005**, *97* (4), 1688-1694.
129. Işıklan, N.; Kurşun, F.; İnal, M., *Journal of Applied Polymer Science* **2009**, *114* (1), 40-48.
130. Işıklan, N.; Kurşun, F.; İnal, M., *Carbohydrate Polymers* **2010**, *79* (3), 665-672.
131. Ma, P.; Xiao, C.; Li, L.; Shi, H.; Zhu, M., *Eur Polym J* **2008**, *44* (11), 3886-3889.

132. Omagari, Y.; Kaneko, Y.; Kadokawa, J.-i., *Carbohydrate Polymers* **2010**, 82 (2), 394-400.
133. Kim, J. H.; Lee, S. B.; Kim, S. J.; Lee, Y. M., *Polymer* **2002**, 43 (26), 7549-7558.
134. Gao, C.; Liu, M.; Chen, S.; Jin, S.; Chen, J., *Int J Pharm* **2009**, 371 (1-2), 16-24.
135. Morch, Y. A.; Donati, I.; Strand, B. L.; Skjak-Braek, G., *Biomacromolecules* **2007**, 8 (9), 2809-14.
136. Fox, S. C.; Li, B.; Xu, D.; Edgar, K. J., *Biomacromolecules* **2011**, 12, 1956-1972.

2.7 Copyright Authorization

6/5/13

Rightslink Printable License

ELSEVIER LICENSE TERMS AND CONDITIONS

Jun 05, 2013

This is a License Agreement between Siddhesh N Pawar ("You") and Elsevier ("Elsevier") provided by Copyright Clearance Center ("CCC"). The license consists of your order details, the terms and conditions provided by Elsevier, and the payment terms and conditions.

All payments must be made in full to CCC. For payment instructions, please see information listed at the bottom of this form.

Supplier	Elsevier Limited The Boulevard, Langford Lane Kidlington, Oxford, OX5 1GB, UK
Registered Company Number	1982084
Customer name	Siddhesh N Pawar
Customer address	240 ICTAS Building on Stanger St. Blacksburg, VA 24061
License number	3154821352987
License date	May 23, 2013
Licensed content publisher	Elsevier
Licensed content publication	Biomaterials
Licensed content title	Alginate derivatization: A review of chemistry, properties and applications
Licensed content author	Siddhesh N. Pawar, Kevin J. Edgar
Licensed content date	April 2012
Licensed content volume number	33
Licensed content issue number	11
Number of pages	27
Start Page	3279
End Page	3305
Type of Use	reuse in a thesis/dissertation
Portion	full article
Format	both print and electronic
Are you the author of this Elsevier article?	Yes
Will you be translating?	No
Order reference number	

<https://s100.copyright.com/CustomerAdmin/PLF.jsp?ref=c95212c-2d2c-4610-b971-2771784f3478>

1/5

Chapter 3: Organic Dissolution of Alginates and Epimer-selective Acetylation Thereof

(Used with permission of The American Chemical Society: *Pawar S.N., Edgar K.J.*

Biomacromolecules 2011; 12(11):4095-4103)

3.1 Abstract

Alginates are (1→4) linked linear copolysaccharides composed of β -D-mannuronic acid (M) and its C-5 epimer, α -L-guluronic acid (G). Several strategies to synthesize organically modified alginate derivatives have been reported, but almost all chemistries are performed in either aqueous or aqueous-organic media. The ability to react alginates homogeneously in organic solvents would open up access to a wide range of new chemistries and derivatives. However, past attempts have been restricted by the absence of methods for alginate dissolution in organic media. We therefore report a strategy to dissolve tetrabutylammonium (TBA) salts of alginic acid in polar aprotic solvents containing tetrabutylammonium fluoride (TBAF). Acylation of TBA-alginate was performed under homogeneous conditions, such that both M and G residues were acetylated up to a total degree of substitution (DS) \approx 1.0. Performing the same reaction under heterogeneous conditions resulted in selective acylation of M residues. Regioselectivity in the acylated alginate products was studied and degradation under basic reaction conditions was probed.

3.2 Introduction

Alginates are unbranched polysaccharide copolymers consisting of 1→4 linked β-D-mannuronic acid (M) and its C-5 epimer α-L-guluronic acid (G). The natural copolymer is an important component of algae such as kelp, and is also an exopolysaccharide of bacteria including *Pseudomonas aeruginosa*. It is comprised of sequences of M (M-blocks) and G (G-blocks) residues interspersed with MG sequences (MG-blocks). Alginates are derived from either algal or bacterial sources. The copolymer composition, sequence and molecular weights vary with the source and species that produce the copolymer. Due to the abundance of algae in water bodies, there is a large amount of alginate material present in nature. While industrial alginate production is approximately 30,000 metric tons annually, it is estimated to comprise less than 10% of the bio-synthesized alginate material.¹ Therefore there is significant additional potential to use designed sustainable biomaterials based on alginates.

The advent of organic solvents with the power to dissolve hitherto recalcitrant polysaccharides has greatly enabled the synthesis of novel derivatives with unique properties, including those with highly regioselective substitution². The chemical modification of alginates can be performed at the two secondary C-2 and C-3 hydroxyl groups, and the C-6 carboxylic acid group; almost all such modifications to date have of necessity involved aqueous solutions or dispersions of alginate in organic solvents. Several chemistries have been reported, taking advantage of these functional groups to synthesize alginate derivatives.³ Syntheses of acetylated alginate derivatives were among the earliest attempts at their chemical modification. Acid catalyzed esterification was used to obtain alginic acetates, wherein partial or complete substitution of hydroxyl groups was reported.⁴⁻⁶ Alternatively, acetylation was performed using ketene as a gaseous reagent to react with alginates in a swollen state.⁷⁻⁸ Selective acetylation of M residues was reported at low degree of substitution (DS) values, by reaction of Ca-alginate

beads swollen in a pyridine-acetic anhydride reagent mixture.⁹ As higher DS values were attained, G residues were also reacted.

The ease of dissolution of hydrophilic alginate salts in aqueous media has prompted the use of aqueous carbodiimide chemistry for synthesis of several alginate derivatives. For example, carboxylic acid groups on the alginate backbone were reacted with long chain alkylamines to synthesize hydrophobically substituted carboxamides.¹⁰ Carbodiimide coupling in aqueous media was also used for attachment of cell signaling molecules such as galactose moieties¹¹⁻¹³ and RGD containing peptides,¹⁴⁻¹⁵ and for covalent crosslinking of alginates.¹⁶ Several articles have reported the synthesis of amphiphilic alginate derivatives by attaching hydrophobic molecules to the backbone. Among these reports is oxidation of the hydroxyl groups to form aldehydes, and their subsequent reaction via reductive amination.¹⁷ Hydrophobic alginates were also prepared starting from commercially available propylene glycol esters of alginic acid, by nucleophilic displacement of the esters using long chain alkylamines.¹⁸⁻²⁰ In addition, long chain alkyl bromides were shown to react with tetrabutylammonium (TBA) carboxylates of alginates by S_N2 chemistry for the synthesis of hydrophobic esters of the alginate C-6 carboxyl.²¹⁻²²

Chemical modification of alginates in aqueous media also has been explored for the synthesis of covalently crosslinked matrices. Crosslinked alginates useful for chromatography and as superabsorbent materials were prepared by reacting the OH groups with epichlorohydrin in the presence of alkali.²³⁻²⁴ Crosslinking using glutaraldehyde, through the formation of acetal linkages, has also been reported.²⁵⁻³⁰ In addition, alginate gels were prepared by formation of amide linkages via reaction of the backbone carboxylic acid groups,³¹ and by partial oxidation followed by subsequent crosslinking using adipic dihydrazide.³² In an alternate strategy,

photocrosslinking of alginates bearing methacrylate groups was reported for the preparation of hydrogel beads.³³

We have found only two reports describing the reaction of alginates in organic reaction media. The first reported dissolution of the TBA salt of alginic acid (TBA-alginate) in dimethylsulfoxide (DMSO),²¹ while the second described dissolution of the TBA-alginate in N,N-dimethylformamide (DMF).³¹ In our hands, TBA-alginate is only partially soluble in DMSO. However, in the presence of a dissolution promoter such as TBAF, the TBA salts of alginic acid were *completely soluble* in DMSO, DMF, DMAc and DMI. *These solvent systems afforded clear and transparent solutions of TBA-alginate with complete dissolution in a few minutes.*

In the current paper, we report data supporting partial dissolution of TBA-alginate in DMSO, and complete dissolution in DMSO, DMF, DMAc and DMI in the presence of TBAF. Furthermore, we report chemical modification (acylation) of TBA-alginates in solution, both in the presence and absence of TBAF. We report on the type, extent, and pattern of acylation attainable vs. solvent system. Molecular weight analysis was performed to determine the degradation of the polysaccharide under basic conditions.

3.3 Experimental

3.3.1 Materials and methods

Five alginate samples were used for the study. Each was represented as ‘Mxxx’, where M stands for mannuronate and xxx denotes the % of M residues in the sample. For example, M063 signifies a sample containing 63% M and 37% G residues. M100 alginate was isolated from an

epimerase-negative mutant of *Pseudomonas fluorescens*, and was graciously provided by Dr. Gudmund Skjåk-Bræk at the Norwegian University of Science and Technology, Trondheim, Norway. M063 alginate, an alginic acid sodium salt from brown algae (low viscosity, Na-alginate) was acquired from Sigma. M029, M013 and M000 alginates were kindly provided by Dr. Anne Tøndervik at SINTEF Materials and Chemistry, Department of Biotechnology, Trondheim, Norway. Sample M029 was isolated from *Laminaria Hyperborea*. M013 was mannuronan (polyM) epimerised in vitro with recombinant AlgE6. M000 consisted of G-blocks with an average $DP_n \sim 20$.

Water used for the experiments was deionized. All other chemicals were used as supplied, unless otherwise specified. Hydrochloric acid (technical grade, HCl), ethanol (95% denatured), ethyl acetate (HPLC grade), DMSO (HPLC grade), DMAc (HPLC grade), DMF and sodium sulfate (granular, 10-60 mesh) were obtained from Fisher. DMSO, DMAc and DMF were dried using 4 Å molecular sieves. 1,3-Dimethyl-2-imidazolidinone (98%; DMI), tetrabutylammonium fluoride trihydrate (99%; TBAF), pyridine (99+%; dried using 4Å° molecular sieves), sodium carbonate (99.5%, extrapure, anhydrous; Na_2CO_3), hexanoic anhydride (99%, Hex_2O) and acetic anhydride (99+%; Ac_2O) were purchased from Acros Organics. Tetrabutylammonium hydroxide (1.0 M in water; TBAOH) was received from Fluka Analytical. Ethylene glycol was obtained from BDH. Lithium chloride (99%; LiCl), anhydrous DMSO ($\geq 99.9\%$), tetrabutylammonium cyanide (TBACN), hexafluorobenzene (99.5+%, NMR grade; C_6F_6), propionic anhydride (97%, Pr_2O) and deuterium oxide (99.9 atom% D; D_2O) containing 0.75% 3-(trimethylsilyl)propionic-2,2,3,3- d_4 acid, sodium salt for NMR were acquired from Sigma-Aldrich. KBr used for FTIR analysis was obtained from International Crystal Labs.

For ^1H -NMR, sample preparation was carried out by dissolving 8-10 mg of polymer in 1.5 mL of D_2O . The solution was filtered using a 1- μ syringe filter into a standard 5-mm NMR tube to remove unwanted particulates. Spectra were acquired using a Varian Unity 400 MHz spectrometer with manual shimming. A standard two-pulse sequence was applied to suppress the residual HDO peak, wherein an observation pulse width (pw) of 11.0 s, second pulse width (p1) of 22.0 s, first relaxation delay (d1) of 2.0 s and second relaxation delay (d2) of 4.2 s were used. The acquisition temperature was 85 $^\circ\text{C}$ for all samples, and the number of scans obtained was 64.

FTIR spectra were acquired using a Thermo Electron Nicolet 8700 instrument in transmission mode. Samples were prepared using the KBr pellet method. Alginate (1 mg) was mixed with 99 mg of KBr using a mortar and pestle. The mixture was compressed in the sample holder between two screws to form a KBr disc. 64 scans were obtained for each spectrum.

Dynamic light scattering (DLS) data was obtained using a Malvern Instruments Zetasizer Nano-ZS. Sample preparation was performed by adding 1 mg of M063 TBA-alginate to 1 mL each of DMSO (**I**) and 1 mg/mL DMSO/TBAF solution (**II**). **I** was passed directly through a 0.2- μ syringe filter prior to measurement. **II** was diluted 10X to get a TBA-alginate concentration of 0.1 mg/mL in 0.1 mg/mL DMSO/TBAF. The solution was passed through a 0.2- μ syringe filter prior to measurement. A glass cuvette with square aperture was used for both experiments.

DS value calculation by ^1H -NMR was carried out by integrating the O-acetyl multiplet peak centered at ~ 2.2 ppm (I_{AC}) against the polymer backbone region ~ 3.5 -5.5 ppm (I_{BB}). I_{AC} accounts for 3X protons, assigned to the acetyl $-\text{CH}_3$ group. I_{BB} accounts for $(7-\text{DS}_{(\text{AC})})\text{X}$ protons. The signals observed in the backbone region of the ^1H -NMR spectrum were assumed to comprise of 5 sugar ring protons and 2 hydroxyl (total of 7) protons. Since the ^1H -NMR spectrum was obtained in D_2O , part of the $-\text{OH}$ groups undergo deuterium exchange to form –

OD groups. The extent of this deuterium exchange defines the “proton fraction” and depends strongly on the polysaccharide chain conformation.³⁴ The proton fraction value for alginate acetates was unknown, and therefore it was assumed that all of the two –OH proton signals were visible in the ¹H-NMR spectrum. The following formula was used to calculate the DS value.

$$DS_{(Ac)} = (7I_{AC}) / (3I_{BB} + I_{AC})$$

Elemental analysis was performed using %CHN analyzer with - combustion/thermal conductivity detector (TCD) and %O analyzer with pyrolysis. Freeze drying of alginates was performed using Labconco® Freezone 4.5 lyophilizer. Dialysis was performed against water in a 4 L beaker using dialysis tubing (MWCO 3500 Da) for 3 days, by replacing the water twice each 24 hrs.

Molecular weight measurements were performed using SEC-MALS-dRI technique. A solvent and sample delivery system consisting of solvent reservoir, on-line degasser, isocratic pump and auto-injector from Agilent Technologies, Santa Clara, CA, USA was used for the experiments. A TSKgel Guard Alpha column (6.0 mm ID × 4.0 cm, 13 μm) was connected in series with a TSKgel Alpha-M column (7.8 mm ID × 30 cm, 13 μm) for size exclusion. The column outlet was connected to a DAWN HELEOS-II MALS detector and to an OPTILAB T-rEX dRI detector, both obtained from Wyatt Technologies, Santa Barbara, CA, USA. Both detectors were calibrated using 5k and 20k molecular weights PEG standards. The mobile phase used for alginate dissolution was 0.05 M Na₂SO₄/0.01 M EDTA, pH 6 containing 2 ppm NaN₃. An alginate concentration of 1 mg/mL was used with a flow rate of 0.5 mL/min and an injection volume of 100 μL. All solutions were passed through 0.2μ nylon syringe filters prior to injection. Data from light scattering and the differential refractometer were processed using Astra (v. 5.3.4.20) software supplied by Wyatt Technologies.

3.3.2 Synthesis of TBA-alginate

A procedure described by Babak et al.²¹ was followed, with modifications. HCl (0.6 N, 30 mL) was added to ethanol (30 mL) in a beaker. Na-alginate (2 g) was added to the mixture and stirred overnight at 4 °C. The mixture was filtered under vacuum using coarse filter paper. The solid obtained, alginic acid was washed thoroughly with ethanol and acetone, and dried overnight in the vacuum oven model at 40 °C. Thoroughly dried alginic acid thus obtained was dispersed in 100 mL water. Aqueous TBAOH was added dropwise with continuous stirring until the polymer was fully dissolved and the pH was adjusted between 7.0-10.0. The solution obtained was dialyzed, filtered to remove any unwanted particulates and freeze dried to yield white TBA-alginate polymer. The ¹H-NMR and FTIR spectra for TBA-alginate are shown in the Supporting Information as **Figures 3.8 and 3.9**.

¹H NMR (400 MHz, D₂O) δ 5.14 – 3.61 (m, alginate backbone), 3.22 – 3.13 (t, NCH₂CH₂CH₂CH₃ of TBA), 1.72 – 1.59 (m, NCH₂CH₂CH₂CH₃ of TBA), 1.45 – 1.32 (m, NCH₂CH₂CH₂CH₃ of TBA), 0.96 (t, NCH₂CH₂CH₂CH₃). FTIR (KBr pellet method): 3400 cm⁻¹, hydroxyl O–H stretching; 2850-2960 cm⁻¹, aliphatic C–H stretching, 1610 cm⁻¹, carboxylate C–O stretching.

3.3.3 Homogeneous synthesis of alginate acetate in DMSO/TBAF using acetic anhydride

TBAF (1 g, 3.82 mmol) was dissolved in DMSO (10 mL) to give a 10% (w/v) solution. The DMSO/TBAF solvent mixture was added to TBA-alginate (150 mg) in a 3-neck flask equipped with a condenser under N₂ atmosphere, and stirred at room temperature until a clear

solution was obtained. The temperature of the solution was raised to 40 °C, and pyridine (0.5 mL, 6.14 mmol) and acetic anhydride (0.5 mL, 5.29 mmol) were added. The reaction was stirred for 2 h at 40 °C, then the polymer was precipitated in ~150 mL of ethyl acetate. The solid was filtered under gravity using fluted coarse porosity filter paper and dried in the vacuum oven overnight. The dried crude product was added to ~30 mL of water and stirred, while 0.1 N Na₂CO₃ solution was added dropwise until the polymer dissolved and the pH was adjusted between 7.0-10.0. The solution thus obtained was dialyzed, filtered to remove any unwanted particulates and freeze dried to yield white TBA alginate acetate. The ¹H-NMR and FTIR spectra for TBA-alginate acetate are shown in **Figures 3.2 and 3.3**.

¹H NMR (400 MHz, D₂O) δ 5.56 – 3.51 (m, alginate backbone), 3.30 – 3.08 (t, NCH₂CH₂CH₂CH₃ of TBA), 2.39 – 1.91 (m, COCH₃ of acetate), 1.75 – 1.57 (m, NCH₂CH₂CH₂CH₃ of TBA), 1.48 – 1.32 (m, NCH₂CH₂CH₂CH₃ of TBA), 0.96 (t, NCH₂CH₂CH₂CH₃). FTIR (KBr pellet method): 1740 cm⁻¹, ester C=O stretching vibration; 1250 cm⁻¹, ester C–O stretching vibration; 3400 cm⁻¹, hydroxyl O–H stretching; 2850-2960 cm⁻¹, aliphatic C–H stretching, 1610 cm⁻¹, carboxylate C–O stretching. DS for product **12** in **Table 3.2** by ¹H-NMR = 0.76. Elemental composition for product **12** in **Table 3.2**: Calculated theoretically using DS 0.76 and assuming 3 moles water of hydration, C, 35.64%; H, 5.78%; N, 0.14%; O, 58.44%; Calculated by ¹H-NMR assuming 3 moles water of hydration, C, 38.26%; H, 6.27%; N, 0.42%; O, 55.04%; Found by elemental analysis, C, 35.59%; H, 5.18%; N, 0.14%; O, 54.36%.

3.3.4 Heterogeneous synthesis of alginate acetate in DMSO

DMSO (10 mL) was added to TBA-alginate (150 mg) in a 3-neck flask equipped with a condenser under N₂ atmosphere, and stirred at room temperature until the polymer fibers were

well dispersed in the solvent. The temperature of the solution was raised to 40 °C, and pyridine (0.5 mL, 6.14 mmol) and acetic anhydride (0.5 mL, 5.29 mmol) were added. The reaction was stirred for 2 h at 40 °C, then the polymer was precipitated in ~150 mL of ethyl acetate. The solid was filtered under gravity using fluted coarse porosity filter paper and dried in the vacuum oven overnight. The dried crude product was added to ~30 mL of water and stirred, while 0.1 N Na₂CO₃ solution was added dropwise until the polymer dissolved and the pH was adjusted between 7.0-10.0. The solution thus obtained was dialyzed, filtered to remove any unwanted particulates and freeze dried to yield white alginate acetate. The ¹H-NMR and FTIR spectra for heterogeneously acetylated TBA-alginate are shown in the Supporting Information as **Figures 3.10 and 3.11**.

¹H NMR (400 MHz, D₂O) δ 5.44 – 3.50 (m, alginate backbone), 5.29 – 2.00 (m, COCH₃ of acetate). FTIR (KBr pellet method): 1740 cm⁻¹, ester C=O stretching vibration; 1250 cm⁻¹, ester C–O stretching vibration; 3400 cm⁻¹, hydroxyl O–H stretching; 2850-2960 cm⁻¹, aliphatic C–H stretching, 1610 cm⁻¹, carboxylate C–O stretching. DS for product **2** in **Table 3.4** by ¹H-NMR = 0.48.

3.3.5 Homogeneous synthesis of alginate acetate in DMSO/TBAF using acetyl chloride

TBAF (1 g, 3.82 mmol) was dissolved in DMSO (10 mL) to give a 10% (w/v) solution. The DMSO/TBAF solvent mixture was added to TBA-alginate (150 mg) in a 3-neck flask equipped with a condenser under N₂ atmosphere, and stirred at room temperature until a clear solution was obtained. The temperature of the solution was raised to 70 °C, and pyridine (0.5 mL, 6.14 mmol) and acetyl chloride (0.5 mL, 7.03 mmol) were added. The reaction was stirred for 2 h at 70 °C, then the polymer was precipitated in ~150 mL of ethyl acetate. The solid was

filtered under gravity using fluted coarse porosity filter paper and dried in the vacuum oven overnight. The dried crude product was added to ~30 mL of water and stirred, while 0.1 N Na₂CO₃ solution was added dropwise until the polymer dissolved and the pH was adjusted between 7.0-10.0. The solution thus obtained was dialyzed, filtered to remove any unwanted particulates and freeze dried to yield white alginate acetate. The ¹H-NMR and FTIR spectra for TBA-alginate acetate synthesized using acetyl chloride are shown in the Supporting Information as **Figures 3.12 and 3.13**.

¹H NMR (400 MHz, D₂O) δ 5.31 – 3.51 (m, alginate backbone), 3.24 – 3.11 (t, NCH₂CH₂CH₂CH₃ of TBA), 2.26 – 2.05 (m, COCH₃ of acetate), 1.73 – 1.59 (m, NCH₂CH₂CH₂CH₃ of TBA), 1.46 – 1.32 (m, NCH₂CH₂CH₂CH₃ of TBA), 1.01 – 0.90 (t, NCH₂CH₂CH₂CH₃ of TBA). FTIR (KBr pellet method): 1740 cm⁻¹, ester C=O stretching vibration; 1250 cm⁻¹, ester C–O stretching vibration; 3400 cm⁻¹, hydroxyl O–H stretching; 2850–2960 cm⁻¹, aliphatic C–H stretching, 1610 cm⁻¹, carboxylate C–O stretching. DS for product **7** in **Table 3.2** by ¹H-NMR = 0.08.

3.3.6 Homogeneous synthesis of alginate propionate in DMSO/TBAF using propionic anhydride

TBAF (1 g, 3.82 mmol) was dissolved in DMSO (10 mL) to give a 10% (w/v) solution. The DMSO/TBAF solvent mixture was added to TBA-alginate (150 mg) in a 3-neck flask equipped with a condenser under N₂ atmosphere, and stirred at room temperature until a clear solution was obtained. The temperature of the solution was raised to 40 °C, and pyridine (0.5 mL, 6.14 mmol) and propionic anhydride (0.5 mL, 3.9 mmol) were added. The reaction was stirred for 2 h at 40 °C, then the polymer was precipitated in ~150 mL of ethyl acetate. The solid was filtered under gravity using fluted coarse porosity filter paper and dried in the vacuum oven

overnight. The dried crude product was added to ~30 mL of water and stirred, while 0.1 N Na_2CO_3 solution was added dropwise until the polymer dissolved and the pH was adjusted between 7.0-10.0. The solution thus obtained was dialyzed, filtered to remove any unwanted particulates and freeze dried to yield white alginate propionate. The ^1H -NMR and FTIR spectra for homogeneously synthesized TBA-alginate propionate are shown in the Supporting Information as **Figures 3.14 and 3.15**.

^1H NMR (400 MHz, D_2O) δ 5.54 – 3.43 (m, alginate backbone), 3.24 – 3.12 (t, $\text{NCH}_2\text{CH}_2\text{CH}_2\text{CH}_3$ of TBA), 2.67 – 2.27 (broad s, COCH_2CH_3 of propionate), 1.73 – 1.59 (m, $\text{NCH}_2\text{CH}_2\text{CH}_2\text{CH}_3$ of TBA), 1.44 – 1.32 (m, $\text{NCH}_2\text{CH}_2\text{CH}_2\text{CH}_3$ of TBA), 1.20 – 1.03 (t, COCH_2CH_3 of propionate), 1.00 – 0.91 (t, $\text{NCH}_2\text{CH}_2\text{CH}_2\text{CH}_3$ of TBA). FTIR (KBr pellet method): 1740 cm^{-1} , ester $\text{C}=\text{O}$ stretching vibration; 1250 cm^{-1} , ester $\text{C}-\text{O}$ stretching vibration; 3400 cm^{-1} , hydroxyl $\text{O}-\text{H}$ stretching; 2850-2960 cm^{-1} , aliphatic $\text{C}-\text{H}$ stretching, 1610 cm^{-1} , carboxylate $\text{C}-\text{O}$ stretching. DS for product **8** in **Table 3.2** by ^1H -NMR = 0.31.

3.3.7 Synthesis of anhydrous DMSO/TBAF solvent system

A procedure described by Heinze et al.³⁵ was adapted, wherein TBACN (1.026 g, 3.82 mmol) was purged with N_2 gas in a round bottom flask. Anhydrous DMSO (10 mL) was added to the flask to dissolve the TBACN at room temperature. C_6F_6 (73.2 μL , 0.636 mmol) was added to the TBACN solution to give an intense red solution which was stirred at room temperature for 1 h, after which it was used to dissolve TBA-alginate. The solubility of the polymer in the anhydrous DMSO/TBAF mixture was confirmed by visual inspection, as the freeze dried solid TBA-alginate dissolved over about one hour.

3.4 Results and discussion

We began our studies with a systematic evaluation of the solubility of alginic acid and its sodium and TBA salts in common solvents. The solubility of alginates depends strongly on the state of the backbone carboxylic acid groups. Results from our solubility study are shown in **Table 3.1**. Alginic acid with its carboxylic acid groups in their protonated form was not fully soluble in any solvent system examined, including water. Neutralization of alginic acid with Na^+ or TBA^+ ions yielded Na-alginate and TBA-alginate respectively. Na-alginate dissolved fully in water, but was not fully soluble in any organic medium examined. TBA-alginate was fully soluble in water, ethylene glycol and polar aprotic solvents containing TBAF, but did not dissolve in any other solvent systems under consideration.

Table 3.1: Solubility of alginates in various solvents at a concentration of 15 mg/mL

	H ₂ O	EG	DMAc	DMF	DMSO	DMAc/ LiCl	DMF/ TBAF	DMSO/ TBAF	DMAc/ TBAF	DMI/ TBAF
Alginic acid	-	-	-	-	-	-	-	-	-	-
Na-alginate	+	-	-	-	-	-	-	-	-	-
TBA-alginate	+	+	-	-	-	-	+	+	+	+

(+) complete solubility and (-) partial or no solubility; EG = ethylene glycol

The difference in solubility between alginic acid and its two salt forms most likely arises from their differing abilities to H-bond to other alginate molecules. The inability to fully dissolve alginic acid in all media may be explained by substantial H-bonding interactions resulting from the presence of a carboxylic acid H-donor in addition to the two hydroxyl groups per monosaccharide unit. In the case of Na- and TBA-alginate, only two hydroxyl group donors are present, and the polymer-polymer H-bond interactions are significantly reduced. Furthermore,

the highly polar carboxylate anions enhance water solubility. The solubility of TBA-alginate in organic media likely results from an increased hydrophobicity due to the N-butyl chains and disruption of H-bonding by the bulky TBA ion (which also is likely to lead to a larger interionic distance, enhancing affinity of the polyanion for water). Na^+ ions are more hydrophilic and smaller in size compared to TBA^+ ions, which makes Na-alginate insoluble or partially soluble in organic media.

The extent to which a solvent can dissolve alginates depends on its ability to overcome the intra- and intermolecular H-bonds present in the polymer. Since water is highly effective at breaking H-bond interactions, it can easily dissolve both Na- and TBA-alginate. Single component dipolar aprotic solvents such as DMSO, DMF, DMAc and DMI were incapable of fully dissolving alginates in any form. However, in the presence of the dissolution promoter TBAF, all four solvents solubilized TBA-alginate fully at room temperature. DMSO/TBAF is an excellent solvent system for cellulose, providing fast dissolution at room temperature.³⁵⁻⁴² In the present study, a 15 mg/mL solution of M063 TBA-alginate could be prepared by room temperature dissolution in DMSO or DMF at TBAF concentrations of 1% (w/v). DMAc and DMI required higher concentrations of TBAF, wherein complete dissolution was achieved at concentrations of 10% TBAF (w/v). It is known that both the strongly electronegative fluoride anion and the bulky TBA cation are both important for the dissolution of polysaccharides in DMSO/TBAF.³⁶ The fluoride ion is a strong H-bond acceptor and is highly effective in competing with the hydroxyl and acetal oxygen atoms in polysaccharides, thus reducing interactions between polymer chains.⁴³ TBAF exists as a trihydrate, and the bound water has also been thought to play a key role in the dissolution mechanism. DMAc/LiCl is the most popular solvent system for cellulose dissolution, since it is well-suited for a wide variety of derivative-

forming chemistries.⁴⁴ The most commonly used procedure for cellulose dissolution requires thermal activation of the polymer in DMAc, followed by the addition of LiCl and overnight stirring.⁴⁵⁻⁴⁶ We examined the utility of the DMAc/LiCl system for alginate dissolution, following similar procedures to those used in cellulose dissolution. We found however that DMAc/LiCl is incapable of fully dissolving alginates in either protonated or salt (Na^+ , TBA^+) form.

The impact of added TBAF on solubility of TBA-alginate in DMSO was studied in further detail, by adding equal amounts of the TBA salt of M063 to pure DMSO, and separately to 1.1% (w/v) TBAF in an equal amount of DMSO. **Figure 3.1** shows an image of the two mixtures. It was observed that the alginate fibers in DMSO (left) were incompletely dissolved, but in the presence of TBAF (right), the TBA-alginate dissolved completely. However, the polymer did partly dissolve in DMSO alone, in spite of the cloudy appearance of the mixture, as confirmed by ^1H -NMR and DLS measurements. **Figures 3.16(a)** and **(b)** in the Supplemental Information show the data obtained. In the ^1H -NMR spectra, the ratio of integration of the polymer backbone protons (3.3-5.3 ppm) to that of the $\text{DMSO-}d_6$ solvent peak at 2.5 ppm was calculated. The backbone:solvent ratio obtained in pure DMSO was ~1:25, whereas a ratio of ~1:5 was obtained for DMSO/TBAF. Thus, a higher concentration of the polymer in DMSO could be achieved by the addition of TBAF as a dissolution promoter. The intensity size distribution plots obtained using DLS support the conclusion that a fraction of the polymer chains dissolved in DMSO in the absence of TBAF. However, the intensity average sizes obtained for TBA-alginate solutions in DMSO and DMSO/TBAF were greater than 100 nm. These values were very high compared to what is typically observed for fully solvated polymer chains. This may indicate that TBA-alginate chains aggregate in DMSO.

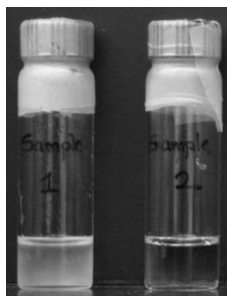
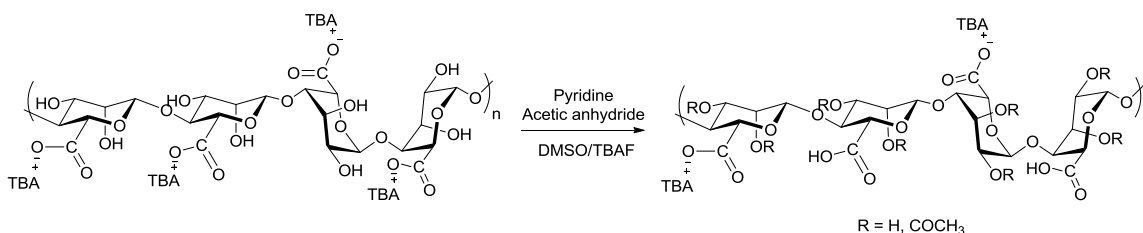


Figure 3.1: Partial dissolution of alginate M063 in DMSO (left) and complete dissolution in DMSO/TBAF (right) at a TBAF concentration of 1.1% (w/v). Alginate concentration in both vials was 15 mg/mL

The most exciting aspect of the discovery was that dipolar aprotic solvents such as DMSO, DMF, DMAc or DMI fully dissolved TBA-alginate in the presence of TBAF. The potential of these solvent systems for TBA-alginate derivatization was studied by homogeneous acetylation using Ac_2O /pyridine (**Scheme 3.1**). Partial acetylation was achieved, affording a product that was insoluble in water. Neutralization using 0.1M Na_2CO_3 was required to make the product water-soluble. **Figure 3.2** shows the ^1H -NMR spectrum of a purified M063 alginate acetate product. The O-acetyl peak appearing at ~ 2.2 ppm confirms the formation of acetate ester groups. The polymer backbone peaks appear in the region ~ 3.5 - 5.5 ppm. The HDO solvent peak at ~ 4.2 ppm was suppressed using a specific pulse sequence (see Experimental section). The protons from the butyl chains of TBA appear at shifts centered at ~ 0.9 , 1.4, 1.7 and 3.2 ppm, indicating that some of the carboxyls are still present as TBA salts in the product. **Figure 3.3** shows the FTIR spectrum of M063 alginate acetate. The peaks at 1740 cm^{-1} and 1250 cm^{-1} were assigned to the C=O and C–O stretching vibrations from the acetate ester.

The elemental composition for homogeneously acetylated M063 alginate acetate product was determined by two methods. The first method used elemental analysis, which gave C-35.59%, H-5.18%, N-0.14% and O-54.36%. The second method employed ^1H -NMR

spectroscopy by integration of the TBA proton peaks against the backbone proton signals. This method, assuming DS = 0.76 and 3 moles water of hydration yielded C-38.26%, H-6.27%, N-0.42% and O-55.04%. These methods were compared with theoretical percentages, calculated by assuming a DS = 0.76 and 3 moles of water of hydration. The composition obtained using this technique was C-35.64%, H-5.78%, N-0.14% and O-58.44%. The ^1H -NMR technique results may be less reliable based on the knowledge that the solvent suppression pulse sequence employed affects the intensities of other signals in the spectra, thus changing the integration values.⁴⁷ The experimental and theoretically calculated elemental composition values were in fairly close agreement when ~3 moles water of hydration was accounted for. When the water of hydration was not taken into consideration, the values obtained using the two methods were quite different. The % of saccharide units existing as TBA salts can be calculated using the %N value obtained by elemental analysis. For example, in a product with acetyl DS of 0.76, the maximum possible %N value is 3.13 for 100% monosaccharide units in TBA salt form. Therefore, a %N value of 0.14 (as obtained by elemental analysis for product **12** in **Table 3.2**) corresponds to about 2.6% saccharide units present as their TBA salts. The partial TBA salts of alginic acid may be converted to 100% Na-salts using ion-exchange. Converting the polymer from its salt form to the protonated form using ion-exchange may be more challenging due to precipitation of alginic acid acetate from water.



Scheme 3.1: Acetylation of TBA-alginate

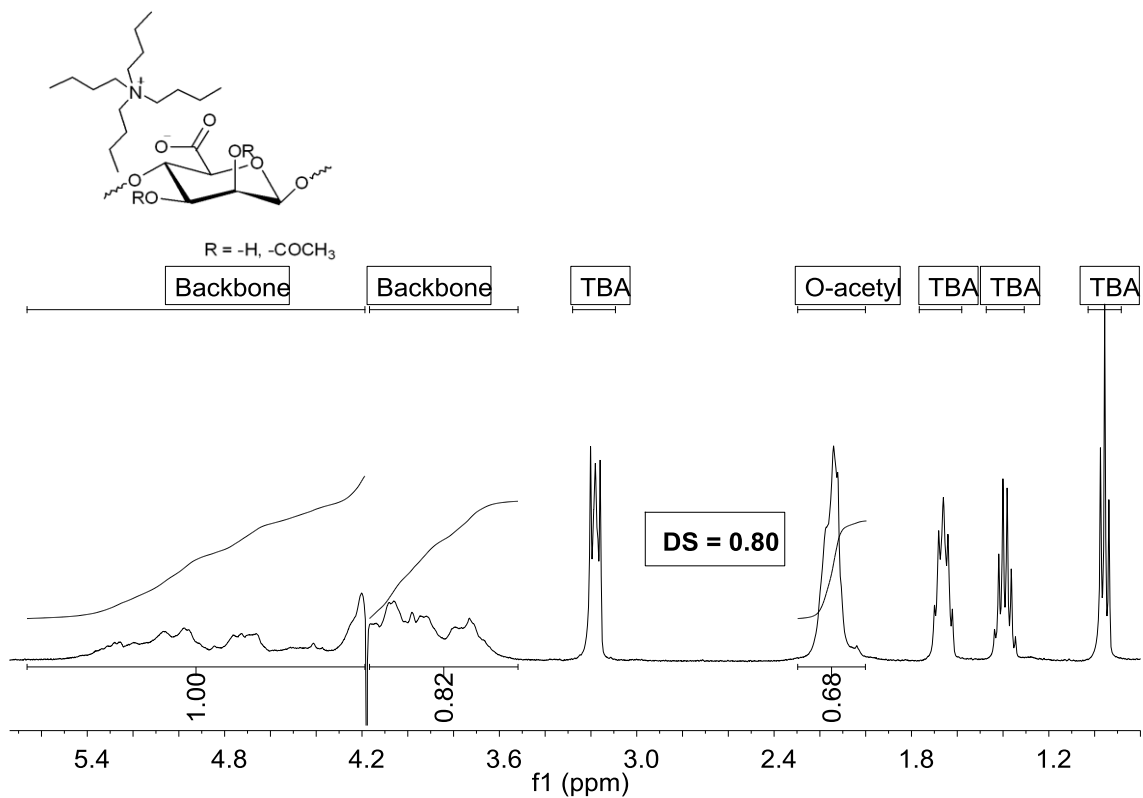


Figure 3.2: ¹H-NMR spectrum of alginate acetate synthesized from alginate M063

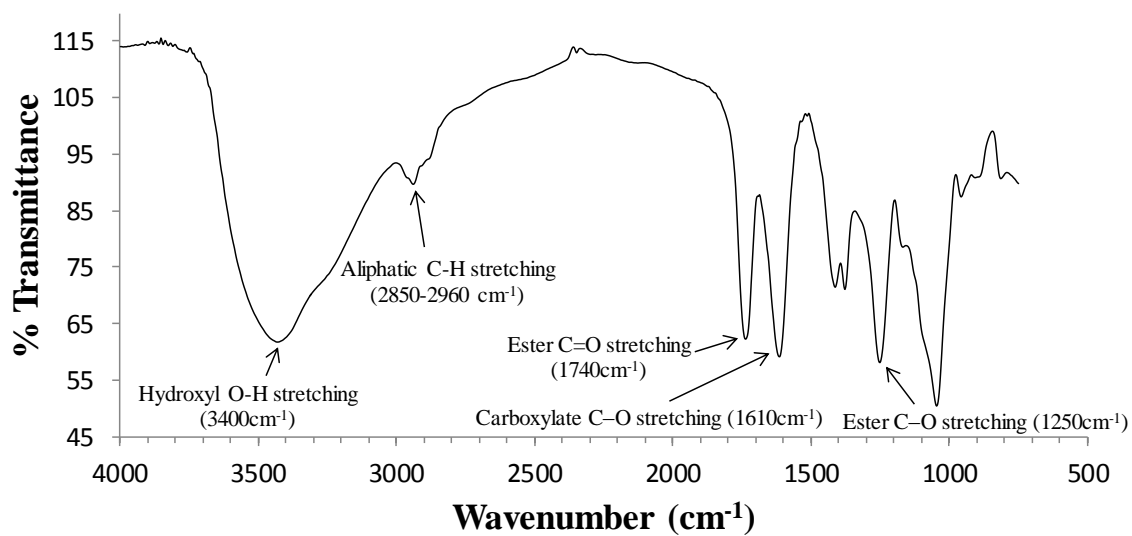


Figure 3.3: FTIR spectrum of alginate acetate synthesized from alginate M063

Acylation reactions of alginate M063 are summarized in **Table 3.2**. Homogeneous acetylation performed in DMF, DMAc, DMI and DMSO with excess Ac₂O afforded DS values ranging between 0.74-0.85, as indicated for products **1-4**. Acetylation using acetic anhydride in DMSO may lead to side reactions through Pummerer rearrangement.⁴⁸ Since products **1-4** gave fairly similar DS values, it was concluded that Pummerer rearrangement did not significantly impact the acylation reaction. In an effort to increase the DS value obtained, a second addition of Ac₂O was carried out and the reaction continued for 2 h; this afforded DS(Ac) of 1.01 (product **5**). We thought the water of hydration of the commercial TBAF might be restricting the maximum DS(Ac) obtained, so performed the reaction under anhydrous conditions by synthesizing TBAF in situ.³⁵ Alginate acetate synthesized under anhydrous conditions yielded a DS value of 1.05 (product **6**). Synthesis of alginate acetate using acetyl chloride (product **7**) afforded only a DS(Ac) of 0.08. This result was surprising since acid chlorides are typically more reactive than the corresponding acid anhydrides. Reaction of TBA alginate with propionic anhydride afforded alginate propionate (product **8**) of DS(Pr) 0.31. The reduction in reactivity with alginate as chain length of the anhydride increases is striking; indeed, hexanoic anhydride did not appear to react with TBA alginate (product **9**) at all. This is surely due in part to steric reasons, but perhaps is also caused by the difficulty of mixing the highly polar, polyanionic alginate and the rather hydrophobic longer chain anhydrides.

Table 3.2: Acylation of alginates and the corresponding DS values

Product	Acyl Reagent	Molar ratio (Alg:Pyr:Acyl)	Solvent	TBAF % (w/v)	DS
1	Ac ₂ O	1:17:15	DMF	10	0.74
2	Ac ₂ O	1:17:15	DMAc	10	0.85
3	Ac ₂ O	1:17:15	DMI	10	0.80
4	Ac ₂ O	1:17:15	DMSO	10	0.80
^a 5	Ac ₂ O	1:17:15	DMSO	10	1.01
^b 6	Ac ₂ O	1:17:15	DMSO	10	1.05
7	AcCl	1:17:19	DMSO	10	0.08
8	Pr ₂ O	1:17:11	DMSO	10	0.31
9	Hex ₂ O	1:17:6	DMSO	10	0.00
10	Ac ₂ O	1:34:29	DMSO	1	0.98
11	Ac ₂ O	1:20:20	DMSO	1	0.89
12	Ac ₂ O	1:10:10	DMSO	1	0.76
13	Ac ₂ O	1:4:4	DMSO	1	0.70
14	Ac ₂ O	1:2:2	DMSO	1	0.29
15	Ac ₂ O	1:1:1	DMSO	1	0.13

DS values measured using ¹H-NMR. All reactions performed in DMSO using M063 sample at 40 °C for 2 hours.

^asecond addition of Ac₂O and reaction continued for 2 more hours.

^breaction performed in anhydrous DMSO/TBAF solvent.

A recent article on cellulose derivatization in DMSO/TBAF reported the effect of TBAF concentration on the DS value achieved.³⁶ A high concentration of TBAF in the reaction mixture was shown to have a limiting effect on the DS values for cellulose derivatives. To probe the effect of TBAF concentration on alginate esterification, acetylation was performed in 1% (w/v) DMSO/TBAF solution. A DS value of 0.98 was achieved for product **10**. Products **11-15** resulted from acetylation under varying molar ratios of acetylation reagent to alginate. The DS could be influenced by the molar ratio of the added reagent to alginate, but only up to an apparent limit of DS(Ac) ~1.0 (**Table 3.2**).

We hypothesized two possible causes for this apparent upper limit on attainable alginate acetate DS. One cause could be that the reaction is highly regioselective, reacting only with

either the 2-OH or 3-OH on the alginate monosaccharides. The second possibility could be greater reactivity of either the M or G monosaccharide units towards acetylation; given the significant conformational change that occurs upon epimerization of M to G in the natural alginate, this seemed a possibility. To better understand the selectivity issues, acetylation was performed using alginates containing varying M/G ratios. **Table 3.3** shows the DS values obtained for TBA alginates acetylated both homogeneously in DMSO/TBAF and (partly) heterogeneously in DMSO.

Table 3.3: Homogeneous and heterogeneous acetylation of alginates and the corresponding DS values

Product	Alginate	DS _{Homogeneous}	DS _{Heterogeneous}
1	M100	0.80	0.91
2	M063	0.80	0.48
3	M029	0.78	0.63
4	M013	0.78	0.54
5	M000	0.82	0.72

DS values measured using ¹H-NMR. All reactions employed TBA alginate at 100 mg/mL DMSO using alginate monosaccharide unit:pyridine:acetic anhydride molar ratio of 1:17:15; homogeneous reactions also employed 100 mg TBAF/mL DMSO.

Under homogeneous reaction conditions, the DS values obtained were nearly identical (~0.8) across the entire range of alginate M/G ratios. This proves that the reaction was not selective for M vs. G, and that both M and G residues could be acetylated. **Figure 3.4** shows the ¹H-NMR spectrum obtained for M100 alginate acetate. Peak assignments for partially acetylated alginates containing 100% M were previously reported by Skjåk-Bræk et al.⁴⁹ Accordingly, peak A was assigned as the H-3 signal from M residues monoacetylated at the 3-OH position and peak B was assigned as the H-3 signal from M residues acetylated at both 2-OH and 3-OH positions. Thus, both 2- and 3-OH positions on M residues could be acetylated under homogeneous

conditions. **Figure 3.5** shows stacked ^1H -NMR spectra of homogeneously acetylated alginate samples represented in **Table 3.3**. While peaks A and B were assigned for M100 alginate, peak assignments for samples containing G residues were not possible due to severe overlap of signals. 2D-COSY studies of alginate acetates containing G residues failed to identify the H-H correlations in the backbone region due to the broad nature of the peaks. Therefore, regioselectivity between the 2-OH and 3-OH positions on G residues was difficult to determine with certainty.

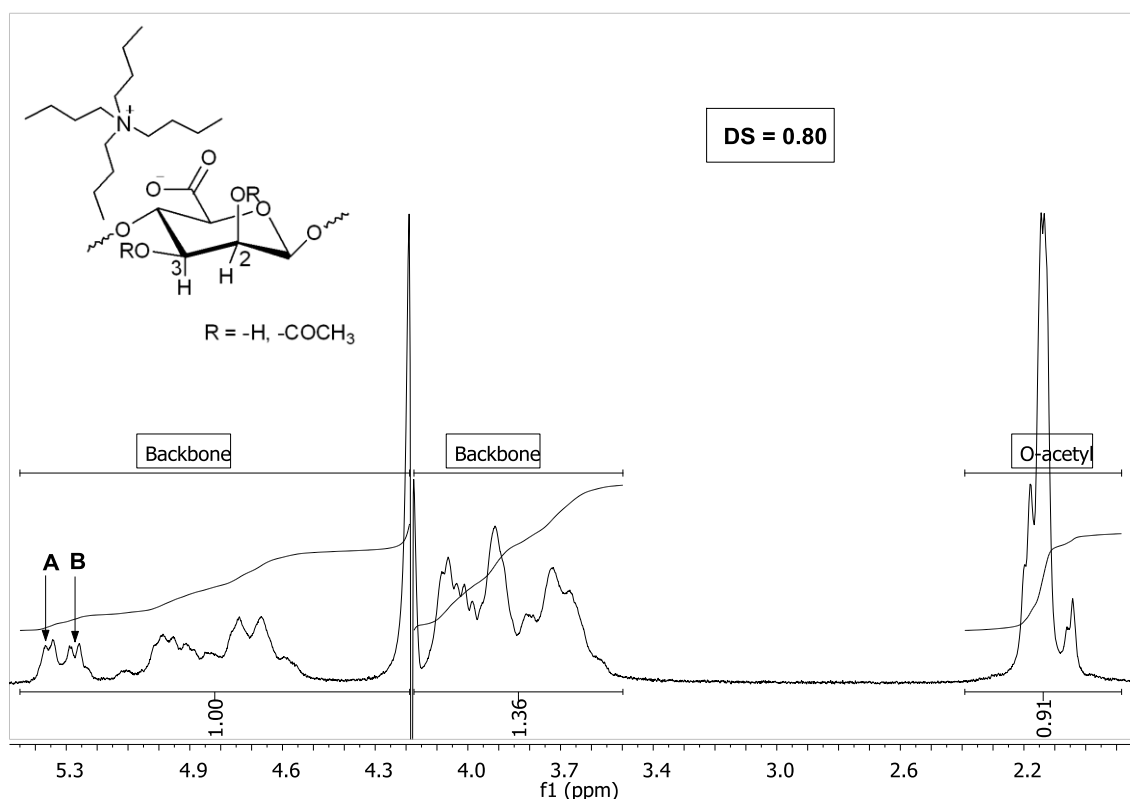


Figure 3.4: ^1H -NMR spectrum of alginate acetate synthesized from alginate M100. Peak A represents H-3 from M residues monoacetylated at position 3. Peak B represents H-3 from M residues diacetylated at positions 2 and 3. Peaks A and B assigned according to previously published literature⁴⁹

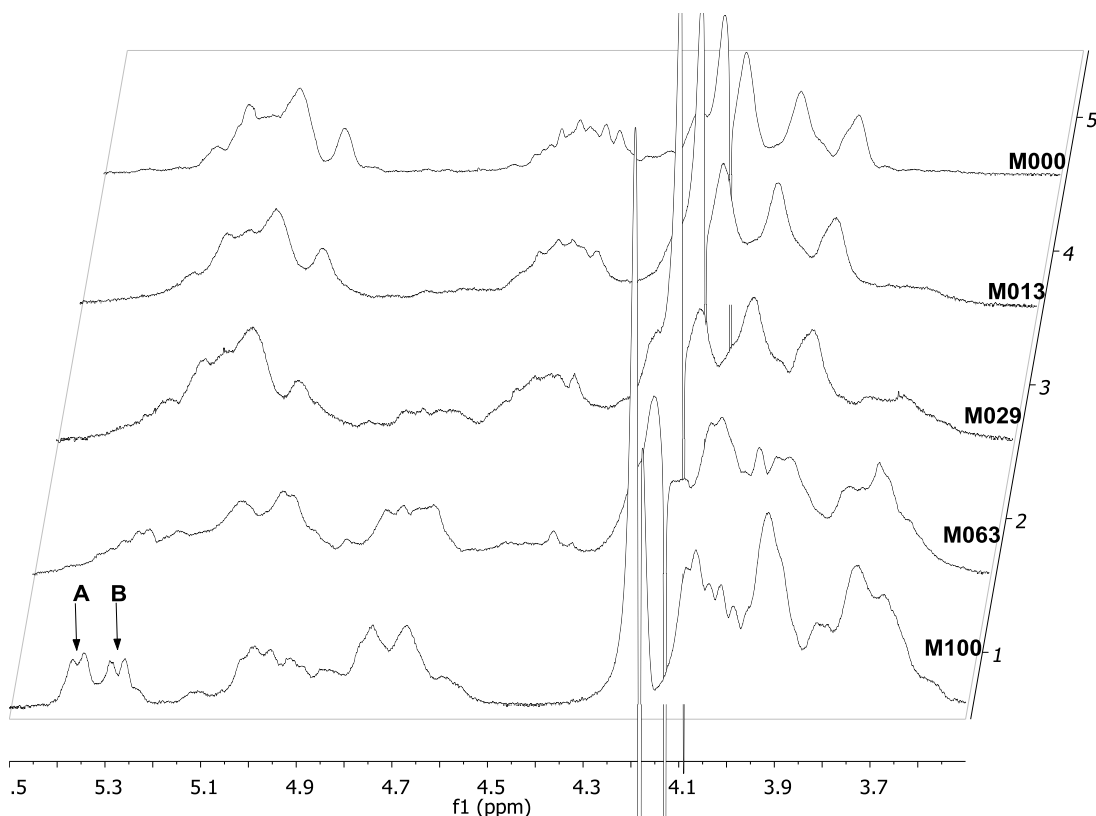


Figure 3.5: ^1H -NMR spectra of homogeneously acetylated alginates from Table 3.3. Peak A represents H-3 from M residues monoacetylated at position 3. Peak B represents H-3 from M residues diacetylated at positions 2 and 3. Peaks A and B assigned according to previously published literature⁴⁹

Acetylation of TBA alginates performed in DMSO without added TBAF, that is under partly heterogeneous conditions, afforded more variable DS values compared to homogeneous acetylation, as shown in **Table 3.3**. While homogeneous acetylation gave similar DS values for alginates across all M/G ratios, the products of heterogeneous reactions yielded DS values that varied with the M/G ratios of the starting polymers. This variance in heterogeneous reaction product DS may result from the differing extent of partial solubility among various TBA-alginate samples in DMSO, which may in turn depend on factors including molecular weight, M/G ratios, and block copolymer structure.

Figure 3.6 shows stacked ^1H -NMR spectra of heterogeneously acetylated alginate samples from **Table 3.3**. The spectrum for M100 alginate acetate shows the two peaks A and B, previously assigned as the H-3 signal from M residues monoacetylated at the 3-OH position, and H-3 signal from M residues diacetylated at both 2-OH and 3-OH positions respectively. Therefore, heterogeneous reactions could yield products where both hydroxyl positions on M residues were substituted. However, in the case of alginates containing G residues, heterogeneous reactions yielded products where the two peaks C and D, with shifts of 5.08 and 4.47 ppm respectively were predominant. The predominance of these peaks was not observed in the case of homogeneous reaction products shown in **Figure 3.5**. Previous assignments for alginates made using ^1H -NMR have shown that the peak at ~5.08 ppm arises from the H-1 signal of G residues in GGG, MGG and GGM triads. The peak centered at ~4.47 ppm on the other hand arises from the H-5 signal in GGG triads.⁵⁰ Thus, the predominance of peaks C and D in heterogeneously acetylated alginates suggests that GGG triad sequences remained relatively unreacted. G-blocks were therefore preserved, resulting in selective acetylation of M residues.

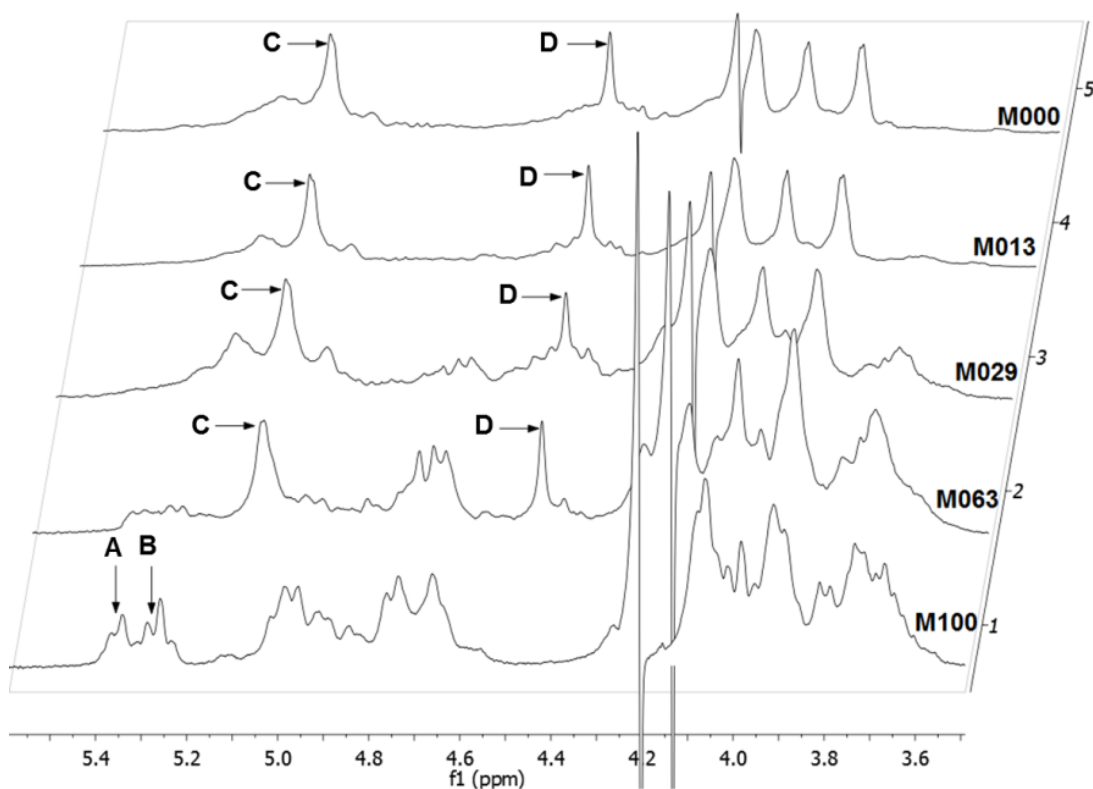


Figure 3.6: ^1H -NMR spectra of heterogeneously acetylated alginates from Table 3.3. Peak A represents H-3 from M residues monoacetylated at position 3. Peak B represents H-3 from M residues diacetylated at positions 2 and 3. Peak C represents H-1 from unreacted GGG, MGG and GGM triad sequences. Peak D represents H-5 from unreacted GGG triad sequences. Peaks A, B, C and D were assigned according to previously published literature⁴⁹⁻⁵⁰

The difference in the DS values and distribution observed between homogeneous and heterogeneous reaction products could be related to the partial solubility of TBA-alginate in DMSO. A possible explanation may be that the fraction dissolving in DMSO contains a higher number of M-blocks, thus facilitating the selective acetylation of M residues. A contrasting picture is seen for homogeneous reactions in DMSO/TBAF, where all polymer chains were fully solubilized. Thus, there is an equal accessibility for G-blocks, M-blocks and MG-blocks, which may result in a more statistical distribution of acetyl groups. The fact that the DS value for alginate acetates could not be increased significantly beyond ~ 1.0 under any attempted

conditions is still a conundrum. A potential explanation for this limited DS is based on monosaccharide ring electronic effects. The uronate ring in unreacted TBA-alginate contains one electron-withdrawing substituent at the C-5 position. During acetylation, the monoacetate product is formed first by reaction at one of the two hydroxyl groups. The monoacetylated uronate ring now bears two electron-withdrawing substituents; the first is the C-5 carboxylate and the second is the acetyl substituent. It is likely that with two electron-withdrawing substituents present, the reactivity of the second hydroxyl group is significantly lowered. The DS value may therefore be limited to ~ 1.0 when pyridine/anhydride is used as the acyl reagent system. An alternate theory may be based on the stereochemistry of the monosaccharide residues. In an M residue, the 2-OH group is axial and may possibly interact with the C-4 proton through 1,3-diaxial interactions, thus favoring substitution at the 3-OH position. In a G residue, an exactly opposite scenario is likely, wherein the 3-OH group is axial and could interact with the C-5 proton through 1,3-diaxial interactions. Substitution of the 2-OH position may therefore be favored on G units. Thus, in either of the two residues, stereochemistry could favor the reaction of one out of the two hydroxyl groups, therefore limiting the DS to ~ 1.0 . At this time we cannot be certain whether one of these mechanisms, or some other mechanism is the source of the apparent acyl DS limitation.

Finally, uronic acids are known to be base sensitive and degrade via β -elimination at higher pH values.⁵¹⁻⁵² Although pyridine is a mild base, it may still degrade the polymer during reaction. Furthermore, fluoride from TBAF is also known to be a strong base⁵³. Molecular weight measurements were therefore performed on M063 alginate acetates that were reacted for different time periods, and compared to unreacted TBA-alginate. PDI was calculated using the M_n and M_w values. Elemental analysis was performed for each sample to determine the %N

content. This %N value was then used to calculate the fraction of carboxylate groups existing as TBA salts (%TBA). **Table 3.5** in the Supporting Information shows the experimental and theoretically calculated % atomic composition values obtained for the alginates shown in **Table 3.4**. Knowing the DS value and the %TBA, an average monosaccharide molar mass was calculated. The Mn value was then divided by the average monosaccharide molar mass to determine the DP. **Table 3.4** shows the data obtained. The results clearly show significant chain degradation. The starting DP (0 min) of 144 is reduced to 66 within the first 15 minutes of reaction. DP continues to decrease throughout the two hours of reaction time. **Figure 3.7** shows the right-shift in the SEC chromatograms for the alginate acetate obtained using light scattering degradation proceeds. As the molecular weight decreases, the elution time increases causing a subsequent right-shift for products with higher reaction times. Clearly, it is desirable to minimize reaction times and temperatures to obtain higher molecular weight products.

Table 3.4: Molecular weight degradation of TBA-alginate during acetylation

Reaction time	DS	M _n (kDa)	M _w (kDa)	PDI	%TBA	DP
0 min	0	56.37	98.18	1.74	64	144
15 min	0.65	20.36	48.88	2.40	13	66
30 min	0.75	13.23	33.32	2.52	10	43
1 h	0.51	8.13	19.61	2.41	7	28
2 h	0.90	2.78	10.91	3.93	7	9

DS values measured using ¹H-NMR. All reactions were performed in 1% (w/v) DMSO/TBAF using M063 sample at 40 °C for 2 hours. Ac₂O was used as the acyl reagent with an Alg:Pyr:Acyl ratio of 1:17:15

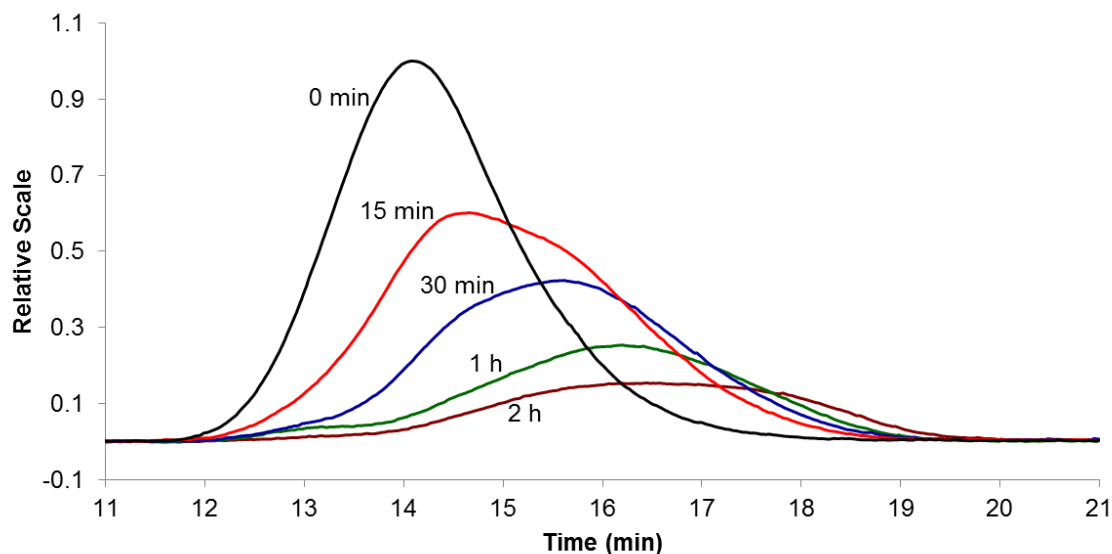


Figure 3.7: Right-shift in the SEC chromatograms obtained using light scattering for the alginate acetates shown in Table 3.4, recorded over increasing reaction time

3.5 Conclusions

In the current study, we report the first four solvent systems (DMSO/TBAF, DMF/TBAF, DMAc/TBAF and DMI/TBAF) that fully dissolve alginic acid, as its TBA salt, and that provide suitable conditions for organic reactions such as esterification. The contrasting results obtained with fully soluble systems (TBA alginate in TBAF/DMSO) versus partially soluble systems (TBA alginate in DMSO not containing any TBAF) illustrate the importance of identifying solvent systems in which alginate is fully soluble, in order to afford equal access of the reagents to alginates independent of factors like molecular weight, M/G ratio, and copolymer sequence. The success we have had in synthesizing alginate acetates and (low DS) alginate propionates is encouraging, since this solvent system permitted us to use relatively mild conditions and avoid the severe degradation to which alginic acid is prone under more aggressive reaction conditions. The ability to modify the polarity of the alginate molecule by adding substituents, such as ester

substituents, is very important if we wish to take advantage of the useful properties of alginates (biocompatibility, biodegradability, natural source, low toxicity, carboxyl content) for the design of drug delivery systems and other biomedical applications. The ability now to dissolve alginate in organic solvents will greatly facilitate such transformations, and the feasibility of chemistries besides esterification of the alginate hydroxyl groups is under active investigation in our group.

3.6 Supporting information

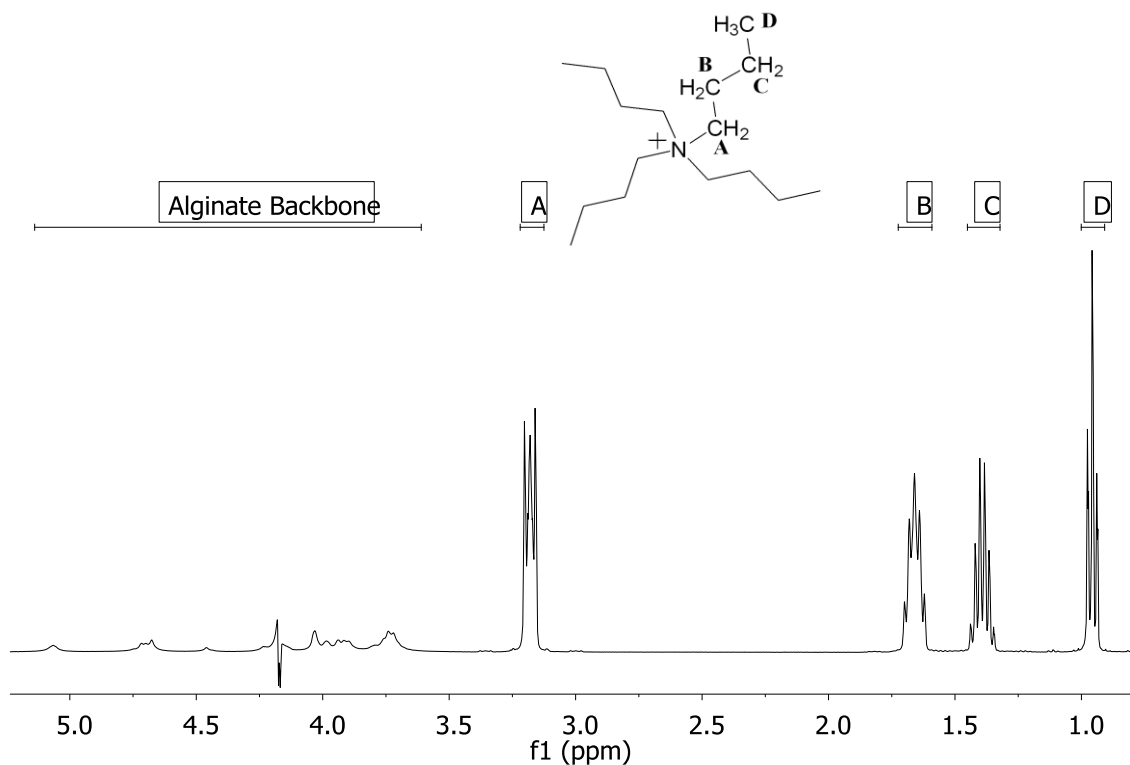


Figure 3.8: ^1H -NMR of M063 TBA-alginate

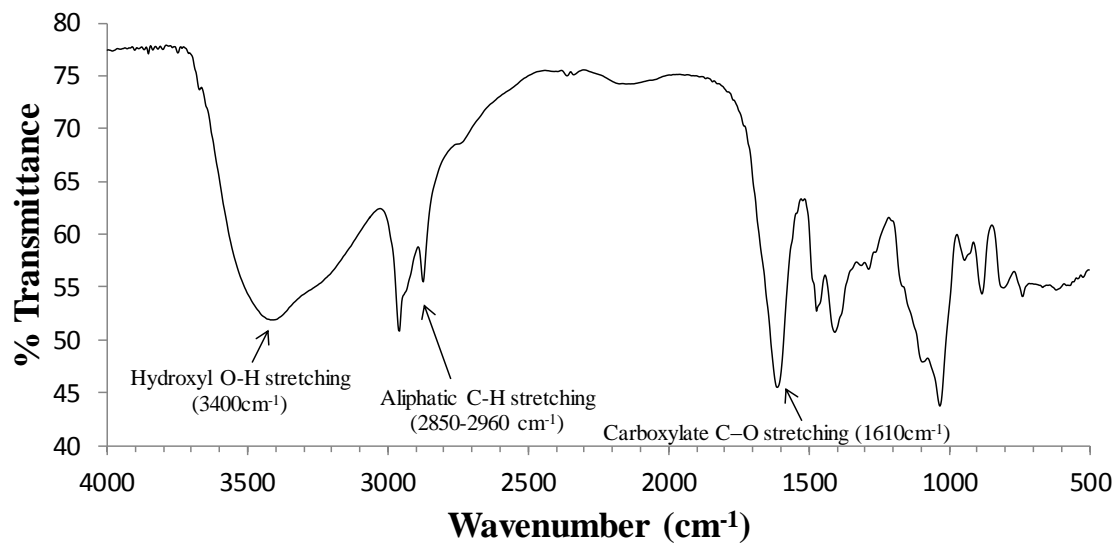


Figure 3.9: FTIR of M063 TBA-alginate

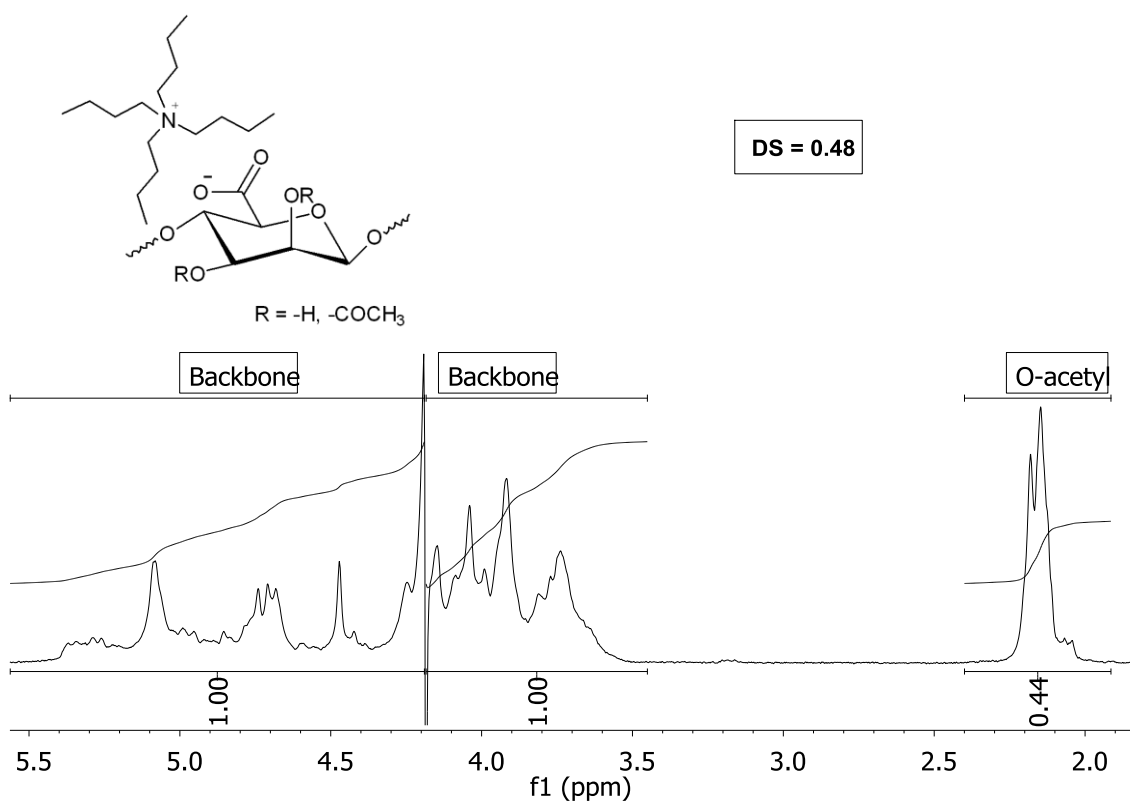


Figure 3.10: ¹H-NMR for product 2 shown in Table 3.4

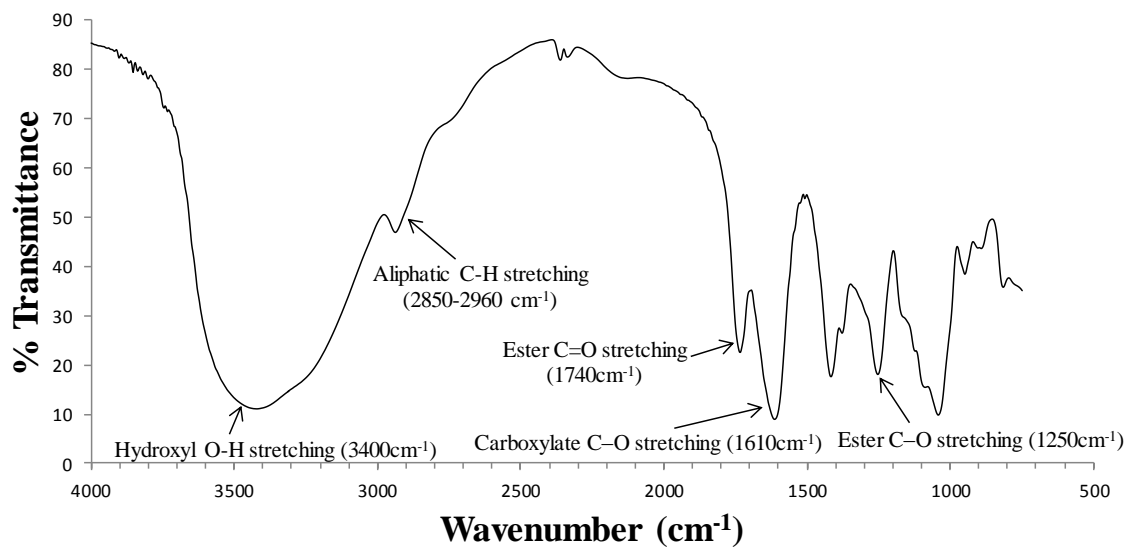


Figure 3.11: FTIR for product 2 shown in Table 3.4

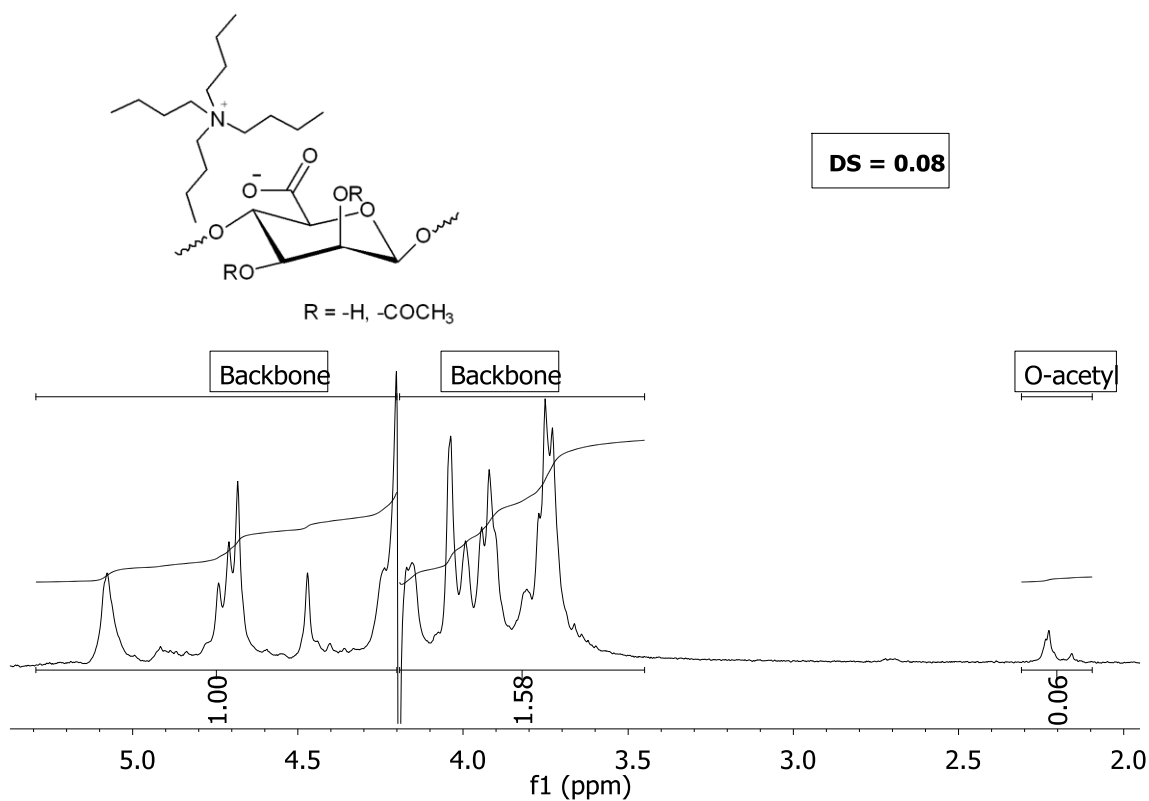


Figure 3.12: $^1\text{H-NMR}$ for product 7 shown in Table 3.2

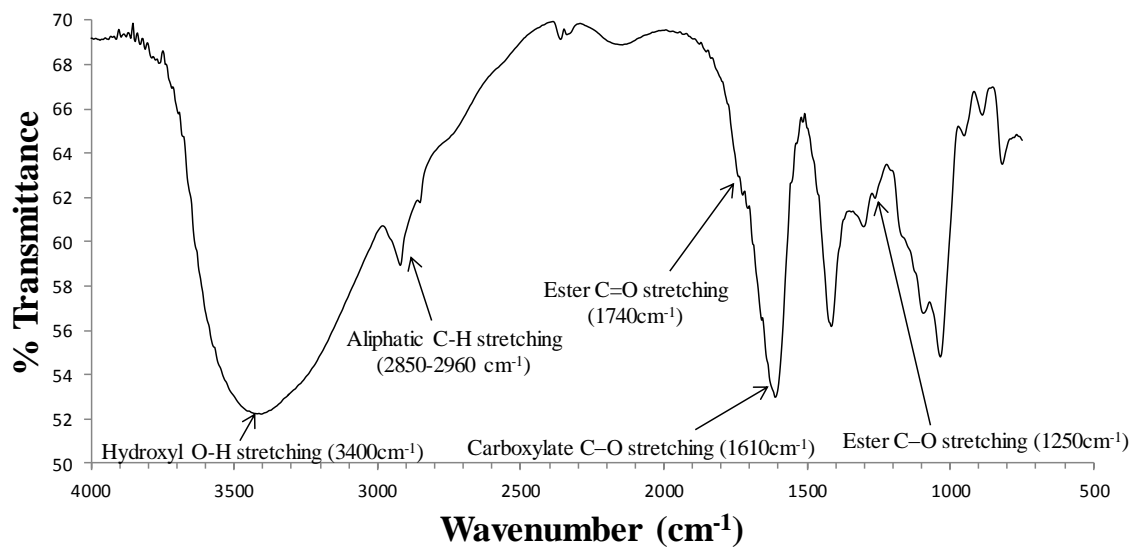


Figure 3.13: FTIR for product 7 shown in Table 3.2

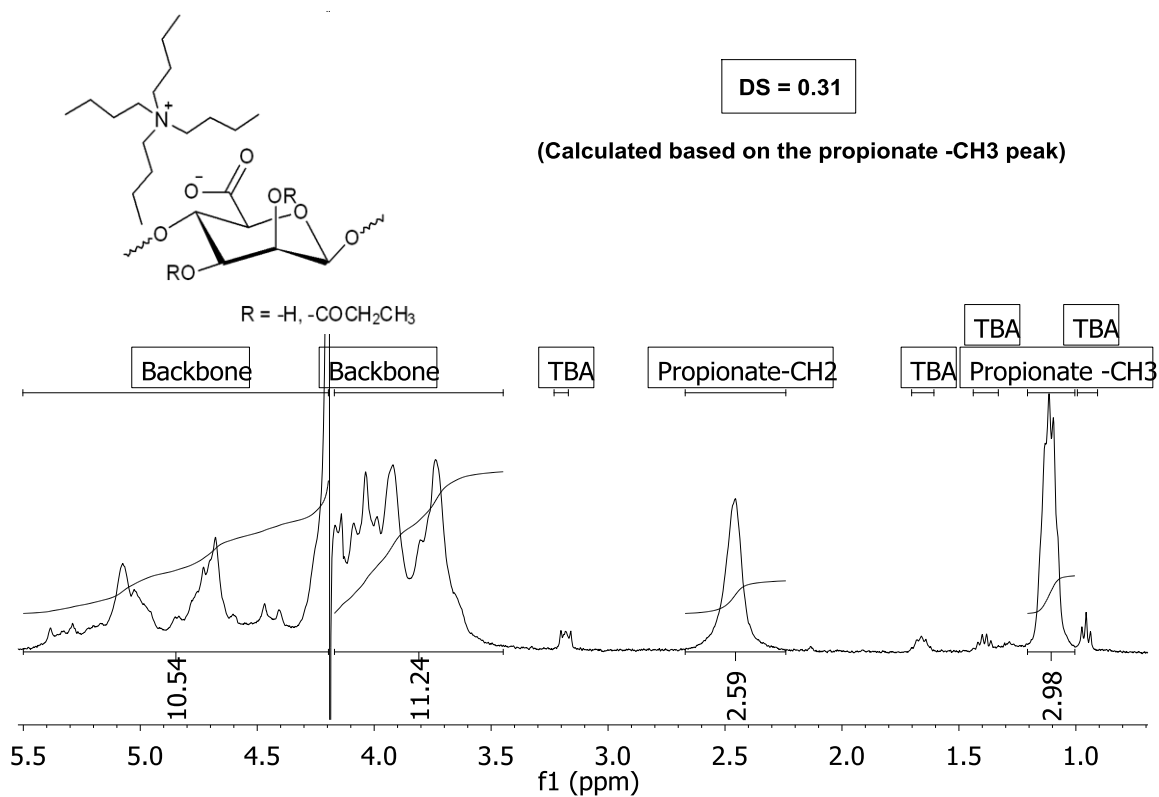


Figure 3.14: ¹H-NMR for product 8 shown in Table 3.2

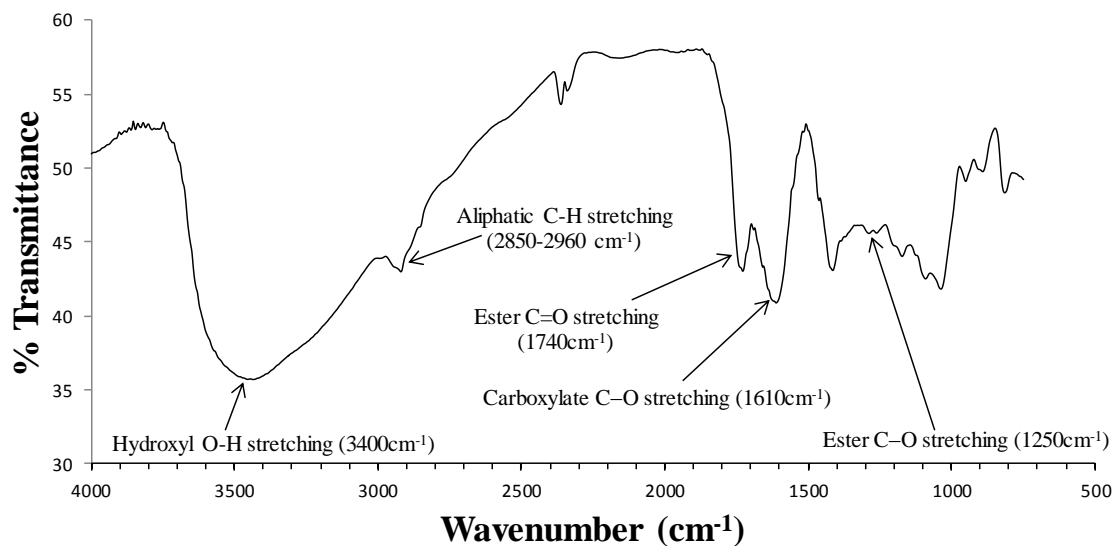


Figure 3.15: FTIR for product 8 shown in Table 3.2

Table 3.5: Experimental and theoretically calculated % elemental compositions of alginate acetates shown in Table 3.4

Reaction time		%C	%H	%O	%N
0 min	Experimental	48.49	9.20	37.98	2.33
	Theoretical	50.77	9.39	37.51	2.33
15 min	Experimental	35.75	5.77	52.73	0.62
	Theoretical	39.03	6.58	53.77	0.62
30 min	Experimental	35.14	5.71	53.11	0.49
	Theoretical	38.36	6.36	54.79	0.49
1 h	Experimental	34.66	5.56	53.03	0.36
	Theoretical	36.48	6.17	56.99	0.36
2 h	Experimental	34.19	5.32	53.58	0.36
	Theoretical	37.81	6.12	55.71	0.36

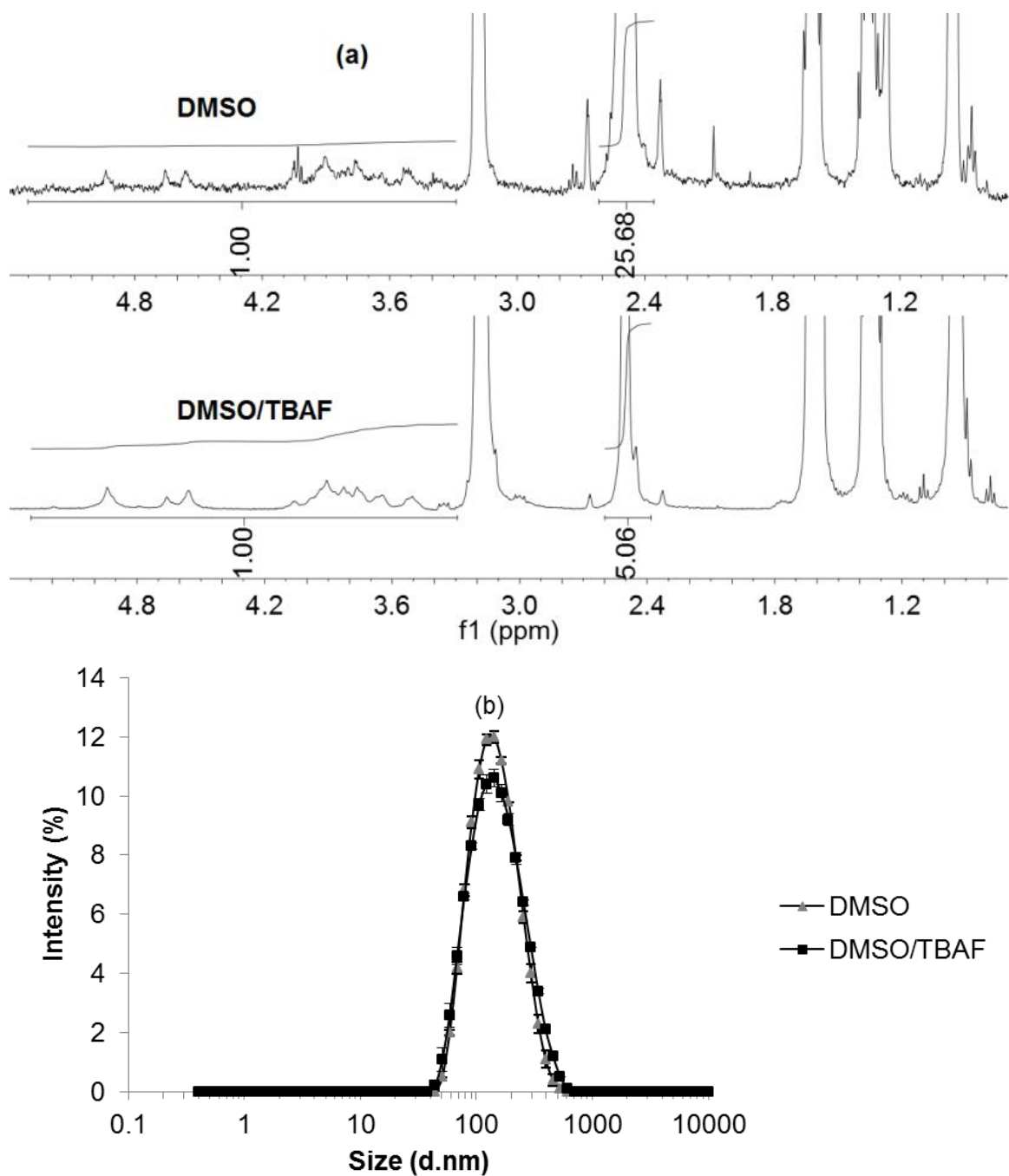


Figure 3.16: (a) ¹H-NMR spectra and (b) DLS intensity plots for TBA-alginate partially dissolved in DMSO and completely dissolved in DMSO/TBAF. ¹H-NMR spectra show integration of the DMSO-d₆ solvent peak at 2.5 ppm against the polymer backbone region between 3.3-5.0 ppm.

3.7 References

1. Draget, K. I., Alginates. In *Handbook of Hydrocolloids*, Phillips, G. O., Williams, P.A., Ed. 2009; pp 379-395.
2. Fox, S. C.; Li, B.; Xu, D.; Edgar, K. J., *Biomacromolecules* **2011**, *12*, 1956-1972.
3. Cathell, M. D.; Szewczyk, J. C.; Schauer, C. L., *Mini-Reviews in Organic Chemistry* **2010**, *7(1)*, 61-67.
4. Chamberlain, N. H., Cunningham, G.E., Speakman, J.B., *Nature* **1946**, *158*, 553.
5. Schweiger, R. G., *J. Org. Chem.* **1962**, *27* (5), 1786-1789.
6. Schweiger, R. G., *J. Org. Chem.* **1962**, *27* (5), 1789-1791.
7. Wassermann, A., *Nature* **1946**, *158*, 271.
8. Wassermann, A., *J. Chem. Soc.* **1948**, 197.
9. Skjåk-Bræk, G.; Paoletti, S.; Gianferrara, T., *Carbohydr. Res.* **1989**, *185* (1), 119-129.
10. Galant, C.; Kjoniksen, A. L.; Nguyen, G. T. M.; Knudsen, K. D.; Nystrom, B., *J. Phys. Chem. B* **2006**, *110* (1), 190-195.
11. Donati, I.; Coslovi, A.; Gamini, A.; Vetere, A.; Campa, C.; Paoletti, S., *Biomacromolecules* **2004**, *5* (1), 186-196.
12. Donati, I.; Vetere, A.; Gamini, A.; Coslovi, A.; Campa, C.; Paoletti, S., *Biomacromolecules* **2003**, *4* (3), 624-631.
13. Yang, J.; Goto, M.; Ise, H.; Cho, C.-S.; Akaike, T., *Biomaterials* **2002**, *23* (2), 471-479.
14. Rowley, J. A.; Madlambayan, G.; Mooney, D. J., *Biomaterials* **1999**, *20* (1), 45-53.
15. Rowley, J. A.; Mooney, D. J., *J. Biomed. Mater. Res.* **2002**, *60* (2), 217-223.
16. Xu, J. B.; Bartley, J. P.; Johnson, R. A., *J. Appl. Polym. Sci.* **2003**, *90* (3), 747-753.

17. Carré, M.-C.; Delestre, C.; Hubert, P.; Dellacherie, E., *Carbohydr. Polym.* **1991**, *16* (4), 367-379.
18. Sinquin, A.; Hubert, P.; Dellacherie, E., *Langmuir* **1993**, *9* (12), 3334-3337.
19. Sinquin, A.; Houzelle, M. C.; Hubert, P.; Choplin, L.; Viriot, M. L.; Dellacherie, E., *Langmuir* **1996**, *12* (16), 3779-3782.
20. Sinquin, A.; Hubert, P.; Dellacherie, E., *Polymer* **1994**, *35* (16), 3557-3560.
21. Babak, V. G.; Skotnikova, E. A.; Lukina, I. G.; Pelletier, S.; Hubert, P.; Dellacherie, E., *J. Colloid Interface Sci.* **2000**, *225* (2), 505-510.
22. Pelletier, S.; Hubert, P.; Lapique, F.; Payan, E.; Dellacherie, E., *Carbohydr. Polym.* **2000**, *43* (4), 343-349.
23. Grasselli, M.; Diaz, L. E.; Cascone, O., *Biotechnol. Tech.* **1993**, *7* (10), 707-712.
24. Moe, S. T.; Skjåk-Bræk, G.; Smidsrød, O., *Food Hydrocolloids* **1991**, *5* (1-2), 119-123.
25. Yeom, C. K.; Lee, K.-H., *J. Appl. Polym. Sci.* **1998**, *67*, 209-219.
26. Kim, J. H.; Jegal, J.; Kim, J. H.; Lee, K. H.; Lee, Y., *J. Appl. Polym. Sci.* **2003**, *89* (11), 3046-3051.
27. Kim, Y.-J.; Yoon, K.-J.; Ko, S.-W., *J. Appl. Polym. Sci.* **2000**, *78* (10), 1797-1804.
28. Riyajan, S.-A.; Sakdapipanich, J., *Polym. Bull.* **2009**, *63* (4), 609-622.
29. Chan, A. W.; Whitney, R. A.; Neufeld, R. J., *Biomacromolecules* **2008**, *9* (9), 2536-45.
30. Chan, A. W.; Whitney, R. A.; Neufeld, R. J., *Biomacromolecules* **2009**, *10* (3), 609-616.
31. Leone, G.; Torricelli, P.; Chiumiento, A.; Facchini, A.; Barbucci, R., *J. Biomed. Mater. Res.-A* **2008**, *84A* (2), 391-401.
32. Bouhadir, K. H.; Hausman, D. S.; Mooney, D. J., *Polymer* **1999**, *40* (12), 3575-3584.

33. Rokstad, A. M.; Donati, I.; Borgogna, M.; Oberholzer, J.; Strand, B. L.; Espevik, T.; Skjåk-Bræk, G., *Biomaterials* **2006**, 27 (27), 4726-4737.
34. Hills, B. P.; Cano, C.; Belton, P. S., *Macromolecules* **1991**, 24 (10), 2944-2950.
35. Köhler, S.; Heinze, T., *Macromol. Biosci.* **2007**, 7 (3), 307-314.
36. Ass, B. A. P.; Frollini, E.; Heinze, T., *Macromol. Biosci.* **2004**, 4 (11), 1008-1013.
37. Fidale, L. C.; Kohler, S.; Prechtel, M. H. G.; Heinze, T.; El Seoud, O. A., *Cellulose* **2006**, 13 (5), 581-592.
38. Heinze, T.; Dicke, R.; Koschella, A.; Kull, A. H.; Klotz, E. A.; Koch, W., *Macromol. Chem. Phys.* **2000**, 201 (6), 627-631.
39. Heinze, T.; Lincke, T.; Fenn, D.; Koschella, A., *Polym. Bull.* **2008**, 61 (1), 1-9.
40. Hussain, M. A.; Liebert, T.; Heinze, T., *Macromol. Rapid. Commun.* **2004**, 25 (9), 916-920.
41. Ramos, L.; Frollini, E.; Koschella, A.; Heinze, T., *Cellulose* **2005**, 12 (6), 607-619.
42. Ramos, L. A.; Frollini, E.; Heinze, T., *Carbohydr. Polym.* **2005**, 60 (2), 259-267.
43. Ostlund, A.; Lundberg, D.; Nordstierna, L.; Holmberg, K.; Nyden, M., *Biomacromolecules* **2009**, 10 (9), 2401-2407.
44. McCormick, C. L.; Callais, P. A., *Polymer* **1987**, 28 (13), 2317-2323.
45. Edgar, K. J.; Arnold, K. M.; Blount, W. W.; Lawniczak, J. E.; Lowman, D. W., *Macromolecules* **1995**, 28 (12), 4122-4128.
46. Liebert, T. F.; Heinze, T. J., *Biomacromolecules* **2001**, 2 (4), 1124-32.
47. Salomonsen, T. J., H.M.; Larsen, F.H.; Engelsen, S.B., The Quantitative Impact of Water Suppression on NMR Spectra for Compositional Analysis of Alginates. In *Magnetic Resonance*



in Food Science: Challenges in a Changing World, Gujonsdottir, M.; Belton, P.; Webb, G., Eds.

The Royal Society of Chemistry: 2009; pp 12-19.


48. Johnson, C. R.; Phillips, W. G., *J. Am. Chem. Soc* **1969**, *91* (3), 682-687.
49. Skjåk-Bræk, G.; Grasdalen, H.; Larsen, B., *Carbohydr. Res.* **1986**, *154*, 239-50.
50. Grasdalen, H., *Carbohydr. Res.* **1983**, *118* (Jul), 255-260.
51. Haug, A. L., B.; Smidsrød, O., *Acta Chem. Scand.* **1967**, *21*, 2859-2870.
52. Haug, A. L., B.; Smidsrød, O., *Acta Chem. Scand.* **1963**, *17*, 1466-1468.
53. Sun, H.; DiMagno, S. G., *J. Am. Chem. Soc.* **2005**, *127* (7), 2050-1.

3.8 Copyright Authorization

4/5/13 RightsLink® by Copyright Clearance Center



[Home](#) [Create Account](#) [Help](#)

**ACS Publications** High quality. High impact.

Title: Chemical Modification of Alginates in Organic Solvent Systems
Author: Siddhesh N. Pawar and Kevin J. Edgar
Publication: Biomacromolecules
Publisher: American Chemical Society
Date: Nov 1, 2011
Copyright © 2011, American Chemical Society

User ID
Password
☐ Enable Auto Login
[Forgot Password/User ID?](#)

LOGIN

If you're a copyright.com user, you can login to RightsLink using your copyright.com credentials. Already a RightsLink user or want to [learn more?](#)

PERMISSION/LICENSE IS GRANTED FOR YOUR ORDER AT NO CHARGE

This type of permission/license, instead of the standard Terms & Conditions, is sent to you because no fee is being charged for your order. Please note the following:

- Permission is granted for your request in both print and electronic formats, and translations.
- If figures and/or tables were requested, they may be adapted or used in part.
- Please print this page for your records and send a copy of it to your publisher/graduate school
- Appropriate credit for the requested material should be given as follows: "Reprinted (adapted) with permission from (COMPLETE REFERENCE CITATION). Copyright (YEAR) American Chemical Society." Insert appropriate information in place of the capitalized words.
- One-time permission is granted only for the use specified in your request. No additional uses are granted (such as derivative works or other editions). For any other uses, please submit a new request.

[BACK](#)[CLOSE WINDOW](#)

Copyright © 2013 Copyright Clearance Center, Inc. All Rights Reserved. [Privacy statement](#). Comments? We would like to hear from you. E-mail us at customercare@copyright.com

Chapter 4: Ca⁺²-Induced Gelation of Alginate Acetates for Tailored Hydrogels

(Adapted from Pawar, S.N., Bowden, S., McQuilling, J.P., Opara, E.C., Edgar, K.J.; Manuscript under review)

4.1 Abstract

Alginates are (1→4) linked linear copolysaccharides composed of β-*D*-mannuronic acid (M) and its C-5 epimer, α-*L*-guluronic acid (G). Several routes to synthesize alginate acetates have previously been described. We recently reported on methods to acetylate alginates either non-selectively or M-selectively. We hypothesized that while the non-selective acetates would be incapable of forming Ca⁺⁺-gels, the M-selective acetates would be more amenable to crosslinking. We herein report on our attempts to synthesize Ca⁺²-crosslinked alginate microbeads after acetylation. As we expected, it was not possible to form beads using randomly acetylated alginates within practical concentration ranges. M-selective alginate acetates however formed beads at relevant concentrations, thus highlighting the role of G blocks in alginate gelling by Ca⁺² crosslinking. The effects of reagent stoichiometry (pyridine and acetic anhydride) on degree of substitution (DS) and molecular weight were studied. Their influence upon solution viscosities, and the formation and mechanical strength of microbeads were studied with the intention of drawing conclusions about what reaction conditions may be best suited to bead formation. Furthermore, we discuss the relative merits of using ¹H-NMR or titration for DS measurement.

4.2 Introduction

Alginates are unbranched copolysaccharides consisting of 1→4 linked β-D-mannuronic acid (M) and its C-5 epimer α-L-guluronic acid (G). The natural copolymer is an important component of algae such as kelp, and is also a biofilm-forming exopolysaccharide of bacteria including *Pseudomonas aeruginosa*. It is comprised of sequences of M (M-blocks) and G (G-blocks) residues interspersed with MG sequences (MG-blocks)¹. Based on the desired functionality, alginate properties are tuned in nature by enzymatically (C-5 epimerase) varying composition (M/G ratio) and sequence², and also by adjusting molar mass. Alginate is an important industrial polysaccharide and is isolated from kelp in quantities up to 30,000 metric tons annually. However, this is estimated to comprise less than 10% of the biosynthesized alginate materials³. The large abundance of algae in water bodies (and the potential for algae farming) therefore offers significant additional potential to use designed sustainable biomaterials based on alginates.

Development of powerful organic solvent systems capable of dissolving recalcitrant polysaccharides has enabled routes to achieve regioselective transformations, leading to derivatives with novel properties.⁴ We have previously shown that in the case of alginates, selection of the appropriate medium for performing a particular reaction can greatly influence regioselectivity.⁵ Acylation of tetrabutylammonium (TBA) salts of alginate by complete solubilization in DMSO/TBAF (tetrabutylammonium fluoride) solvent provided derivatives with non-selective substitution of both epimers (M/G). In contrast, acylation under conditions of partial alginate solubilization in DMSO provided derivatives with preferential substitution on M residues. Prior to our report, several methods had been described for the synthesis of acetylated alginates.⁶ Acid-catalyzed acetylation was described as leading to partially and fully substituted

derivatives.⁷⁻⁹ An alternate route to acetylation was developed using ketene, a gaseous reagent which reacted with alginates in the swollen state.^{10, 11} However, the selectivity of this ketene chemistry was not reported. Selective acetylation of M residues was described by forming Ca-alginate beads and swelling them in a pyridine-acetic anhydride reagent mixture.¹² M residues reacted in preference to G residues at low degrees of substitution (DS). As the DS approached its limiting value, G residues reacted and epimer selectivity was compromised.

Alginates are most well known for their ability to form hydrogels by crosslinking with bivalent cations. Gel formation is driven by G-block sequences which associate via multidentate chelation to form tightly held junction points.¹³ In addition, MG-block sequences provide assistance by forming relatively weaker junctions.¹⁴ Hydrogel formation is not possible in the absence of G residues. The importance of these physically crosslinked systems in medicine and biology is immense.¹⁵ Alginates are currently used as dressing materials in the treatment of acute or chronic wounds.¹⁶ They play a central role in facilitating the progression of cystic fibrosis wherein alginate biofilms are secreted by bacteria for immunoprotection¹⁷; conversely, alginate oligomers have been proposed for therapy of cystic fibrosis patients, by competitively inhibiting alginate-mucin binding.¹⁸ One of the more impactful applications of alginates is in diabetes therapy.¹⁹ Diabetes is a globally prevalent disease, currently affecting about 285 million people worldwide.²⁰ Type 1 diabetes is a significant cause of morbidity and mortality in young adults. In addition, secondary diabetic complications may arise in the form of increased risk of heart attack and stroke, and decreased life expectancy.^{20, 21} Current standard treatment regimens for Type 1 diabetes include daily insulin injections to control blood glucose. While intensive insulin therapy can adequately control blood glucose levels so as to permit most normal activities, it cannot duplicate the continuous monitoring and response of a functional pancreas, and does not totally

eradicate secondary diabetic complications and adverse side effects such as unwanted weight gain and hypoglycemia.^{22, 23}

An alternative treatment modality for Type 1 diabetes is replacement of the missing β -cells via transplantation of the pancreas.^{24, 25} This treatment method is capable of achieving normal glycemic levels along with prevention, and even reversal of secondary complications. The islets of Langerhans are the most preferred source of insulin secreting β -cells.²⁶ It is however essential to prevent immune responses that may result from transplantation of foreign islet cells. Microencapsulation within alginate beads is a convenient way to accomplish this goal. We have previously described the principle of immunoisolation by islet encapsulation within alginates.²⁵ Upon cell encapsulation within alginate microbeads, a permselective poly-L-ornithine (PLO) coating is applied which is permeable to small molecules such as nutrients, oxygen and water, but impermeable to large entities such as immune cells and antibodies. Finally, an outer alginate layer is applied to prevent interactions between positively charged PLO and negatively charged proteins and cells *in vivo*.

While alginates play a very important role in the design of the bioartificial pancreas, there appear to be no reports on the use of hydrophobically modified alginates for this application. Hydrophobic modifications may be envisioned as an excellent tool to fine-tune the diffusion/transport properties of alginates encapsulating β -cells. In addition, gel instabilities arising from Na^+ - Ca^+ ion exchange may be suppressed by making the alginate gel more hydrophobic. However, to be able to use modified alginates for encapsulation, a primary criterion is the preservation of its ability to form ionic gels. In the current article, we report on the potential of acetylated alginates to form Ca^{+2} induced gels. The effects of variables including acetylation reaction conditions, corresponding DS values, molecular weights and M/G ratios and

viscosities were studied to establish clear correlations with the gelling abilities of the modified alginates. In addition, we noticed in following up our earlier alginate acetylation studies that there were unexplained variations in DS values, and herein we describe investigation of the cause of those variations, and development of a superior method for determination of DS(acetyl). Furthermore, we describe our investigations of the relative mechanical strength of microbeads made either from alginate or acetylated alginate.

4.3 Experimental

4.3.1 Materials

Four alginates were used in the study and are represented as A-D. ‘A’ and ‘B’, were high-mannuronic alginic acid sodium salts extracted from brown algae with viscosities of $\geq 2,000$ cP and 100-300 cP respectively (measured as 2% aqueous solutions). ‘C’ and ‘D’ were alginic acid sodium salts with high M and high G contents respectively. The molecular weights and M/G compositions of A-D are listed in **Table 4.1**. In addition, an ultrapure grade of alginate ‘LVM’ with a low viscosity and high M content commonly used for islet encapsulation was also studied for comparative analyses.

Water used in the experiments was deionized. Hydrochloric acid, reagent alcohol (histological grade), hexanes (HPLC grade), dimethylsulfoxide (HPLC grade), 5 N standardized NaOH solution, 1 N standardized HCl solution, ethyl acetate and calcium chloride (CaCl_2) were purchased from Fisher Scientific (Fair Lawn, NJ). Acetic anhydride (Ac_2O ; 99+%), pyridine (Pyr; anhydrous, 99.0%), tetrabutylammonium hydroxide (TBAOH; 40 wt%, 1.5 M solution in water) and sodium carbonate (99.8% anhydrous powder) were obtained from Acros. Deuterium

oxide (99.9 atom% D; D₂O) containing 0.75% 3-(trimethylsilyl)propionic-2,2,3,3-d₄ acid, sodium salt for NMR, NaCl, 4-(2-hydroxyethyl)-1-piperazineethanesulfonic acid (HEPES), and alginates ‘A’ and ‘B’ were acquired from Sigma-Aldrich (St. Louis, MO). Alginates ‘C’ and ‘D’ were acquired from FMC BioPolymer (Philadelphia, PA). KBr used for FTIR analysis was purchased from International Crystal Labs. Ultrapure low-viscosity high mannuronic acid (LVM) alginate was obtained from Novamatrix (Sandvika, Norway).

4.3.2 Synthesis of TBA-alginate

For conversion of Na-alginate to its protonated form, a procedure described by Babak et al.²⁷ was followed with modifications. HCl (0.6 N, 120 mL) was mixed with ethanol (120 mL) in a beaker. Na-alginate (8 g) was added to the mixture and stirred overnight at 4 °C. The mixture was filtered, the solid (alginic acid) washed thoroughly with ethanol followed by acetone, and dried overnight *in vacuo* at 60 °C. Thoroughly dried alginic acid was then dispersed in 200 mL water. TBAOH was added dropwise with continuous stirring at room temperature until the polymer was fully dissolved and the pH was adjusted to 10.0. If the solution was too viscous, small amounts of water were added until a final viscosity was reached at which the solution could be easily stirred. The aqueous TBA-alginate solution was then premixed with reagent alcohol. The premix was precipitated in a mixture of ethyl acetate-hexane. The solvent ratios used were aqueous alginate acetate : ethanol : ethyl acetate : hexane = 1:3:12:3. The precipitate was then filtered under vacuum and dried *in vacuo* at 60 °C. The ¹H-NMR and FTIR spectra for TBA-alginate are shown in the Supporting Information as **Figures 4.11** and **4.12** respectively.

¹H NMR (500 MHz, D₂O) δ 5.82 – 3.46 (m, alginate backbone), 3.19 (t, NCH₂CH₂CH₂CH₃ of TBA), 1.67 (m, NCH₂CH₂CH₂CH₃ of TBA), 1.40 (m, NCH₂CH₂CH₂CH₃

of TBA), 0.97 (t, $\text{NCH}_2\text{CH}_2\text{CH}_2\text{CH}_3$). FTIR (KBr pellet method): 3400 cm^{-1} , hydroxyl O–H stretching; $2850\text{--}2960\text{ cm}^{-1}$, aliphatic C–H stretching, 1610 cm^{-1} , carboxylate C–O stretching. Elemental composition TBA-alginate ‘A’ measured by elemental analysis: C, 57.30%; H, 9.76%; N, 2.82%. This composition corresponds to roughly 78% TBA and 22% Na salt.

4.3.3 Synthesis of alginate acetate

DMSO (350 mL) was added to TBA-alginate (7 g) in a 3-neck flask. The mixture was blended using a mechanical stirrer at room temperature until the polymer was fully dispersed. The temperature of the mixture was raised to $40\text{ }^\circ\text{C}$. Ac_2O was added followed by pyridine at the desired molar ratios. The suspension was stirred for 30 min, and then the polymer was precipitated in 3500 mL of ethyl acetate. The solid was filtered under gravity using fluted filter paper and dried *in vacuo* at $60\text{ }^\circ\text{C}$. The dried crude solid was crushed into a powder using mortar and pestle, and the powder was added to $\sim 50\text{--}250\text{ mL}$ of water. While the mixture was stirring, 1 M Na_2CO_3 solution was added dropwise to dissolve the polymer. The pH was adjusted to 10.0. The solution was added dropwise to 500 mL ethanol to precipitate the sodium salt of alginate acetate. The resulting solid was filtered under vacuum and dried *in vacuo* at $60\text{ }^\circ\text{C}$. A second purification was carried out by dissolving the dry product in water and re-precipitating in ethanol before drying *in vacuo*. The ^1H -NMR and FTIR spectra for alginate acetate A.P10.Ac20 from **Table 4.2** are shown in **Figures 4.1** and **4.2**.

Analytical results for A.P10.Ac20 are as follows. ^1H NMR (500 MHz, D_2O) δ 5.69 – 3.31 (m, alginate backbone), 2.45–1.80 (m, COCH_3 of acetate). FTIR (KBr pellet method): 1740 cm^{-1} , ester C=O stretching vibration; 1250 cm^{-1} , ester C–O stretching vibration; 3400 cm^{-1} , hydroxyl O–H stretching; $2850\text{--}2960\text{ cm}^{-1}$, aliphatic C–H stretching, 1610 cm^{-1} , carboxylate C–O

stretching. $DS_{\text{NMR}} = 2.0$. $DS_{\text{Titration}} = 0.85$. Elemental composition, as measured experimentally using elemental analyzer: C, 35.00%; H, 4.51%; N, 0.09%; O, 44.05%. Theoretical compositions were determined using a spreadsheet in which %TBA values were varied from 0-100% and the corresponding elemental percentages were calculated. By inserting the DS value ($DS_{\text{Titration}} = 0.85$ for this example) and assuming an appropriate number of moles of water of hydration (1 for this example), theoretical compositions that were closest matching to the experimental values were determined. The %TBA corresponding to that composition was then used for average molar mass calculations. For A.P10.Ac20, the theoretically calculated composition was C, 37.39%; H, 4.41%; N, 0.09%; O, 49.24%. This corresponded to a %TBA value of 1.6. For all alginate acetates listed in **Table 4.2**, the %TBA values and their calculated average repeat unit molar masses are shown in **Table 4.6** of Supporting Information.

4.3.4 Synthesis of Ca-alginate beads

Solutions of M-acetylated alginate (3%, 5%, 7.5% w/v) and a solution of 1.5% non-acetylated sodium alginate (sample A) were prepared in deionized water and placed on a shaker in a warm room (37°C) for 24 hours. Each alginate solution (3 mL) was placed in a 5 mL syringe and passed through a 2-nozzle microfluidic encapsulator²⁸ at a flow rate of 0.2 mL/min and fixed air pressure (0.5, 1, 1.5 or 2 psi). The capsules were dropped into 45 mL of cross-linking solution (1.1% w/v CaCl_2) in a 100/20 mm Petri dish with continuous stirring.

4.3.5 DS_{NMR} measurement

For ^1H -NMR, sample preparation was carried out by dissolving ~10 mg of polymer in 0.6 mL D_2O containing TMS standard. Spectra were acquired using a JEOL 500 MHz spectrometer with automatic shimming. An automatic water suppression pulse was applied to suppress the residual HDO peak. The acquisition temperature was 85 °C for all samples, and 64 scans were obtained for each. All spectra were processed using MestReNova version: 6.2.1-7569. DS value calculation was carried out by evaluating the ratio of the integral of the O-acetyl peak centered at ~2.2 ppm (I_{AC}) to that of the polymer backbone region ~3.5-5.5 ppm (I_{BB}). I_{AC} accounts for 3X protons, assigned to the acetyl $-\text{CH}_3$ group. I_{BB} accounts for $(7-\text{DS}_{(\text{Ac})})\text{X}$ protons. The following formula was used to calculate DS(acetyl) from these integrals:

$$DS_{\text{NMR}} = \frac{7I_{\text{AC}}}{(3I_{\text{BB}} + I_{\text{AC}})}$$

4.3.6 $\text{DS}_{\text{Titration}}$ measurement

Titration was performed by reacting alginate acetates with excess NaOH to hydrolyze the esters. NaOH molecules remaining after hydrolysis were then back-titrated with HCl to measure the moles of acetate present. Specifically, 50 mg alginate acetate was weighed into a 25 mL 3-neck flask. To this, 10.0 mL of standardized 0.1 N NaOH solution was added and stirred overnight at room temperature. Potentiometric titrations were performed using a pH electrode (Inlab 413, Mettler-Toledo International, Inc.). The electrode was inserted into the 3-neck flask, 0.1 mL aliquots of standardized 0.1 N HCl solution added, the solution allowed to stir for 30 seconds and the pH measured. Total volume of HCl added was 15 mL. Two plots were made using the recorded data. pH was first plotted against the volume of HCl added. Derivative $d(\text{pH})$

was plotted in a second graph against the volume of HCl added. Inflexion point was recorded as the volume at which peak maximum was attained in the d(pH) plot.

Moles of acetate present in the alginate acetate used for titration (50 mg) were calculated as follows:

$$\text{Moles of acetate (M)} = \text{Initial moles of NaOH} - \text{Moles remaining after hydrolysis}$$

DS was then calculated as:

$$DS_{\text{Titration}} = \frac{M}{\text{No. of uronic acid residues in sample (N)}} \quad \text{Equation (1)}$$

Where,

$$N = \frac{0.05}{417(x) + 198(1-x) + 42(DS_{\text{Titration}})} \quad \text{Equation (2)}$$

‘x’ refers to the fraction of alginate acetate existing as TBA-salts. Correspondingly, (1-x) is the fraction existing as Na-salts. The value of ‘x’ can be expressed in terms on ‘DS’ as follows:

$$x = \frac{(198 + 219x + 42(DS_{\text{Titration}}))A}{1400} \quad \text{Equation (3)}$$

‘A’ is the % elemental composition of nitrogen measured using %CHN analyzer with combustion/thermal conductivity detector (TCD) and %O analyzer with pyrolysis. Equation (3) was substituted in Equation (2), which was in turn plugged in to Equation (1) to calculate $DS_{\text{Titration}}$.

4.3.7 FTIR measurement

FTIR spectra were acquired using a Thermo Electron Nicolet 8700 instrument in transmission mode. Samples were prepared using the KBr pellet method. Alginate (1 mg) was mixed with 99 mg of KBr in a mortar-pestle. The mixture was compressed in the sample holder between two screws to form a KBr disc. 64 scans were obtained for each spectrum.

4.3.8 SEC analysis

Molecular weight measurements were performed using SEC-MALS-dRI technique. A solvent and sample delivery system consisting of solvent reservoir, on-line degasser, isocratic pump and auto-injector from Agilent Technologies, Santa Clara, CA, USA was used for the experiments. Three Waters columns were connected in series - UltrahydrogelTM Linear (7.8×300 mm), UltrahydrogelTM 500 (7.8×300 mm) and UltrahydrogelTM 120 (7.8×300 mm). The columns were preceded by an UltrahydrogelTM Guard column (6×40 mm). The column outlet was connected to a DAWN HELEOS-II MALS detector and to an OPTILAB rEX dRI detector, both obtained from Wyatt Technologies, Santa Barbara, CA, USA. The mobile phase used for alginate dissolution was 0.05 M Na₂SO₄/0.01 M EDTA, pH 6 containing 2 ppm NaN₃. An alginate concentration of 1-2 mg/mL was used with a flow rate of 0.8 mL/min and an injection volume of 100 μ L. All solutions were passed through 0.2 μ nylon syringe filters prior to injection. Data from light scattering and the differential refractometer were processed using Astra (v. 6.0.6.13) software supplied by Wyatt Technologies.

4.3.9 Viscosity measurement

A Brookfield LVDV-II+PRO CP viscometer (Middleboro, MA) with a CP-52 spindle attached was connected to a 23°C water bath and RheoCalc program was used to collect the viscosity data. Various solutions of non-acetylated alginate A, the M-acetylated alginates (3%, 5.5%, 6%, 6.5%, 7% and 7.5% w/v) and a solution of 1.5% non-acetylated LVM were placed on a shaker in a warm room (37°C) for 24 hours. A 0.5 mL sample aliquot was placed in the spindle

plate of the Brookfield viscometer and spun for two minutes at <99% torque to remove air bubbles and spread the sample evenly. Each sample was run for five 60-second loops, each separated by one second, decreasing in shear rate with each subsequent loop. The shear rate values corresponded to a range of 10% to 99% torque in order to maximize the accuracy of the readings. Viscosity data were collected at one second intervals during each loop. Three 0.5 mL samples were run for each alginate preparation. Each sample was run three times. The viscosity data were averaged for each concentration of alginate examined. Viscosity, measured in Pa.s, was plotted against shear rate.

4.3.10 Imaging of Microbeads

Microbeads were placed in a 24-well plate containing approximately 0.2 mL of cross-linking solution. Images were taken at 4x and 10x using an Olympus IX-71 Inverted Microscope. Scale bars were added to the image to determine microbead size.

4.3.11 Mechanical Strength Testing of Microbeads

The mechanical strength of the microbeads was assessed using the osmotic stress and mechanical stress procedures described previously²⁹. In the osmotic stress test, briefly microbeads measuring 500-600 μM in diameter were generated using a 2-channel air jacket microencapsulator. Osmotic stress test was conducted by placing 100 microbeads/well in a 48 well plate with 1 mL distilled H_2O and then incubating at 37 °C for 2 h. The microbeads were then washed with a mixed solution of 0.9% saline and 0.25% CaCl_2 prior to assessment of the numbers of broken and intact microbeads using an inverted light microscope. In the mechanical

stress test, groups of 350 microbeads were placed in T-25 flasks containing approximately 6.5 g of 3 mm inert soda lime beads (VWR Scientific Products Corporation) and 5 mL of the mixed 0.9% saline and 0.25% CaCl_2 solution. Microbeads from each group were then subjected to mechanical stress for 48 h by shaking at 100 rpm using a Max Q 3000 Shaker (Thermo Scientific). The percentages of broken and unbroken capsules were then determined by visual analysis under an inverted microscope.

4.3.12 Statistical evaluation of data

Quantitative data for mechanical strength studies of microbeads are presented as mean \pm standard deviation and were statistically evaluated using One-Way ANOVA with Tukey-Kramer multiple comparisons test. Differences between data were considered significant at $p < 0.05$.

4.4 Results and Discussion

In order to perform a systematic study correlating gel-forming ability to acetylation reaction conditions, DS, molecular weight and M/G ratio, careful selection of starting alginates was essential. **Table 4.1** shows molar masses and compositions of alginates A-D used in this study. ‘A’ and ‘D’ represent alginates with the lowest and highest F_G (fraction of G residues) values respectively. ‘B’ and ‘C’ possess intermediate F_G values. While F_G indicates the total fraction of G units within the alginate chain, it includes those G units in G-blocks, MG-blocks and interspersed residues. For the study of gelling properties, perhaps a more significant parameter would be F_{GG} (fraction of G residues neighboring another G residue) – the fraction representing G residues involved in G-block formation. ‘D’ therefore possesses the largest

fraction of G-blocks followed by LVM, ‘C’ and ‘A’, while ‘B’ has the lowest fraction of G-blocks. Molar mass analysis of the starting Na-alginates shows that ‘A’ had the highest while ‘C’ had the lowest DP_n value. LVM, ‘B’ and ‘D’ had intermediate DP_n , the former being slightly smaller. As the Na^+ salts were converted to their corresponding TBA^+ salts, the DP_n values for all four alginates decreased. This is not surprising since alginates undergo degradation in the presence of both acids (via hydrolysis)^{30, 31} and bases (via β -elimination).^{32, 33} Molecular weight (MW) loss can therefore occur due to the presence of both HCl and TBAOH in two separate synthesis steps. During conversion to its TBA salt, the DP_n of alginate A decreased by 658 (72% drop). This ΔDP_n value was much larger compared to those of alginates B, C and D, whose average chain lengths were lowered by 134, 132 and 177 (44, 57 and 49% drops) respectively.

Table 4.1: Molecular weights, PDI, DP_n and M/G compositions of alginates A-D used in the study

		M_n (KDa)	M_w (KDa)	PDI	DP_n	ΔDP_n	F_G	F_M	F_{GG}	F_{GM}	F_{MM}
LVM	Na^+	61	111	1.821	308	-	0.49	0.51	0.26	0.23	0.28
A	Na^+	180	251	1.394	909	-	0.33	0.67	0.21	0.12	0.55
	TBA^+	97	197	2.031	251	658					
B	Na^+	60	101	1.683	303	-	0.37	0.63	0.19	0.18	0.45
	TBA^+	68	108	1.588	169	134					
C	Na^+	46	116	2.522	232	-	0.40	0.60	0.27	0.13	0.47
	TBA^+	39	70	1.795	100	132					
D	Na^+	71	123	1.732	359	-	0.62	0.38	0.56	0.06	0.32
	TBA^+	72	117	1.625	182	177					

M_n , M_w and PDI measured using aqueous SEC. F_G , F_M , F_{GG} , F_{GM} and F_{MM} calculated by 1H -NMR using a method previously described in the literature^{34, 35}

The reaction variables employed during acetylation (reagent molar ratios, time and temperature) affect final properties such as DS, molecular weight and ability to form Ca-crosslinked hydrogels. We suspected that in order to obtain functional alginate acetate calcium gels, it would be of critical importance to balance the extent and placement of acetylation with

the amount of molecular weight loss occurring during acylation. We were interested specifically in the effects of pyridine (because of its potential catalysis of base-catalyzed chain degradation) and Ac₂O molar equivalents (mainly impacting product DS_{acetyl} and the location of acetyl groups, we thought) on final properties. **Table 4.2** lists the experiments conducted to probe these effects, and the corresponding results. In Series I, pyridine molar equivalents were varied from 2-20 while using a large excess (20 equivalents) of Ac₂O. This series therefore illuminated the effect of pyridine molar excess on final properties at a high concentration of Ac₂O. Similarly, Series II showed the effect of varying the pyridine molar equivalents on final properties at low concentrations of Ac₂O. In Series III, the Ac₂O molar equivalents were varied from 2-20 while keeping the pyridine equivalents constant at 10, thus providing insight into the effect of Ac₂O molar excess on final properties. Finally, Series IV shed light on the effects of changes in the alginate composition and sequence.

Table 4.2: Molar ratios used for acetylation, DS values as measured by titration, and aqueous SEC results for corresponding products

Series	Sample ID	Molar Ratio	DS _{Titration}	M _n (KDa)	M _w (KDa)	PDI	DP _n
I	A.P2.Ac20	1:2:20	0.98	15	58	3.867	57
	A.P10.Ac20	1:10:20	0.85	27	66	2.444	106
	A.P20.Ac20	1:20:20	0.92	17	49	2.882	65
II	A.P2.Ac2	1:2:2	0.40	35	99	2.829	145
	A.P10.Ac2	1:10:2	0.30	60	140	2.333	259
	A.P20.Ac2	1:20:2	0.40	36	79	2.194	151
III	A.P10.Ac2	1:10:2	0.30	60	140	2.333	259
	A.P10.Ac5	1:10:5	0.69	41	156	3.805	166
	A.P10.Ac10	1:10:10	0.80	26	91	3.500	103
	A.P10.Ac20	1:10:20	0.85	27	66	2.444	106
IV	B.P10.Ac10	1:10:10	0.96	39	141	3.615	151
	C.P10.Ac10	1:10:10	0.90	32	81	2.531	125
	D.P10.Ac10	1:10:10	0.97	36	79	2.194	138

UAR:Uronic acid residue; Molar ratios expressed as UAR:Pyridine:Ac₂O

We have previously described a method to prepare TBA-salts of alginic acid for dissolution in organic solvents and further reaction in those solvents⁵. Since commercially available alginates are typically Na-salts, it is essential first to protonate the salts using ethanolic HCl to form alginic acids. TBAOH can then be added to form the corresponding TBA-salts. Our previously described TBA-alginate isolation procedure used dialysis and freeze-drying as the final purification steps. However for processing larger (gram) quantities of material on a lab scale, these purification steps may require several weeks for final product recovery. In addition, we noticed that freeze drying of extremely viscous solutions caused inconsistencies in physical appearance, for example between portions of the same solution dried in separate flasks. We therefore developed a faster precipitation workup procedure which yielded products that were free of physical inconsistencies. The aqueous TBA-alginate solution was first premixed with ethanol. The premix was then added dropwise to an ethyl acetate-hexane mixture. Ethanol was necessary since water and ethyl acetate are immiscible without a compatibilizing solvent. The presence of hexane in the non-solvent aided filtration by yielding a harder precipitate which was easier to filter. **Figures 4.11** and **4.12** in the supporting information show the ¹H-NMR and FTIR spectra of TBA-alginate (A) respectively. The percentage of uronic acid residues existing as TBA salts was quantified using elemental analysis. **Table 4.5** in the Supporting Information shows the elemental compositions and % TBA contents of TBA-alginates A-D.

We have previously described the heterogeneous acetylation of TBA-alginate in DMSO as a method to achieve selective reaction of M residues on the backbone ⁵. Water-soluble alginate acetates were recovered as final products. **Figures 4.1** and **4.2** depict the ¹H-NMR and FTIR spectra of product A.P10.Ac20 shown in **Table 4.2**. The O-acetyl peak appearing at ~2.2 ppm confirms the presence of acetate esters. The polymer backbone peaks appear in the region

~3.5-5.5 ppm. The HDO solvent peak at ~4.2 ppm was eliminated using a water suppression experiment. In the FTIR spectrum, the peaks at 1740 cm^{-1} and 1250 cm^{-1} were assigned to the C=O and C–O stretching vibrations from the acetate ester. These peaks were absent in the FTIR spectrum of TBA-alginate shown in **Figure 4.12** of supporting information.

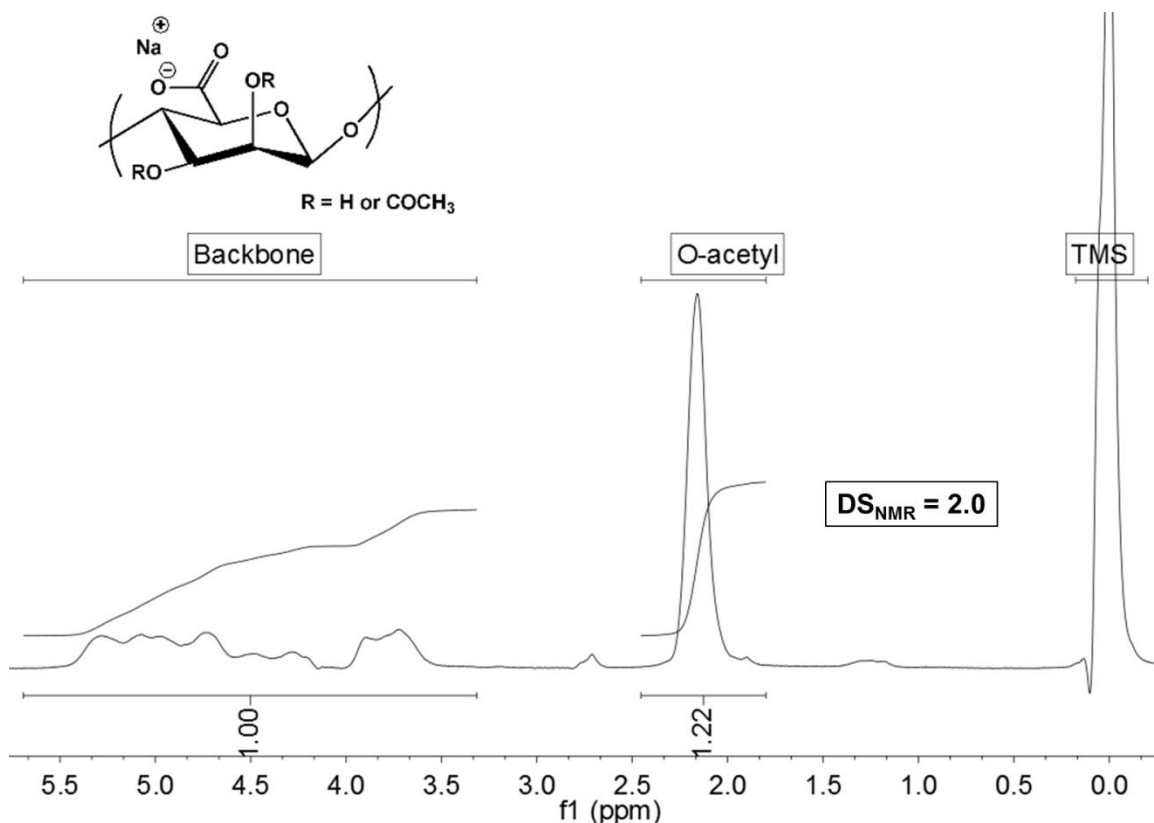


Figure 4.1: ^1H -NMR spectrum of alginate acetate A.P10.Ac20 from Table 4.2. HDO peak suppression used during acquisition

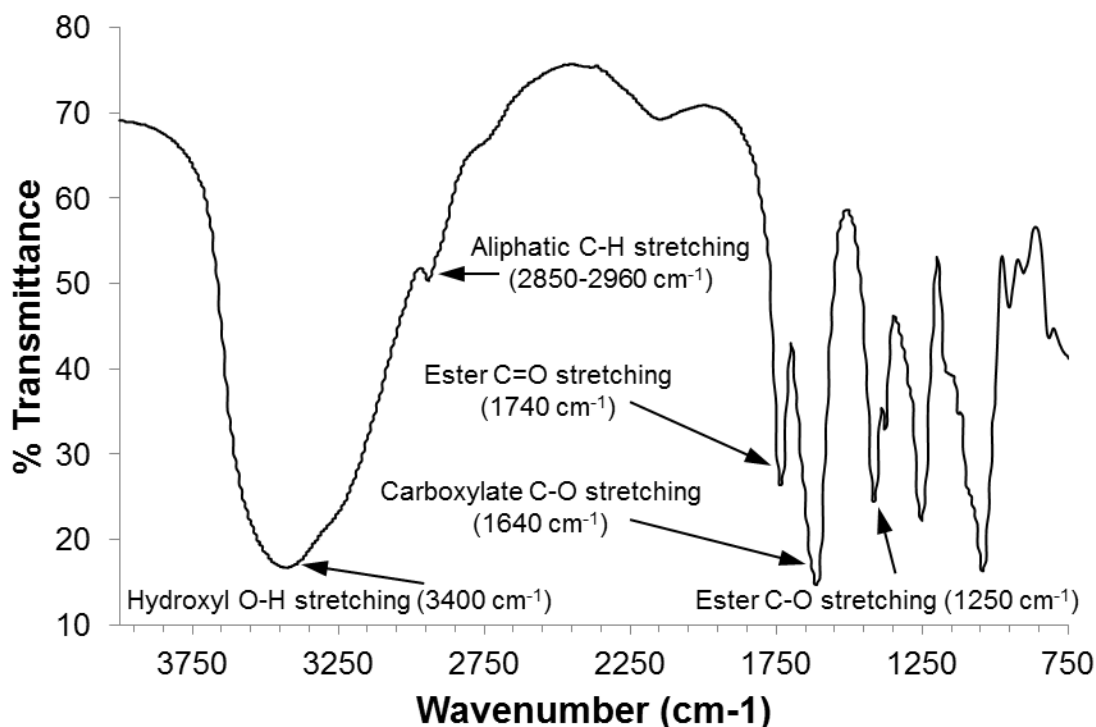


Figure 4.2: FTIR spectrum of alginate acetate A.P10.Ac20 from Table 4.2

We expressed in our previous publication describing alginate acetates the concern that the accuracy of DS calculations based on ^1H NMR measurements may be questionable, since HDO solvent suppression affects the intensities of adjacent signals in the spectra, thus changing the integration values³⁶. A demonstration of the impact of HDO solvent peak suppression upon integration values follows. The ^1H NMR spectrum in **Figure 4.1** illustrates the result of application of a water suppression pulse sequence during acquisition. Based on integration, DS_{NMR} was found to be 2.0. A second spectrum for the same product A.P10.Ac20 is shown in **Figure 4.3**. In this case a regular pulse sequence was applied during acquisition, but signal suppression was carried out post acquisition using NMR processing software (listed in experimental). DS_{NMR} in this case was calculated to be 1.28. The disparity between the two DS

values clearly demonstrates how water suppression can change peak integration ratios and lead to inaccuracy.

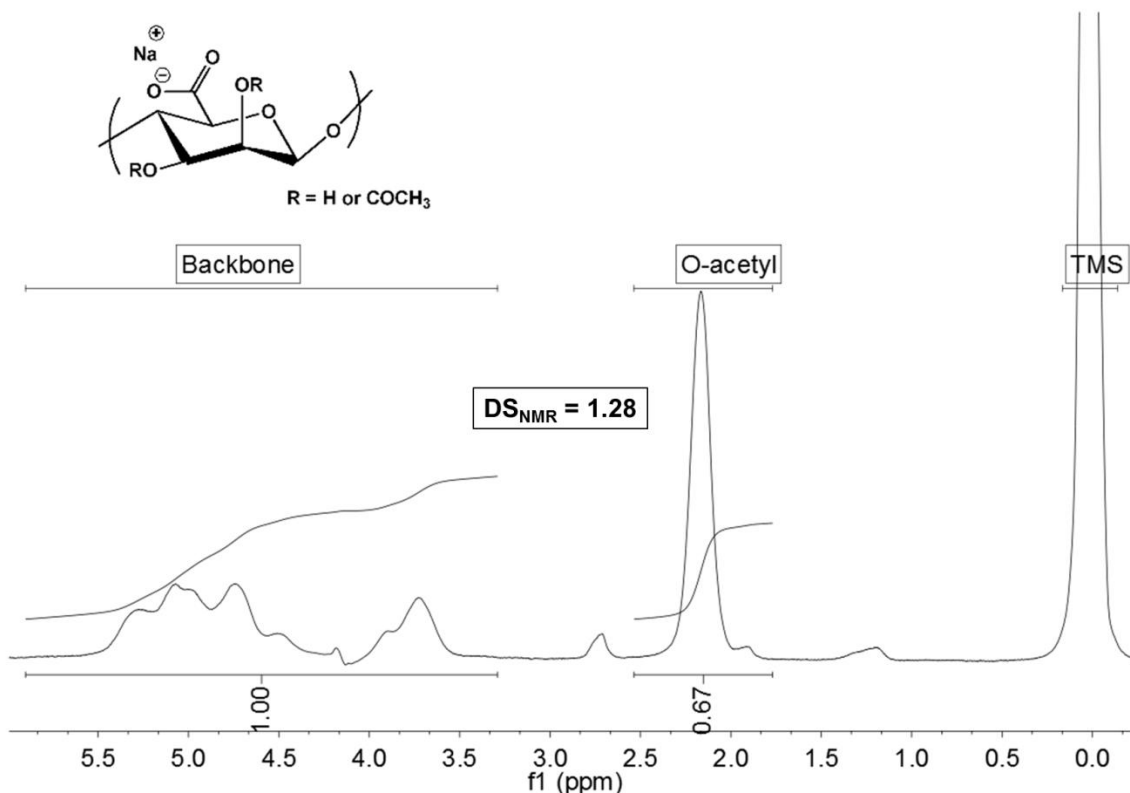


Figure 4.3: ^1H -NMR spectrum of alginate acetate A.P10.Ac20 from Table 4.2. HDO peak suppression carried out post acquisition using NMR processing software

In order to circumvent this problem, we developed a method to determine DS values based on titration. DS measurement by saponification of polysaccharide esters using aqueous NaOH, and back titration of the excess base is an old, reliable and accurate technique³⁷. We therefore saponified known quantities of alginate acetates using standardized NaOH solution, and back-titrated the excess base using standardized HCl solutions. The moles of NaOH consumed were equivalent to the moles of acetate present in the known quantity of sample. $\text{DS}_{\text{Titration}}$ values were then calculated using Equations 1-3 described in the Experimental section. **Figures 4.4** and **4.5** show the potentiometric titration [pH] and derivative [d(pH)] plots for

alginate A.P10.Ac20 from **Table 4.2**. As expected, the pH plot yields a sigmoidal decay curve while the d(pH) plot gives a singular peak corresponding to the inflexion point. $DS_{\text{Titration}}$ for A.P10.Ac20 was calculated to be 0.85. Thus, assuming that the well-understood and widely practiced titration method yields an accurate DS value, it is evident that $^1\text{H-NMR}$ with its water suppression issues overestimates the DS value for these alginate acetates. This overestimation is consistent for all alginate acetates described in **Table 4.2**. A comparison of DS values based on $^1\text{H-NMR}$ vs. titration is presented in **Table 4.6** of the Supporting Information.

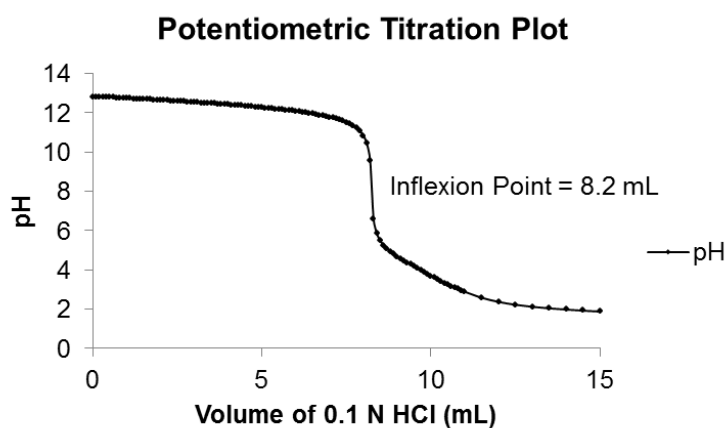


Figure 4.4: Potentiometric titration [pH] plot for alginate acetate A.P10.Ac20 from Table 4.2

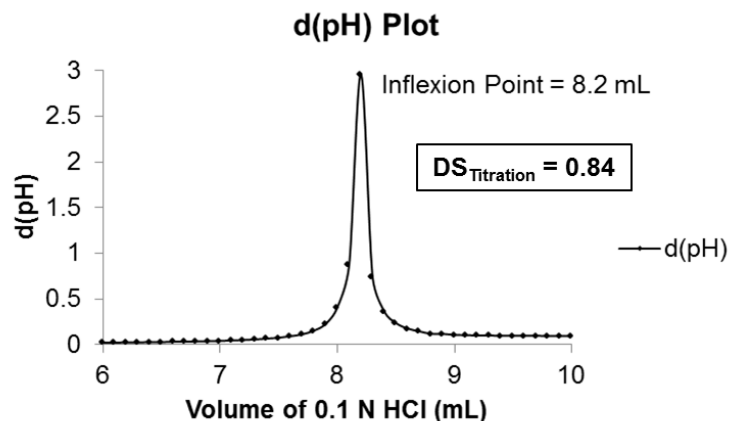


Figure 4.5: Potentiometric titration derivative [d(pH)] plot for alginate acetate A.P10.Ac20 from Table 4.2

A comparison of $DS_{\text{Titration}}$ values for alginate acetates shown in **Table 4.2** provides insight into the effect of reagent molar equivalents. In Series I the pyridine molar equivalents were varied while a large excess of Ac_2O was added, examining the impact of pyridine molar excess at high Ac_2O molar equivalents. $DS_{\text{Titration}}$ values ranged between 0.85-0.98; they did not change drastically with increasing pyridine molar excess. This supports our previous findings that the maximum possible DS value in alginates acetylated using this method tends to be limited, for reasons that are not well-understood, to ≤ 1.0 . Series II looked at the impact of pyridine molar excess at lower Ac_2O molar equivalents; the products in this series had acetate DS values in the range of 0.30-0.40, again displaying little or no sensitivity to pyridine molar excess. Series III represents experiments in which the pyridine molar equivalents were held constant, but the Ac_2O equivalents were varied. With increasing molar excess of Ac_2O , acetate $DS_{\text{titration}}$ values increased as expected; this method can therefore be used to control the acetate DS of alginate acetates.

MW analysis reveals that it is challenging to completely shut down the loss of molar mass during acetylation of the labile alginates. This is clear from comparison of the DP_n of the alginate starting material A-TBA (251) to those of the reaction products listed in **Table 4.2**. When a large excess of Ac_2O (20 equivalents) was used, MW loss was most pronounced. DP_n values for Series I were measured as 57, 106 and 65 for 2, 10 and 20 equivalents of pyridine respectively. **Figure 4.6** shows the shifts in the SEC chromatograms obtained using a refractive index detector for alginate acetates listed in **Table 4.2**. Consistent with the strong influence of the molar equivalent ratio of acetic anhydride per M/G monosaccharide, alginates from Series I show the shortest elution times, signifying strong MW degradation. In contrast, Series II in which 2 equivalents of Ac_2O were employed instead of 20, measured DP_n values were 145 and 151. A reduction in the loss of MW at lower Ac_2O /monosaccharide equivalents is supported by the positions of the peaks on the chromatograms, wherein A.P2.Ac2 and A.P20.Ac2 appear to shorter elution times compared to Series I. In Series III, measured DP_n values were 259, 166, 103 and 106 for 2, 5, 10 and 20 molar equivalents of Ac_2O respectively. Correspondingly, the SEC chromatograms showed longer elution times with higher Ac_2O equivalents used in the reaction. This analysis clearly indicates that acetic anhydride had a stronger effect on chain degradation compared to pyridine. This was surprising to us; we expected that pyridine-catalyzed elimination reactions (loss of the C-5 proton followed by elimination of the linkage hydroxyl from C-4) would be a significant cause of DP and MW loss and would become even more important at higher molar excesses of pyridine. The lack of consistent impact (Series I) upon DP_n makes it clear that the pyridine molar excess is not a critical factor. We are not sure of the cause of the large impact from increasing acetic anhydride equivalents upon DP_n loss. Certainly pyridinium acetate, the by-product of acetylation, could be a catalyst for alginate chain cleavage. If this were

the primary cause for DP_n loss, then the higher the DS (acetyl) achieved, the higher the degree of chain cleavage that would be expected, since increasing DS (acetyl) causes concomitant increase in pyridinium acetate by-product. The entries of Series III neither contradict this notion, nor prove it.

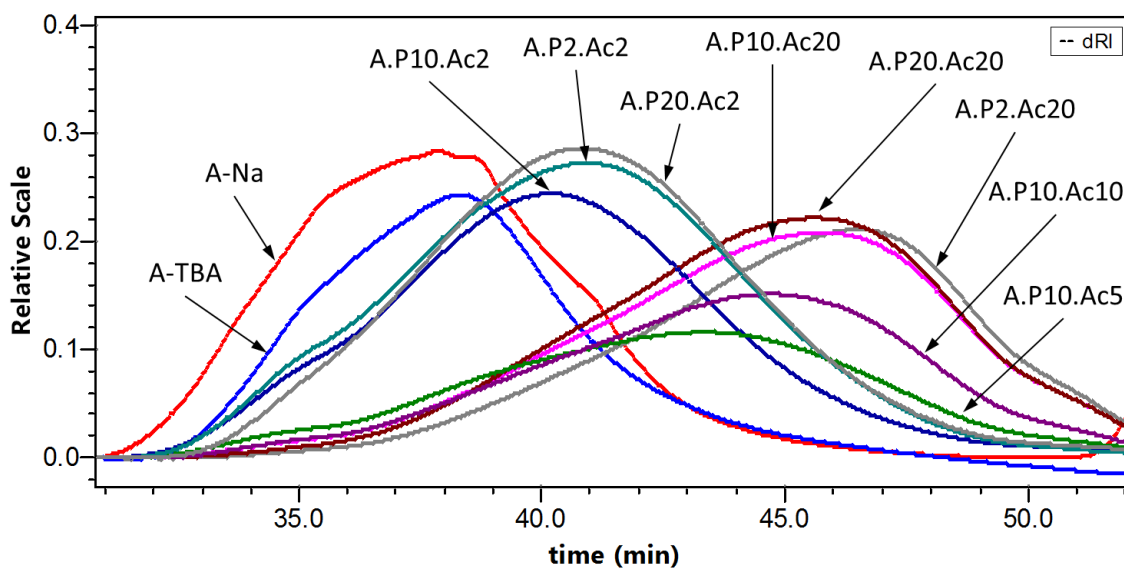


Figure 4.6: SEC chromatograms of alginate acetates in Series I, II and III from Table 4.2

Changes in DS and loss in molecular weight with changing acetylation conditions appear to significantly impact the ability of alginate acetates to form Ca-crosslinked gels. Our experiments show that when alginates were acetylated homogeneously in DMSO/TBAF (thereby acetylating both M and G residues), the products were incapable of forming Ca-crosslinked microspheres even at concentrations as high as 25%. We therefore focused exclusively on the method by which alginates were acetylated heterogeneously in DMSO, the results from which are described in **Table 4.2**.

Figure 4.7 shows the optical microscopy images of microbeads prepared starting with alginate concentrations of 3, 5 and 7.5%, and an air pressure of 0.5 psi. For unmodified sodium

alginate A-Na ($DP_n = 909$), while spherical microbeads with minimal imperfections were made at 3%; at 5% and 7.5% concentrations, tailing was observed due to the high viscosity of the alginate solutions. When ultrapure LVM ($DP_n = 308$) was used, spherical microbeads with minimal imperfections were prepared with 3 and 5% solutions. At 7.5% tailing was observed. As a general observation, ultrapure alginates formed smoother and more transparent microbeads. This is advantageous since only ultrapure grades of alginate are medically relevant in order to prevent toxicity issues. The alginate acetates of Series I, which had relatively high DS (acetyl) due to the high excesses of acetic anhydride used, did not form microbeads at any concentration/air pressure combination. This series consists of products that not only have high degrees of acetylation, but also are most strongly degraded. This combination appears to prevent bead formation altogether. The bead-forming abilities of alginates in Series III, synthesized using increasing molar equivalents of acetic anhydride were then compared. Results using A.P10.Ac2 showed that at, DS (acetyl) 0.3 and $DP_n = 259$ (2 molar equiv Ac_2O), a 3% solution yielded spherical beads with no tailing. At 5%, uniform beads with small tails were observed. At 7.5%, the microbeads contained both tails and occurrences of polymorphism. At higher DS (0.69) and lower DP_n (166) (5 molar equiv Ac_2O), overall beads were not as well shaped as those seen with 2 equivalents Ac_2O . Microbeads were malformed at both 3% and 5% concentrations. At 7.5%, spherical beads were observed, but with high incidence of polymorphism. In the case of the highest DS alginate acetate (0.80, with lowest DP_n (103)), made with 10 equiv Ac_2O per monosaccharide, no bead formation was observed at 3 and 5% concentrations since alginate droplets were unable to break the surface tension of the calcium chloride crosslinking solution. Clearly in this case, DS (acetate) (and the resulting hydrophobicity) was an influential factor. At 7.5 %, beads could be prepared, but were malformed.

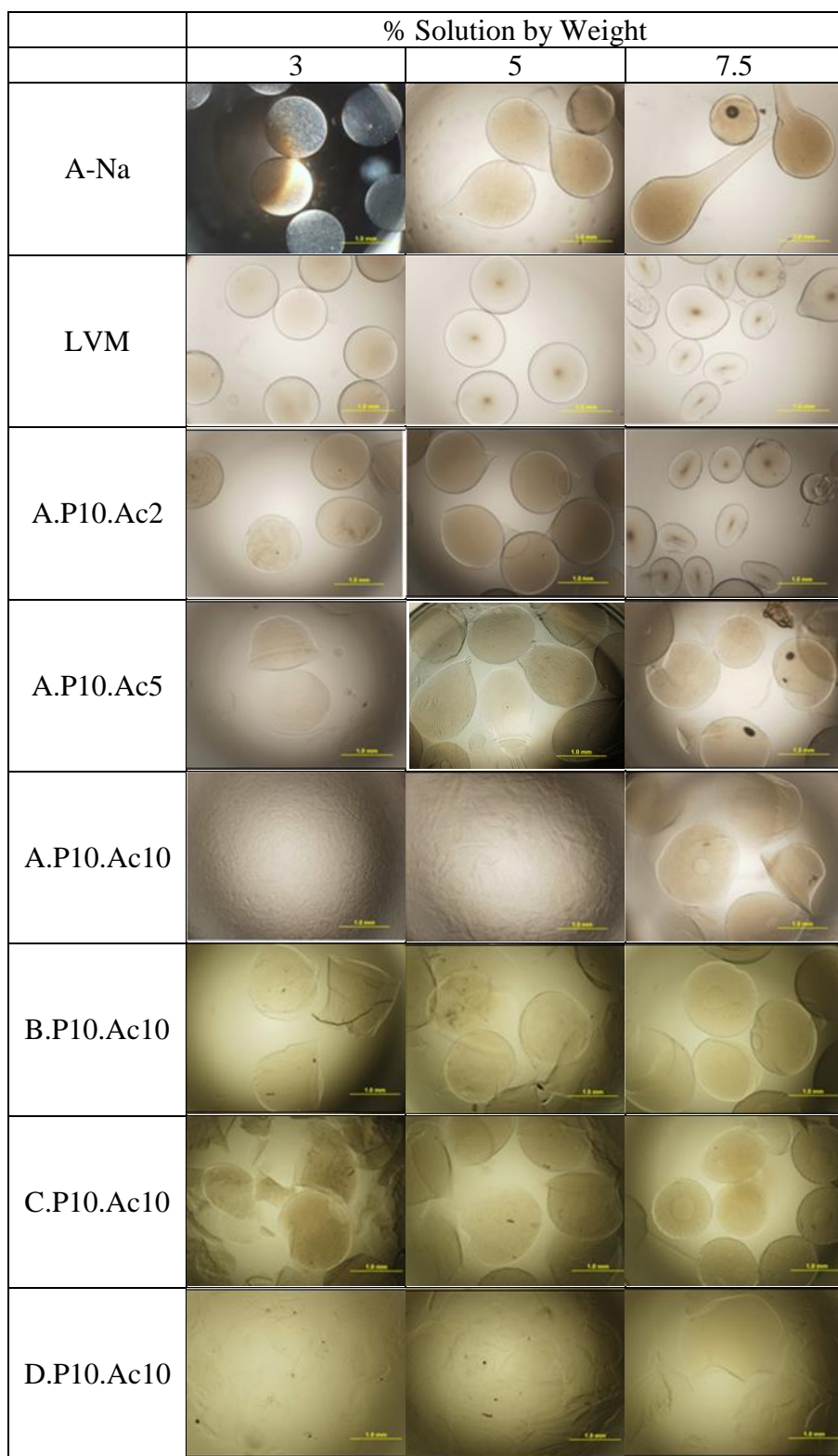


Figure 4.7: Microscopic images of capsules formed using alginate acetates from Table 4.2

The results shown above highlight the existence and position of a window of alginate acetate structure and preparation conditions, in which uniform and perfectly spherical alginate acetate microbeads can be synthesized. On the one hand, unmodified alginates with very high molecular weights (providing high solution viscosities) show undesirable tailing effects. On the other hand, alginate acetates with high DS (acetate) values that are significantly degraded may have difficulty forming microbeads altogether. In addition, malformation and polymorphism may be observed as undesirable side effects. From the examples demonstrated above, A.P10.Ac2 (DS = 0.3 and $DP_n = 259$) seems to be within the operating window; 3% solutions of this alginate acetate yielded perfectly shaped microbeads with no undesirable features such as tailing or polymorphism.

Figure 4.8 shows the viscosity vs. shear rate plots for alginates used to generate the microbeads shown in **Figure 4.7**. Since Series I did not show any microbead formation, viscosity studies of these samples were not undertaken. The data shown in **Figure 4.8** is summarized numerically in **Table 4.3**, wherein the viscosity of solutions at concentrations of 3, 5 and 7.5% has been reported. Viscosity is measured in Pa.s at a shear rate of 1 s^{-1} . Clearly, unmodified A-Na and LVM show high viscosities at the concentrations being studied. Acetylation causes a definite drop in viscosity, as noted from the viscosity values of reacted alginates. This drop in viscosity may result from a loss in MW as well as disruption of intra- and interchain H-bonding. Considering the specific example of A.P10.Ac2, even at a fairly low acetyl $DS_{\text{titration}}$ value of 0.3 and DP_n of 259, there is a >90% reduction in viscosity compared to A-Na at all three concentrations. This clearly demonstrates the manner in which even small DS(acetate) values can have a significant impact of the physical properties of alginates. Since viscosity of alginate solutions is an important criterion in the preparation of microbeads, it is evident that one would

have to account for changes occurring in the physical nature, and adjust the microbead processing parameters accordingly.

Table 4.3: Viscosities of alginate acetates from Table 4.2 at various concentrations

	Viscosity at shear rate = 1 s^{-1} (Pa.s)		
	3%	5%	7.5%
A-Na	4709	17146	21314
LVM	3803	6996	18705
A.P10.Ac2	89	342	1409
A.P10.Ac5	84	254	715
A.P10.Ac10	25	62	102
B.P10.Ac10	123	229	1983
C.P10.Ac10	276	407	637
D.P10.Ac10	2001	4410	1203

*Measurements performed at room temperature

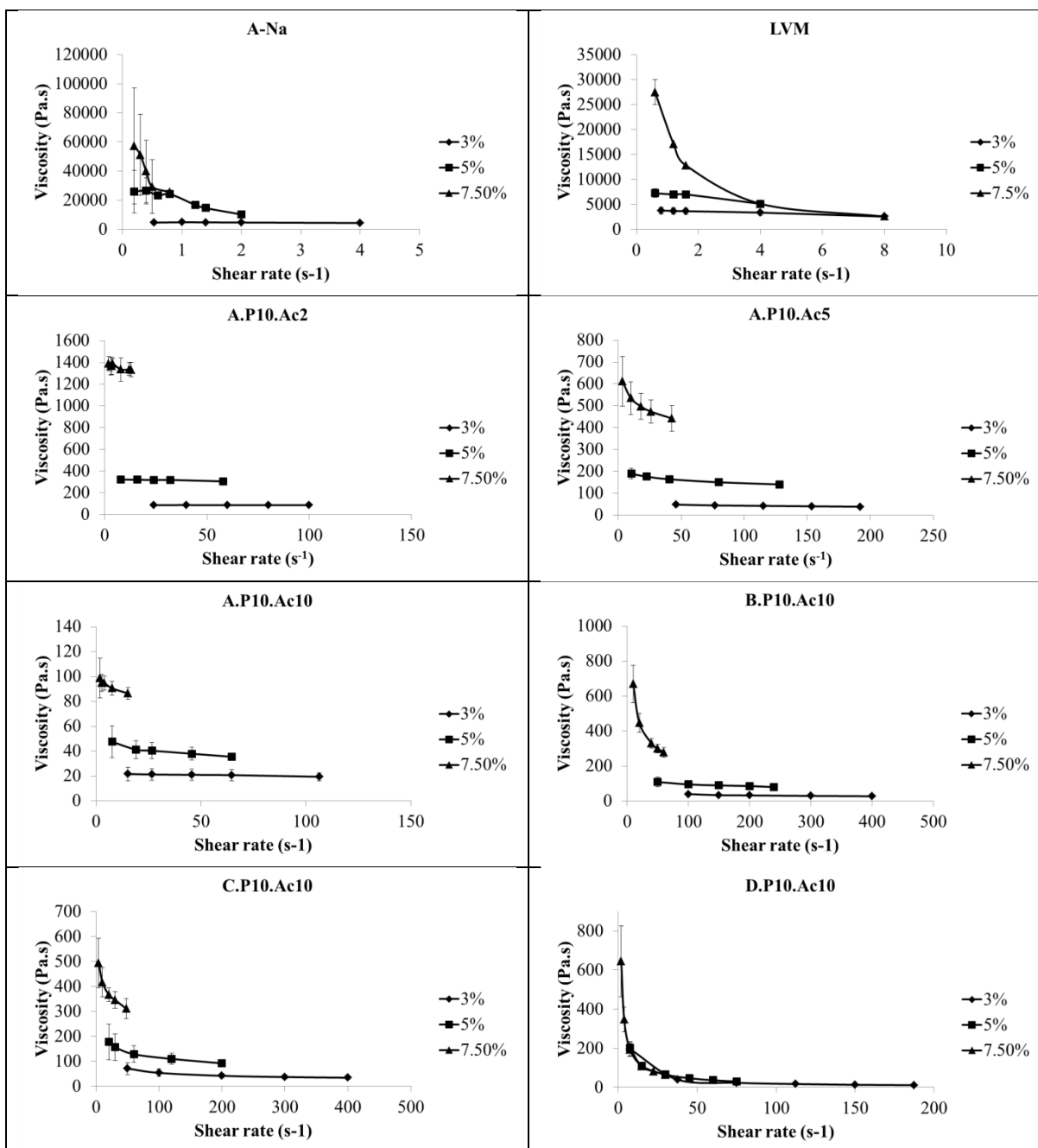


Figure 4.8: Viscosity vs. shear rate plots for alginate acetates from Table 4.2 at various concentrations, measured at room temperature

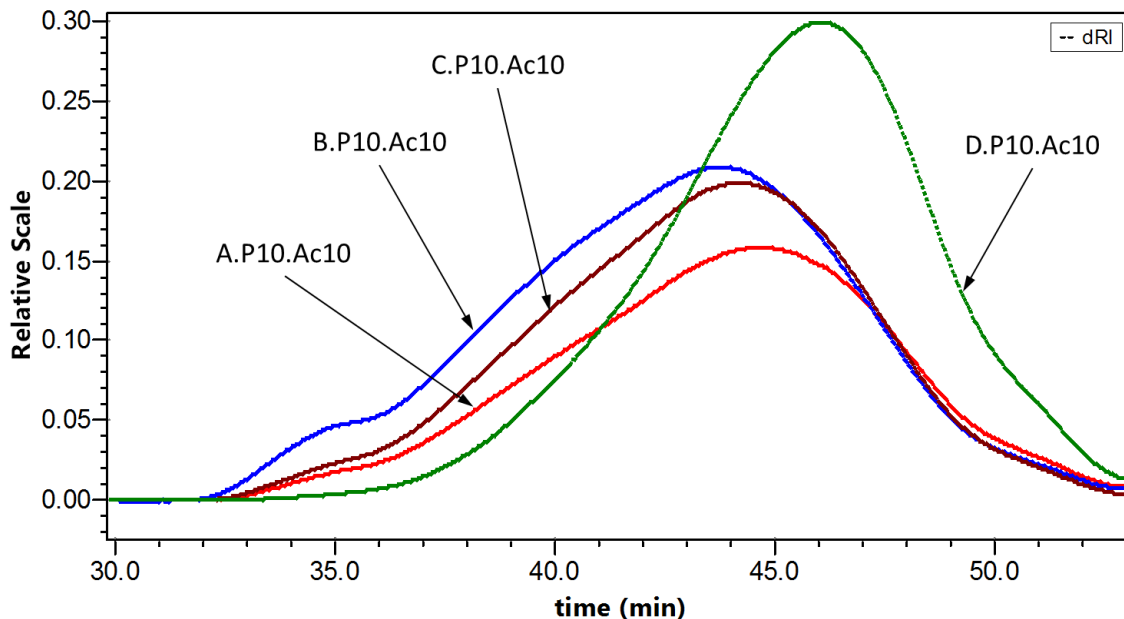


Figure 4.9: SEC chromatograms of alginate acetates in Series IV from Table 4.2

Figure 4.9 shows the SEC chromatograms of alginates A, B, C and D acetylated under identical conditions. The final DP_n values were measured as 103, 151, 125 and 138 respectively. As mentioned previously, microbead formation using A.P10.Ac10 ($DS_{\text{titration}} = 0.80$, $DP_n = 103$ and $F_{GG} = 0.21$) was successful only at a concentration of 7.5%; the beads were however malformed. Lower concentration solutions were not suitable. In the case of alginate B.P10.Ac10 ($DS_{\text{titration}} = 0.96$, $DP_n = 151$ and $F_{GG} = 0.19$), 3 and 5% solutions yielded malformed microbeads. At a concentration of 7.5% however, spherical beads were obtained at an air pressure of 0.5 psi. Nearly identical results were achieved using C.P10.Ac10 ($DS_{\text{titration}} = 0.90$, $DP_n = 125$ and $F_{GG} = 0.27$), wherein 3 and 5% solutions yielded malformed microbeads but 7.5% solutions produced perfectly spherical beads. For alginate D.P10.Ac10 ($DS_{\text{titration}} = 0.97$, $DP_n = 138$ and $F_{GG} = 0.56$), no bead formation was achieved at any concentration.

Comparing the DP_n values of alginates in Series IV, A.P10.Ac10 was more degraded compared to its B, C and D counterparts. This may be why A.P10.Ac10 could at best form

malformed capsules, while B.P10.Ac10 and C.P10.Ac10 yielded perfectly spherical microbeads at a concentration of 7.5%. Surprisingly, microbeads could not be formed using D.P10.Ac10 at any of the three concentrations studied. This result is unexpected because not only does D.P10.Ac10 have a DP_n comparable to its B and C counterparts, but also has the highest F_{GG} value of all for alginates A-D. Longer G-blocks would be expected to enhance the ability to form Ca-crosslinked gel microspheres. However this is not the case, perhaps because for D.P10.Ac10 we now have longer non-acetylated G-block sequences compared to its A, B, and C counterparts. Since non-acetylated sequences are not as hydrophobic as acetylated sequences, they would tend to associate with each other. In the case of D.P10.Ac10, it is easier for long hydrophilic stretches to self-associate forming non-acetylated G-block clusters, whereas it may be difficult to form such clusters when the blocks are not very long, as is the case for A, B and C. This hypothesis may also perhaps explain why the viscosity of D.P10.Ac10 solutions is lowered when the concentration is increased from 5 to 7.5%. At concentrations of 3 and 5%, the density of non-acetylated G-block clusters is not high enough for a known shear rate (1 s^{-1} , **Table 4.2**) to cause disruption of the clusters. However, at 7.5%, the cluster density is high enough, whereby the same shear rate can now disrupt the clusters and cause a lowering of measured viscosity.

The stability of alginate acetate microbeads towards osmotic and mechanical stresses is an important criterion governing their applicability as biomedical implants. In this study, since A.P10.Ac2 showed the most promising microbead forming ability, its osmotic and mechanical stress results were compared to those of A-Na and LVM. **Table 4.4** shows stability measured in terms of the number of broken beads after exposure to stress. The data is presented graphically in **Figure 4.10**. Clearly, microbeads formed from A.P10.Ac2 ($DP_n = 259$) have lower osmotic and mechanical stability compared to A-Na ($DP_n = 909$). However, compared to LVM ($DP_n = 308$),

there does not seem to be a statistically significant difference in the percentage of broken beads. Since LVM is commonly used for encapsulation, we can safely state that the stability of alginate acetates is in the workable range. The reduced stability of alginate acetate compared to unreacted Na-alginate may be caused by the DP loss during TBA salt formation and acetylation, and/or due to changes in crosslink density because of the acetate substituents in alginate acetate.

Table 4.4: Osmotic and mechanical stress effects, measured as % of broken microbeads

Sample	Conc. (%)	Osmotic Stress Test % Broken Capsules		Mechanical Stress Test % Broken Capsules	
		Average	Std. Dev.	Average	Std. Dev.
A.P10.Ac2	5	27.74	11.33	31.42	16.16
A-Na	5	2.25	3.82	12.02	2.85
LVM	1.5	19.61	4.59	15.36	9.88

For osmotic stress test: 1.5% LVM vs. 5% A-Na, $p < 0.001$; 1.5% LVM vs. 5% A.P10.Ac2, no significant difference; 5% A-Na vs. 5% A.P10.Ac2, $p < 0.001$. For mechanical stress test: 1.5% LVM vs. 5% A-Na, no significant difference; 5% A-Na vs. 5% A.P10.Ac2, $p < 0.05$; 1.5% LVM vs. 5% A.P10.Ac2, $p < 0.05$.

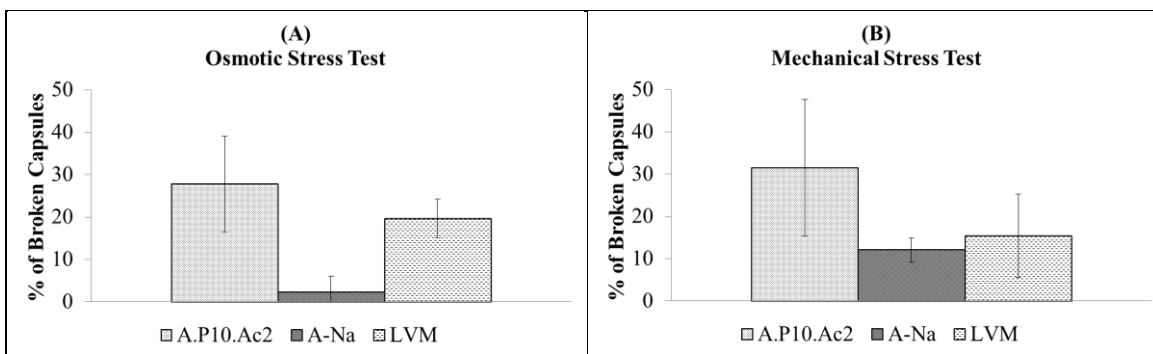


Figure 4.10: (A) Osmotic and (B) mechanical stress effects, measured as % of broken microbeads. For osmotic stress test: 1.5% LVM vs. 5% A-Na, $p < 0.001$; 1.5% LVM vs. 5% A.P10.Ac2, no significant difference; 5% A-Na vs. 5% A.P10.Ac2, $p < 0.001$. For mechanical stress test: 1.5% LVM vs. 5% A-Na, no significant difference; 5% A-Na vs. 5% A.P10.Ac2, $p < 0.05$; 1.5% LVM vs. 5% A.P10.Ac2, $p < 0.05$.

4.5 Conclusions

Acylation chemistry is one of the most widely used methods for polysaccharide modification. The ability to acylate alginates without significant degradation can be a useful tool for fine-tuning physical properties to meet the needs of specific applications. Chemical modification of hydrogel-forming alginates has the potential to allow the attachment of various functional moieties to the polysaccharide backbone. The nature and function of these moieties could range from those that make alginate significantly more hydrophobic, to those that allow it to interact specifically in biological environments, to those that can enable covalent crosslinking of chains in addition to the ionic crosslinks. The current study looks in detail at how control of the degree of acetylation, position of acetylation (M vs. G), and the concomitant chain cleavage reaction impact the ability of alginate acetates to form functional, partly hydrophobic Ca-gels.

In order to use acylated alginates as Ca-crosslinked hydrogels, it is important that acylation be selective for M residues. Indeed, we show herein that homogeneous acetylation of alginates provides randomly substituted alginate acetates, for which the solution concentrations required for microbead formation were so high that they were out of the practical working range. However, M-selective acetylation products afforded microbeads in a practically feasible concentration range of 3-7.5%. When acetylated using the pyridine/acetic anhydride reagent system, the molar equivalents of acetic anhydride used per monosaccharide had a direct impact on DS (acetyl) and DP_n , and thereby on the ability of final products to form Ca^{+2} -crosslinked microbeads. While DS values could be controlled using the amount of Ac_2O added, there appeared to be a ceiling ($DS \approx 1.0$) beyond which no more acetate substitution took place on the alginate backbone, consistent with our earlier study of alginate dissolution in organic solvents (TBAF/polar aprotic solvent such as DMSO) followed by hydroxyl esterification^{5, 38}. It is possible that this is related to our recent observation that TBAF catalyzes deacylation of

cellulose esters³⁸, but the cause of the apparent limit on alginate acylation in this system will require further investigation. Since DS (acetyl) has such a powerful impact on alginate acetate gelation and other physical properties, accurate measurement of this parameter is crucial. We demonstrate herein the successful development of a titration method to determine DS(acetyl) that replaces the former ¹H NMR method, which was plagued by the need to suppress the water peak, strongly influencing DS results. This more reliable method for DS(acetyl) determination is a crucial element as we attempt to realize the potential of alginate acetates as delivery systems for cells and molecules.

Molecular weight loss during acetylation seems to be unavoidable, given the sensitivity of alginate to both acidic and basic reaction conditions. While both acetic anhydride and pyridine have the potential to cause chain degradation, we report here the surprising discovery that the presence of excess acetic anhydride accelerates degradation much more effectively than does excess pyridine. Furthermore, the data presented herein on the gelling abilities of alginate acetates clearly proves that products that are more degraded have difficulty forming microbeads. Therefore, if one desires to synthesize Ca-crosslinked alginate acetate gel microspheres, the amount of acetic anhydride added in the reaction needs to be considered as a key factor. While high DS values can be attained only in the presence of large excesses of Ac₂O, these excesses also lead to more extensive DP_n loss. Fortunately, these studies clearly demonstrate that alginate acetates with only a relatively low DS (acetyl) (ca. 0.3) show excellent ability to gel and form capsules in the presence of Ca⁺² ions. Since these alginate acetates can be made using only small excesses of acetic anhydride, this opens the door to synthesis of materials for encapsulation and delivery by the process described herein. Once acetylated, the viscosity of the alginate solution drops significantly. Because of a drop in viscosity, microbead synthesis is directly affected.

While very high viscosities may be undesirable as they cause artifacts such as tailing, very low viscosities prevent the alginate droplets from breaking the surface tension of CaCl_2 bath solution, thereby preventing bead formation. We demonstrate in this work a processing window for forming perfectly spherical microbeads from alginate acetates of the proper DP and DS, accessible by the methods we have described. Furthermore, we have shown that while the osmotic and mechanical stability may be reduced due to acetylation, it is still in the workable range by analogy to the similar stability of LVM microbeads routinely used for encapsulation.

4.6 Supporting information

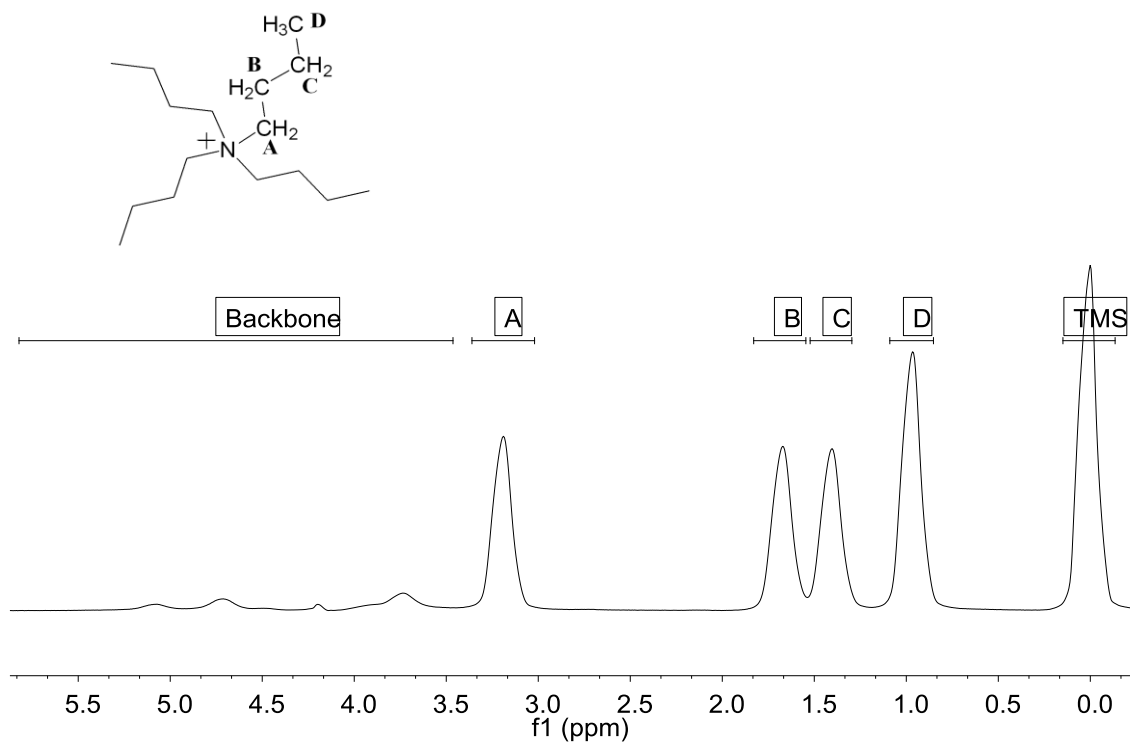


Figure 4.11: ^1H -NMR of TBA-alginate 'A'

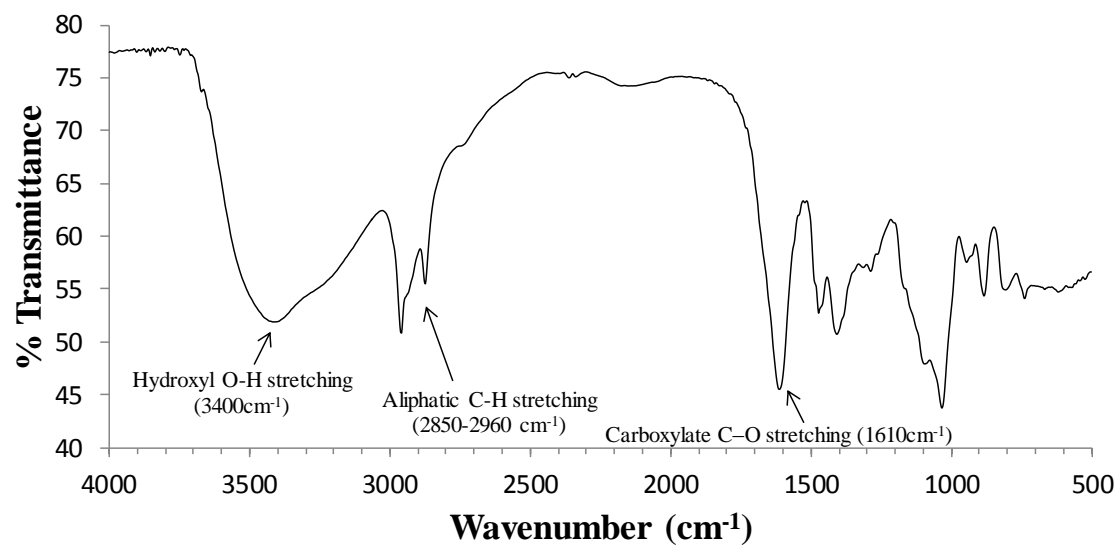


Figure 4.12: FTIR of TBA-alginate 'A'

Table 4.5: Elemental compositions and percent salt contents of TBA-alginates A-D

Alginate	Elemental Composition			Calculated Salt Content	
	% C	% H	% N	% TBA ⁺	% Na ⁺
A	57.30	9.76	2.82	78	22
B	57.87	10.42	2.95	85	15
C	56.46	10.46	2.86	80	20
D	57.57	10.57	2.89	82	18

Table 4.6: Percent TBA contents of alginate acetates, corresponding average repeat unit molar masses and DS values, as measured by ¹H-NMR and titration

Series	Sample ID	% TBA	Avg. Repeat Unit Molar Mass	DS	
				¹ H-NMR	Titration
I	A.P2.Ac20	3.0	264	1.93	0.98
	A.P10.Ac20	1.6	255	2.02	0.85
	A.P2.Ac20	2.3	260	2.06	0.92
II	A.P2.Ac2	3.6	241	0.86	0.40
	A.P10.Ac2	1.6	232	0.90	0.30
	A.P20.Ac2	2.5	238	0.71	0.40
III	A.P10.Ac2	1.6	232	0.90	0.30
	A.P10.Ac5	1.2	248	1.53	0.69
	A.P10.Ac10	1.5	253	1.74	0.80
	A.P10.Ac20	1.6	255	2.02	0.85
IV	B.P10.Ac10	1.3	259	1.67	0.96
	C.P10.Ac10	1.0	256	1.64	0.90
	D.P10.Ac10	2.2	261	1.64	0.97

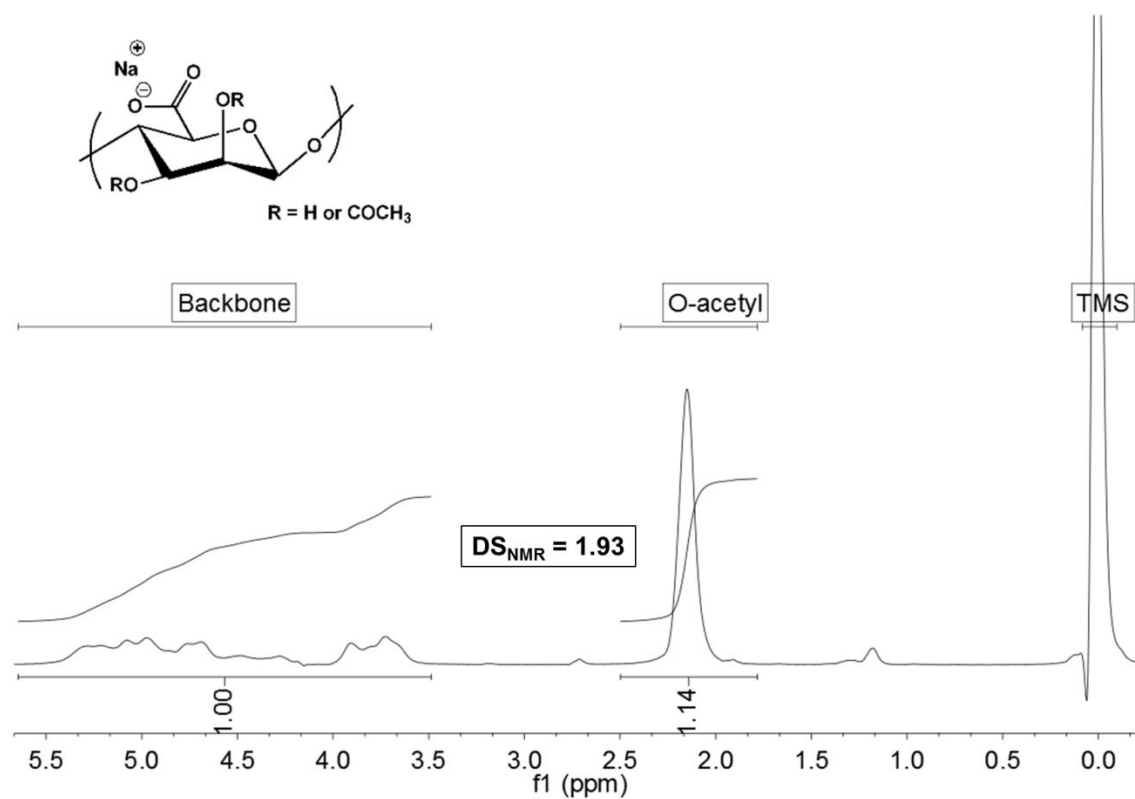


Figure 4.13: ^1H -NMR spectrum of alginate acetate A.P2.Ac20 from Table 4.2. HDO peak suppression pulse applied during acquisition

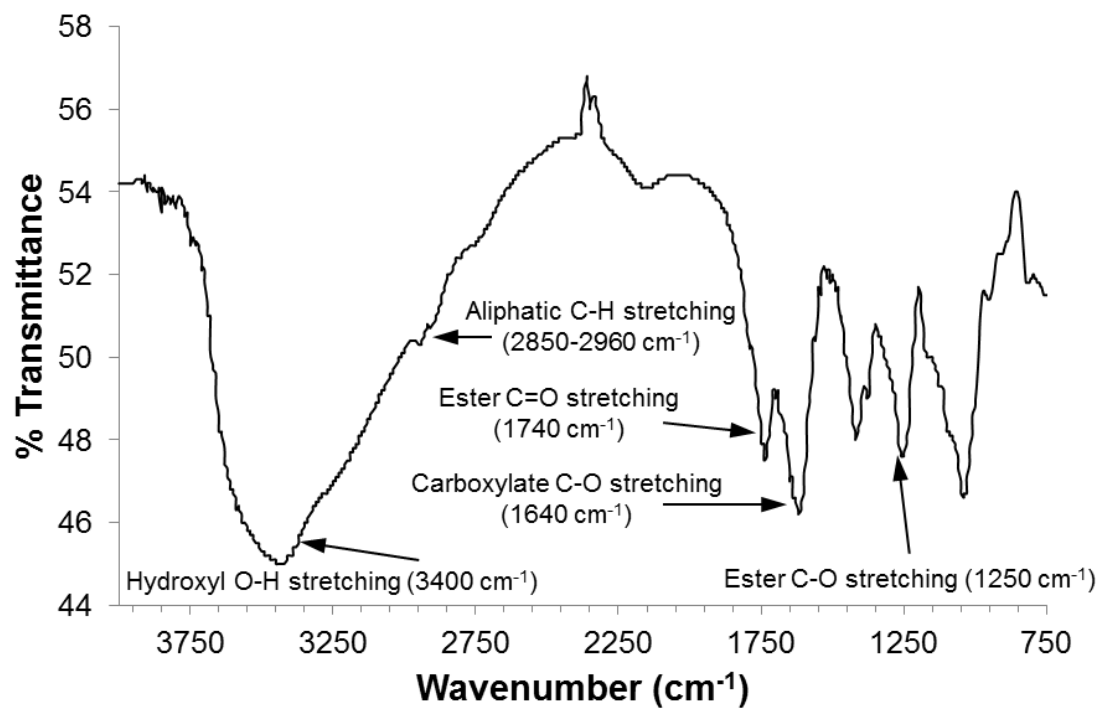


Figure 4.14: FTIR spectrum of alginate acetate A.P2.Ac20 from Table 4.2

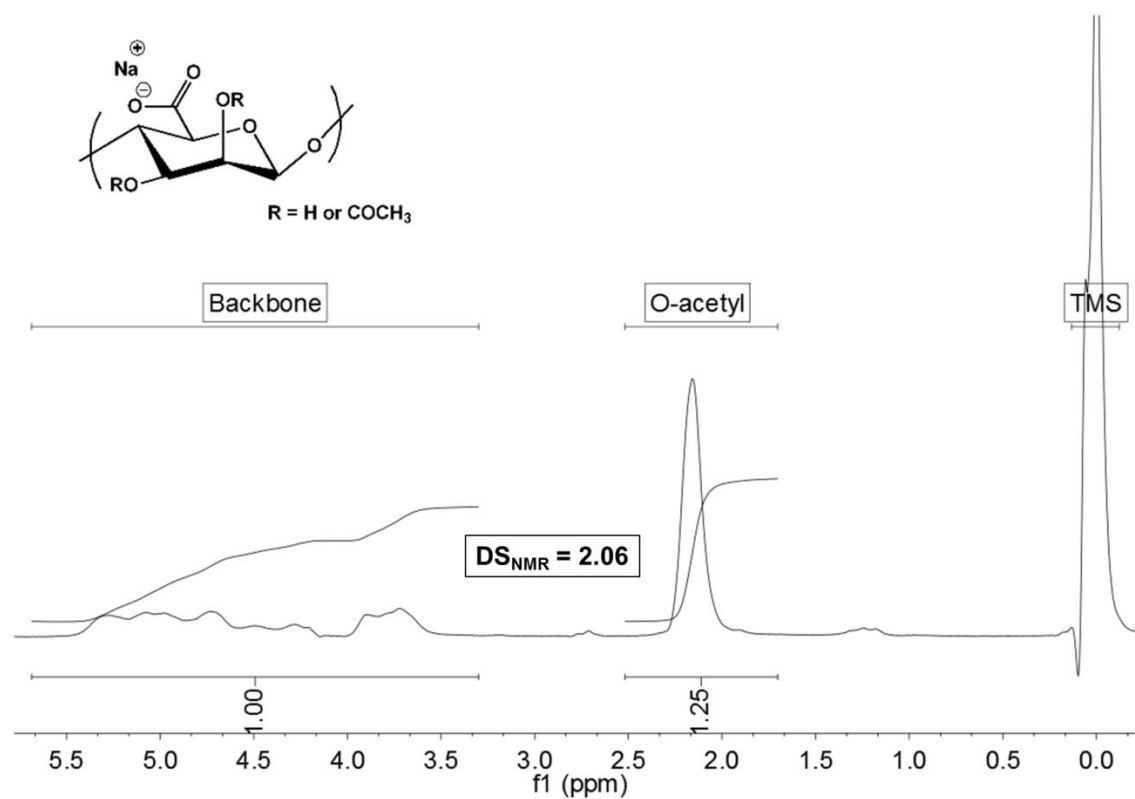


Figure 4.15: ¹H-NMR spectrum of alginate acetate A.P2.Ac20 from Table 4.2. HDO peak suppression pulse applied during acquisition

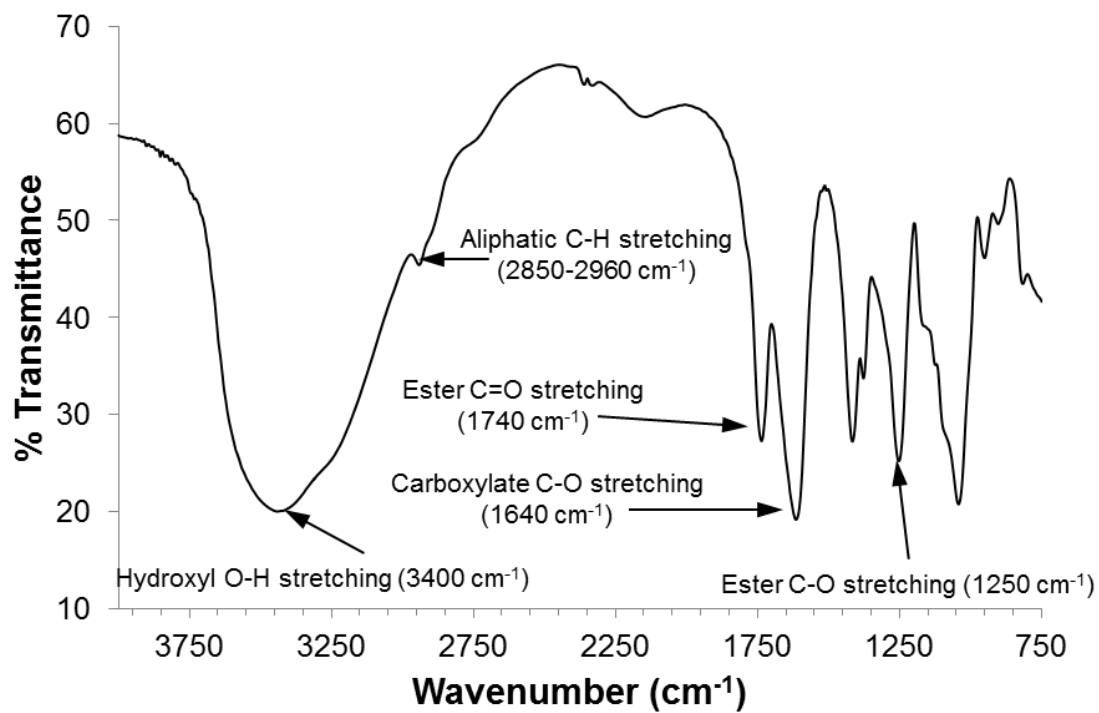


Figure 4.16: FTIR spectrum of alginate acetate A.P2.Ac20 from Table 4.2

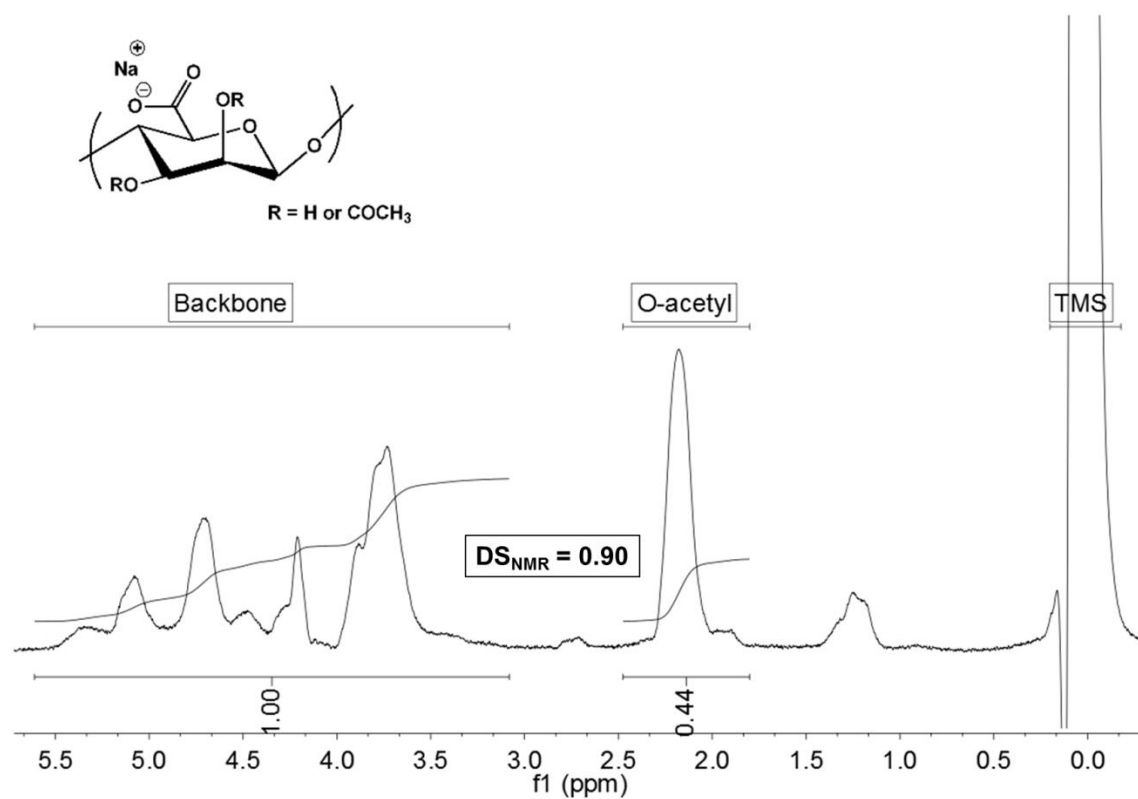


Figure 4.17: ^1H -NMR spectrum of alginate acetate A.P10.Ac2 from Table 4.2. HDO peak suppression pulse applied during acquisition

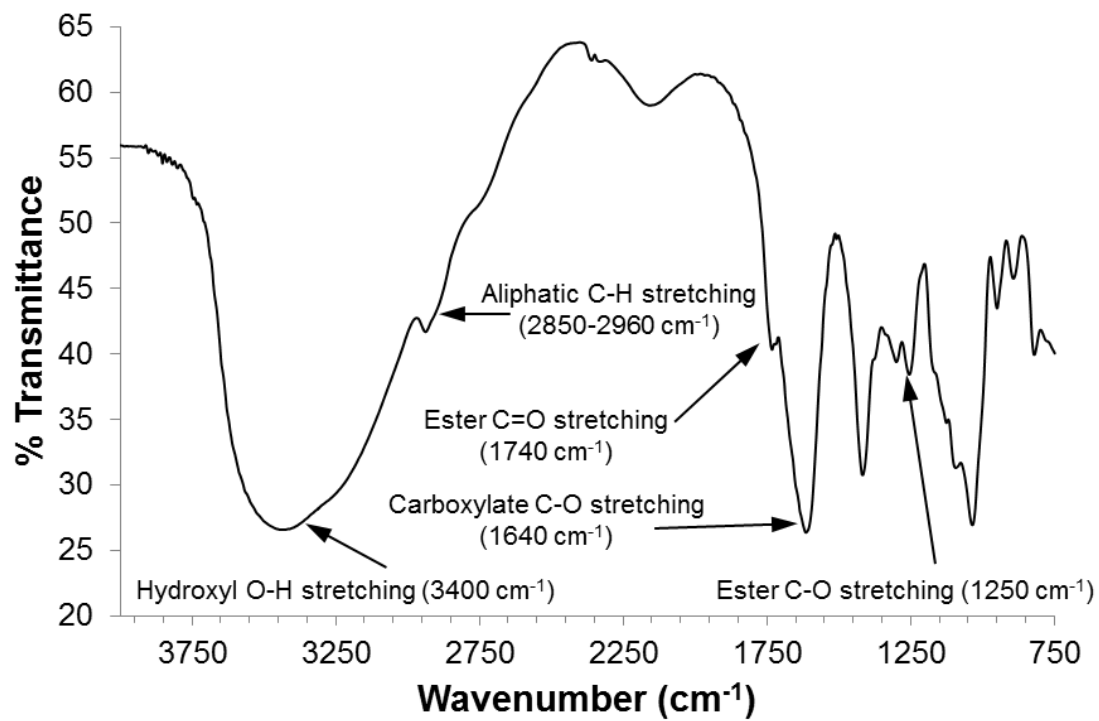


Figure 4.18: FTIR spectrum of alginate acetate A.P10.Ac2 from Table 4.2

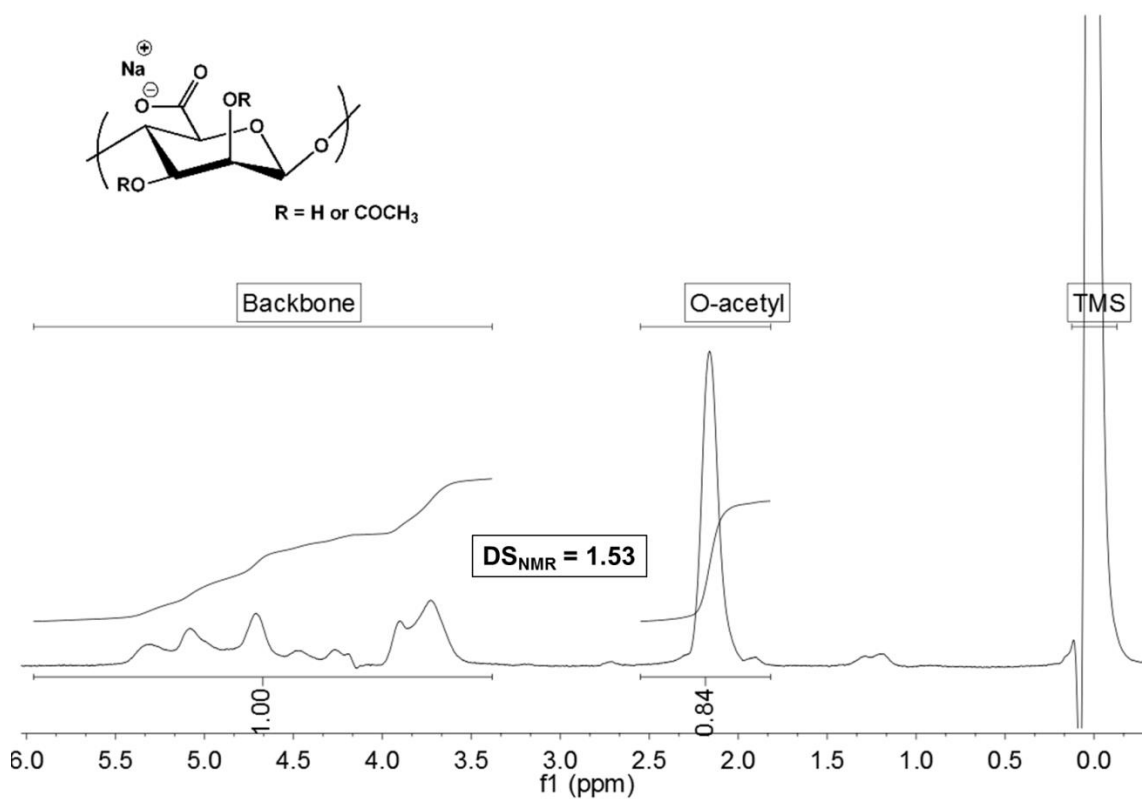


Figure 4. 19: ^1H -NMR spectrum of alginate acetate A.P10.Ac5 from Table 4.2. HDO peak suppression pulse applied during acquisition

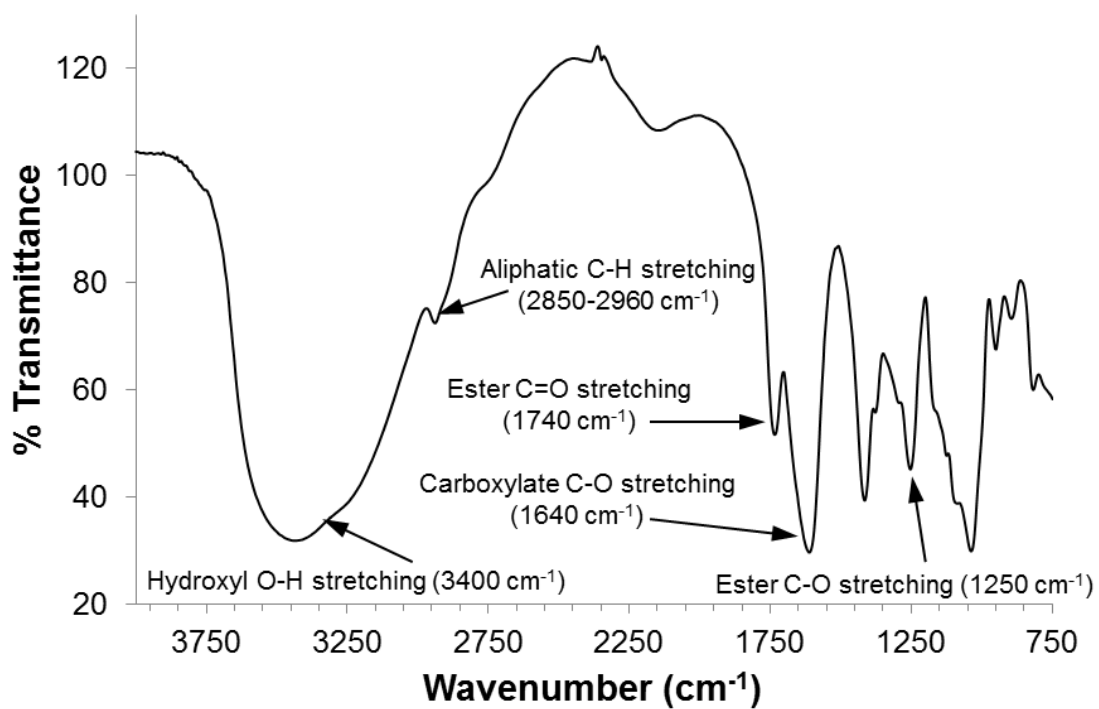


Figure 4.20: FTIR spectrum of alginate acetate A.P10.Ac5 from Table 4.2

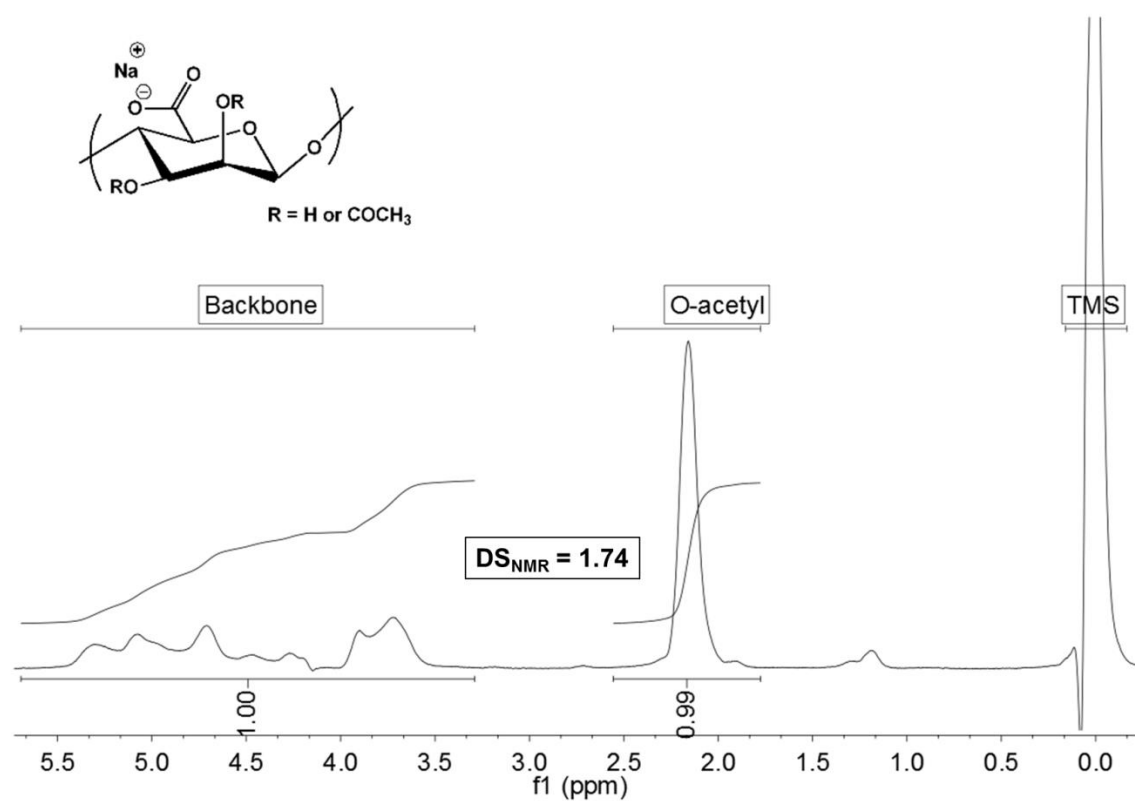


Figure 4.21: ^1H -NMR spectrum of alginate acetate A.P10.Ac10 from Table 4.2. HDO peak suppression pulse applied during acquisition

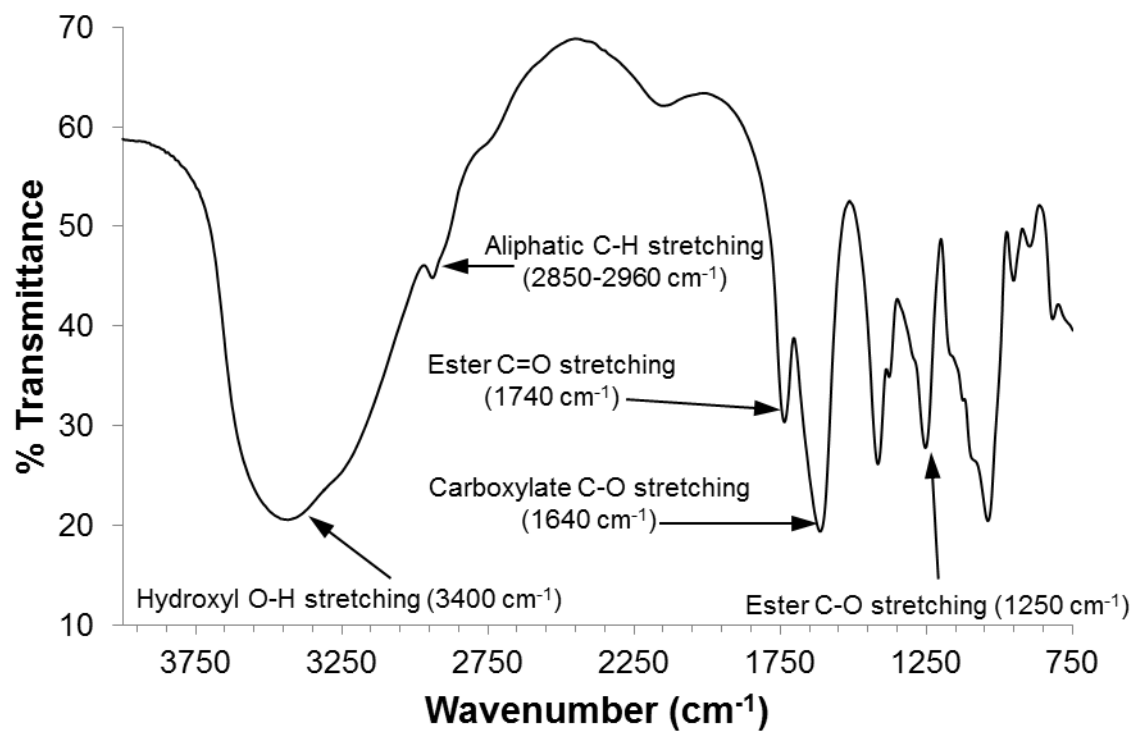


Figure 4.22: FTIR spectrum of alginate acetate A.P10.Ac10 from Table 4.2

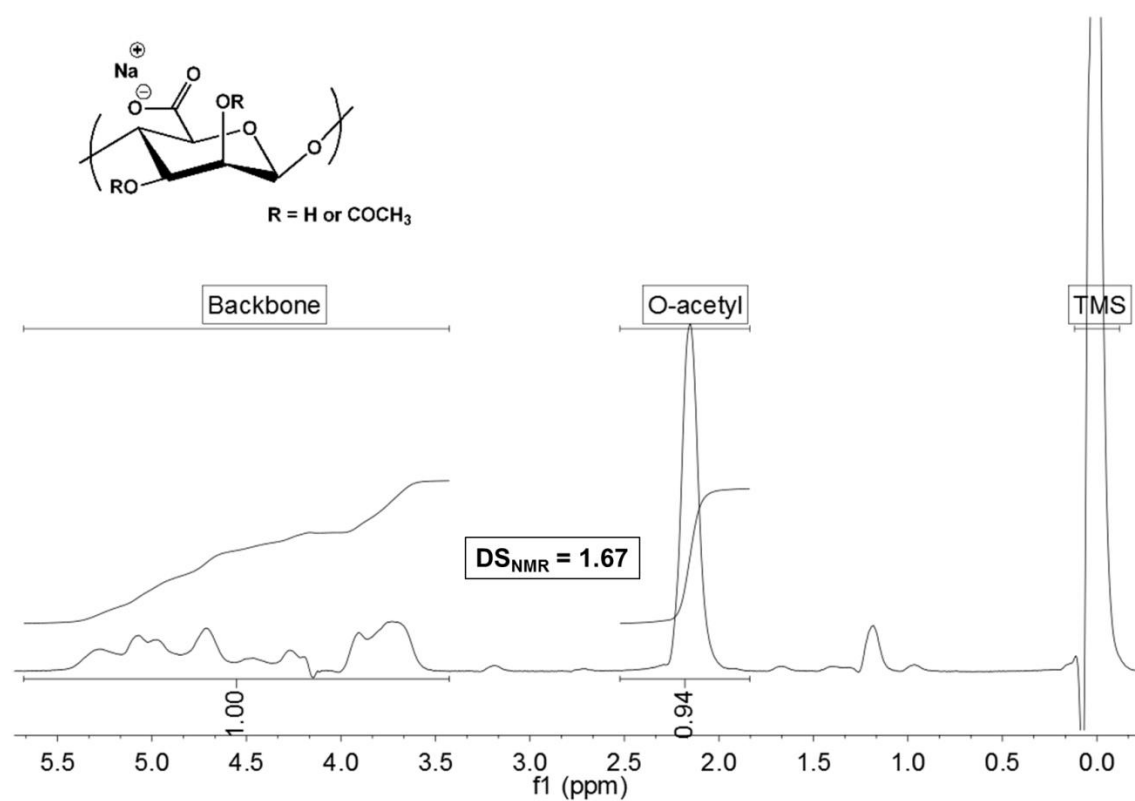


Figure 4.23: ^1H -NMR spectrum of alginate acetate B.P10.Ac10 from Table 4.2. HDO peak suppression pulse applied during acquisition

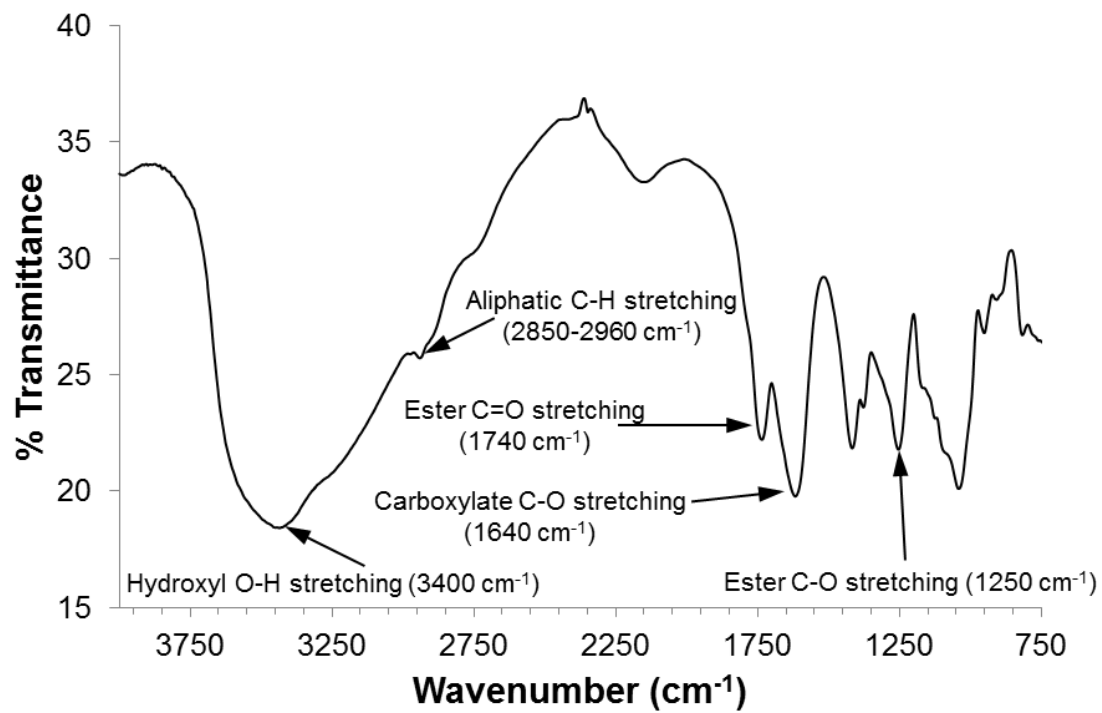


Figure 4.24: FTIR spectrum of alginate acetate B.P10.Ac10 from Table 4.2

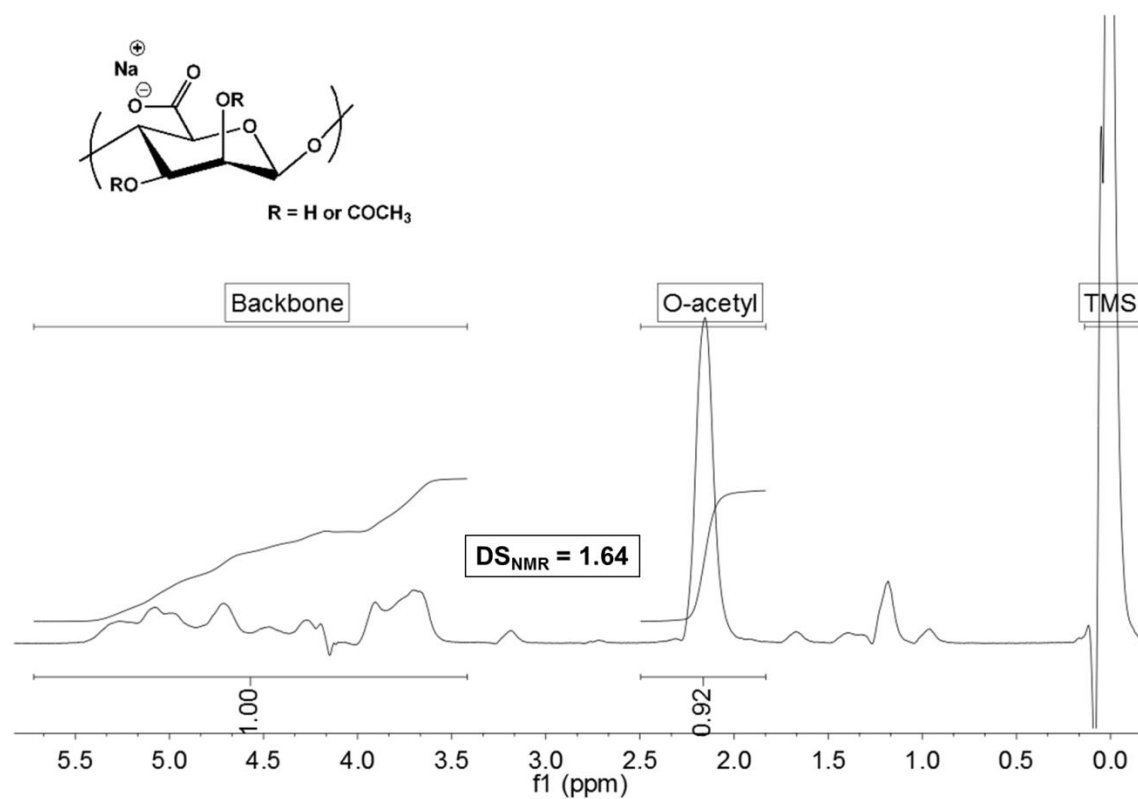


Figure 4.25: ^1H -NMR spectrum of alginate acetate C.P10.Ac10 from Table 4.2. HDO peak suppression pulse applied during acquisition

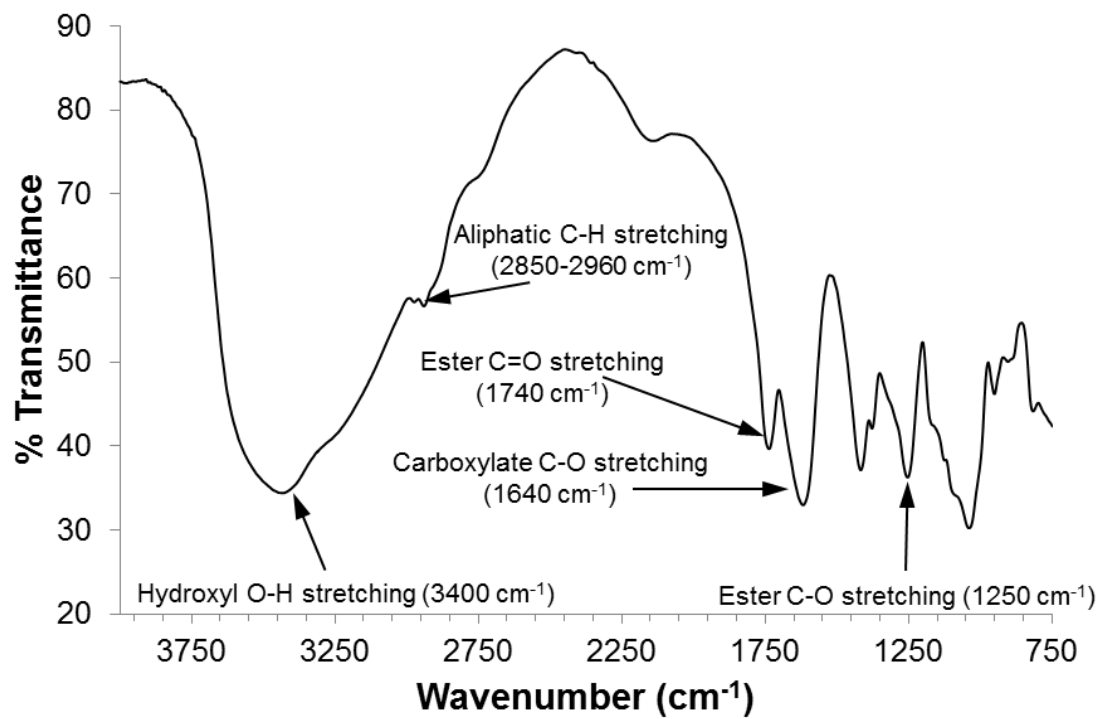


Figure 4.26: FTIR spectrum of alginate acetate C.P10.Ac10 from Table 4.2

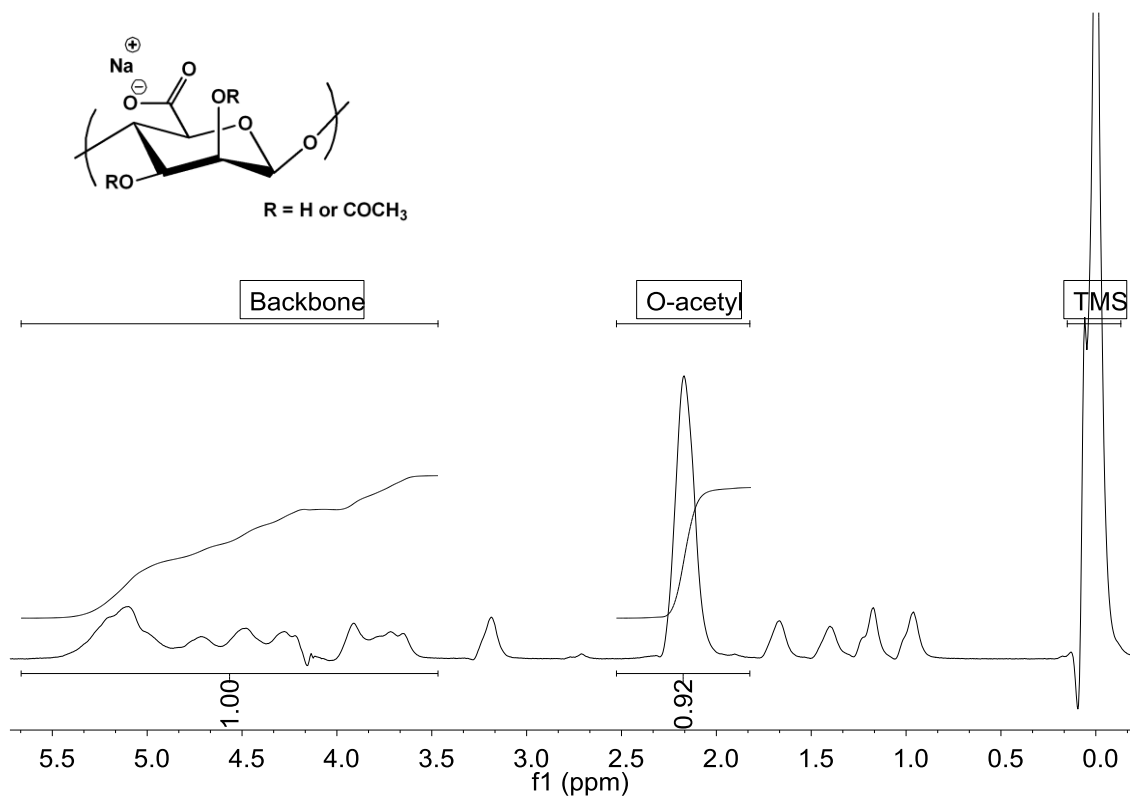


Figure 4.27: ^1H -NMR spectrum of alginate acetate D.P10.Ac10 from Table 4.2. HDO peak suppression pulse applied during acquisition

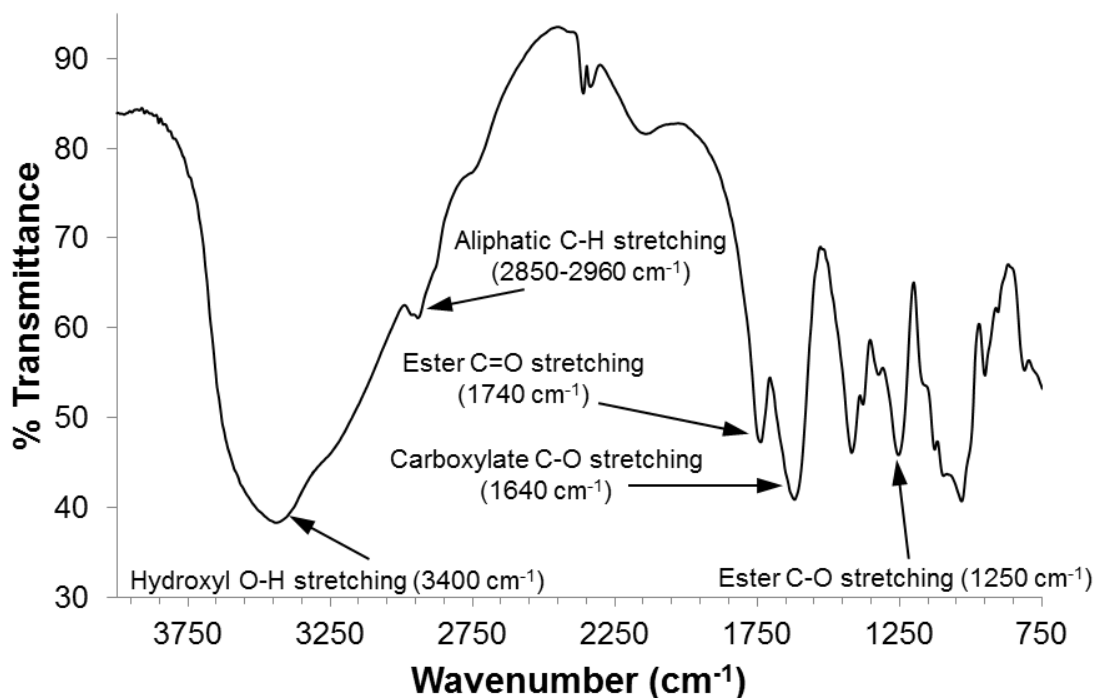


Figure 4.28: FTIR spectrum of alginate acetate D.P10.Ac10 from Table 4.2

4.7 References

1. Draget, K. I.; Smidsrod, O.; Skjak-Braek, G., Alginates from Algae. In *Polysaccharides and Polyamides in the Food Industry*, Steinbuchel, A.; Rhee, S. K., Eds. Wiley-VCH: Weinheim, 2005; pp 1-30.
2. Morch, Y. A.; Donati, I.; Strand, B. L.; Skjak-Braek, G., Molecular engineering as an approach to design new functional properties of alginate. *Biomacromolecules* **2007**, 8, (9), 2809-14.
3. Draget, K. I., Alginates. In *Handbook of Hydrocolloids*, Phillips, G. O., Williams, P.A., Ed. 2009; pp 379-395.

4. Fox, S. C.; Li, B.; Xu, D.; Edgar, K. J., Regioselective esterification and etherification of cellulose: a review. *Biomacromolecules* **2011**, 12, (6), 1956-72.
5. Pawar, S. N.; Edgar, K. J., Chemical Modification of Alginates in Organic Solvent Systems. *Biomacromolecules* **2011**, 12, (11), 4095-4103.
6. Pawar, S. N.; Edgar, K. J., Alginate derivatization: A review of chemistry, properties and applications. *Biomaterials* **2012**, 33, (11), 3279-3305.
7. Chamberlain, N. H., Cunningham, G.E., Speakman, J.B., Alginic acid diacetate. *Nature* **1946**, 158, 553.
8. Schweiger, R. G., Acetylation of Alginic Acid. I. Preparation and Viscosities of Algin Acetates. *J. Org. Chem.* **1962**, 27, (5), 1786-1789.
9. Schweiger, R. G., Acetylation of Alginic Acid. II. Reaction of Algin Acetates with Calcium and Other Divalent Ions. *J. Org. Chem.* **1962**, 27, (5), 1789-1791.
10. Wassermann, A., Alginic Acid-acetate. *Nature* **1946**, 158, 271.
11. Wassermann, A., Alginic Acid-acetate. *J. Chem. Soc.* **1948**, 197.
12. Skjåk-Bræk, G.; Paoletti, S.; Gianferrara, T., Selective acetylation of mannuronic acid residues in calcium alginate gels. *Carbohydr. Res.* **1989**, 185, (1), 119-129.
13. Sikorski, P.; Mo, F.; Skjåk-Bræk, G.; Stokke, B. r. T., Evidence for Egg-Box-Compatible Interactions in Calcium Alginate Gels from Fiber X-ray Diffraction. *Biomacromolecules* **2007**, 8, (7), 2098-2103.
14. Donati, I.; Holtan, S.; Mørch, Y. A.; Borgogna, M.; Dentini, M.; Skjåk-Bræk, G., New hypothesis on the role of alternating sequences in calcium-alginate gels. *Biomacromolecules* **2005**, 6, (2), 1031-40.

15. Lee, K. Y.; Mooney, D. J., Alginate: Properties and biomedical applications. *Prog. Polym. Sci.* **2012**, 37, (1), 106-126.
16. Boateng, J. S.; Matthews, K. H.; Stevens, H. N. E.; Eccleston, G. M., Wound healing dressings and drug delivery systems: A review. *J Pharm Sci-US* **2008**, 97, (8), 2892-2923.
17. Ramsey, D. M.; Wozniak, D. J., Understanding the control of *Pseudomonas aeruginosa* alginate synthesis and the prospects for management of chronic infections in cystic fibrosis. In *Mol. Microbiol.*, 2005; Vol. 56, pp 309-322.
18. Khan, S.; Tondervik, A.; Sletta, H.; Klinkenberg, G.; Emanuel, C.; Onsoyen, E.; Myrvold, R.; Howe, R. A.; Walsh, T. R.; Hill, K. E.; Thomas, D. W., Overcoming Drug Resistance with Alginate Oligosaccharides Able To Potentiate the Action of Selected Antibiotics. *Antimicrob Agents Chemother* **2012**, 56, (10), 5134-5141.
19. Soonshiong, P.; Feldman, E.; Nelson, R.; Heintz, R.; Yao, Q.; Yao, Z. W.; Zheng, T. L.; Merideth, N.; Skjåk-Bræk, G.; Espevik, T.; Smidsrød, O.; Sandford, P., Long-Term Reversal of Diabetes by the Injection of Immunoprotected Islets. *P Natl Acad Sci USA* **1993**, 90, (12), 5843-5847.
20. Zhang, P.; Zhang, X.; Brown, J.; Vistisen, D.; Sicree, R.; Shaw, J.; Nichols, G., Global healthcare expenditure on diabetes for 2010 and 2030. *Diabetes Res Clin Pract* **2010**, 87, (3), 293-301.
21. Chukwuma, C., Sr., Type I diabetic nephropathy: clinical characteristics and economic impact. *J Diabetes Complicat.* **1993**, 7, (1), 15-27.
22. The Diabetes Control and Complications Trial Research Group. Weight gain associated with intensive therapy in the diabetes control and complications trial. . *Diabetes Care* **1988**, 11, (7), 567-73.

23. The Diabetes Control and Complications Trial Research Group. The effect of intensive treatment of diabetes on the development and progression of long-term complications in insulin-dependent diabetes mellitus. . *N Engl J Med* **1993**, 329, (14), 977-86.
24. White, S. A.; Shaw, J. A.; Sutherland, D. E., Pancreas transplantation. *Lancet* **2009**, 373, (9677), 1808-17.
25. Opara, E. C.; Mirmalek-Sani, S. H.; Khanna, O.; Moya, M. L.; Brey, E. M., Design of a bioartificial pancreas(+). *J Investig Med* **2010**, 58, (7), 831-7.
26. Harlan, D. M.; Kenyon, N. S.; Korsgren, O.; Roep, B. O., Current advances and travails in islet transplantation. *Diabetes* **2009**, 58, (10), 2175-84.
27. Babak, V. G.; Skotnikova, E. A.; Lukina, I. G.; Pelletier, S.; Hubert, P.; Dellacherie, E., Hydrophobically associating alginate derivatives: Surface tension properties of their mixed aqueous solutions with oppositely charged surfactants. *J. Colloid Interface Sci.* **2000**, 225, (2), 505-510.
28. Tendulkar, S.; Mirmalek-Sani, S. H.; Childers, C.; Saul, J.; Opara, E. C.; Ramasubramanian, M. K., A three-dimensional microfluidic approach to scaling up microencapsulation of cells. *Biomed Microdevices* **2012**, 14, (3), 461-9.
29. Darrabie, M. D.; Kendall, W. F., Jr.; Opara, E. C., Characteristics of Poly-L-Ornithine-coated alginate microcapsules. *Biomaterials* **2005**, 26, (34), 6846-52.
30. Timell, T. E., The acid hydrolysis of glycosides: I. general conditions and the effect of the nature of the aglycone. *Can. J. Chem.* **1964**, 42, 1456.
31. Smidsrød, O. H., A.; Larsen, B., The influence of pH on the Rate of Hydrolysis of Acidic Polysaccharides. *Acta Chem Scand* **1966**, 20, 1026-34.

32. Tsujino, I.; Saito, T., A new unsaturated uronide isolated from alginase hydrolysate. *Nature* **1961**, 192, 970-1.
33. Preiss, J.; Ashwell, G., Alginic Acid Metabolism in Bacteria. *J Biol Chem* **1962**, 237, (2), 309-316.
34. Penman, A.; Sanderson, G. R., A method for the determination of uronic acid sequence in alginates. *Carbohydr Res* **1972**, 25, (2), 273-282.
35. Grasdalen, H.; Larsen, B.; Smidsrød, O., PMR Study of the Composition and Sequence of Uronate Residues in Alginates. *Carbohydr Res* **1979**, 68, (1), 23-31.
36. Salomonsen, T. J., H.M.; Larsen, F.H.; Engelsen, S.B., The Quantitative Impact of Water Suppression on NMR Spectra for Compositional Analysis of Alginates. In *Magnetic Resonance in Food Science: Challenges in a Changing World*, Gujonsdottir, M.; Belton, P.; Webb, G., Eds. The Royal Society of Chemistry: 2009; pp 12-19.
37. Heinze, T.; Liebert, T.; Koschella, A., Structure Analysis of Polysaccharide Esters. In *Esterification of Polysaccharides*, Springer Berlin Heidelberg: 2006; pp 143-167.
38. Xu, D. G.; Edgar, K. J., TBAF and Cellulose Esters: Unexpected Deacylation with Unexpected Regioselectivity. *Biomacromolecules* **2012**, 13, (2), 299-303.

Chapter 5: Synthesis of Alginate Esters via Carboxyl Group Modification

(Adapted from Pawar, S.N., Edgar, K.J.; Manuscript under preparation)

5.1 Abstract

Alginates are (1→4) linked linear copolysaccharides composed of β -D-mannuronic acid (M) and its C-5 epimer, α -L-guluronic acid (G). Several strategies to synthesize carboxyl modified alginate derivatives exist in the literature. A large majority of the findings however take advantage of aqueous chemistries, such as carbodiimide coupling reactions. Based on our previous report on the homogeneous dissolution of TBA-alginate, we now describe the use of TBAF based two component solvent systems as media for the synthesis of carboxyl modified alginate esters. Partially and fully esterified derivatives such as benzyl, butyl ethyl and methyl alginate were synthesized via reaction with the corresponding alkyl halides. The newly synthesized derivatives were soluble in polar aprotic solvents without the addition of TBAF. Saponification was performed to demonstrate that -COOH groups were selectively reacted over -OH groups to form esters. Furthermore, DS was measured using both NMR and titration to show that the two methods yielded similar values. Later, we demonstrated the utility of the alginate esters to enhance aqueous solubility of the flavonoid naringenin by formation of solid dispersions.

5.2 Introduction

Alginates are unbranched polysaccharides consisting of 1→4 linked β -D-mannuronic acid (M) and its C-5 epimer α -L-guluronic acid (G). They are isolated from one of two major sources - algae such as kelp, or as an exopolysaccharide of bacteria such as *Pseudomonas aeruginosa*. The alginate microstructure is unique and comprises M (M-blocks) and G (G-blocks) residues interspersed with MG sequences (MG-blocks). Source and species dependent variability exists between alginates in terms of their copolymer composition, sequence and molecular weights. This variance is often used as a tool to control final properties in a number of natural functions. For example, in *Laminaria hyperborea*, the stipe and holdfast require high strength and rigidity and therefore contain alginates having higher fractions of G residues. In contrast, the leaves of the plant which require flexibility for flotation in streaming water possess alginates with lower fractions of G residues. Due to the abundance of algae in water bodies, there is a large amount of alginate material present in nature. Industrial alginate production is approximately 30,000 metric tons annually, and is estimated to comprise less than 10% of the biosynthesized alginate material.¹ Therefore there is significant additional potential to design sustainable biomaterials based on alginates.

One of the most obvious and effective ways to design high performance biomaterials is by chemically reacting the functional groups available on the alginate backbone. Alginate being a water soluble polysaccharide in salt form, the use of aqueous chemistries such as EDC/NHS coupling reactions to make esters/amides is a widely used strategy.² While aqueous phase reactions can be a good way to modify polysaccharides, they do not match the versatility that organic phase reactions can offer. This is clearly demonstrated through the rich body of literature published on organic dissolution and derivatization of cellulose.³ A major factor that

differentiates alginates from cellulose is the presence of ionizable carboxylic acid functionalities on the former's backbone. The charges play a crucial role in dictating organic solubility of alginates; in fact, until recently no organic solvent systems had been described that would permit full dissolution of alginate. Addressing this key problem, we have recently shown that it is possible to dissolve alginates in two-component organic media consisting of polar aprotic solvents (such as DMSO, DMF, DMAc or DMI) and the salt tetrabutylammonium fluoride (TBAF).⁴ Furthermore, water soluble alginate acetates up to $DS_{\text{acetyl}} \sim 1.0$ were synthesized by reaction of alginate hydroxyl groups.

A disadvantage with the TBAF based two-component solvent systems is that the salt is hydrated and there is always a small percentage of water present in the mixture. Furthermore, it has been shown by our group that TBAF is useful as a reagent for regioselective deacylation of cellulose esters.⁵ Although not experimentally confirmed, a similar deacylation reaction occurring *in situ* could be the source of the limitation we have observed in alginate acylations, where alginate acetate product DS_{acetyl} has not exceeded ~ 1.0 . We would therefore like to develop alginate derivatives that would dissolve in organic media without the addition of TBAF. From our past studies, no single component organic solvent (including ionic liquids) is capable of fully dissolving (tetrabutylammonium) TBA-salts of alginic acid. The ability to dissolve alginates in water-free organic media will be advantageous in two ways. Firstly, it will permit the use of organic reagents that are incompatible with water, thereby enabling new pathways to alginate functionalization. Secondly, it will enable solvent-based processing methods, which may extend the applicability of alginates beyond its current scope (which involves mostly aqueous processing). Substitution of alginate at the carboxyl group to form an ester is one potential approach to the preparation of derivatives with such properties. Within our scope of knowledge,

we are aware of two prior instances where alginate esters have been synthesized via carboxyl group modification.² The first derivative is a commercially available alginate ester – propylene glycol alginate, synthesized by reaction with propylene oxide. The second known set of reports has detailed the reaction of TBA-alginate with dodecyl bromide to prepare dodecyl alginate in DMSO.⁶⁻⁸ However the maximum DS_{dodecyl} value reported was 0.12. Through this work we intend to study the reaction of TBA-alginate with alkyl halides by homogeneous dissolution in TBAF containing solvent systems. Furthermore, we shall study the impact of this derivatization method on enhancing the organic solubility of alginates.

In order to demonstrate the potential utility of organo-soluble alginate derivatives, we chose to test the performance of alginate carboxylate esters for amorphous solid dispersion of naringenin (Nar). Nar is the aglycone of naringin, a flavonoid that confers a bitter taste to citrus fruits. Among several potential Nar health benefits, it is well known to possess hypolipidemic and anti-diabetic properties, and is therefore of great interest in the treatment of high cholesterol and diabetes.⁹⁻¹⁰ In addition, like many other flavonoids, it is an antioxidant and is of importance in cancer prevention and treatment.¹¹ Recently, it was shown that Nar inhibits the secretion of hepatitis C virus (HCV) in infected patients, and is a regulator of cytochrome P450 enzymes, which are critical elements in drug metabolism.¹²⁻¹³ While Nar possesses favorable activity against a host of diseases, it suffers from poor water solubility, which is a cause of its low oral bioavailability. The Nar molecule is hydrophobic by nature ($\log P = 2.628$), is highly crystalline with a melting point of 250 °C, and has low reported aqueous solubility.¹⁴ To be able to use Nar effectively in therapeutic formulations or dietary supplements, improving its aqueous solubility and bioavailability is critical.

One approach that has been of interest for enhancing the solubility of poorly water soluble drugs is through formation of amorphous solid dispersions (ASD).¹⁵⁻¹⁶ ASD formation is a method by which drug crystallinity can be suppressed by trapping the drug molecules in a metastable amorphous state via molecular dispersions with high glass transition temperature (T_g) polymers. Polymer matrices chosen by previous ASD designers have been selected from polymers that had already been included in drug formulations approved by the FDA for some other purpose (so by definition not designed for ASDs). Polyvinylpyrrolidone (PVP) for example, is a synthetic polymer that is well suited for SD formulations.¹⁷ Another class of polymers that has shown promise is carboxyl-containing cellulose derivatives. These cellulose derivatives have high T_g values, availability of OH and COOH groups for secondary interactions with the drug, and the ability to tailor hydrophobicity using the type and DS of other substituents. As a result of these properties, properly designed cellulose derivatives make excellent ASD polymers. Most well-known among other cellulose derivatives are hydroxypropylmethylcellulose acetate succinate (HPMCAS),¹⁸ carboxymethylcellulose acetate butyrate (CMCAB),¹⁹⁻²⁰ and more recently from our laboratory, cellulose ω -carboxy alkanoates including cellulose acetate adipate propionate (CAAdP).²¹⁻²⁴

Thus far, within our scope of knowledge, alginate derivatives have not yet been explored for SD formulations. A major reason behind this is that it has never before been made soluble in single-component organic media for ease of processing. In the current manuscript, we describe new routes to synthesizing alginate derivatives that are soluble in single component polar aprotic solvents as well as certain ionic liquids. Using bimolecular substitution nucleophilic (S_N2) reactions, the alginate carboxylate groups were esterified, whereby fully substituted (DS = 1.0) derivatives were possible. The solubility properties of the derivatives were studied and peak

assignments were performed using alginates enriched in M and G residues. Furthermore, the use of derivatives having partial DS in enhancing aqueous solubility of Nar was demonstrated.

5.3 Experimental

5.3.1 Materials

Four alginates were used for the study. We represented each as 'Mxxx', where M stands for mannuronate and xxx denotes the % of M residues in the sample. For example, M063 signifies a sample containing 63% M and 37% G residues. M100 alginate was isolated from an epimerase-negative mutant of *Pseudomonas fluorescens* in the laboratory of , Prof. Gudmund Skjåk-Bræk.²⁵ M063 alginate, an alginic acid sodium salt (algal source undisclosed) was from Sigma. M060 alginate (algal source undisclosed) was from FMC BioPolymer. M000 was an alginate containing G-blocks with an average $DP_n \sim 20$ from the laboratory of Dr. Anne Tøndervik.

Water used in the experiments was deionized. Reagent alcohol (histological grade), hexanes (HPLC grade), DMSO (HPLC grade), DMF (HPLC grade), 5 N standardized NaOH solution, 1 N standardized HCl solution, sodium iodide [NaI], potassium chloride [KCl], potassium phosphate monobasic [KH_2PO_4] and ethyl acetate were purchased from Fisher Scientific (Fair Lawn, NJ). Benzyl bromide (98%) [BzBr], iodoethane (98%) [EtI], 1-iodobutane (98%) [BuI], 1-methyl-2-pyrrolidone (99.5%, extra dry) [NMP] and tetrabutylammonium hydroxide (TBAOH; 40 wt%, 1.5 M solution in water) were obtained from Acros (Fair Lawn, NJ). Deuterium oxide (99.9 atom% D; D_2O) containing 0.75% 3-(trimethylsilyl)propionic-2,2,3,3- d_4 acid sodium salt for NMR, (\pm)-naringenin, and iodomethane [MeI] were obtained from

Sigma-Aldrich (St. Louis, MO). KBr used for FTIR analysis was purchased from International Crystal Labs (Garfield, NJ). DMSO-d₆ for NMR was acquired from Cambridge Isotope Laboratories, Inc. (Andover, MA).

5.3.2 Synthesis of TBA-alginate

For conversion of Na-alginate to its protonated form, a procedure described by Babak et al.⁶ was followed with modifications. HCl (0.6 N, 120 mL) was mixed with reagent alcohol (120 mL) in a beaker. Na-alginate (8 g) was added to the mixture and stirred overnight at 4 °C to convert Na-alginate to alginic acid. The percentage of Na-salts protonated to the acid form was not determined since the purpose was to subsequently synthesize TBA-alginate from alginic acid. The mixture was filtered, then the solid (alginic acid) was washed thoroughly, sequentially with alcohol and acetone. The solid product was dried overnight *in vacuo* at 60 °C. Fully dried alginic acid was then dispersed in 200 mL water. TBAOH was added dropwise with continuous stirring at room temperature until the polymer was dissolved and the pH was adjusted to 10.0. If the solution was too viscous, small amounts of water were added until a final viscosity was reached at which the solution could be easily stirred. The aqueous TBA-alginate solution was then premixed with reagent alcohol. The premix was precipitated in a mixture of ethyl acetate-hexane. The solvent ratios used were aqueous alginate acetate : ethanol : ethyl acetate : hexane = 1:3:12:3. The precipitate was then filtered under vacuum and dried *in vacuo* at 60 °C. The ¹H-NMR and FTIR spectra for TBA-alginate are shown in the Supporting Information as **Figures 5.8** and **5.9** respectively.

¹H NMR (500 MHz, D₂O) δ 5.82 – 3.46 (m, alginate backbone), 3.19 (t, NCH₂CH₂CH₂CH₃ of TBA), 1.67 (m, NCH₂CH₂CH₂CH₃ of TBA), 1.40 (m, NCH₂CH₂CH₂CH₃

of TBA), 0.97 (t, $\text{NCH}_2\text{CH}_2\text{CH}_2\text{CH}_3$). FTIR (KBr pellet method): 3400 cm^{-1} , hydroxyl O–H stretching; $2850\text{--}2960\text{ cm}^{-1}$, aliphatic C–H stretching, 1610 cm^{-1} , carboxylate C–O stretching. Elemental composition TBA-alginate M060 measured by elemental analysis: C, 56.46%; H, 10.46%; N, 2.86%. This composition corresponds to roughly 80% TBA and 20% Na salt.

5.3.3 Synthesis of benzyl alginate

TBAF (0.1 g, 0.32 mmol) was dissolved in DMF (10 mL) at room temperature. TBA-alginate (0.15 g) was then added and the mixture stirred until the polymer was dissolved. The temperature was then raised to $80\text{ }^\circ\text{C}$. Benzylation was carried out using either BzBr or benzyl iodide (BzI). In case of BzBr, the necessary equivalents of reagent were directly added to the alginate solution. For BzI, the reagent was synthesized starting from BzBr and then added to the alginate solution. Upon reagent addition, the solution was stirred at $80\text{ }^\circ\text{C}$ for 30 min, after which it was precipitated in ethyl acetate ($\sim 150\text{ mL}$). The precipitate was recovered and dried *in vacuo* at $60\text{ }^\circ\text{C}$. Dry crude benzyl alginate was then dissolved in DMF ($\sim 1.5\text{ mL}$), precipitated in ethyl acetate, filtered and dried *in vacuo*; this step was repeated one more time. The dry solid obtained thereafter was benzyl alginate. The synthesis of BzI reagent is described as follows.

Benzyl iodide: NaI (0.535 g, 3.6 mmol) was dissolved in 5 mL of acetone (dried over 3 \AA molecular sieves) under N_2 pressure at room temperature. To this solution BzBr (0.43 mL, 3.6 mmol) was added. Upon addition, NaBr precipitated as a white solid, which was filtered out and discarded. To the filtrate, 1 mL of DMF (solvent for benzyl alginate synthesis) was added, and acetone removed from the mixture using a rotary evaporator. BzI solution of DMF was thus obtained, and was immediately used for benzyl alginate synthesis.

For benzyl alginate shown in **Figures 5.1** and **5.2**: ^1H NMR (500 MHz, DMSO- d_6) δ 7.48 – 7.23 (m, H9-13), δ 5.43 – 3.16 (m, H1-5), 5.20 (m, H7). ^{13}C NMR (500 MHz, DMSO- d_6) δ 169.15 – 166.33 (m, C6), δ 135.24 – 125.33 (m, C8-13), δ 102.94 – 91.41 (m, C1), δ 80.88-61.39 (m, C2-5), δ 65.62 (m, C7). FTIR (KBr pellet method): 3400 cm^{-1} , hydroxyl O–H stretching; 2850-2960 cm^{-1} , aliphatic C–H stretching; 1740 cm^{-1} , ester C=O stretching; 1250, ester C–O stretching. Elemental composition: C, 46.62%; H, 4.70%; N, 0.04%; O, 41.99%.

5.3.4 Synthesis of methyl alginate

TBAF (0.1 g, 0.32 mmol) was dissolved in DMF (10 mL) at room temperature. TBA-alginate (0.15 g) was then added and the mixture stirred until the polymer was dissolved. The temperature was then raised to 40 °C. Methyl iodide was added at once (molar equivalents varied by experiment) to the alginate solution. Upon reagent addition, the solution was stirred at 40 °C for 30 min, after which it was precipitated in ethyl acetate (~150 mL). The precipitate was recovered and dried *in vacuo* at 60 °C. Dry crude methyl alginate was then dissolved in DMF (~1.5 mL), precipitated in ethyl acetate, filtered and dried *in vacuo*; this step was repeated one more time. The dry solid obtained thereafter was methyl alginate.

For methyl alginate shown in **Figures 5.19** and **5.20** of Supporting Information: ^1H NMR (500 MHz, DMSO- d_6) δ 6.00 – 3.49 (m, H1-5), δ 3.73 (m, H7). ^{13}C NMR (500 MHz, DMSO- d_6) δ 169.36 – 166.43 (m, C6), δ 114.918 – 92.09 (m, C1), δ 80.91-61.63 (m, C2-5), δ 51.53 (m, C7). FTIR (KBr pellet method): 3400 cm^{-1} , hydroxyl O–H stretching; 2850-2960 cm^{-1} , aliphatic C–H stretching; 1740 cm^{-1} , ester C=O stretching; 1250, ester C–O stretching. Elemental composition: C, 40.38%; H, 5.20%; N, 0.11%; O, 49.24%.

5.3.5 Synthesis of ethyl alginate

TBAF (0.1 g, 0.32 mmol) was dissolved in DMF (10 mL) at room temperature. TBA-alginate (0.15 g) was then added and the mixture stirred until the polymer was dissolved. Temperature was then raised to 60 °C. Ethylation was carried out using either EtI wherein the necessary equivalents of reagent were directly added to the alginate solution. Upon reagent addition, the solution was stirred at 60 °C for 30 min, after which it was precipitated in ethyl acetate (~150 mL). The precipitate was recovered and dried *in vacuo* at 60 °C. Dry crude ethyl alginate was then dissolved in DMF (~1.5 mL), precipitated in ethyl acetate, filtered and dried *in vacuo*; this step was repeated one more time. The dry solid obtained thereafter was ethyl alginate.

For ethyl alginate shown in **Figures 5.21** and **5.22** of Supporting Information: ^1H NMR (500 MHz, DMSO- d_6) δ 6.00 – 3.49 (m, H1-5), δ 3.73 (s, H7). ^{13}C NMR (500 MHz, DMSO- d_6) δ 169.36 – 166.43 (m, C6), δ 114.918 – 92.09 (m, C1), δ 80.91-61.63 (m, C2-5), δ 39.50 (m, C7). FTIR (KBr pellet method): 3400 cm^{-1} , hydroxyl O–H stretching; 2850-2960 cm^{-1} , aliphatic C–H stretching; 1740 cm^{-1} , ester C=O stretching; 1250, ester C–O stretching. Elemental composition: C, 40.31%; H, 5.37%; N, 0.11%; O, 48.98%.

5.3.6 Synthesis of butyl alginate

TBAF (0.1 g, 0.32 mmol) was dissolved in DMF (10 mL) at room temperature. TBA-alginate (0.15 g) was then added and the mixture stirred until the polymer was dissolved. Temperature was then raised to 80 °C. Butylation was carried out using either BuI wherein the necessary equivalents of reagent were directly added to the alginate solution. Upon reagent

addition, the solution was stirred at 80 °C for 30 min, after which it was precipitated in ethyl acetate (~150 mL). The precipitate was recovered and dried *in vacuo* at 60 °C. Dry crude butyl alginate was then dissolved in DMF (~1.5 mL), precipitated in ethyl acetate, filtered and dried *in vacuo*; this step was repeated one more time. The dry solid obtained thereafter was butyl alginate.

For butyl alginate shown in **Figures 5.23** and **5.24** of Supporting Information: ^1H NMR (500 MHz, DMSO- d_6) δ 5.95 – 3.44 (m, H1-5), δ 4.13 (m, H7), δ 1.63 (m, H8), δ 1.38 (m, H9), δ 0.93 (m, H10). ^{13}C NMR (500 MHz, DMSO- d_6) δ 169.57 – 166.60 (m, C6), δ 113.25 – 92.71 (m, C1), δ 80.21-61.91 (m, C2-5), δ 64.42 (m, C7), δ 29.64 (m, C8), δ 18.04 (m, C9), δ 12.85 (m, C10). FTIR (KBr pellet method): 3400 cm^{-1} , hydroxyl O–H stretching; 2850-2960 cm^{-1} , aliphatic C–H stretching; 1740 cm^{-1} , ester C=O stretching; 1250, ester C–O stretching. Elemental composition: C, 50.52%; H, 6.91%; N, 0.07%; O, 40.72%.

5.3.7 Saponification of esters

Benzyl alginate with DS 1.0 (131 mg) was added to water (13 mL) forming a suspension. To this suspension, 1M NaOH solution (1.3 mL) was added and stirred for 30 min. Over time, the alginate dissolved. It was then precipitated in reagent alcohol (~150 mL), filtered, the solid recovered and dried *in vacuo* at 60 °C. The dry solid was dissolved in water and re-precipitated in reagent alcohol, followed by filtration and drying *in vacuo* at 60 °C.

5.3.8 NMR Analysis

For all alginate esters, the solid sample (40-50 mg) was dissolved in DMSO-d6 (~0.7 mL) by applying heat. Spectra were acquired using a JEOL 500 MHz spectrometer with automatic shimming, and the acquisition temperature was 85 °C. Number of scans acquired was 16 for ¹H-NMR and DQF-COSY, 250 for HMQC and HSQC, and 13,000 for ¹³C-NMR. All spectra were processed using MestReNova version: 8.0.2-11021. For water soluble samples, an automatic water suppression pulse was applied to suppress the residual HDO peak. For benzyl alginate, DS value calculation was carried out by integrating the benzyl aromatic peaks appearing at 7.48 – 7.23 ppm (*I*_{Aromatic}) against the region appearing around 5.43 – 3.16 ppm, which contains the backbone and benzyl CH₂ signals (*I*_{Backbone+Methylene}). *I*_{Aromatic} accounts for 5X protons while *I*_{Backbone+Methylene} accounts for 7+2(X) protons. The following formula was then used to calculate the DS value.

$$DS_{Benzyl} = \frac{7I_{Aromatic}}{5I_{Backbone+Methylene} - 2I_{Aromatic}}$$

To calculate the DS values for ethyl and butyl alginate derivatives, the methyl peak of the ester appearing at ~0.93 ppm (*I*_{Methyl}) was integrated against the region appearing at 5.95 – 3.44 ppm, which contains the backbone and ester CH₂ signals (*I*_{Backbone+Methylene}). *I*_{Methyl} accounts for 3X protons while *I*_{Backbone+Bz,methylene} accounts for 7+2(X) protons. The following formula was then used to calculate the DS value.

$$DS_{Butyl/Ethyl} = \frac{7I_{Methyl}}{3I_{Backbone+Methylene} - 2I_{Methyl}}$$

DS value of methyl alginate could not be calculated using ¹H-NMR due to the overlap of the methyl ester peak with the backbone region.

5.3.9 FTIR measurement

FTIR spectra were acquired using a Thermo Electron Nicolet 8700 instrument in transmission mode. Samples were prepared using the KBr pellet method. Alginate (1 mg) was mixed with 99 mg of KBr using a mortar and pestle. The mixture was compressed in the sample holder between two screws to form a KBr disc. 64 scans were obtained for each spectrum.

5.3.10 Elemental analysis

Measurements were performed using %CHN analyzer with a combustion/thermal conductivity detector (TCD) and %O analyzer with pyrolysis.

5.3.11 DS measurement by titration

Titration was performed by reacting alginate esters with excess NaOH to hydrolyze the ester groups. NaOH molecules remaining after hydrolysis were then back-titrated with HCl to measure the moles of acetate present. For example in the case of benzyl alginate, 250 mg solid was weighed into a 50 mL 3-neck flask. To this, 25.0 mL of standardized 0.1 N NaOH solution was added and stirred overnight at room temperature. The water insoluble polymer dissolved over time. Potentiometric titrations were performed using a pH electrode (Inlab 413, Mettler-Toledo International, Inc.). The electrode was inserted into the 3-neck flask, 0.1 mL aliquots of standardized 0.1 N HCl solution added, the mixture allowed to stir for 30 seconds and the pH measured. Total volume of HCl added was 30 mL. Two plots were made using the recorded data. pH was first plotted against the volume of HCl added. Derivative $d(pH)$ was plotted in a second

graph against the volume of HCl added. Inflexion point was recorded as the volume at which peak maximum was attained in the d(pH) plot.

Moles of ester groups present in the sample used for titration (250 mg) was calculated as follows:

$$\text{Moles of ester (M)} = \text{Initial moles of NaOH} - \text{Moles remaining after hydrolysis}$$

DS was then calculated as:

$$DS_{\text{Titration}} = \frac{M}{\text{No. of uronic acid residues in sample (N)}} \quad \text{Equation (1)}$$

Where,

$$N = \frac{0.25}{(266 \times DS_{\text{Titration}}) + (198 \times (1 - DS_{\text{Titration}}))} \quad \text{Equation (2)}$$

Equation (2) was plugged in to Equation (1) to calculate $DS_{\text{Titration}}$.

5.3.12 Synthesis of solid dispersions

Three solid dispersions were prepared starting from three different alginate ester derivatives – ethyl, butyl and benzyl. In each case, the alginate derivative (180 mg) was dissolved in 4 mL NMP by applying heat. Once the solution was cool, naringenin (60 mg) was added and dissolved at room temperature. The solution was then precipitated in ice-cold water (100 mL) and filtered to recover the wet solid, which was then placed in the freezer overnight before lyophilizing.

5.3.13 Alginate ester solubility in water

To test the solubility of alginate ester in water, the solid (4 mg) was added to D₂O (1 mL), heat applied and stirred using a vortex mixer. The suspension was passed through a syringe filter to separate the solid, while the filtrate was added to a 5 mm NMR tube for acquisition.

5.3.14 Nar calibration curves

To plot calibration curves, Nar was dissolved in NMP at a concentration of 1 mg/mL. The NMP solution was then diluted to concentrations of 0.02, 0.015, 0.01 and 0.005 mg/mL using buffer solution, and UV-Vis spectra were obtained for each dilution. Two buffers solutions were used in the study: pH 6.8 and 1.2. The absorbance wavelengths monitored were 316 nm in pH 6.8 buffer, and 291 nm in pH 1.2 buffer.

5.3.15 Measurement of % drug loading

Drug loading was measured by dissolving the solid dispersion in NMP at a concentration of 1 mg/mL. The NMP solution was then diluted to a concentration of 0.02 mg/mL in pH 6.8 buffer, and UV-Vis spectrum obtained. The absorbance at 316 nm was recorded and the concentration of Nar in the solution was determined using the Nar calibration plot. Drug loading was then calculated as follows:

$$\text{Percent Drug loading} = \frac{\text{Nar concentration in } \frac{\text{mg}}{\text{mL}} \text{ as measured by UV}}{0.02} \times 100$$

5.3.16 Nar release studies

Nar samples (pure or solid dispersion) were dispersed in 100 mL buffer (pH 6.8 or 1.2) in amber glass flasks at Nar concentrations of 0.07 mg/mL, and stirred at room temperature. Aliquots (1.5 mL) were withdrawn at appropriate time intervals and replaced with 1.5 mL of fresh dissolution medium after each sampling to maintain constant volume. UV-Vis absorption of each aliquot was recorded after centrifugation at 14,000 rcf (relative centrifugal force) for 10 min.

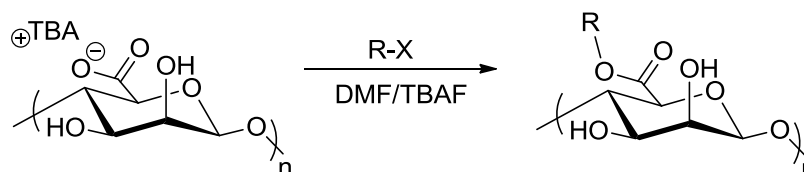
5.4 Results and Discussion

Since alginates are predominantly water soluble polysaccharides, it has been a persistent effort in our laboratory to find diverse organic solvents capable of dissolving them for subsequent derivatization. Our previous findings have shown that a minimum requirement necessary to solubilize alginates in organic media is the exchange of their inorganic counterions (such as Na^+ or Ca^{+2}) with organic counterions (such TBA^+). However, even after this requirement is satisfied, TBA-alginate can only dissolve in polar aprotic solvents (DMSO, DMF, DMI and DMAc) with the addition of the dissolution promoter TBAF. These two-component solvent systems can serve as homogeneous reaction media, whereby it may now be feasible to react the available functional groups on alginate backbone to synthesize derivatives with high degrees of substitution (DS). Our hope was that upon derivatization, the new derivatives will show improved solubility properties, and perhaps dissolve in single component organic solvents. Having single component solvents will not only eliminate the use of TBAF (and thereby avoid the accompanying water of TBAF hydration, as well as the potential for side reactions caused by the presence of fluoride ion) but also allow easier processing for intended applications.

There are two available functional group types on the alginate backbone that may be used for derivatization. We have previously shown that upon acetylation of the -OH groups up to $DS_{\text{acetyl}} = 1.0$, the derivatives were water-soluble and showed no single component organic solubility. Furthermore, propionylation yielded alginate propionate up to $DS_{\text{propionyl}} = 0.31$, but its solubility was still limited to water. At this point, we hypothesized that while hydrophobic groups could be attached to the alginate backbone via -OH group modification, the charges imparted by carboxylate moieties presented significant hydrophilic character to the backbone to prevent organic dissolution, particularly since we were unable to achieve the maximum theoretical DS of 2.0 upon acylation of alginate hydroxyls in these solvent systems. We therefore adopted a strategy of carboxyl group esterification as a potential method for synthesis of a new class of organo-soluble alginate derivatives.

Selective reaction of carboxylate (COO^-) over hydroxyl (-OH) groups is advantaged, since the former is a stronger nucleophile. The difference in nucleophilicity can be used to selectively react the carboxylate groups with substrates that can undergo S_N2 substitution. The ability to do so in our new alginate solvent systems⁴ afforded the additional possibility of complete substitution on the carboxyl groups, as well as the possibility that no added base would be needed since alginate carboxyls are already ionized in our solvent systems. We therefore reacted alginate in solution with several halide reagents to prepare the corresponding esters. This reaction of carboxylates with halides is non-catalyzed and does not entail the use of extreme pH environments. Such conditions are favorable for preserving the molecular weight of the sensitive polysaccharide alginate during reaction. It is well known that alginates suffer a loss in molar mass in both strongly acidic²⁶⁻²⁷ and strongly alkaline solutions.²⁸⁻²⁹ Modification of alginates

under mild pH conditions is therefore often preferred. A general reaction scheme for the esterification of alginate carboxylate groups using alkyl halides is shown in **Scheme 5.1**.



Scheme 5.1: General reaction scheme for esterification of alginates using alkyl halides

We first synthesized the benzyl ester by reaction of TBA-alginate with BzBr. $DS_{\text{benzyl}} = 0.44$ was achieved when the reaction was performed at 80 °C for 30 min. ^1H -NMR spectrum of the product is shown in **Figure 5.10** in the Supporting Information. Knowing that the theoretical maximum DS_{benzyl} value is 1.0, this indicates that 44% of the available carboxylate groups were substituted. What is more significant however is the fact that this is the first demonstration of the capability to react alginate with a hydrophobic organo-soluble reagent such as BzBr. Since BzBr is water immiscible, achieving the same level of substitution by performing the reaction in an aqueous medium could be anticipated as a challenge. In addition, a relatively rapid reaction under mild pH conditions can allow preservation of molar mass during reaction. This highlights the benefits of being able to dissolve alginates in organic solvents. We sought to achieve $DS_{\text{benzyl}} > 0.44$, preferably full substitution, so took the approach of replacing BzBr with a benzyl reagent that possesses a better leaving group. For example, when TBA-alginate was reacted with BnI at 80 °C for 30 min, we were able to synthesize fully substituted benzyl alginate with $DS_{\text{benzyl}} = 1.0$. This to our knowledge is the first demonstration of complete substitution at the carboxyl group position to form alginate esters. **Figure 5.1** shows the ^1H and ^{13}C -NMR spectra of fully substituted benzyl alginate.

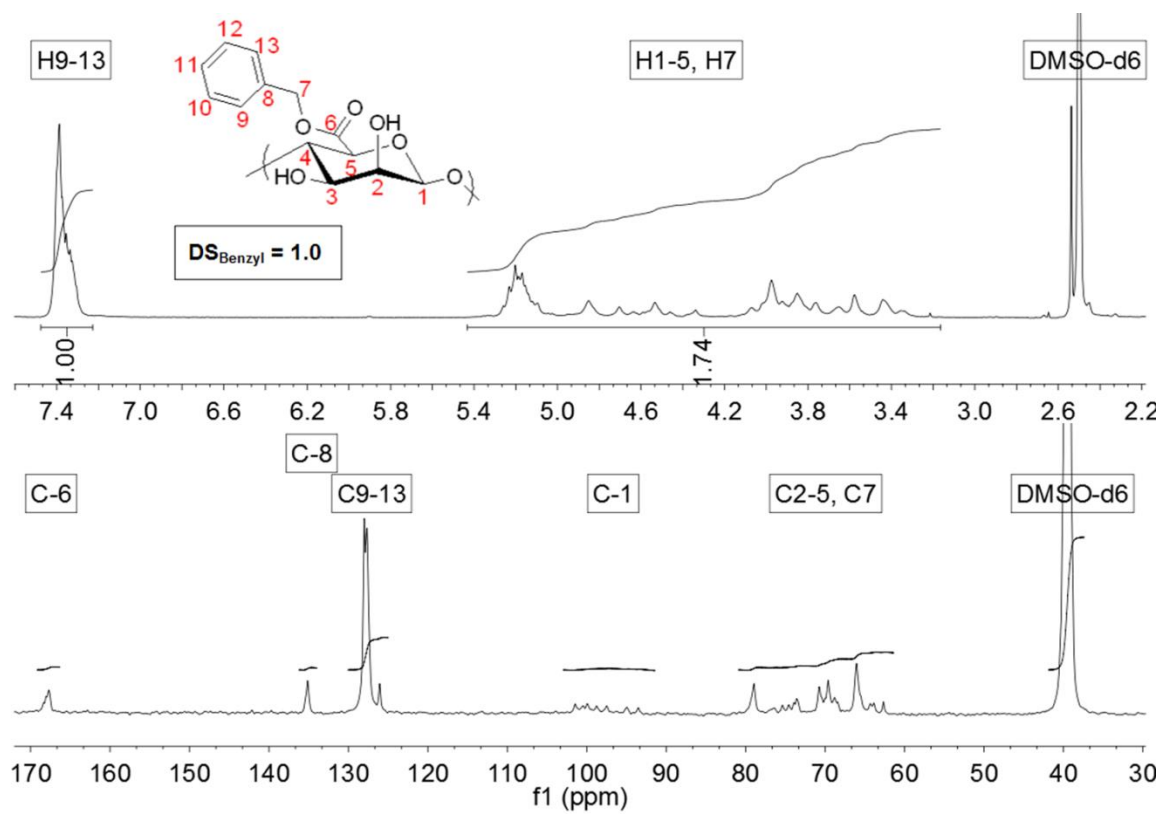


Figure 5.1: ^1H and ^{13}C -NMR spectra of benzyl alginate with $\text{DS}_{\text{benzyl}} = 1.0$

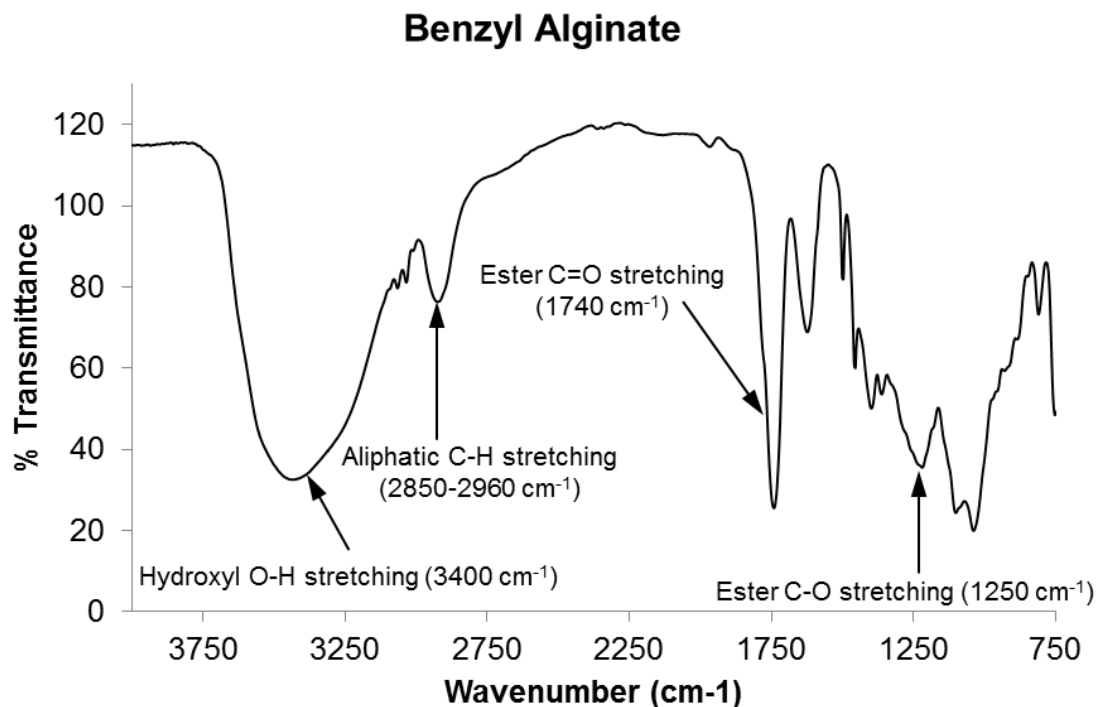
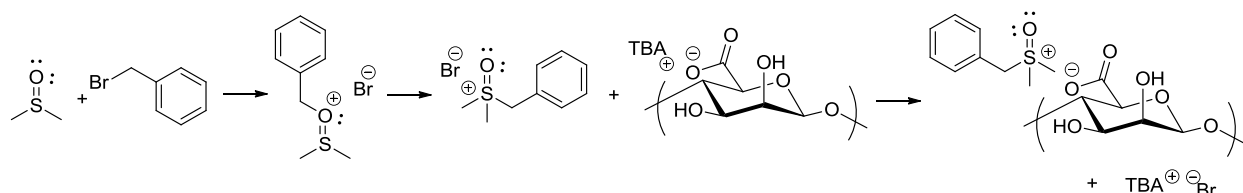


Figure 5.2: FTIR spectrum of benzyl alginate with $DS_{\text{benzyl}} = 1.0$

The ability to dissolve TBA-alginate in a variety of TBAF based two-component solvent systems has important implications in the preparation of alginate esters. This can be demonstrated through an example in which we first used DMSO/TBAF as reaction solvent for benzyl alginate synthesis. Our results indicate that while alginate carboxyl groups were benzylated, DMSO participated as a reactive solvent forming benzyldimethyloxosulfonium salts of alginate. A probable mechanism by which this reaction proceeds is shown in **Scheme 5.2**. The ^1H -NMR spectra of all benzyl alginates synthesized in DMSO/TBAF showed a consistent peak ~ 2.9 ppm, as indicated by (*) in **Figure 5.10** of Supporting Information. The reactivity of DMSO with alkyl halides is previously documented, wherein the alkyl halide can first react with the DMSO oxygen to give alkyloxydimethylsulfonium halide, which further rearranges to the more stable form of the salt yielding alkyldimethyloxosulfonium halide.³⁰ Due to the reactivity of

DMSO with alkyl halides, DMF/TBAF proved to be a more suitable solvent system for alginate ester syntheses. Benzyl alginate with $DS_{\text{benzyl}} = 1.0$, free of side reactions could be prepared in DMF/TBAF by reaction of TBA-alginate with BnI at 80 °C for 30 min. As observed in **Figure 5.1**, the peak around ~2.9 ppm was absent.



Scheme 5.2: Postulated side reaction of DMSO with benzyl bromide leading to the formation of benzyldimethyloxosulfonium salts of alginate

In order to prove that the reaction of benzyl iodide was indeed chemoselective towards alginate carboxylate groups, the product esters were hydrolyzed by treatment with aqueous NaOH. Any ether groups formed via –OH group reactions would not hydrolyze, being unreactive with aqueous alkali. We therefore compared the ^1H NMR spectra of benzyl alginate before and after hydrolysis. Benzyl alginate is insoluble in the aqueous NaOH medium at first, but dissolves as it reacts. Therefore the NMR spectrum of benzyl alginate was acquired in DMSO- d_6 , while that of the hydrolyzed product was acquired in D_2O (**Figure 5.3**). It is evident that the aromatic peaks observed in the benzyl alginate spectrum are completely absent after hydrolysis. This confirms that the signals arising in the aromatic region for benzyl alginate arose only from carboxylate ester moieties, and not from benzyl ethers of the hydroxyl groups. This is strong support for the general notion that reaction of TBA alginate with alkyl halides in homogeneous solution is strongly chemoselective for reaction of the carboxylate groups in preference to the hydroxyl groups.

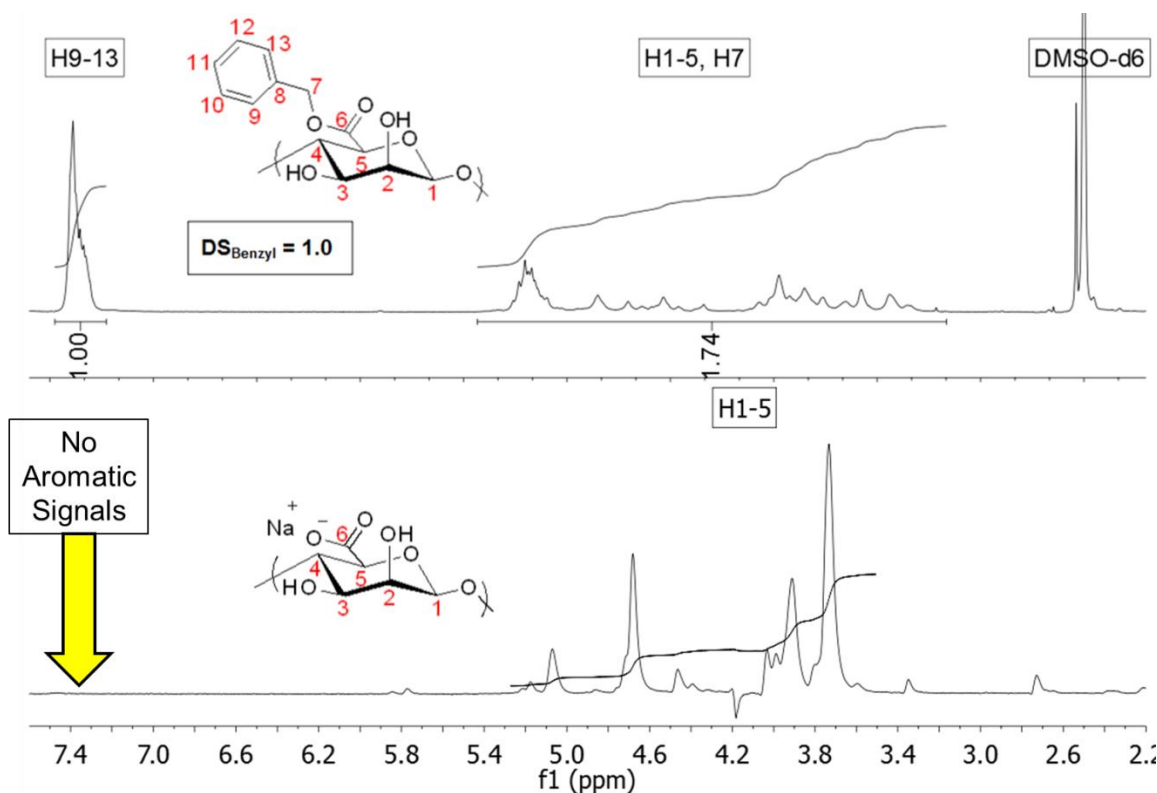


Figure 5.3: ¹H-NMR spectra of benzyl alginate pre (top) and post hydrolysis (bottom)

Previous studies in our laboratory have shown that in the case of alginate acetates, ¹H-NMR integration methods lead to consistent overestimation of DS_{acetyl} values. This overestimation is a result of suppression of the residual HDO signal, which reduces the intensity of certain neighboring alginate backbone signals. A titration-based method was therefore developed to accurately measure DS_{acetyl}. While suppression of the residual HDO is not required when the NMR solvent is DMSO-d₆, it is still worthwhile to verify the accuracy of DS measurement by ¹H NMR. Benzyl alginate was therefore hydrolyzed in an aqueous NaOH solution of known molarity; the solid was initially insoluble in the medium but dissolved over time as the ester groups were hydrolyzed. The moles of NaOH remaining after hydrolysis were measured by titration against standardized HCl. The amount of titrant used was employed to

calculate the moles of ester present, and therefore the DS_{benzyl} . **Figure 5.4** shows the potentiometric titration and $d(pH)$ plots for benzyl alginate. **Table 5.1** shows a comparison of the DS values as measured using $^1\text{H-NMR}$ and titration. It is clear that both methods yield the same value for DS_{benzyl} , thus confirming that $^1\text{H-NMR}$ can be used as a reliable method for DS measurement.

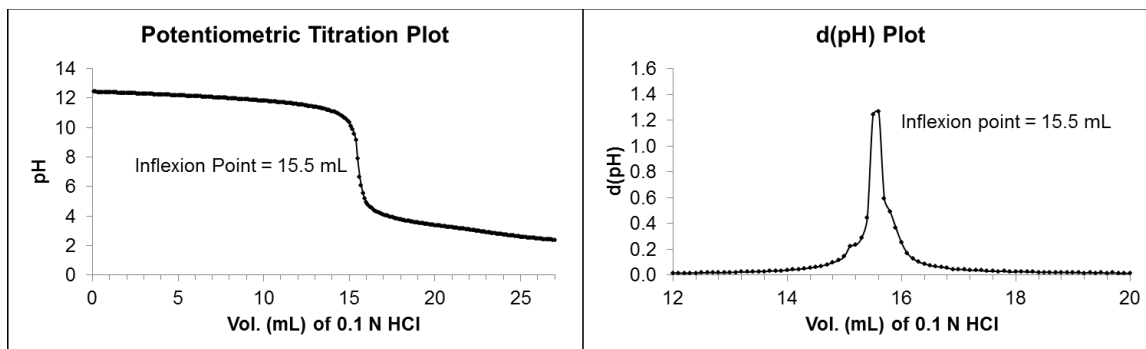


Figure 5.4: Potentiometric titration [left] and $d(pH)$ [right] plots for benzyl alginate

Table 5.1: Comparison of DS_{benzyl} values measured using $^1\text{H NMR}$ and titration

DS_{benzyl}	
$^1\text{H-NMR}$	Titration
1.0	1.0

Peak assignments for alginate esters can be performed using 2D-NMR spectroscopy. As a general observation, dissolving alginate derivatives in DMSO-d_6 for NMR resulted in better peak resolution compared to D_2O , where peak overlap appeared to be more severe. To facilitate interpretation of NMR spectra and assign signals arising from M and G residues, we took the approach of esterifying the homopolymers M100 and M000, and using their simplified spectra as guideposts for interpretation of copolymer spectra. The homopolymeric alginates are not commercially available, but M100 can be prepared from bacterial culture of epimerase-deficient bacteria,²⁵ while M000 can be obtained from extensive exposure of natural alginate co-polymers

to a series of alginate epimerases *in vitro*.³¹⁻³⁴ We then prepared butyl esters of alginates having varying M/G compositions in order to perform the necessary peak assignments. **Figure 5.5** and **5.6** show the stacked ^1H and ^{13}C NMR spectra of butyl alginates.

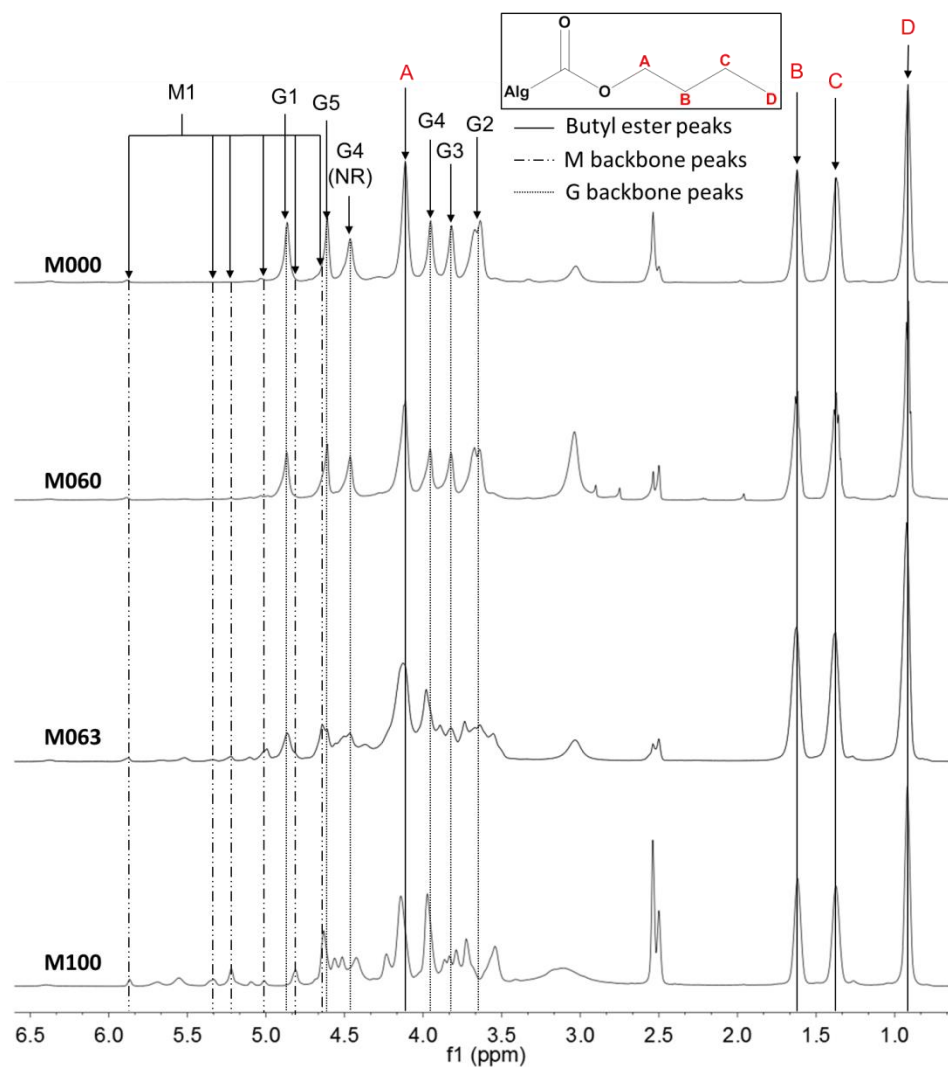


Figure 5.5: Stacked ^1H -NMR spectra of butyl alginates of varying M contents

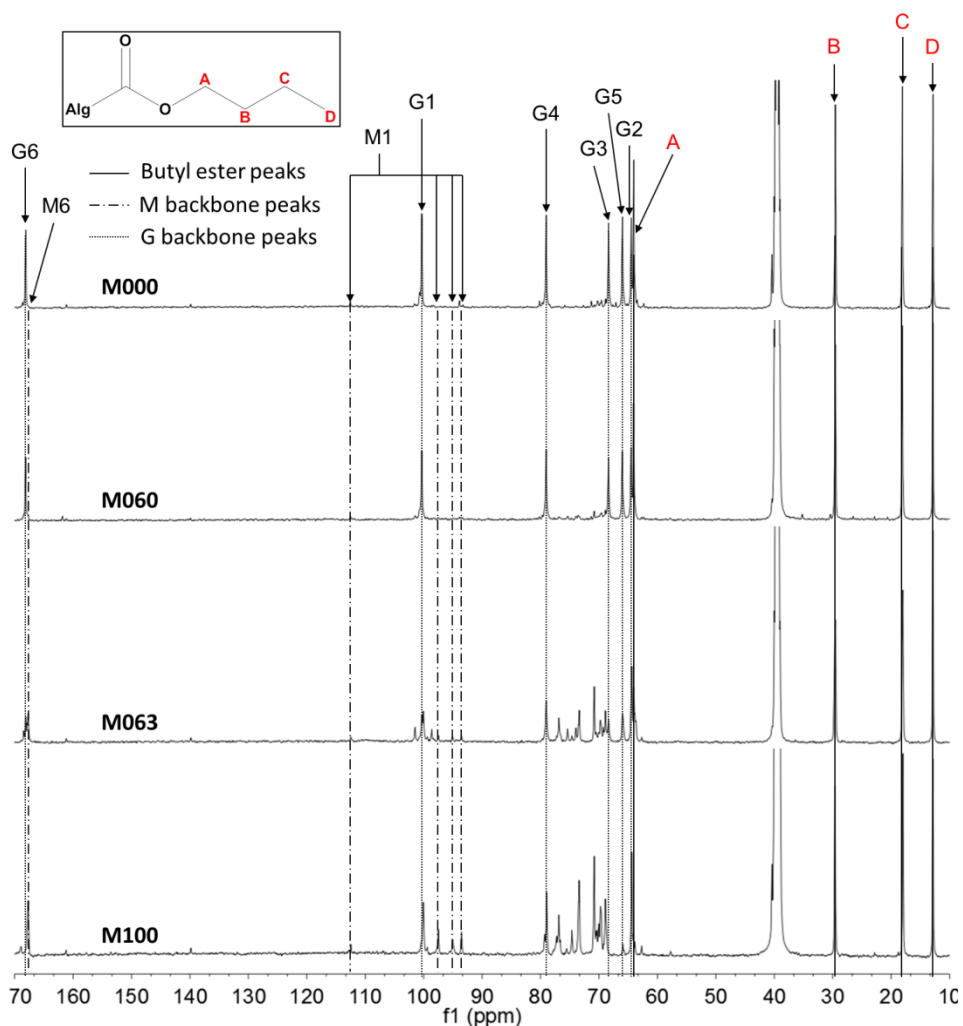


Figure 5.6: Stacked ^{13}C -NMR spectra of butyl alginates of varying M contents

For peak assignment, we used a strategy wherein the anomeric signals were first identified based on their shifts in the ^{13}C -NMR spectrum. Then, using a combination of DQF-COSY (^1H - ^1H coupling) and HMQC (^1H - ^{13}C coupling) correlation spectroscopy techniques, all remaining peaks were assigned. We observed that upon esterification, peak assignment for G residues was relatively simpler compared to M residues. For example, in the case of the butyl ester of M000 alginate, only one anomeric peak was observed which was correlated to the corresponding G backbone peaks. Conversely, for the butyl ester of M100 alginate, at least five

separate anomeric signals were identified, and their correlations to corresponding M backbone peaks were challenging using the techniques chosen. Furthermore, cross peaks obtained in the 2D-NMR spectra were not well resolved in the case of M100. As the fraction of M residues in the backbone increased, the complexity arising in the NMR spectra increased correspondingly, and analysis became more challenging. We were nevertheless able to clearly assign signals arising from G residues in all alginate samples. The DQF-COSY and HMQC spectra for all four alginates are shown in **Figures 5.11 – 5.18** of Supporting Information. In addition, all backbone peak shifts for G residues, and anomeric peak shifts for M residues are listed in **Table 5.5** of Supporting Information.

Table 5.2: Alginate esters, their DS values and corresponding solubility properties

Derivative	Solubility		
	DMSO, DMF, NMP, DMAc, DMI	Methanol, Isopropanol, Acetone	Water
Benzyl alginate DS = 1.0	S	I	I
Butyl alginate DS = 1.0	S	I	I
Ethyl alginate DS = 1.0	S	I	I
Methyl alginate DS = 1.0	S	I	I

S = soluble, I = insoluble, P = partially soluble

Synthesis of alginate esters using carboxylate modification can afford derivatives with a range of structures and properties based on the reagent and stoichiometry used. To demonstrate this, we synthesized methyl and ethyl alginate in addition to the benzyl and butyl ester derivatives. The ^1H , ^{13}C -NMR and FTIR spectra of methyl, ethyl and butyl alginate are shown in **Figures 5.19 – 5.24** of the Supporting Information. **Table 5.2** shows the solubility properties of ester derivatives with different DS values. The utility of alginate esters can be demonstrated

using an application that takes advantage of their ability to dissolve in organic solvents without the addition of a dissolution promoter such as TBAF. We were specifically interested in understanding whether these novel alginate derivatives had the potential to enhance the solubility of poorly water-soluble drugs such as Nar. Solid dispersions have previously been defined as “a drug substance entrapped (or “dissolved”) in a carrier, usually a hydrophilic polymer.”³⁵ By forming molecular dispersions of the drug with the polymer, suppression or disruption of drug crystallinity is possible; such dispersions are termed “amorphous solid dispersions” (ASDs). By hindering crystal lattice formation of high-melting drugs, increases in the rate of dissolution and bioavailability have been reported.³⁶ Important criteria for the selection of appropriate polymers in SD formulations include their non-toxicity, miscibility with hydrophobic drugs (facilitated by specific interactions, for example hydrogen bonding or ionic interactions) and a trigger mechanism (such as pH sensitivity) for drug release. In addition, the polymer must be capable of providing stability against drug crystallization in both solid and solution states.

Several methods for the synthesis of ASDs are possible based on solvent processing. The first step involves dissolution of the drug and polymer in a common organic solvent or mixture of solvents. The solvent/s can then be removed using methods such as evaporation under reduced pressure, for example by rotary evaporation, film casting, or spray drying. Each of these methods however requires the use of low-medium range boiling solvents such as acetone, methanol, methylene chloride, acetonitrile or ethanol. Unfortunately, the alginate esters we synthesized were not soluble in any of these solvents; their solubility was restricted to high-boiling polar aprotic solvents such as DMSO, DMF, DMI, DMAc and NMP. Due to this limitation, we chose a co-precipitation method, wherein the drug and polymer were dissolved in NMP, followed by co-precipitation in cold water. For the current Nar release study, we compared partially esterified

benzyl, butyl and ethyl alginate derivatives listed in **Table 5.2**. Partially esterified derivatives have a fraction of carboxylate groups that remain non-esterified, thus providing a pH dependent release mechanism. None of the three derivatives in question showed complete water solubility. However, we imagined that any partial water solubility may affect the percent drug loading of the resulting solid dispersion, and hence its release performance. The water solubility of the each derivative was therefore tested using $^1\text{H-NMR}$ following exposure to D_2O . **Figure 5.25** in Supporting Information shows the spectra, wherein the alginate backbone region has been shaded grey. It is evident that the ethyl derivative shows partial solubility in D_2O , while the butyl and benzyl derivatives do not show any water solubility. Owing to this partial solubility of ethyl alginate in water, loss of polymer occurs during SD preparation. A direct result of this is that actual drug loading is higher compared to the theoretically expected loading. On the contrary, butyl and benzyl alginate SDs yielded percent drug loadings that were lower than the theoretically expected values. **Table 5.3** shows the compositions of the SDs, and the theoretical and actual percent drug loading values.

Table 5.3: SD compositions, along with theoretical and actual drug loading

Derivative	Drug:Alginate Wt. Ratio	Theoretical drug loading	Actual drug loading
Ethyl alginate	1:3	25%	42%
Butyl alginate	1:3	25%	21%
Benzyl alginate	1:3	25%	19%

We studied the release of Nar from the solid dispersions in aqueous solutions buffered at pH 1.2 (simulating gastric environment) and 6.8 (simulating small intestinal environment). **Figure 5.7** shows the Nar release curves obtained. Compared to pur Nar (Blank), all three alginate derivatives showed enhancement in drug solubility at both pH values. **Table 5.4** shows the maximum percent Nar release achieved for all SD formulations and the corresponding

solubility enhancement factors. Ethyl and benzyl alginates showed solubility enhancement factors that were close to ~1.50, while that of butyl alginate ASD were slightly higher (ca. 2.25). It is worthwhile at this point to compare these factors with the ones reported for carboxyl-containing cellulose derivatives [Li, Liu, Edgar et al.; manuscript under review]. HPMCAS clearly yields the best improvement in Nar aqueous solubility with an enhancement factor of 14. CMCAB and CAAAdP have factors of 5 and 4 respectively, and are closer to the values yielded by alginate esters.

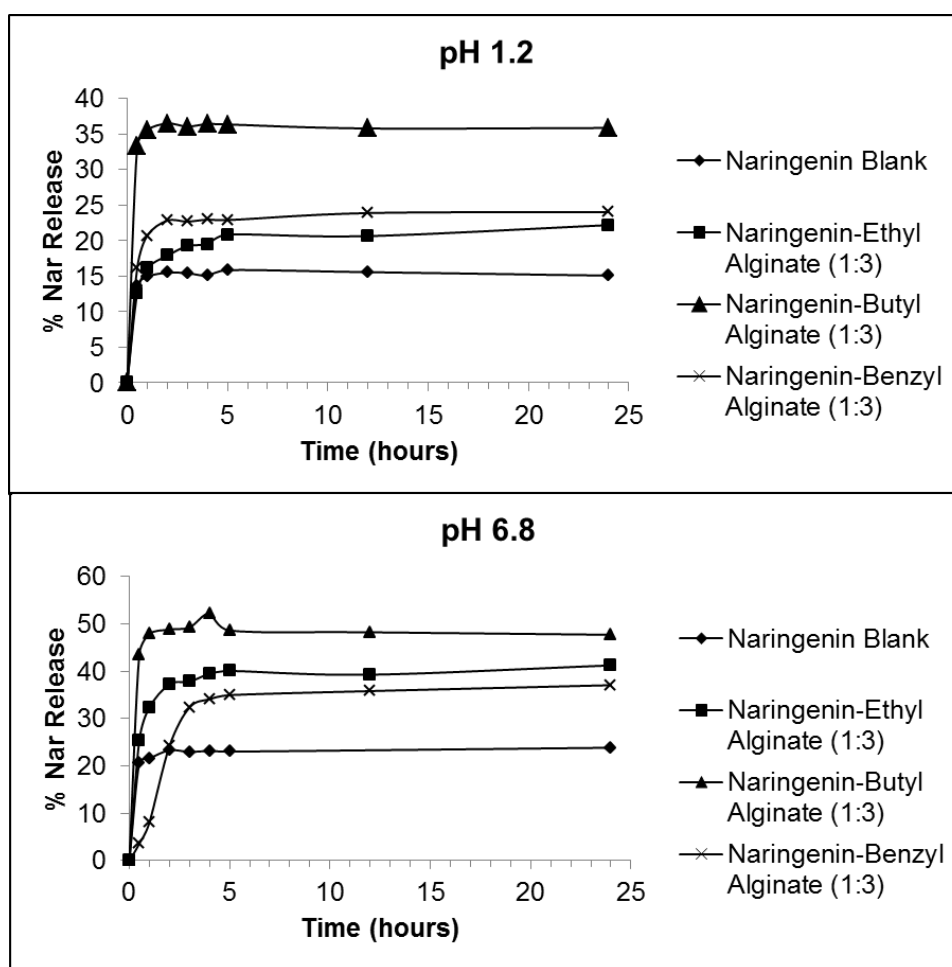


Figure 5.7: Nar release profiles studied at pH 1.2 (top) and pH 6.8 (bottom)

In order for alginate derivatives to be competitive as matrix polymers, there is clearly a need for improvement in their solubility enhancement factors. However, the purpose of this study is simply to demonstrate that modifying alginates in this fashion can lead to derivatives capable of solubility enhancement of poorly water-soluble drugs. Going forward, there may be several avenues possible for performance optimization. Firstly, the ability to dissolve alginates in low boiling solvents can be expected to have a significant impact on the ease of ASD formation. Allowing the use of solvent evaporation techniques such as film casting, vacuum evaporation and spray drying could significantly impact the nature of the solid dispersions formed. Solvent evaporation is perhaps the most flexible, practical technique for SD formation; melt extrusion is often preferred when it is practical, but it is restricted to cases where both drug and polymer have sufficient thermal stability. Extending the solubility profiles of alginate derivatives to permit dissolution in low-boiling solvents should be possible by functionalization of the available –OH groups in addition to the –COOH groups. Furthermore, varying the DS and type of both carboxyl and hydroxyl substituents should allow fine-tuning of the hydrophilicity-hydrophobicity balance to achieve optimal performance. To realize the best possible solid-state stabilization, determination of the glass transition temperatures (T_g) of the alginate derivatives will be key. In addition, XRD studies will be necessary to determine the extent to which alginate derivatives are able to suppress drug crystallinity. In summary, our data demonstrates the principle that alginate esters are capable of enhancing solubility of poorly water-soluble drugs, but there is ample room for performance enhancement using multitude of strategies. We therefore believe that alginates hold the promise to be interesting candidates for achieving improved dissolution and bioavailability of poorly water-soluble drugs.

Table 5.4: Maximum percent Nar released and solubility enhancement factors for the SDs studied

SD	pH 1.2		pH 6.8	
	Maximum Nar Conc. (mg/mL)	Solubility enhancement factor	Maximum Nar Conc. (mg/mL)	Solubility enhancement factor
Nar Blank	1.11×10^{-2}	-	1.67×10^{-2}	-
Nar:Ethyl alginate (1:3)	1.55×10^{-2}	1.40	2.89×10^{-2}	1.73
Nar:Butyl alginate (1:3)	2.55×10^{-2}	2.30	3.65×10^{-2}	2.19
Nar:Benzyl alginate (1:3)	1.68×10^{-2}	1.52	2.59×10^{-2}	1.55
Nar/HPMCAS	-	-	-	14 ^a
Nar/CMCAB	-	-	-	5 ^a
Nar/CAAdP	-	-	-	4 ^a

^aData reported by Edgar et al.[Li, Liu, Edgar et al.; manuscript under review]

5.5 Conclusion

With a growing emphasis on the use of renewable resource materials and the potential to harvest algae in abundance, alginates have great promise as the source of polysaccharide derivatives for demanding applications. Herein we have demonstrated chemoselective modification of the alginate carboxyl group to provide a variety of esters, with DS controllable by stoichiometry, that broadens the palette of available alginate derivatives and provides a new route for their synthesis. We build on our previous finding that TBA salts of alginate were soluble in two component polar aprotic solvent systems such as DMSO/TBAF, showing that these organosoluble alginate salts react directly with alkyl halide reagents exclusively at the carboxylate groups on the alginate backbone. A relatively fast reaction of alginates with alkyl iodides presents the opportunity to achieve high DS products without significant loss of molar mass. The resulting carboxyl ester derivatives, including benzyl, butyl, ethyl and methyl alginates, have good solubility in polar aprotic solvents such as (DMSO, DMF, DMAc, DMI and

NMP) without addition of the dissolution promoter TBAF. These new derivatives, with enhanced organic solubility and significantly modified properties, promise to find applications for which the natural alginate polymer would not be suited.

It is clear from this work that the type of halide reagent used strongly influences reactivity and hence achievable DS. While alkyl bromides do react with TBA alginate in organic solution to give partially carboxyl-esterified products, switching to alkyl iodide reagents permitted synthesis of completely substituted (DS 1.0) alginate esters at the proper stoichiometry. This work further demonstrates the importance of choosing the correct solvent system from the several polar aprotic solvents that effectively dissolve TBA alginate in the presence of TBAF. The use of DMSO afforded side products from reactions of the solvent with the alkyl halides, while amide solvents like DMF permitted smooth and clean alginate carboxylate alkylation with no observed side reactions. It proved possible to discount the possibility of competing hydroxyl alkylation by saponification of the product esters followed by NMR analysis to demonstrate the absence of residual alkyl ether groups; this saponification methodology was also a useful tool, coupled with back titration, to confirm the DS values measured by ^1H NMR and to provide an alternative analysis method that might in under some circumstances be preferred to ^1H NMR. 2D-NMR analysis of alginates was also performed for samples with varying M contents. We were able to show that the complexity of NMR spectra grew as the percentage of M residues in the backbone increased. Peak assignments were performed to identify all backbone signals arising from G residues. Because of the complex spectra with overlapping signals and cross peaks from M residues, only the anomeric signals of these residues were identified.

We utilized the improved solubility of alginates in organic media upon esterification to help us demonstrate one potential area of utility for these alginate carboxylate esters, for the preparation of solid dispersion drug delivery systems. Partially esterified benzyl, butyl and ethyl alginates were used for the study because the fraction of carboxylate groups which remain non-esterified provide pH sensitivity. Fully esterified alginate with DS 1.0 would have no free carboxylates present on the backbone to enable pH dependent release activity. We circumvented the low solubility of these esterified alginates in volatile organic solvents by using co-precipitation from polar aprotic solvents, which proved to be an efficient method for making solid dispersions of drugs in alginate ester matrices. Some of the alginate derivatives tested had partial solubility in water (e.g. ethyl alginate); this led to solid dispersions containing a higher percentage of drug (and lower percentage of alginate ester) than was targeted. Water-insoluble alginates like benzyl or n-butyl alginate afforded dispersions with the target percent drug. We find that these solid dispersions do enhance the aqueous solution concentration of naringenin by small amounts, roughly 1.5 – 2X, and surmise that more hydrophobic alginate derivatives might give higher solution concentrations of Nar by better retarding crystal growth and/or slowing nucleation. More broadly, this new method for chemoselective alginate carboxyl modification opens the door to design of regioselectively modified alginates with tailored structure and hydrophobic/hydrophilic balance, revealing fresh possibilities for utilization of this abundant natural polysaccharide.

5.6 Supporting information

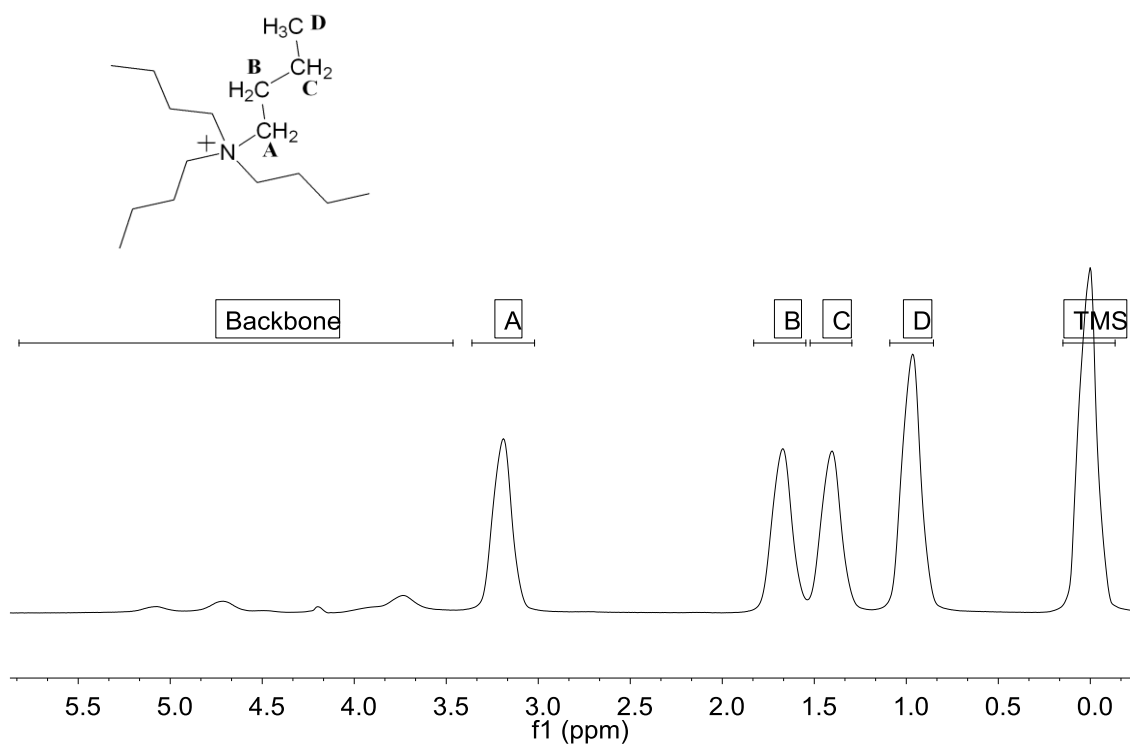


Figure 5.8: ^1H -NMR of TBA-alginate

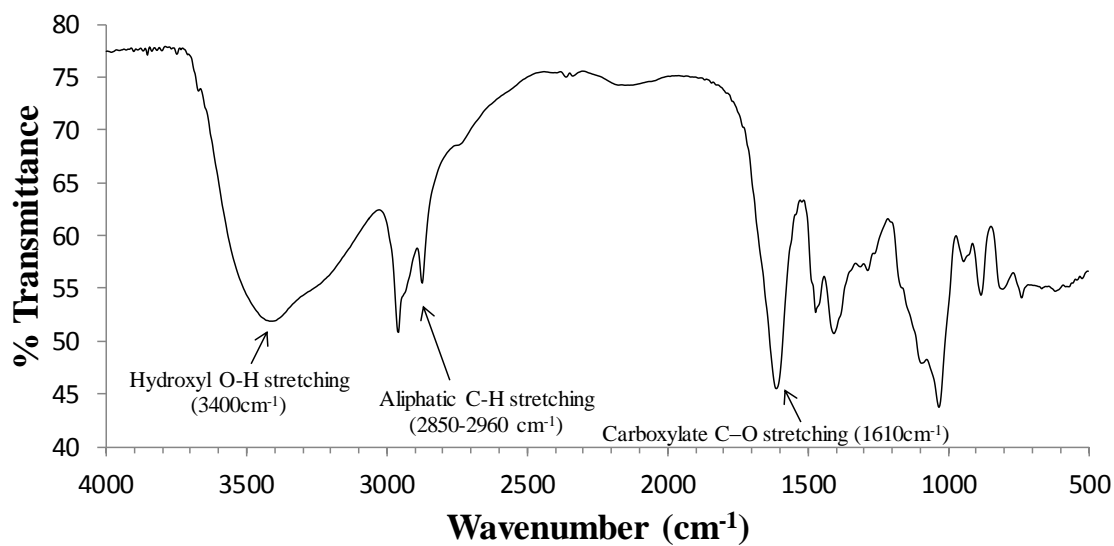


Figure 5.9: FTIR of TBA-alginate

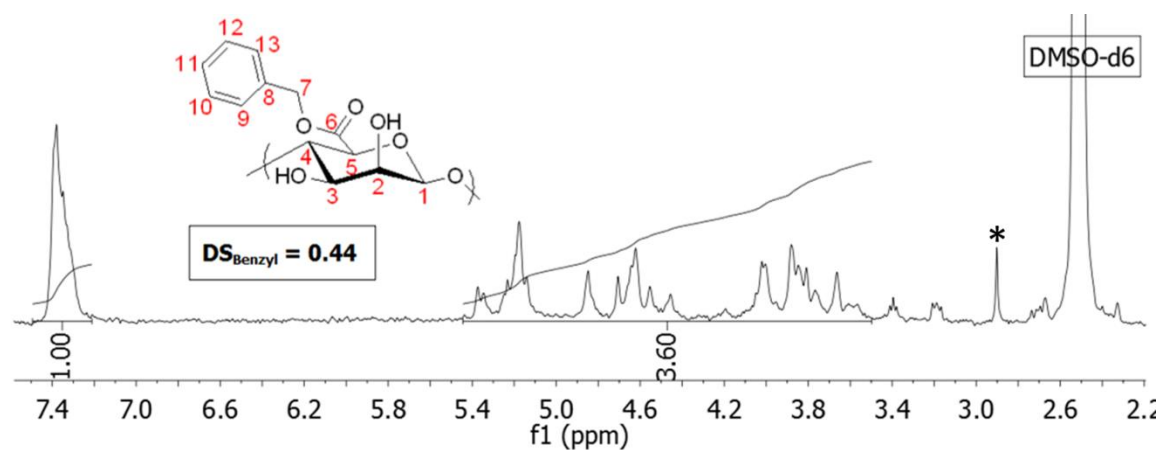


Figure 5.10: ^1H -NMR spectrum of benzyl alginate with DS 0.44 synthesized using BzBr

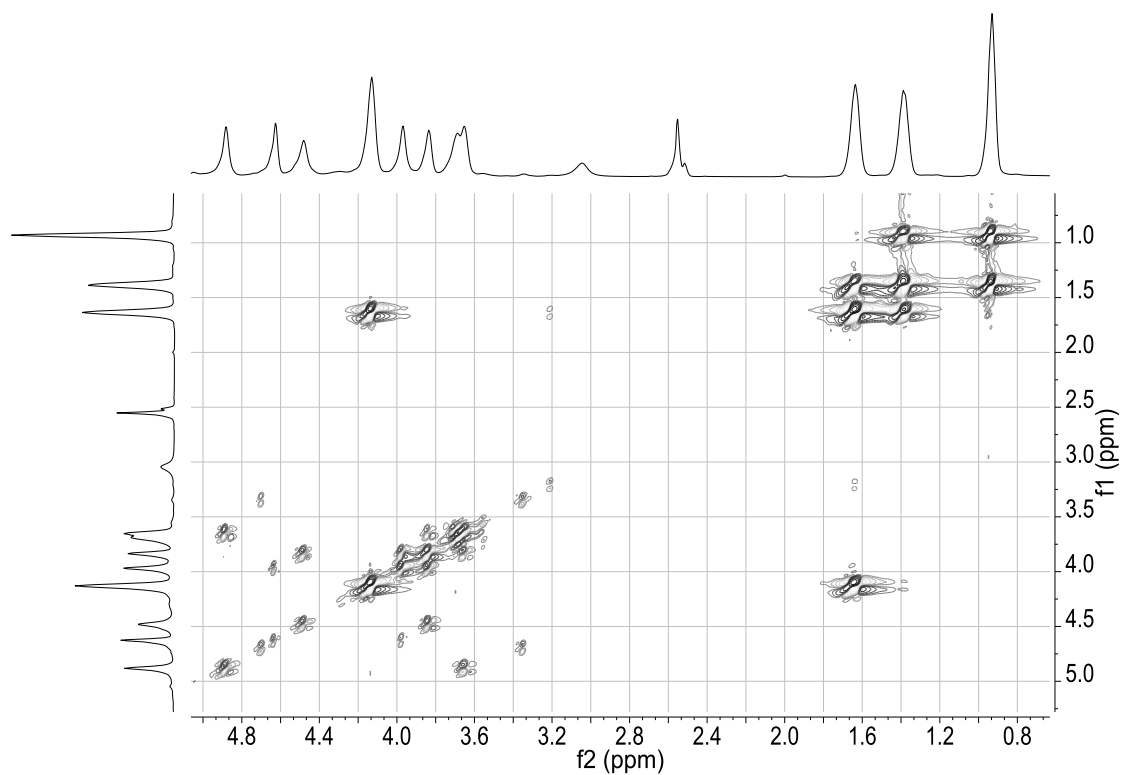


Figure 5.11: DQF-COSY spectrum of benzyl alginate M000

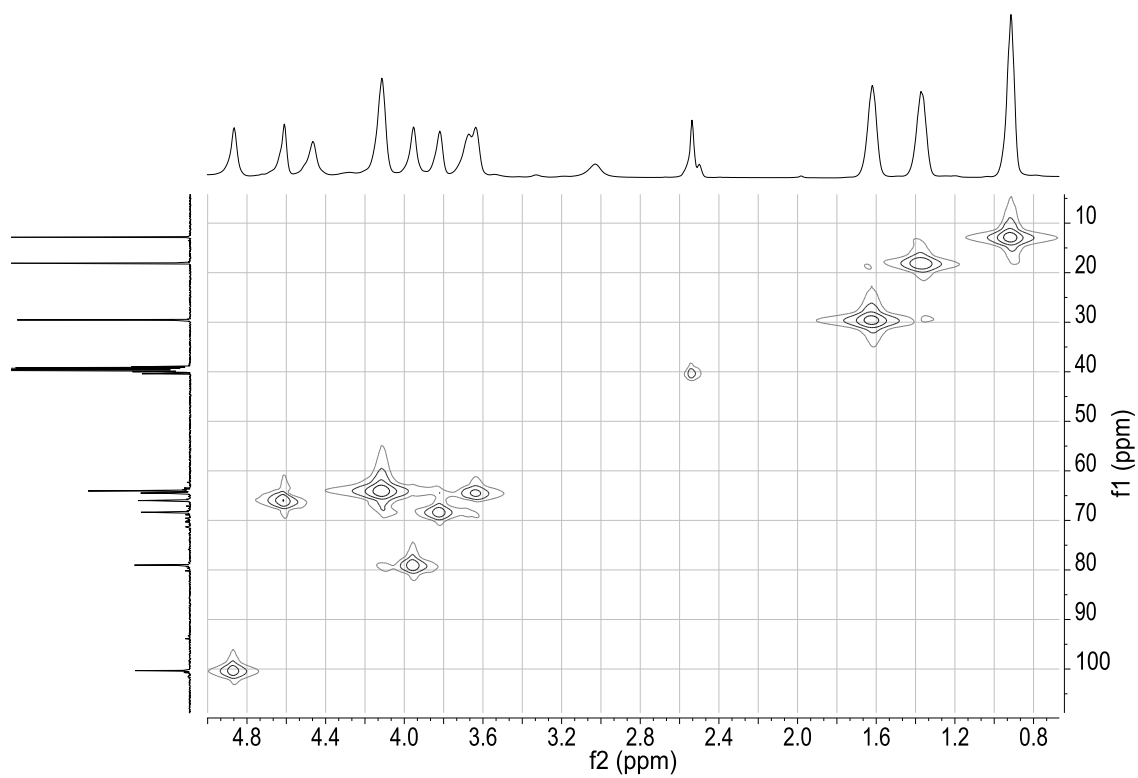


Figure 5.12: HMQC spectrum of benzyl alginate M000

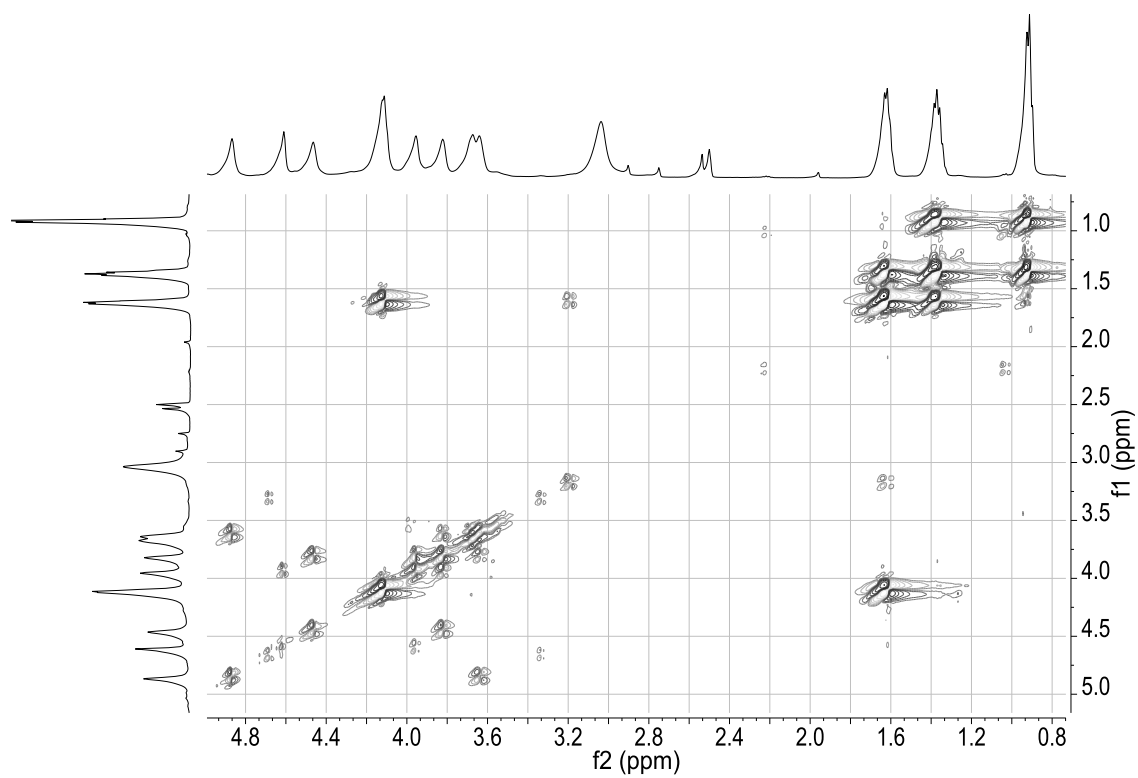


Figure 5.13: DQF-COSY spectrum of benzyl alginate M060

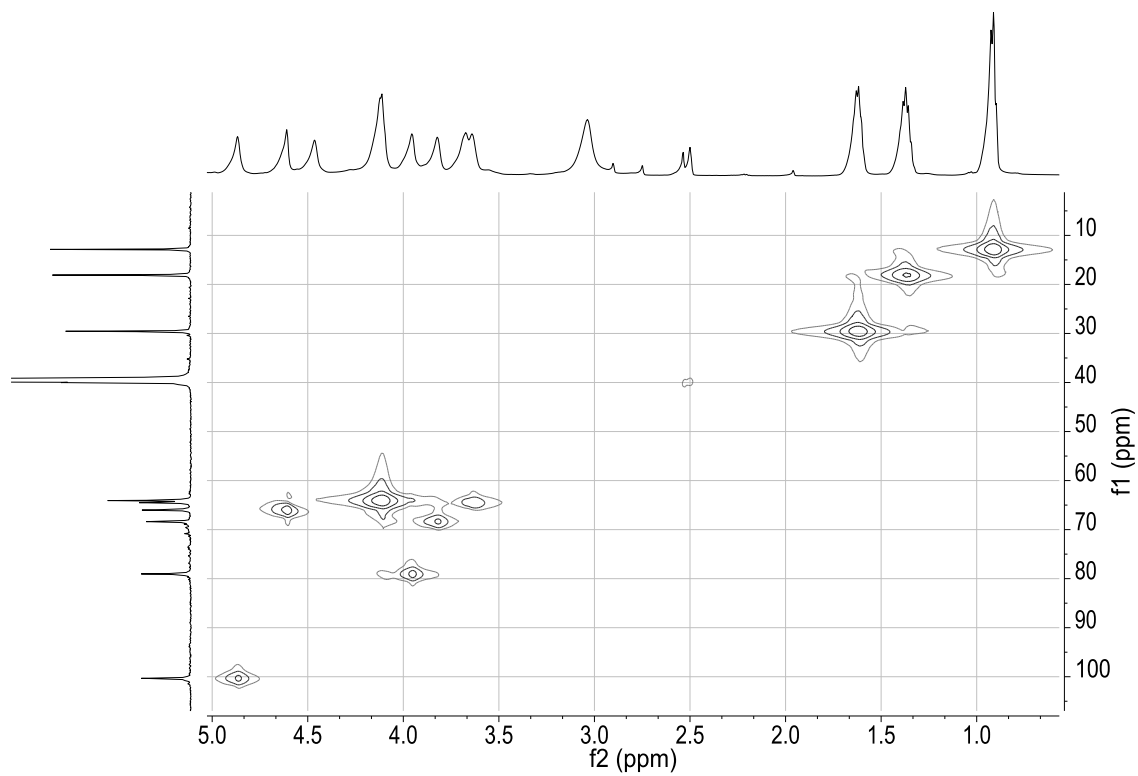


Figure 5.14: HMQC spectrum of benzyl alginate M060

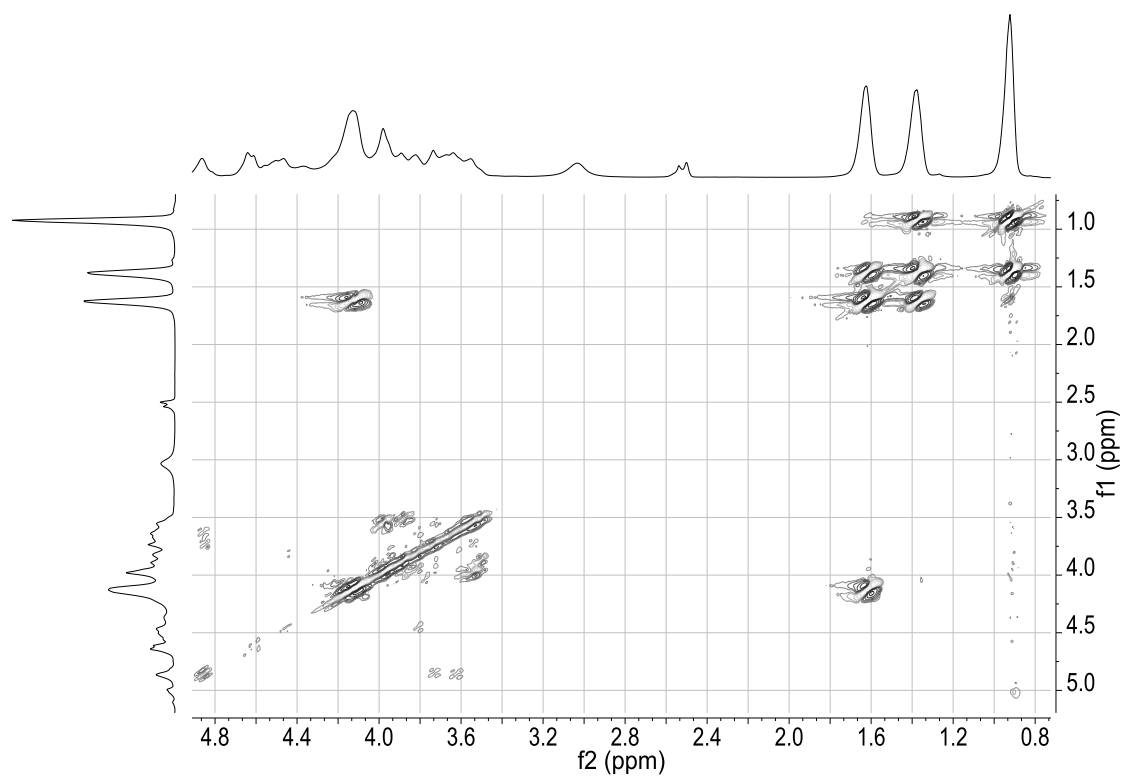


Figure 5.15: DQF-COSY spectrum of benzyl alginate M063

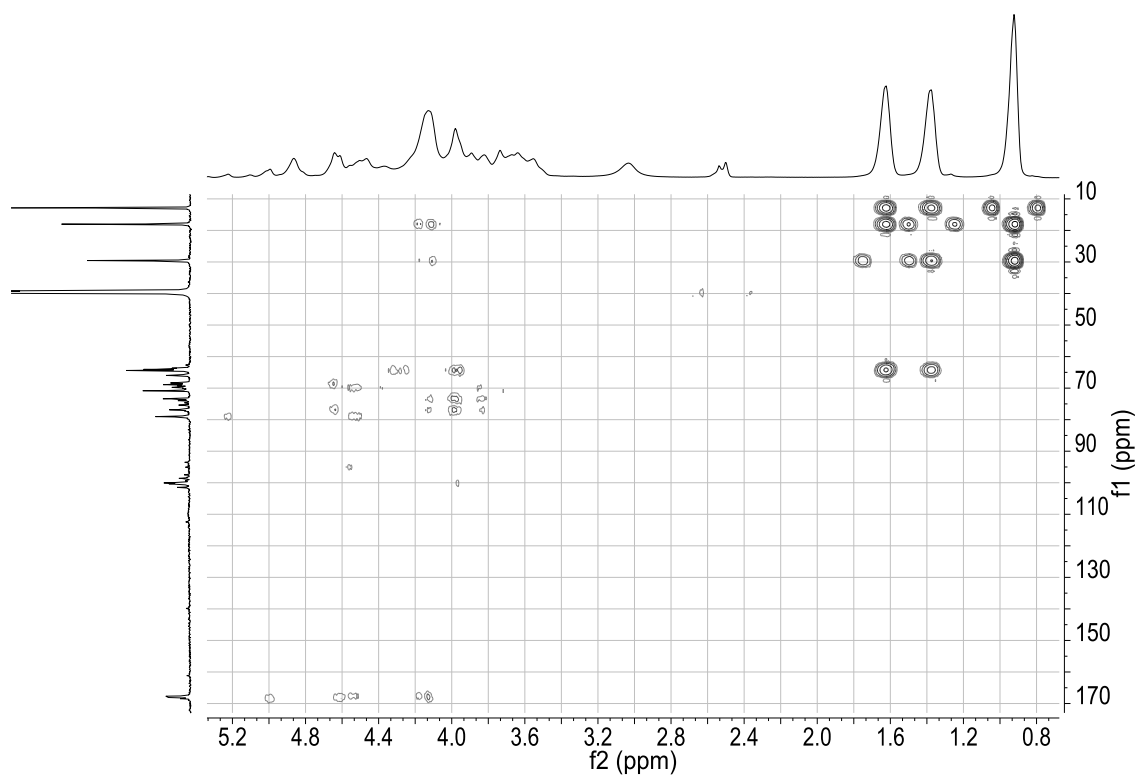


Figure 5.16: HMBC spectrum of benzyl alginate M063

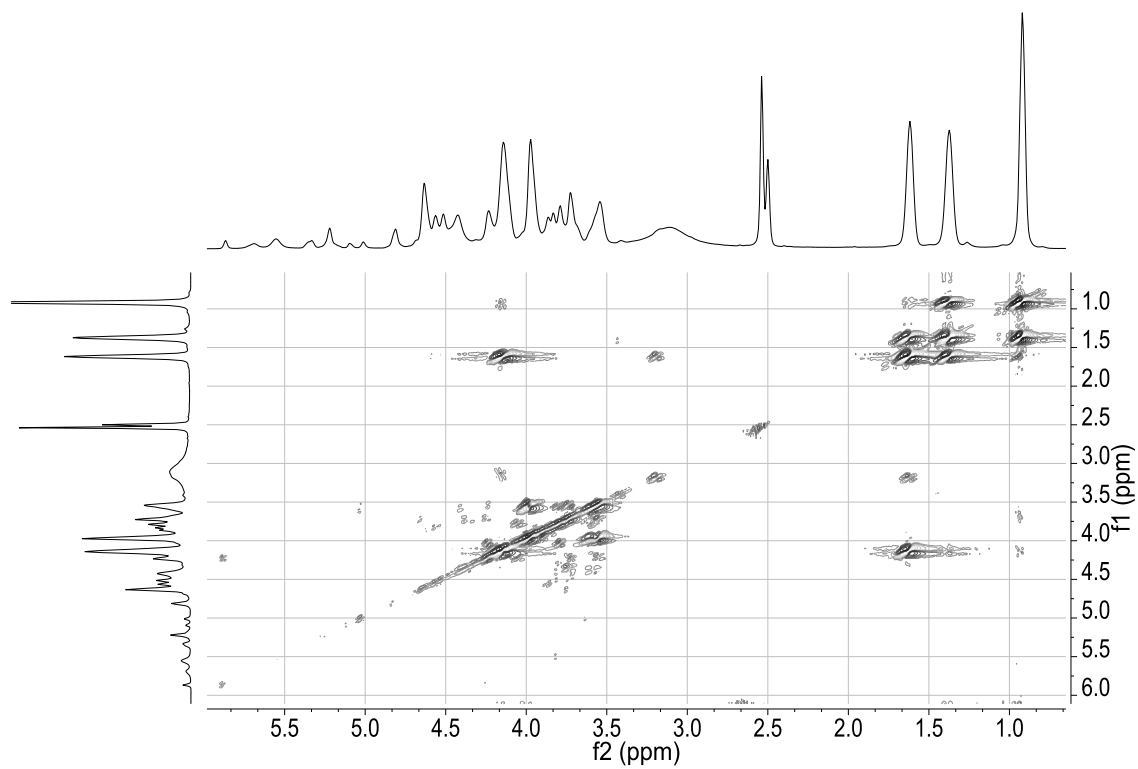


Figure 5.17: DQF-COSY spectrum of benzyl alginate M100

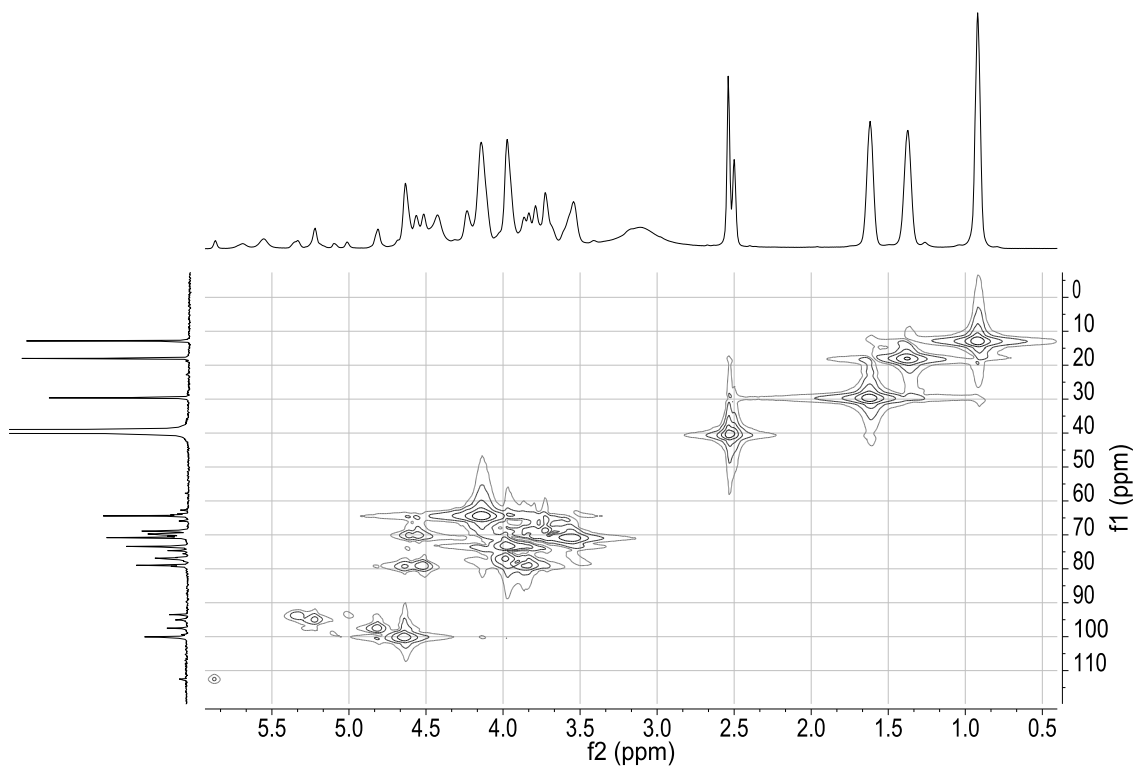


Figure 5.18: HMQC spectrum of benzyl alginate M100

Table 5.5: ^1H and ^{13}C -NMR peak shifts in butyl alginates

G Residues			M Residues		
Position	^1H -NMR Shift	^{13}C -NMR Shift	Position	^1H -NMR Shift	^{13}C -NMR Shift
G1	4.86	100.32	M1	5.87	112.46
G2	3.64, 3.67	64.06, 64.49	M1	4.64	100.05
G3	3.82	68.36	M1	4.82	97.49
G4	3.95	79.03	M1	5.22	95.07
G4(NR)	4.46	71.30	M1	5.34, 5.01	93.51
G5	4.61	65.99			
G6	-	168.09			

NR: non-reducing

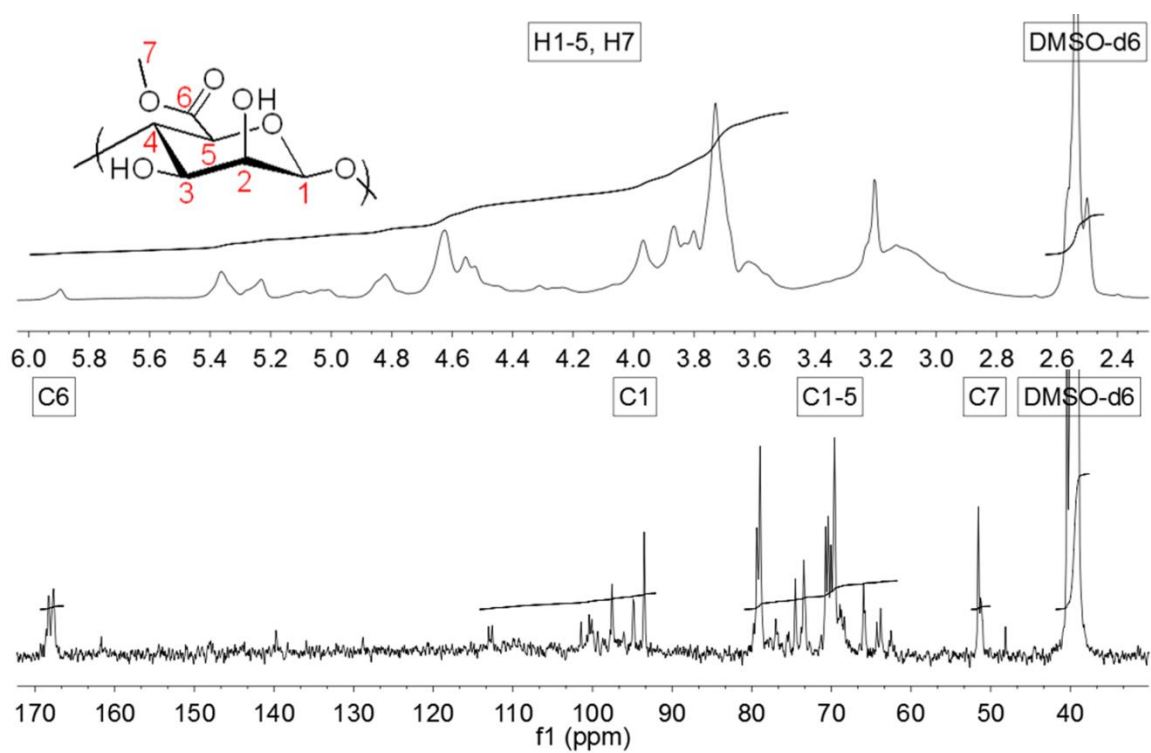


Figure 5.19: ^1H and ^{13}C -NMR of methyl alginate

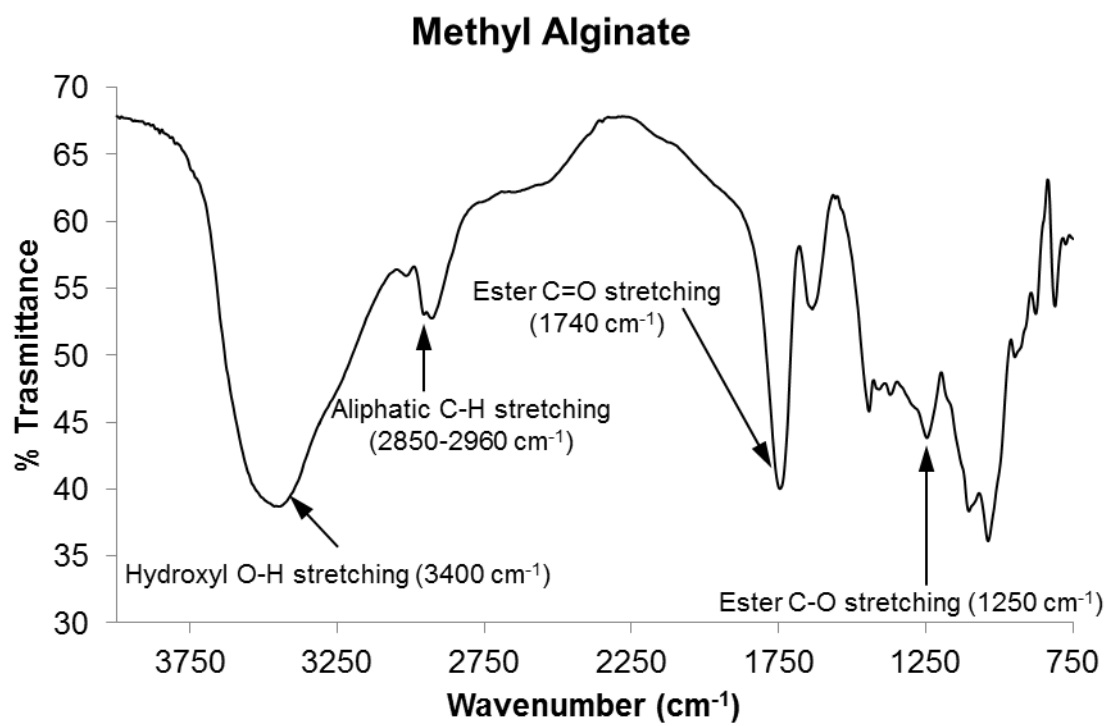


Figure 5.20: FTIR of methyl alginate

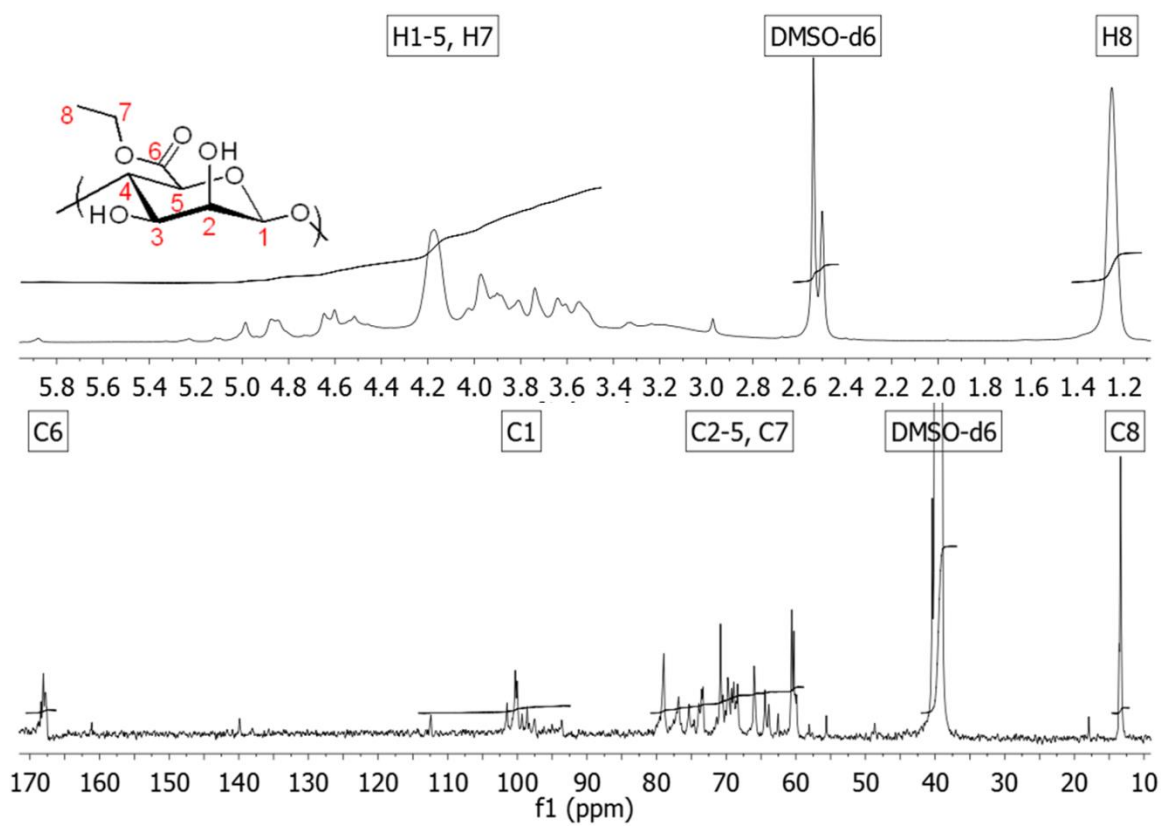


Figure 5.21: ^1H and ^{13}C -NMR of ethyl alginate

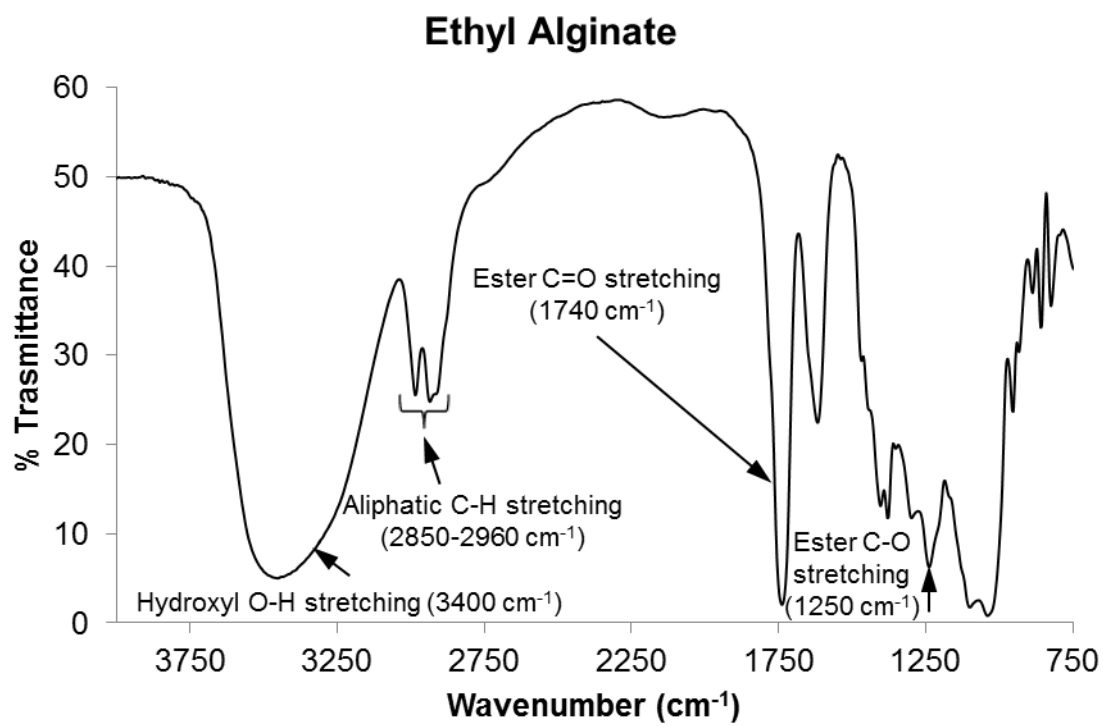


Figure 5.22: FTIR of ethyl alginate

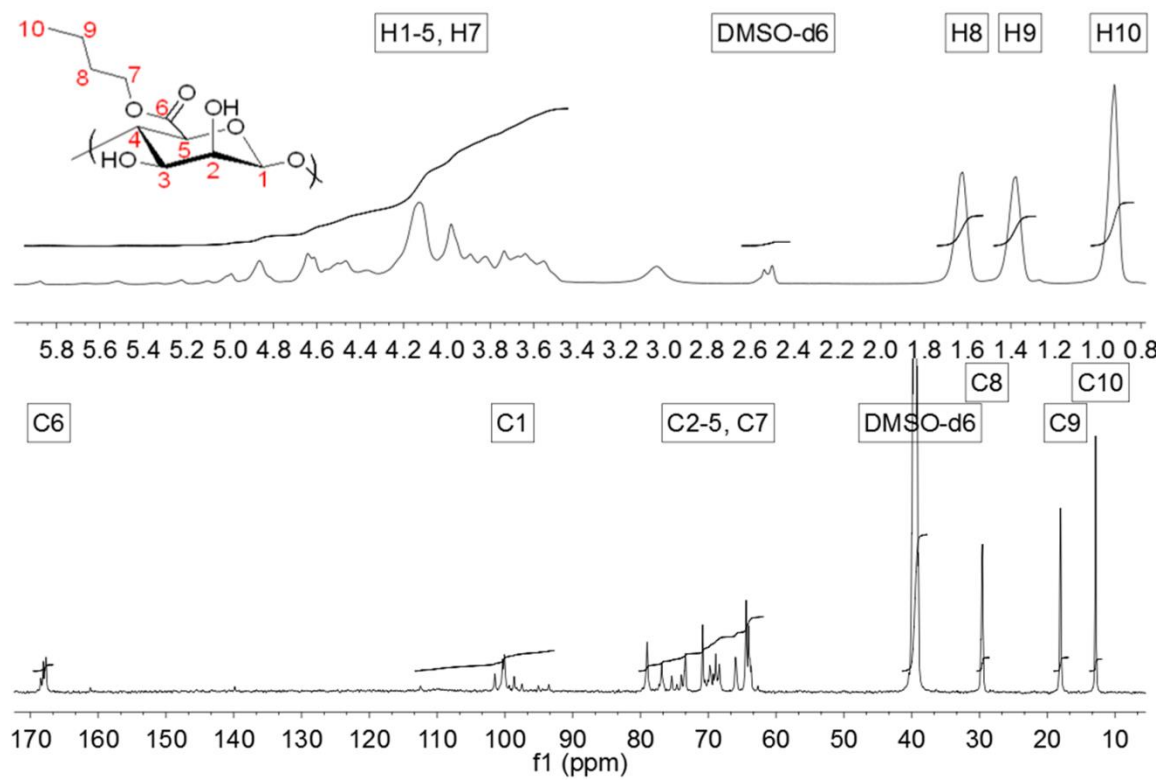


Figure 5.23: ^1H and ^{13}C -NMR of butyl alginate

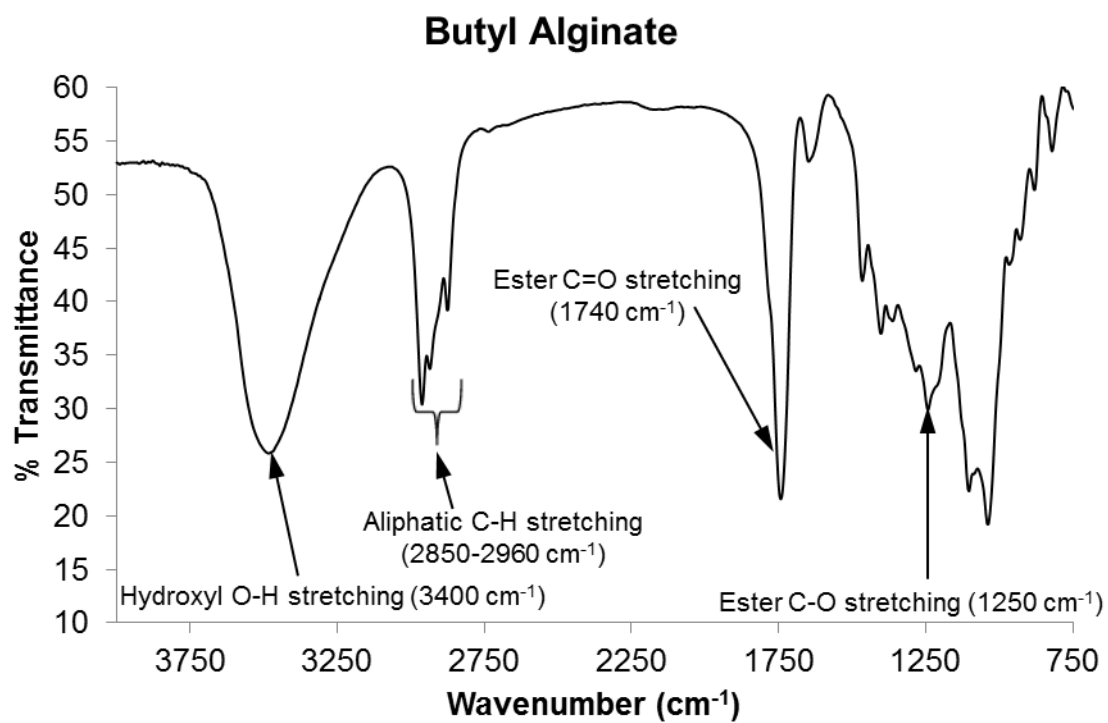


Figure 5.24: FTIR of butyl alginate

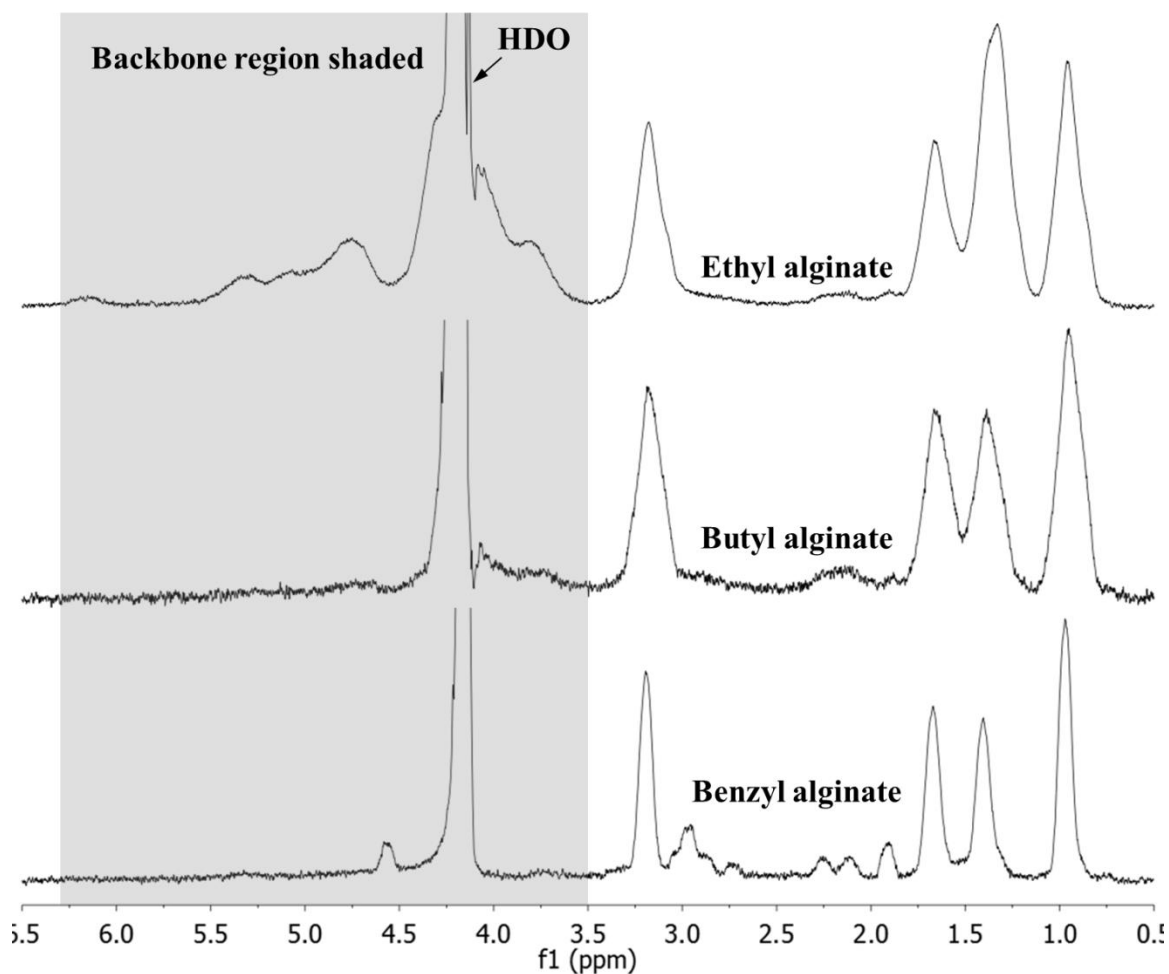


Figure 5.25: ^1H -NMR of partially esterified alginates acquired in D_2O

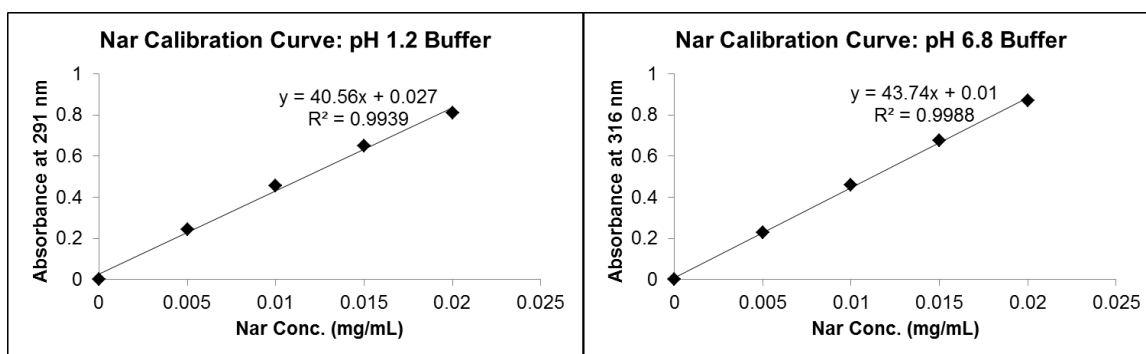


Figure 5.26: Nar calibration curves obtained in pH 1.2 (left) and pH 6.8 (right) buffer

5.7 References

1. Draget, K. I., Alginates. In *Handbook of Hydrocolloids*, Phillips, G. O., Williams, P.A., Ed. 2009; pp 379-395.
2. Pawar, S. N.; Edgar, K. J., *Biomaterials* **2012**, 33 (11), 3279-3305.
3. Liebert, T.; Heinze, T.; Edgar, K. J., Preface. In *Cellulose Solvents: For Analysis, Shaping and Chemical Modification*, American Chemical Society: 2010; Vol. 1033, pp ix-x.
4. Pawar, S. N.; Edgar, K. J., *Biomacromolecules* **2011**, 12 (11), 4095-4103.
5. Xu, D. G.; Edgar, K. J., *Biomacromolecules* **2012**, 13 (2), 299-303.
6. Babak, V. G.; Skotnikova, E. A.; Lukina, I. G.; Pelletier, S.; Hubert, P.; Dellacherie, E., *J. Colloid Interface Sci.* **2000**, 225 (2), 505-510.
7. Pelletier, S.; Hubert, P.; Lapique, F.; Payan, E.; Dellacherie, E., *Carbohydr. Polym.* **2000**, 43 (4), 343-349.
8. Leonard, M.; Rastello de Boisseson, M.; Hubert, P.; Dellacherie, E., *Journal of Biomedical Materials Research Part A* **2004**, 68A (2), 335-342.
9. Borradaile, N. M.; de Dreu, L. E.; Barrett, P. H.; Behrsin, C. D.; Huff, M. W., *Biochemistry-Us* **2003**, 42 (5), 1283-91.
10. Tsai, S. J.; Huang, C. S.; Mong, M. C.; Kam, W. Y.; Huang, H. Y.; Yin, M. C., *J Agric Food Chem* **2012**, 60 (1), 514-21.
11. Du, G.; Jin, L.; Han, X.; Song, Z.; Zhang, H.; Liang, W., *Cancer Res* **2009**, 69 (7), 3205-12.
12. Goldwasser, J.; Cohen, P. Y.; Lin, W.; Kitsberg, D.; Balaguer, P.; Polyak, S. J.; Chung, R. T.; Yarmush, M. L.; Nahmias, Y., *J Hepatol* **2011**, 55 (5), 963-71.

13. Tsujimoto, M.; Horie, M.; Honda, H.; Takara, K.; Nishiguchi, K., *Biol Pharm Bull* **2009**, 32 (4), 671-6.
14. Tommasini, S.; Raneri, D.; Ficarra, R.; Calabro, M. L.; Stancanelli, R.; Ficarra, P., *J Pharm Biomed Anal* **2004**, 35 (2), 379-87.
15. Van Eerdenbrugh, B.; Taylor, L. S., *Mol Pharm* **2010**, 7 (4), 1328-37.
16. Klein, C. E.; Chiu, Y. L.; Awni, W.; Zhu, T.; Heuser, R. S.; Doan, T.; Breitenbach, J.; Morris, J. B.; Brun, S. C.; Hanna, G. J., *J Acq Imm Def* **2007**, 44 (4), 401-410.
17. Kanaze, F. I.; Kokkalou, E.; Niopas, I.; Barmapalexis, P.; Georgarakis, E.; Bikiaris, D., *Drug Dev Ind Pharm* **2010**, 36 (3), 292-301.
18. Curatolo, W.; Nightingale, J. A.; Herbig, S. M., *Pharm Res* **2009**, 26 (6), 1419-31.
19. Posey-Dowty, J. D.; Watterson, T. L.; Wilson, A. K.; Edgar, K. J.; Shelton, M. C.; Lingerfelt, L. R., *Cellulose* **2007**, 14 (1), 73-83.
20. Shelton, M., C.; Posey-Dowty, J., D.; Lingerfelt, L.; Kirk, S., K.; Klein, S.; Edgar, K., J., Enhanced dissolution of poorly soluble drugs from solid dispersions in carboxymethylcellulose acetate butyrate matrices. In *Polysaccharide Materials: Performance by Design*, American Chemical Society: 2009; Vol. 1017, pp 93-113.
21. Kar, N.; Liu, H. Y.; Edgar, K. J., *Biomacromolecules* **2011**, 12 (4), 1106-1115.
22. Liu, H. Y.; Kar, N.; Edgar, K. J., *Cellulose* **2012**, 19 (4), 1279-1293.
23. Ilevbare, G. A.; Liu, H. Y.; Edgar, K. J.; Taylor, L. S., *Crystengcomm* **2012**, 14 (20), 6503-6514.
24. Ilevbare, G. A.; Liu, H. Y.; Edgar, K. J.; Taylor, L. S., *Cryst Growth Des* **2012**, 12 (6), 3133-3143.
25. Chitnis, C. E.; Ohman, D. E., *J Bacteriol* **1990**, 172 (6), 2894-900.

26. Timell, T. E., *Can. J. Chem.* **1964**, *42*, 1456.
27. Smidsrød, O. H., A.; Larsen, B., *Acta Chem Scand* **1966**, *20*, 1026-34.
28. Tsujino, I.; Saito, T., *Nature* **1961**, *192*, 970-1.
29. Preiss, J.; Ashwell, G., *J Biol Chem* **1962**, *237* (2), 309-316.
30. Smith, S. G.; Winstein, S., *Tetrahedron* **1958**, *3* (3), 317-319.
31. Høidal, H. K.; Ertesvåg, H.; Skjåk-Bræk, G.; Stokke, B. T.; Valla, S., *J Biol Chem* **1999**, *274* (18), 12316-12322.
32. Hartmann, M.; Duun, A. S.; Markussen, S.; Grasdalen, H.; Valla, S.; Skjåk-Bræk, G., *Biochim Biophys Acta* **2002**, *1570* (2), 104-12.
33. Hartmann, M.; Holm, O. B.; Johansen, G. A. B.; Skjåk-Bræk, G.; Stokke, B. T., *Biopolymers* **2002**, *63* (2), 77-88.
34. Campa, C.; Holtan, S. v.; Nilsen, N.; Bjerkan, T. M.; Stokke, B. r. T.; Skjåk-Bræk, G., *Biochem. J.* **2004**, *381* (1), 155-164.
35. Shelton, M. C.; Posey-Dowty, J. D.; Lingerfelt, L. R.; Kirk, S. K.; Klein, S.; Edgar, K. J., Enhanced dissolution of poorly soluble drugs from solid dispersions in carboxymethylcellulose acetate butyrate matrices. In *Polysaccharide Materials: Performance by Design*, American Chemical Society: 2009; Vol. 1017, pp 93-113.
36. Hancock, B.; Parks, M., *Pharmaceutical Research* **2000**, *17* (4), 397-404.

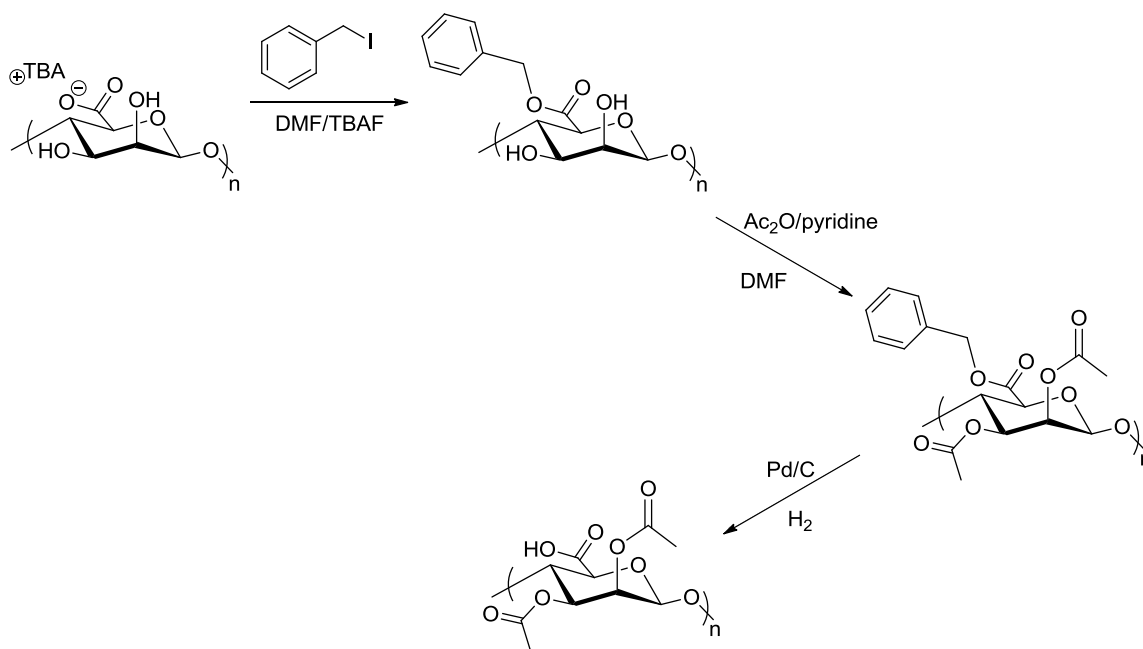
Chapter 6: Summary and Future Work

Sodium alginate in its unmodified form is a water soluble hydrophilic polysaccharide that shows no organic solubility. Through our knowledge of the literature, we recognized that homogeneous organic dissolution of alginates was an aspect of its derivatization chemistry that was not previously explored.[1] We further predicted that if alginates could be dissolved in organic media, new routes to its functionalization could be unlocked, access to useful hydrophobic reagents made possible, and derivatives not previously permissible through aqueous chemistry could be synthesized. Based on this hypothesis, we discovered TBAF based two component solvent systems capable of dissolving tetrabutylammonium (TBA) salts of alginate. Polar aprotic solvents such as DMSO, DMF, DMI or DMAc along with TBAF were able to afford clear solutions of TBA-alginate at room temperature. This was the first ever demonstration of the unequivocal dissolution of alginates in organic media. This discovery has opened up numerous possibilities for the derivatization of alginates using a variety of chemistries and reagents not previously possible. Through our work, we have successfully illustrated some of the possible routes to alginate functionalization. While this was the first demonstration of the use of DMSO/TBAF for solubilizing TBA-alginate, it has previously been reported to dissolve crystalline polysaccharides such as cellulose at room temperature.[2]

Solubilizing alginates in two component solvent systems was made possible by simply exchanging the small inorganic counterions (Na^+ or Ca^{+2}) with a bulky organic counterion (TBA^+). However, it appears that this counterion exchange is not enough to affect single component organic solvent solubility. An ideal scenario could be imagined, wherein alginates are easily soluble in common low-boiling organic solvents such as acetone, methanol, ethanol, chloroform, dichloromethane and so on. Perhaps the only way to achieve this ideal solubility

range is via organic derivatization of the alginate –OH and/or –COOH groups. As of now, we believe that the best way to achieve this is via dissolution and derivatization of TBA-alginate in solvents systems such as DMSO/TBAF.

We demonstrated that the alginate –OH groups can be acetylated using Ac_2O /pyridine in DMSO/TBAF.[3] Knowing that the maximum possible achievable $\text{DS}_{\text{acetyl}}$ is 2.0, we reacted TBA-alginate with large excesses of Ac_2O . Under no circumstances were we able to achieve $\text{DS}_{\text{acetyl}}$ values higher than ~1.0. Clearly, there was a ceiling beyond which no further acetylation occurred when Ac_2O /pyridine was used. We speculated on the reasons why such a ceiling may be observed. One possible explanation relates to the tendency of TBAF to regioselectively deacylate esters of cellulose.[4] A similar reaction occurring in situ during acetylation of alginates may be one explanation for limiting the $\text{DS}_{\text{acetyl}}$ value. In order to further explore the role played by TBAF during acetylation, it would be valuable to perform acetylation homogeneously, but in the absence of TBAF. If $\text{DS}_{\text{acetyl}}$ values higher than 1.0 can be achieved under such conditions, it would confirm our suspicion that the fluoride ions do indeed limit $\text{DS}_{\text{acetyl}}$. However, the homogeneous dissolution of alginates in organic media without TBAF is possible only through derivatives prepared via carboxyl esterification (as demonstrated in Chapter 5). We therefore believe that the alginates esters synthesized in Chapter 5 would be suitable substrates to study acetylation in the absence of TBAF. Notably, the benzyl derivative could be more valuable, considering the possibility of subsequent hydrogenation to remove benzyl groups without hydrogenolysis of acyl esters. **Scheme 6.1** shows a general scheme that may be used for this study.



Scheme 6.1: Suggested route for acylation of benzyl alginate and subsequent hydrogenation to remove benzyl groups

Achieving regioselectivity (reaction of one out of two –OH groups) and epimer selectivity (reaction of one out of the two monosaccharides M and G) during alginate modification is non-trivial. As for regioselectivity, the difference in chemical reactivity between the 2-OH and 3-OH groups is too small to be of much consequence. Perhaps a possible approach to achieving regioselectivity would be to use sterically bulky reagents, similar to a strategy that's commonly used in the derivatization of cellulose.[5] Even though both –OH groups in alginates are secondary, one is axial while the other is equatorial. One may look at this as a window of opportunity to synthesize regioselectively modified alginates. The more difficult challenge however would be the analysis of such alginates. Even with the availability of modern characterization techniques such as 1D/2D-NMR, the complex nature of the alginate backbone poses a daunting analytical task. To achieve epimer-selectivity, we were able to take advantage of the partial solubility of TBA-alginate in DMSO. M-selective acetylation was possible when

the reaction conditions were heterogeneous (DMSO), and non-selective acetates were prepared when alginate was dissolved homogeneously (DMSO/TBAF). While we have shown this to be a possible way to achieve epimer-selective control, other promising routes have been reported for the same.[6] A chemoenzymatic approach would perhaps be most appealing, considering that it offers complete control in terms of epimer-selectivity.

An important aspect of alginate derivatization that cannot be ignored is its susceptibility to molecular weight degradation. Alginates degrade under both acidic and basic pH conditions. When performing acetylation using Ac_2O /pyridine, the acetic acid by product formed had a much stronger effect on degradation compared to pyridine. We further observed that degradation during acetylation could only be minimized at best; it could not be prevented. The impact of molecular weight on the strength of Ca-crosslinked alginate gels is well known. We were further able to prove that in the case of M-selective alginate acetates, molecular weight had a strong influence on the ability to form Ca-crosslinked beads. High $\text{DS}_{\text{acetyl}}$ values coupled with significant loss in MW severely compromised Ca-crosslinking capacity. This observation is a clear demonstration of why it may be important to preserve alginate DP during reaction.

To achieve acylation of alginates while preserving the degree of polymerization (DP_n), formation of acetoacetate esters is an attractive option. The synthesis of cellulose acetoacetate using diketene reagent has previously been reported.[7] Diketene would indeed be the best choice for alginate acetoacetylation since it requires no catalyst and reacts at low temperatures, as shown through cellulose acetoacetates. Such a situation would be ideal to synthesize derivatives without significant loss in DP_n values. However, the highly reactive and at times hazardous nature of diketene can be a deterrent to its use. As part of our work, diketene reactions were not explored due to the fact that it is no longer commercially available and requires

specialized equipment to make. We have therefore envisioned the use of alternate methods for the synthesis of alginate acetoacetates; they are schematically described in **Figure 6.1**. Diketene may be replaced with the acetone-diketene adduct[8], tert-butyl acetoacetate (TBAA)[9] or acetoacetyl imidazolidine reagent to derivatize alginate. While the acetone-ketene adduct and TBAA are commercial reagents, the imidazolidine may be synthesized prior to the alginate reaction. Furthermore, using the ketene acetone adduct, we were able to form alginate acetoacetate with $DS_{\text{acetoacetate}} = 0.31$. **Figure 6.2** shows the ^1H -NMR spectra of the product obtained.

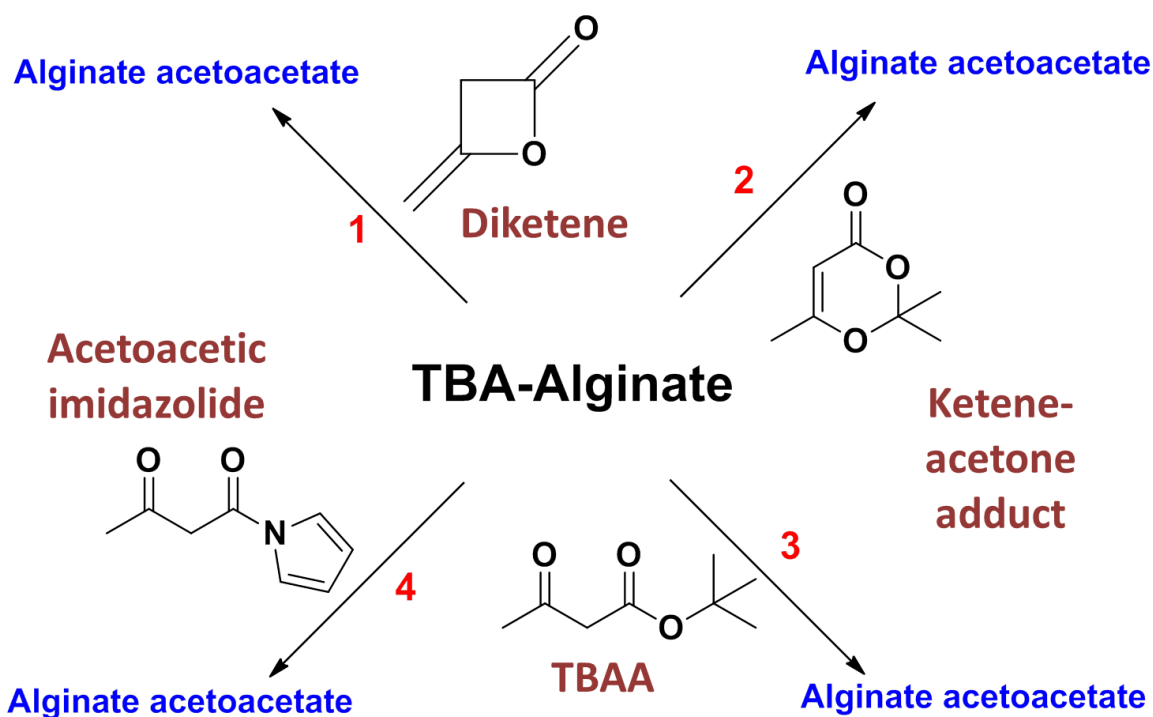


Figure 6.1: Proposed routes to synthesis of alginate acetoacetates

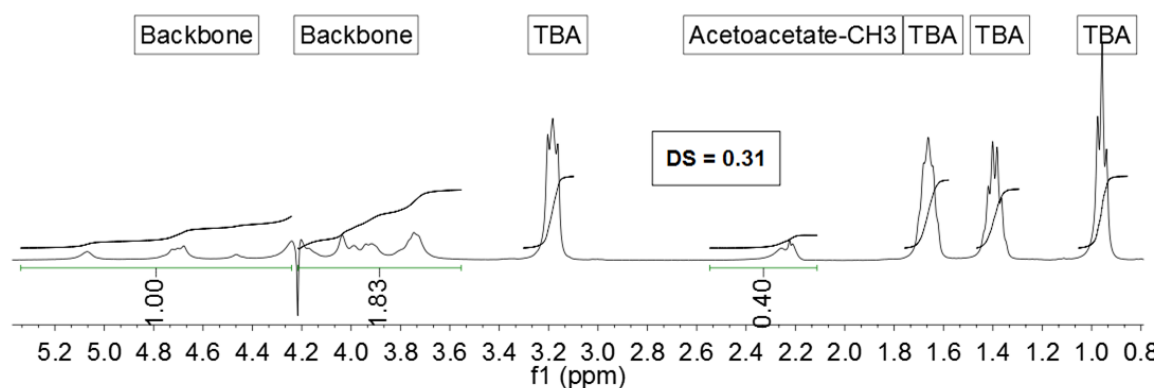


Figure 6.2: ^1H -NMR of alginate acetoacetate

Based on the accomplishments from this work, some general comments can be made about its impact on the area of alginate derivatization. In addition to preparing alginate esters, it is always an attractive option to explore the synthesis of ethers via hydroxyl group modification. Most etherification reactions necessitate the use of strong bases for deprotonating $-\text{OH}$ groups. Knowing that alginates undergo degradation via β -elimination, a competitive side reaction that lowers molecular weight is almost guaranteed. This makes the synthesis of alginate ethers challenging. However, if the MW loss can be controlled under specific conditions, and if the intended applications do not require high MWs, synthesizing alginate ethers would be a novel addition to the field. Like ethers, the synthesis of alginate sulfates is marred by similar difficulties. Alginate sulfates are of interest as heparin analogs due to their anticoagulant properties.[10, 11] Most sulfate syntheses require the use of reagents based on strong acids such as H_2SO_4 . In such harsh conditions, a competitive degradation reaction through a hydrolytic mechanism would be unavoidable. It would therefore be a valuable exercise to consider the use of reagents that are milder compared to H_2SO_4 . Perhaps a reagent such as SO_3 .pyridine complex may lead to sulfation while minimizing loss of molar mass. In conclusion, alginate derivatization is non-trivial, both in terms of actual syntheses and structural characterization. However,

syntheses that use novel chemistries, afford good regioselective control, offer high DS values and limit the loss in molar mass will be valuable additions to alginate research.

6.1 References

1. Pawar SN, Edgar KJ. Alginate derivatization: A review of chemistry, properties and applications. *Biomaterials* 2012;33(11):3279-3305.
2. Ostlund A, Lundberg D, Nordstierna L, Holmberg K, Nyden M. Dissolution and Gelation of Cellulose in TBAF/DMSO Solutions: The Roles of Fluoride Ions and Water. *Biomacromolecules* 2009 Sep;10(9):2401-2407.
3. Pawar SN, Edgar KJ. Chemical Modification of Alginates in Organic Solvent Systems. *Biomacromolecules* 2011;12(11):4095-4103.
4. Xu DG, Edgar KJ. TBAF and Cellulose Esters: Unexpected Deacylation with Unexpected Regioselectivity. *Biomacromolecules* 2012;13(2):299-303.
5. Fox SC, Li B, Xu D, Edgar KJ. Regioselective esterification and etherification of cellulose: a review. *Biomacromolecules* 2011;12(6):1956-1972.
6. Rokstad AM, Donati I, Borgogna M, Oberholzer J, Strand BL, Espevik T, et al. Cell-compatible covalently reinforced beads obtained from a chemoenzymatically engineered alginate. *Biomaterials* 2006;27(27):4726-4737.
7. Edgar KJ, Arnold KM, Blount WW, Lawniczak JE, Lowman DW. Synthesis and Properties of Cellulose Acetoacetates. *Macromolecules* 1995 Jun 5;28(12):4122-4128.
8. Clemens RJ, Hyatt JA. Acetoacetylation with "2,2,6-Trimethyl-4h-1,3-Dioxin-4-One - a Convenient Alternative to Diketene. *J Org Chem* 1985;50(14):2431-2435.

9. Witzeman JS, Nottingham WD. Transacetoacetylation with Tert-Butyl Acetoacetate - Synthetic Applications. *J Org Chem* 1991 Mar 1;56(5):1713-1718.
10. Freeman I, Kedem A, Cohen S. The effect of sulfation of alginate hydrogels on the specific binding and controlled release of heparin-binding proteins. *Biomaterials* 2008;29(22):3260-3268.
11. Freeman I, Cohen S. The influence of the sequential delivery of angiogenic factors from affinity-binding alginate scaffolds on vascularization. *Biomaterials* 2009;30(11):2122-2131.